Photovoltaics International

THE TECHNOLOGY RESOURCE FOR PV PROFESSIONALS

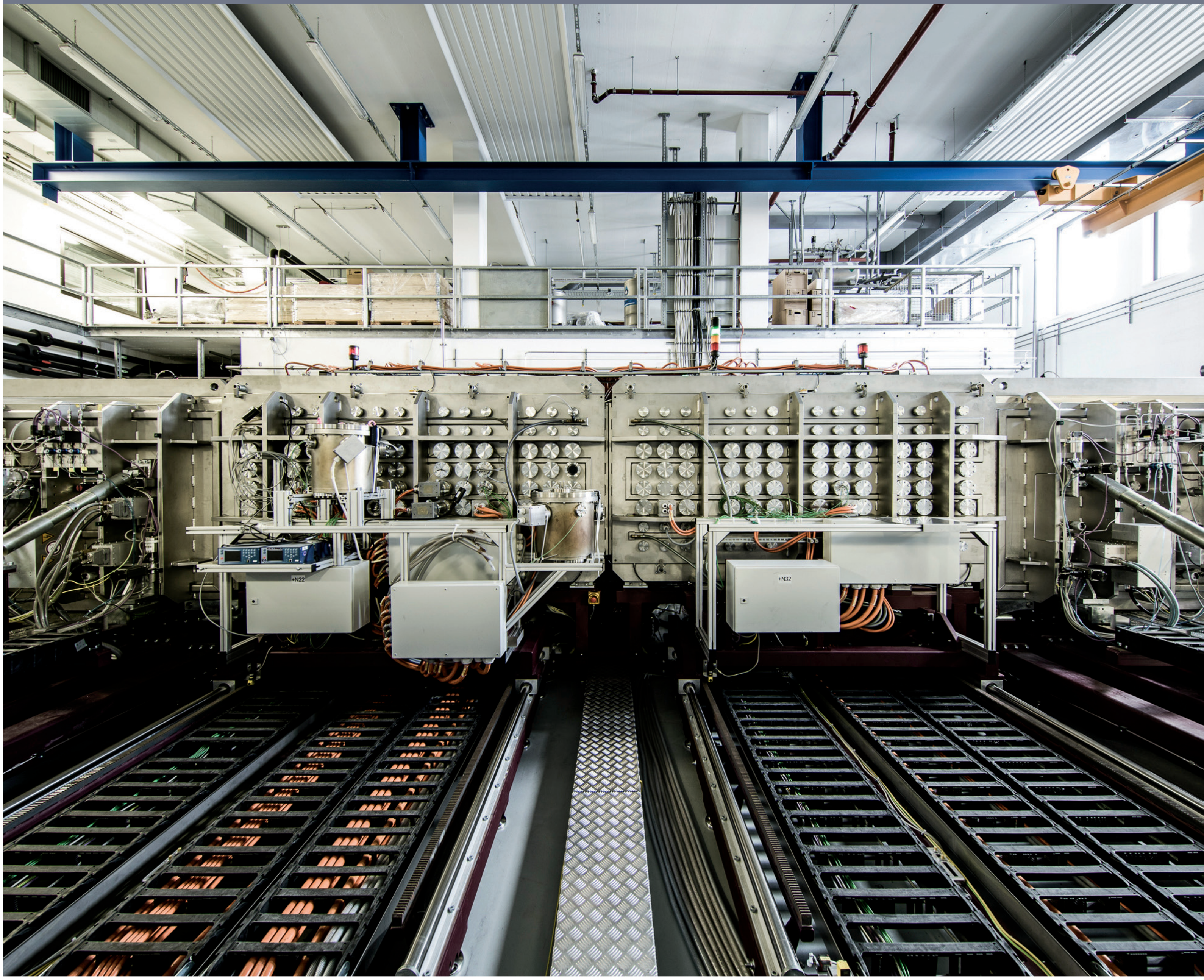

Edition 41

Towards the next generation of high-efficiency Cu(In,Ga)Se2 thin-film solar cells – Sharc25

High-efficiency CIGS cells under the microscope

Transition to Industry 4.0

Opportunities and challenges for the PV sector

On the fabrication of high-efficiency mc-Si PERC-based solar cells on diamond wire-sawn surfaces using industrially viable etching technologies

Improved texturing for diamond wire-sawn multicrystalline silicon wafers

Riding the workhorse of the industry: PERC

Trina Solar on the scope for future PERC efficiency gains

State-of-the-art bifacial module technology

Bifacial technology and performance in review

Advances in module interconnection technologies for crystalline silicon solar cells

Developments in integrated cell to module manufacturing

www.pv-tech.org

JA SOLAR

Harvest the Sunshine

Premium Cells, Premium Modules

+86(10)6361 1888 www.jasolar.com

Foreword

Welcome to Photovoltaics International 41.

An emerging theme in the industry further downstream is the growing variety of bankable PV modules. It's a topic we'll be picking up on 23-24 October at our PV ModuleTech conference in Penang, Malaysia.

This issue of PVI captures the ongoing work to drive improvements across the full range of those technologies. From the exploration of next generation CIGs cells to the commercial improvements of PERC by Trina Solar, this edition neatly captures that variety.

Fraunhofer ISE reviews the latest results from efforts to improve the texturing of diamond wire sawn wafers (p.40). A cost-effective process could help close the gap in efficiencies between mono and multicrystalline solar. The team from Fraunhofer also examine an early large-scale effort by a manufacturer who has been using an alternative plasma-less dry-chemical etching (ADE) method.

Trina Solar presents a roadmap for PERC improvements that it claims could halve costs while pushing efficiencies to 24% in around seven years (p. 54). Doing so will require more than simple tweaking of existing processes but a wholesale R&D effort to improve materials, methods and the development of some specific manufacturing tools.

As the aforementioned variety in cell concepts has developed, the need for a variety of module concepts to best incorporate them has developed. ECN and imec explore the latest developments in integrated cell to module manufacturing approaches from the more familiar multi-busbar and multi-wire to shingling and woven fabric and foil-based module technologies for back contacted cells (p. 93).

In the world of thin-film, ZSW provides an overview of the efforts of the EU-backed Sharc25 project, which has the broad aim of driving CIGSe efficiencies towards 25% (p. 79). ZSW has set a record of 22.6% but as they discuss, improving one aspect of CIGSe cell performance can lead to deterioration of another parameter.

Elsewhere, CSEM INES zooms in on a major limiting factor for silicon heterojunction cells, metallization (p. 65). Replacing silver paste with a lower curing temperature paste creates its own headaches. In this paper they examine the use of copper electroplating as the potential fix.

All the regular features including our news reviews and R&D spending report make a return, plus lots more.

Following on from this bumper edition, PVI42 will be published in Spring 2019.

John Parnell
Head of content
Solar Media Ltd

Photovoltaics International

Published by:
Solar Media Ltd.,
3rd Floor, America House, 2 America Square
London EC3N 2LU, UK
T: +44 (0) 207 871 0122
E info@pv-tech.org
www.pv-tech.org

Publisher: David Owen

Head of Content: John Parnell
Managing Editor: Ben Willis
Commissioning Editor: Adam Morrison
Sub-Editor: Steve D. Brierley
Senior News Editor: Mark Osborne
Reporters: Tom Kenning, Andy Colthorpe
Design: Tina Davidian
Production: Daniel H Brown, Sarah-Jane Lee
Sales Director: David Evans
Account Managers: Adam Morrison, Graham Davie, Lili Zhu

Cover image: In-line CIGS deposition system at ZSW

Image courtesy of ZSW

Printed by Buxton Press

Photovoltaics International
Forty First Edition
Third Quarter, September 2018
Photovoltaics International is a quarterly journal published in February, May, September and December.

Distributed in the USA by Mail Right International, 1637 Stelton Road B4, Piscataway, NJ 08854.

ISSN: 1757-1197

USPS Information
USPS Periodical Code: 025 313

Periodicals Postage Paid at
New Brunswick, NJ
Postmaster: Send changes to:
Photovoltaics International,
Solar Media Ltd., C/o 1637 Stelton Road,
B-4, Piscataway, NJ 08854, USA

Editorial Advisory Board

Photovoltaics International's primary focus is on assessing existing and new technologies for "real-world" supply chain solutions. The aim is to help engineers, managers and investors to understand the potential of equipment, materials, processes and services that can help the PV industry achieve grid parity. The Photovoltaics International advisory board has been selected to help guide the editorial direction of the technical journal so that it remains relevant to manufacturers and utility-grade installers of photovoltaic technology. The advisory board is made up of leading personnel currently working first-hand in the PV industry.

Our editorial advisory board is made up of senior engineers from PV manufacturers worldwide. Meet some of our board members below:

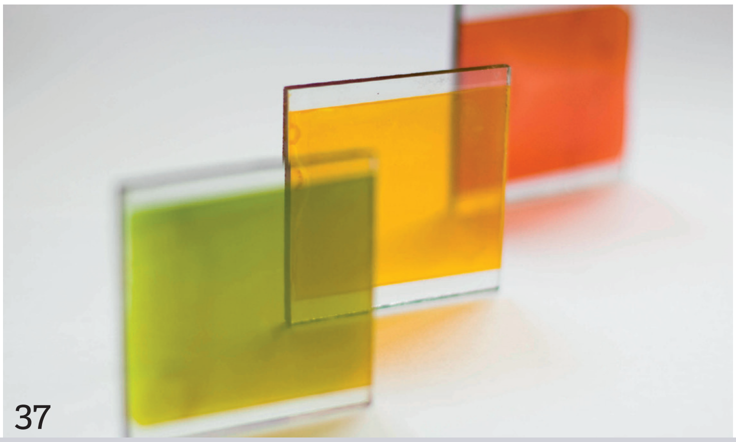

37

77

Contents

Product reviews

Cell Processing: **Aurora**

Aurora Solar launches first measurement tool for TCO layer uniformity on heterojunction cells

Product Outline: Aurora Solar Technologies (AST) has launched the DM-121 and DM-321 measurement systems for heterojunction technology (HJT) cell TCO layer quality control.

Problem: To produce the electrical structure of a HJT cell, it is necessary to apply thin layers of amorphous silicon on both sides of a crystalline silicon wafer as well as transparent, conductive oxide layers (TCO) to absorb the generated power. Optimizing and controlling the uniformity of the TCO layers during cell manufacturing is crucial to maximizing the power and yield of the HJT cells.

Solution: The DM-121 and DM-321 systems measure the front and rear TCO sheet resistances and thicknesses on silicon photovoltaic (PV) wafers. Both sheet resistance and thickness are measured at a series of discrete points along each wafer. Aurora's patented non-contact infrared measurement technology is used in these products and provides accurate real-time measurements for process control and optimization.

Applications: The DM-121 and DM-321 systems measure the front and rear TCO sheet resistances and thicknesses of heterojunction solar cells.

Platform: The systems consists of a specialized pair of DM (formerly Decima) series measurement heads, designed as a unit to fit above and below a wafer conveyor, measuring up to 100% of wafers at full production line speed, and can connect to Aurora's 'Visualize' quality control system for integration of measurements with process tools to provide real-time 3D visualization of intra-tool dynamics, both spatially and by batch. This enables optimization and control of PVD or RPD processes for maximum production line yield and throughput.

Availability: Currently available.

Cell Processing: **VITRONIC**

VITRONIC's 'VINSPEC SOLAR' AOI system extends cell metallization screen life-times

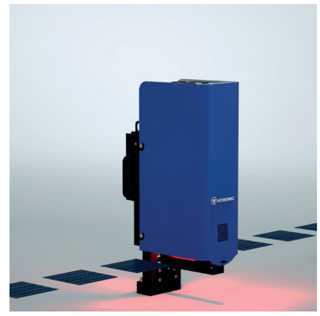

Product Outline: VITRONIC has developed a new solution for post cell-metallization print inspection. Early detection of screen wear with VINSPEC SOLAR extends screen life time (3,000 to 8,000 additional prints) and reduces downtime by 10-30%, because corrective action can be taken immediately, due to fast feedback.

Problem: To achieve highest cell efficiency and to fulfill growing quality requirements in the global PV industry it becomes increasingly important to include optical inspection systems directly at each surface and metallization process. Not only does this approach enable high cell quality in a narrow tolerance range – it also delivers increased efficiency, yield rates and cost reductions.

Solution: The PV industry is constantly demanding technology that helps to gain competitive edge in a rapidly developing market. Automated optical inspection (AOI) plays a key role to meet this objective, ensuring both stable processes and high cell quality along the entire cell production. Optimization of print parameters using the optical inspection data enables adherence to strict quality limits, which reduces average finger width which guarantees optimum efficiency and reduces silver paste usage by between 1-3%.

Applications: Automated optical inspection of solar cells (PERC, PERT, laser openings, Bifacial).

Platform: VITRONIC provides inline AOI systems are able to detect defects at an early stage. Intelligent trend analysis, heat map evaluation and feedback with the production equipment are further benefits of an integrated quality inspection. It allows reliable inspection at finger width of down to <25μm and features closed loop communication for optimized predictive maintenance.

Availability: Available since June 2018.

Cell Processing: **DuPont**

DuPont's 'Solamet' PV21A metallization paste offers better contact performance

Product Outline: DuPont Photovoltaic Solutions has developed a proprietary metallization pastes design that is said to deliver better contact performance and high aspect ratios.

Problem: The continued drive by solar cell producers to push screen printing technology towards finer lines leads to the need to overcome various challenges, such as further improving the contact resistivity as well as the grid line resistance. Nowadays, when more advanced solar cell structures like PERC/ N-PERT enter large-scale production, there is a need to further minimize the contact recombination at the metal and silicon contact interface as it starts to hinder further efficiency improvements for cell structures with higher open circuit voltage.

Solution: Industry-leading performance is proven on a variety of substrates such as diamond wire-sawn wafer and black silicon. TSEC, which specializes in manufacturing high performance, top quality mono- and multi-crystalline solar cells and modules, has observed 21.75% and 20.3% cell efficiency and module power output as high as 315 watts and 300 watts (60 pcs) in its five-busbar half-cut design mono PERC and multi-PERC black cell modules respectively.

Applications: P-type and n-type technologies.

Platform: The Solamet PV21A product family is designed to fulfill all mainstream cell technology, it also includes product series for advanced printing such as double printing, dual print and mesh cross free screen printing.

Availability: Currently available.

Product reviews

Cell Processing: **Manz**

SpeedPicker' 3.0 from Manz provides high-throughput contact-free handling of solar cells

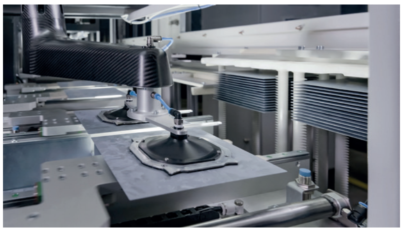

Product Outline: Manz has launched its third generation 'SpeedPicker' 3.0 from its SAS series equipment for the specific handling of crystalline silicon wafers in the manufacturing of solar cells. SpeedPicker provides an automation solution for almost contact-free handling of solar cells throughout their entire production process.

Problem: The shift to higher automation to reduce production cost and improve yields through Industry 4.0 requires wafer and cell solutions with high throughput and contactless handling solutions to reduce breakage rates and minimize contamination.

Solution: Manz has equipped the SpeedPicker with various technological highlights, which make the handling system significantly faster, more precise and gentle on the workpiece and therefore more economical. The SpeedPicker is a slider system which can be used either for unloading the wafers from the transport cassettes by vacuum or loading onto them. This prevents abrasion caused by micro-movements of the wafers on the tray, as was common when belts were used for transport.

Applications: Compatible with all crystalline silicon cell technologies including HJ and IBC cells.

Platform: The SpeedPicker 3.0 offers a maximum throughput of 8,000 wafers per hour. The breakage rate is currently just 0.05%. For efficient integration of the SpeedPicker in new and existing production lines, the system is built on a standardized machine base. The SpeedPicker can also optionally be equipped with colour inspection for quality control of solar cells and coated wafers. Simple connection to a customer-specific MES (Manufacturing Execution System) is also possible.

Availability: Available since June 2018.

Cell Processing: **KOPEL**

KOPEL's probe-bar screening system first for advanced interconnects

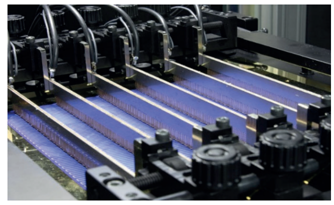

Product Outline: KOPEL has developed the first probe-bar screening of multi-wire interconnection of busbarless solar cells, which provides higher IV measurement stability, data repeatability and durability for longer life cycles.

Problem: The traditional probe pricking method for IV measurement of solar cells is not suited to next-generation solar cells as microcracks in the cells can be generated, while the increased use of multi-wire interconnection in busbarless solar cells means cell alignment accuracy for improved measurement repeatability is reduced significantly.

Solution: The probe system incorporates a patent pending 'flexible spring suspension' (FSS) system, which provides security against the creation of microcracks in the cells being tested and can therefore handle the trend towards thinner and larger wafers, notably for n-type mono solar wafers. The system can therefore operate in a high-speed mode as well as maintain cell alignment accuracy for improved measurement repeatability of IV measurements. It is therefore possible to implement high-speed measurement with not so high accuracy for alignment of PV Cells. Movement of the FSS within elastic deformation region prevents deterioration for longer life.

Applications: R&D to production to improve the accuracy of IV measurement.

Platform: The FSS system provides greater measurement stability. The difference in height of fingers can be followed by the four-wire method and contact made by a continuous line. The influence of shadows can be minimized by a 1mm thick probe bar. When replacing the probe bar it can be completed in a shorter time than before, due to a special mounting frame, contributing to productivity improvement.

Availability: Currently available.

Thin Film: **3D-Micromac**

3D-Micromac's microFLEX laser system designed for patterning of flexible solar cells

Product Outline: 3D-Micromac's microFLEX roll-to-roll laser system is suitable for precisely patterning of flexible CIS/CIGS solar cells as well as organic solar cells for high-throughput applications.

Problem: Flexible PV substrates by nature require flexible manufacturing systems to accommodate a wide range of niche applications, while providing the advantages of low-cost roll-to-roll production.

Solution: The highly versatile microFLEX production platform is the all-in-one solution for the manufacturing of flexible thin films in photovoltaics. It combines high-precision laser processing with cleaning, coating, printing and packaging technologies, as well as inline quality control. The tool can undertake laser structuring, laser patterning, laser cutting, printing and coating as well as laser annealing and laser lift-off. The modular system concept is used with standardized interfaces between the modules to enable a wide variety of applications.

Applications: Roll-to-roll laser patterning of CIS/CIGS and organic solar cells.

Platform: Due to its modular concept various customized solutions are available, reaching from industrial mass production to pilot lines as well as applied research. It enables laser processing on-the-fly or in step and repeat mode and the integration of different laser sources and wavelengths. Various optical setups can be deployed, e.g. galvo scanner, fixed optics, and line beam set-up. The system has the highest precision in web control: down to ± 1 µm tracking error and provides machining under ambient conditions, inert gas atmosphere or vacuum. User-friendly, flexible system control including MES and adaptable to various roll-to-roll or roll-to-sheet configurations.

Availability: Currently available.

Product reviews

PV Modules: **Borealis**

Borealis and Borouge new polyolefin encapsulant films improve long-term module performance and reliability

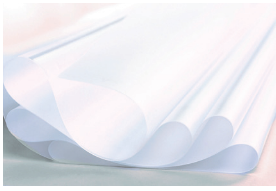

Product Outline: Borealis and Borouge have announce the introduction of two new encapsulant film types based on two new 'Quentys' polyolefin (PO) grades. Borealis Quentys PO encapsulant film now improves the operational reliability of photovoltaic (PV) modules throughout product lifetime, offering better cost efficiency and a sustainable solution for PV modules.

Problem: Extensive independent testing has confirmed that Borealis PO encapsulant film based on Quentys extends the lifetime of solar modules and offers increased power output over the lifespan of the module. Borealis PO encapsulant film is said to outperform conventional ethylene vinyl acetate (EVA), reducing UV-induced module degradation and moisture-induced corrosion, and lowering the incidence of electrochemical failures.

Solution: Two types of Borealis PO encapsulant film are included in the initial launch: the BPO8828F, a front or back encapsulant film in all types of solar modules, and the BPO8828WH a white reflective back encapsulant film for dual glass or standard modules. The PO encapsulant film can help optimize PV module production, resulting in lower costs per watts peak (Wp), due to up to a 50% reduction in lamination cycle in PV module production and lower investment costs needed for increasing output capacity of module production. This enables an improved spread of fixed costs across more modules, with lower per unit module costs.

Applications: PV module encapsulation.

Platform: Borealis PO encapsulant film is the second major application based on Quentys to be launched in 2018, and follows the introduction in May of ICOSOLAR CPO 3G, a co-extruded polypropylene (PP) solar backsheet developed in partnership with ISOVOLTAIC SOLINEX.

Availability: Global availability since the beginning of 2018.

PV Modules: **Endeas**

Endeas launches all-in-one tool to drive down testing cost in PV module manufacturing

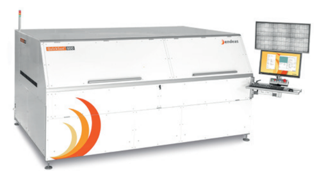

Product Outline: Endeas Oy has launched the 'QuickSun 600', which is the first product to include a class A+A+A+ solar simulator; electroluminescence and visual inspection; and insulation resistance, ground bond and bypass diode tests.

Problem: Competition between leading photovoltaic module manufacturers has forced them to find ways to lower manufacturing costs continually, while introducing technologies that improve the efficiency of modules. Highly efficient modules place high demands on solar simulators, which must be able to measure power output accurately. In addition, increasing assembly line throughput makes it impractical for human operators to keep up with inspecting the quality of manufactured modules.

Solution: The QuickSun 600 tool by Endeas provides a comprehensive collection of final module inspection tests in a single, fully automated machine. The class A+A+A+ solar simulator accurately measures the latest module technologies, including PERC, IBC, HJT and bifacial modules. In addition to precisely measuring the power output of PV modules, the QuickSun 600 enables PV module manufacturers to inspect modules for a comprehensive set of defects automatically. Combining all tests into a single tool makes the QuickSun 600 competitively priced compared to the cost of many separate machines, while ensuring the reliability of test results.

Applications: Final testing of PV modules at high capacity module assembly lines.

Platform: The QuickSun 600 comes with all necessary module handling automation, and modules are loaded and unloaded at a standard production line height. At seven square metre footprint means that it can replace any existing solar simulator without the need for additional space.

Availability: Available since May 2018.

PV Modules: **Meyer Burger**

Meyer Burger's 'Ibex' SWCT stringer system offers increased performance and low manufacturing costs

Product Outline: Meyer Burger's patented SmartWire Connection Technology (SWCT) uses a patented foil-wire electrode with up to 24 round wires to electrically interconnect solar cells and is said to set a benchmark in terms of module performance and low manufacturing costs within the 'Ibex' SWCT stringer system.

Problem: The continued requirement to reduce PV module production costs has led to greater emphasis on cost-competitiveness while increasing module power and production capacity. Manufacturers are evaluating the next generation of cell connection technology in order to reduce the usage of cost-intensive silver.

Solution: SWCT features a dense contact matrix, which reduces electrical resistance and minimizes shading by 25%. The round wires enable a higher light retention in the solar cell and reflect less light back, which further contributes to higher energy efficiency. SWCT does not need any busbar print or soldering pads, reducing silver consumption. On a bifacial HJT solar module for example, a 50% reduction in silver results in 6% lower module material costs.

Applications: SWCT is compatible to all crystalline silicon cell technologies: selective emitter, PERC and Heterojunction (HJT) in both p- and n-type cells.

Platform: The 'Ibex' SWCT stringer uses the SmartWire foil-wire electrode to interconnect solar cells to strings of variable lengths. Its compact and scalable design enables various degrees of throughput and levels of automation. Key features include a unique gripping system and high throughput and a camera system that detects wrong cell orientation and edge defects and is said to achieve a production yield of 98 to 99 %.

Availability: Available since June 2018.

Product reviews

PV Modules: RenewSys

Polyolefin elastomeric encapsulant from RenewSys protects against PID

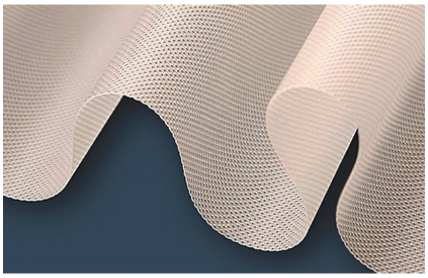

Product Outline: India-based PV module and materials specialist RenewSys has become the first Indian company to receive UL approval and commercialize its polyolefin elastomeric (POE) encapsulant. 'CONSERV E 360 (POE)' has been developed to combine the advantages of TPO as well to provide an effective solution to potential-induced degradation (PID).

Problem: PID is responsible for accelerated PV module performance degradation – maximum power point (MPP) and open circuit voltage (Voc) and reduced shunt resistance, caused by moisture permeation and thermal creeping of the glass.

Solution: CONSERV E 360 (POE) encapsulants exhibit virtually zero PID. A unique method of crosslinking maintains the fine balance between adhesion strength of the encapsulant, with its degree of cross linking. Its unique formulation has also been able to withstand thermal creep at 105 degree Celsius, for 250 hours. It has delivered protection against PID, with extremely low moisture transmission (MVTR.) The encapsulant material resistant to PID helps in reducing power loses on the solar power plants when PV panels with high voltage stress face hot and humid climatic conditions.

Applications: PID protection encapsulant material for glass/glass and glass to backsheet.

Platform: CONSERV E 360 is UL Certified - E 353124, and has an ultra -short lamination time that adds value by decreasing lamination time for the manufacturer, while continuing to offer durability under extreme climatic conditions. CONSERV A 360-14 FC: UL (UL 94, UL 746A & UL746B), IEC 61215, RoHS, 2250 Hrs. DHT TUV Declaration.

Availability: Available since June 2018.

PV Modules: Teamtechnik

Teamtechnik's Stringer TT1400 ECA is designed for sensitive HJT solar cells

Product Outline: teamtechnik has introduced the 'STRINGER TT1600 ECA', which deploys a new adhesive technology and low process temperatures to join high-efficiency bifacial HJT (heterojunction) cells. This process reduces thermal and mechanical stress on the sensitive cells and results in a high string quality.

Problem: It has proved challenging to interconnect powerful HJT cells using existing soldering technology because the performance of the sensitive HJT cells degrades when they are exposed to excessively high temperatures. This also increases the risk of micro-cracks on the typically ultra-thin n-type mono wafers, compared to conventional p-type silicon wafers. The solution needs to be adhesive-based process which replaces the soldering of cells and be automated for high-volume repeatable production.

Solution: ECA is an abbreviation for "electrically conductive adhesive". In this process a conductive glue is applied to both sides of the cell using a screen-printing technique. It is then fully cured at a temperature of roughly 160°C together with the LCRs (Light-Capturing Ribbons), entirely on the string transport. The STRINGER TT1600 ECA production system connects HJT cells with LCRs at a cycle rate of 2.25 seconds. The finished product is a solar module that is designed for extremely high performance and long-life.

Applications: Electrically conductive adhesive technology and low process temperature to join high-efficiency bifacial HJT (heterojunction) cells.

Platform: STRINGER TT1600 ECA system interconnects the cells using a new adhesive technology that reduces thermal and mechanical stresses on the sensitive HJT cells and results in a high string quality. The Stringer TT1400 ECA is also designed for reliable series production with high unit volumes.

Availability: Currently available.

Materials: RCT Solutions

RCT Solutions 'RCT i-UniTex' tool combines texturing capabilities of mono and multi wafers

Product Outline: RCT Solutions 'RCT i-UniTex' tool combines texturing of mono and multi wafers, while providing the most innovative and cost-effective processes.

Problem: Diamond wire (DW) cutting of both multi and mono wafers has provided for lower manufacturing cost as slurries are not required. However, challenges existed for the texturing of wafers to create inverted pyramids for improved light capture.

Solution: DWS multi wafers are processed by RCT Solutions' proven MCCE inline process. In the same tool, also mono wafers can be textured by an advanced MCCE (Metal Catalyzed Chemical Etching) process yielding inverted pyramids. This high efficiency texturing solution, which was limited to laboratory applications in the past is transferred into an inline-MCCE-based, mass production suitable process, which considerably increases the efficiency of the solar cells. Inverted pyramids grow into depths, to further reduce reflections considerably and ensure in the module that low angle incident light is better absorbed thus providing a higher energy yield.

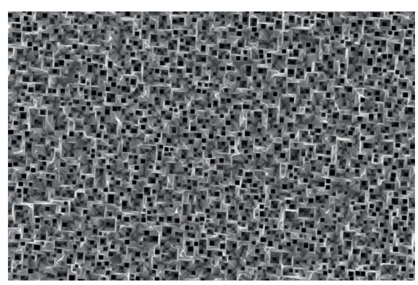

Applications: In-line wafer texturing of mono and multi wafers after diamond wire cutting.

Platform: RCT Solutions supplies the i-UniTex as a five- or 10-lane tool, which provide a throughput of up to 4,200uph and 8,400uph respectively. For finalization of the process in existing tools like b-Tex (batch for mono) or i-Tex (inline for multi), their throughput can be increased since the etch depth requirement is significantly reduced and thus less process time is needed. In case of monocrystalline wafers less additive is required, which saves costs additionally.

Availability: Currently available.

News

EU calls time on Chinese anti-dumping duties

The European Union has officially elected not to extend anti-dumping duties against panels imported from China, with the minimum import price now ceasing to exist from midnight Monday 3 September 2018.

EU DG Trade confirmed that it was in the "best interests of the EU as a whole" to let the measures lapse having considered the needs of manufacturers and the solar supply chain as a whole.

The measures, effective since December 2013, have essentially prevented Chinese manufacturers from dumping solar panels into EU member states by setting a minimum price at which the panels can be imported, protecting domestic manufacturers.

However, the measures have grown controversial and the EU elected to renew them for just 18 months in March last year as opposed to the usual five years.

This was perceived to be an exceptional circumstance and acted as a compromise between the two opposing sides of the case but, having concluded that the market situation had not changed to the extent to justify their extension, the duties will now be allowed to lapse.

Credit: Flickr/Glyn Lowe

The move will not help non-Chinese manufacturers.

REACTION AS MIP ENDS

Marc Rechter, co-founder of integrated solar energy consortium, Solar Synergy Group, said:

Expected impact of MIP ending:

- In terms of Chinese Tier 1 cross margins, with these manufacturers now able to produce for the EU from China (instead of Taiwan or Vietnam) the prices should drop by about €2 cents per Watt which should return their business to profitability;
- This would also imply that CAPEX for EU solar projects can be further reduced which will bring the projects closer to grid-parity across more geographies where developers and IPPs will benefit - but not the non-Chinese manufacturer;
- It is an important signal to the market from the EU as it heads towards an integrated and affordable energy market based on renewables

Short-term impact with respect to PV generation figures is limited.

Other items impacting the growth of solar in the EU:

- The challenges today in the EU are not so much the module prices (EU module manufacturers have mostly disappeared) but rather the regulatory framework conditions;
- Legislation and regulation with respect to solar generation are widely diverse in EU member states, which is a barrier to faster solar energy growth;
- Two further challenges typically observed in the EU include the lack of grid capacity (whether at local level or interconnection) as well as the complex and time-consuming authorisation processes.

CHINA POLICY

Chinese solar companies start posting profit warnings and revenue declines

The first wave of public listed China-based, China centric PV manufacturers reporting first half year financial results offers insight into the impact on companies after the Chinese Government capped utility-scale and distributed generation (DG) PV power plant projects at the end of May 2018.

The Chinese Government's caps on PV power plant deployments, commonly known as '531 New Deal', due to the date the National Development and Reform Commission, the Ministry of Finance and the National Energy Administration, jointly issued new policies to curtail the rapidly expanding domestic market that had led to outstanding FiT payments by the end of 2017, that had ballooned to approximately US$17.5 billion.

Adding to the challenges in the China market was the realisation of a rapid growth in deployments. Notably 2016 and 2017 had already stalled during the second quarter of 2018, before the caps were imposed in June.

The year did not start strongly, although the first quarter is seasonally the weakest quarter for PV deployments, due to winter weather and China New Year, many companies reported operating income below the levels set in first quarter of 2017.

This is in contrast to China's National Energy Administration (NEA) figures that deployments totalled 9.65GW in the first quarter of 2018, a 22% increase over the prior year period.

The official breakdown of installations included 7.68GW of (DG) solar capacity, which increased by 217%, compared to the prior year period.

In contrast, utility-scale installed capacity declined 64% to only 1.95GW in the first quarter of 2018, compared to the prior year period.

Therefore, companies more focused on the utility-scale business, suffered more than those that were focused on the DG market or had a more balanced focus with less exposure to the utility market.

Typically, there has been a strong bounce back in operating income in the second quarter, due primarily to the rush to complete utility-scale projects ahead of the FiT change at the end of June.

According to official figures from China's National Energy Administration, the utility-scale market in China reached 12.06GW of new deployments in the first half of 2018, a year-on-year decrease of 30%, while DG power generation reached 12.24GW, an increase of nearly 72% year-on-year, according to data from China's National Energy Administration.

Notably, the utility market did bounce back strongly in the second quarter with over 10GW installed, while the DG market softened to just over 4.5GW.

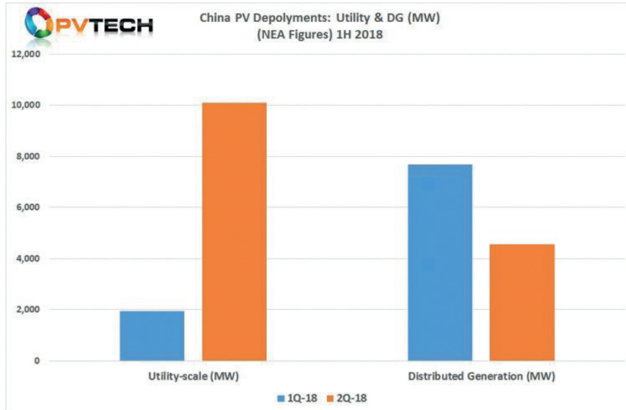

Chinese utility and distributed PV deployments in Q1 and Q2 2018.

ROTH Capital expects 34GW of solar production overcapacity after China caps growth

US-based investment firm ROTH Capital Partners expects as much as 34GW of solar production overcapacity in China in 2018 as a result of the "stark policy pivot" by the Chinese government, which imposed sector caps and feed-in tariff (FiT) mechanism reductions to drastically cap solar installation growth.

ROTH Capital highlighted the critical role China plays in the global solar supply chain, given its manufacturing dominance and lead position in PV deployments, which topped 53GW, with over half the global installed market in 2017.

With activity in the two strongest sectors, utility-scale and distributed generation (DG) markets effectively halted through 2020.

ROTH Capital highlighted: "Our initial estimates suggest we are due for a potential massive 20-30GW of annualized overcapacity in the coming months and quarters without a clear catalyst of rebalance. We expect to see a rapid deterioration in ASPs through the entire supply chain (module all the way to poly), while downstream players will benefit."

As a result, ROTH downgraded its deployment forecast for China in 2018 to 35GW, compared to its previous forecast of 52GW. This would effectively result in a net PV module manufacturing overcapacity of as much as 34GW.

The investment firm also downgraded its global installation forecast by 8GW for 2018, to 91.7GW.

In the critical solar cell manufacturing sector, which has been rapidly expanding, due to the migration to PERC (Passivated Emitter Rear Cell) technology and P-type monocrystalline wafers as part of an industry shift to higher conversion efficiency modules, ROTH expects the sector to add around 19GW of new solar cell capacity in 2018, with a significant share being added in the second half of the year.

However, such expansions could be halted, once the dust settles on the sudden change to China's policy on solar growth.

Indeed, the announcement, "2018 Solar PV Power Generation Notice" by Chinese government agencies, came a day after the largest trade exhibition ended in Shanghai. ROTH Capital echoed the fact that despite days of meetings with leading PV companies at SNEC, there was no warning of what was about to happen.

IHS Markit forecasts global solar demand to increase 11% in 2018 despite China cuts

According to market research firm IHS Markit, solar PV installations in 2018 are expected to reach 105GW, an 11% increase over the prior year when installations topped over 96GW, despite an expected decline in China, due to the sudden capping of growth by new government policies.

IHS Markit noted that its outlook for global PV installations in 2018 has fallen from 113GW to 105GW, directly due to the expected drop in installations as caps were imposed on utility-scale and distributed generation (DG) projects, the two biggest market sectors in the country.

The market research firm is forecasting installations in China will reach 38GW in 2018, down from over 53GW in 2017. Other market research firms are guiding 30GW to 35GW in China after the policy changes.

The significant impact in installations in China is expected to occur in the second half of 2018 and amount to less than half the number installed in the first half of the year, according to IHS Markit.

IHS Markit expects the whole PV supply chain will be impacted by curtailment in China, which will result in a "fiercely competitive environment in international markets, which will lead to aggressive price reductions across the board."

However, avoiding forecasting module ASP decline's such as Bloomberg New Energy Finance (BNEF), IHS Markit said: "At this early stage, the concept of an 'average' price is somewhat meaningless. The final price level will not only depend on China's recent decision, but it will also be influenced by developments around the Minimum Imported Price (MIP) in Europe and India's decisions surrounding safeguard duties and the anti-dumping investigation."

The market research firm summarized the market going forward in 2018 as being "defined by overproduction and intense competition among suppliers."

"Once these lower prices are settled, and the industry has gone through another wave of oversupply, low profitability and consolidation, solar energy will become even more competitive across new markets."

US VS CHINA

US solar safeguard and subsidies 'seriously damaged' our trade interests, China tells WTO

China has filed a complaint at the World Trade Organisation (WTO) against the US' 30% safeguard tariffs on solar imports as well as its renewable energy subsidies, claiming that they distort the global PV market – a move which comes as part of wider trade battle between the two global powers.

A spokesperson from China's Ministry of Commerce said that the tariffs are suspected of violating WTO rules and therefore undermining the WTO's authority. Furthermore, US subsidies for its own domestic PV manufacturing were giving its industry an "unfair competitive advantage and damaged the legitimate rights and interests of China's renewable energy companies".

Both the safeguard and the subsidies "have seriously damaged China's trade interests", said the spokesperson, before adding: "We urge the US to take concrete actions, respect the rules of the WTO, and abandon the wrong practices so that the relevant trade can be restored to normal track."

China's policy overhaul hugely impacted global forecasts.

Credit: Canadian Solar

The US introduced its safeguard tariffs in January this year and while China's own solar policy upheaval has already started reducing solar equipment costs and therefore undermines the impact of the US duties, several Chinese firms have already announced plans to set up module assembly factories within the US since the duty imposition.

After a US spat with India at the WTO, which led to India having to drop its Domestic Content Requirement (DCR) policy, India – like China now – complained to the WTO about the US' own subsidies for its manufacturers in eight states.

Thailand, Vietnam, Malaysia, the Philippines, Singapore, the EU, Taiwan, South Korea and China have all filed complaints about the US tariffs (but not its subsidies) already this year, with China kicking off proceedings as early as 7 February.

The US has now accepted China's requests for consultations.

A communication from the delegation of the US, posted on 28 August, stated: "We stand ready to confer with officials from your mission on a mutually convenient date for these consultations."

MAKE IN INDIA

India pondering 100GW ISTS solar tender linked with manufacturing

India is currently mulling over a plan for a 100GW solar tender to be linked with manufacturing, but with no timeframe put down as yet.

Ministry of New and Renewable Energy (MNRE) secretary Anand Kumar said that the capacity of manufacturing is yet to be decided upon.

The idea so far floated is to bid out the 100GW capacity all in one go and for the projects to be connected to the Interstate Transmission System (ISTS) in a pan-India manner. This is a vastly ambitious scheme, given that India has been incrementally working towards a huge target of 100GW of solar overall by 2022 and with many trials and tribulations on the way. Kumar did, however, hint that the power minister will soon be unveiling another enormous solar target for 2030, in which the 100GW tender could fit in.

2018 has seen India focus less on its solar park initiative and more on standalone ISTS projects for which there are multiple gigawatts of tenders already out. Unlike solar parks, these projects require the developer to acquire land, secure transmission connectivity and take on other risks. The Ministry of Power has now granted solar procurers the option of extending financial close, land acquisition and project completion timeframes to give developers more time to overcome these difficult challenges.

The announcement comes shortly after Solar Energy Corporation of India (SECI) issued a tender for 5GW of PV manufacturing in India to be linked with 10GW of solar project development, but the manufacturing component has now been reduced to 3GW, which is a worrying sign for hopes of the 100GW tender idea.

R&D spending analysis of 20 key PV manufacturers in 2017

By Mark Osborne, senior news editor, Photovoltaics International

Abstract

An analysis of R&D spending of 20 publicly listed PV module manufacturers in 2017 has been undertaken to replace *Photovoltaics International*'s previous list of 12 companies tracked over a 10-year period. A number of the original companies tracked have subsequently de-listed from stock markets and gone private, which meant that a broader analysis, including other listed companies was required to provide a good representation of global R&D spending trends in the PV wafer, cell and module segments of the upstream solar market.

Trina Solar is one of a growing number of PV manufacturers to go private, necessitating a revamp of our R&D tracking.

Selection criteria

Historically, we had tracked 12 publicly listed PV module manufacturers, which had included First Solar, the only thin-film module manufacturer amongst the group, and 11 crystalline silicon module manufacturers: Canadian Solar, Hanwha Q CELLS, JA Solar, JinkoSolar, REC, ReneSola, SolarWorld, SunPower, Suntech, Trina Solar and Yingli Green.

In the 2016 R&D spending report we highlighted that due to a number of these companies withdrawing from stock markets, verifiable data from publicly available annual financial reports was in decline. This trend escalated in 2017, with the result that we could no longer track four companies (REC, Trina Solar, ReneSola and SolarWorld) from the original group of 12.

In the evaluation process of replacing those four module manufacturers it was apparent from long-term broader analysis of R&D spending that a number of emerging major manufacturers had moved into solar cell and module manufacturing in recent years. Notabe among these are GCL Group and LONGi Group, which were historically from the upstream polysilicon and wafer sectors.

Being the largest wafer producers, with GCL-Poly dominant in multicrystalline wafer production and LONGi the dominant monocrystalline wafer producer, the emergence of these companies provided the opportunity to

Credit: Trina Solar

broaden the R&D expenditure analysis beyond the original scope of the last 10 years.

Indeed, the likes of JinkoSolar and JA Solar have historically had meaningful wafer capacity in-house. Both have been aggressively adding new monocrystalline wafer capacity in-line with in-house module assembly capacity expansions. This has always meant that R&D spending within these companies included expenditure on wafer-related technology.

With other upstream manufacturers, such as module encapsulant material specialist Jolywood, moving into cell and module manufacturing and the chance to include some of leading Taiwanese cell producers, such as Motech, NSP and Gintech, which have all had module manufacturing operations, we had the opportunity to analyse R&D spending trends from a larger pool of companies and a larger part of the upstream manufacturing sectors.

As a result, the 2017 R&D spending analysis includes the following 20 PV manufacturers: Canadian Solar, Eging Photovoltaic, First Solar, GCL-Group, Gintech, Hanergy Thin Film, Hanwha Q CELLS, Hareon Solar, JA Solar, JinkoSolar, Jolywood, LONGi Group, Motech Industries, Neo Solar Power, Risen Energy, Solartech Energy, SunPower Corp, Tongwei Group, Wuxi Suntech and Yingli Green.

Analysis criteria

Although we have historically analysed R&D spending of primarily module manufacturers, this and subsequent reports analyse total R&D spending, which in the case of GCL includes GCL-Poly (polysilicon and multi c-Si wafer) and GCL System Integrated (cell and module), combined.

In the case of LONGi, R&D spending is across mono c-Si wafer and subsidiary, LONGi Solar (cell and module), combined. The spending analysis of Tongwei includes polysilicon, cells and modules.

Although all companies in the new selection produce modules at varying capacities, the cases of Neo Solar Power, Motech, Gintech and Solartech have historically been concentrated on merchant cell production.

Therefore, we no longer rank companies specifically from a module R&D spend perspective. Instead, this and subsequent reports will look more holistically at R&D spending trends from the broader upstream supply chain of selected publicly listed companies.

It is also important to note that we have retained historical R&D spending data from the PV module companies that were previously tracked and remain publicly listed but all new additions are tracked from 2012 onwards.

However, in the case of Tongwei the data is compiled from 2014 as it was a new entrant into the PV industry in that year. In the case of Jolywood, data available starts in 2013, as the company became publicly listed in 2014.

Historical R&D spending trends from 2007 to 2016

In retaining historical data that tracked 12 module manufacturers from 2007 through to 2016, combined with data from the expanded list of PV manufacturers, primarily from 2012 through to 2016, (Figure 1) shows a sharp increase in R&D spending in 2014, compared to the two previous years. This increase coincided with a recovery

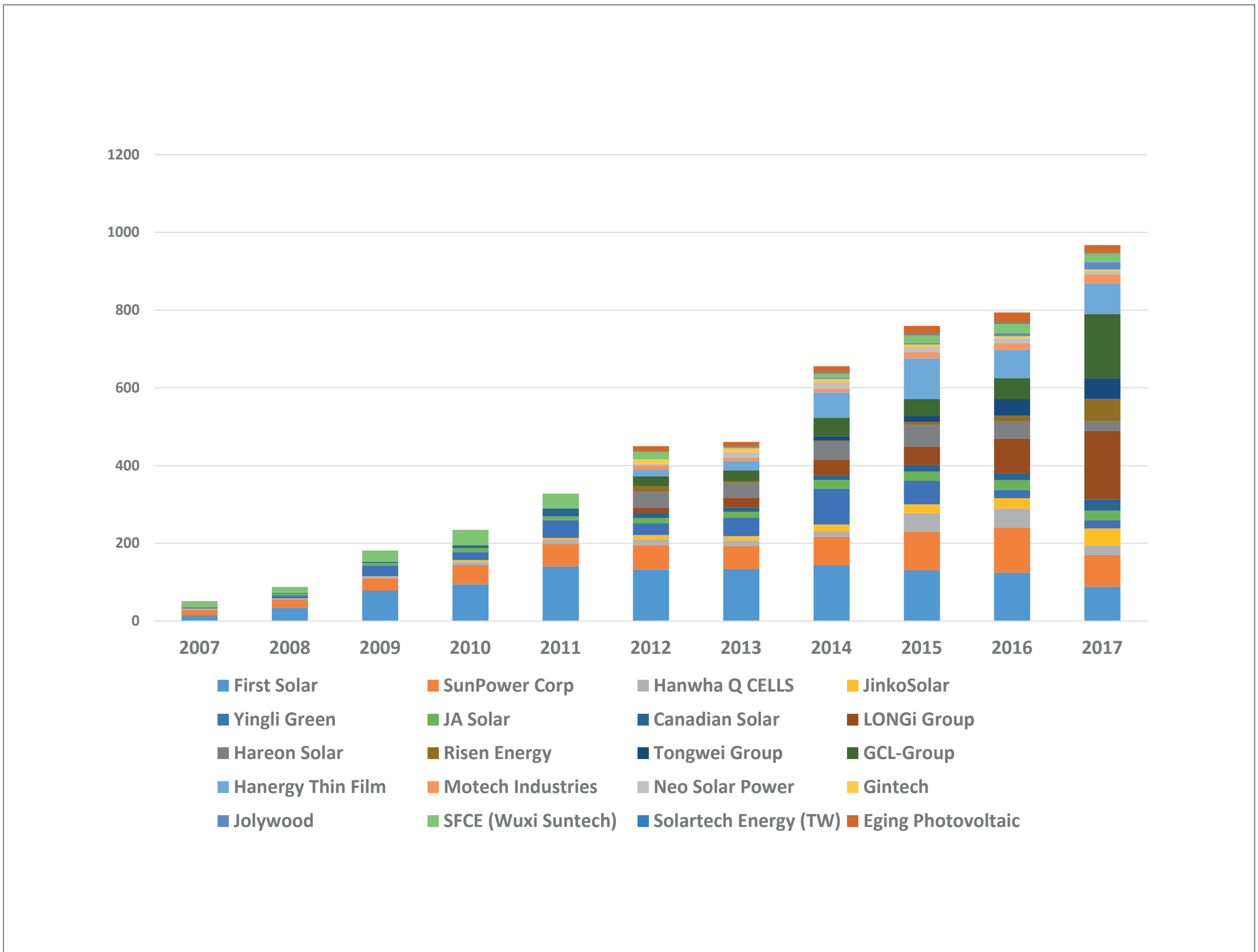

Figure 1. PV manufacturers (publicly listed) annual R&D expenditure, US$ millions 2007 to 2016.

in the PV industry, after several years of extreme overcapacity throughout the supply chain and was a new record at the time.

Cumulative annual R&D spending reached US$880.41 million in 2015, up from US$781.5 million in 2014, up around 12.5%, or almost US$100 million from the previous year.

However, a trend not seen before 2012, which accounted for strong sequential R&D expenditure growth has remained ever since, which has been selective company R&D spending behaviour.

This manifested itself in 2012, when seven companies reduced R&D spending, whilst the others expanded spending. In 2013, the number reducing spending increased to 10 and only three of these (Eging, Suntech and Trina Solar) continued to lower spending in two consecutive years.

In 2014, a total of only three companies (Gintech, Hanwha Q CELLS and Risen) actually lowered R&D spending, reflecting the overall global solar market recovery. Gintech was the only company to lower spending in two consecutive years.

By 2016, the number of companies reducing spending had increased back to seven. This may have been a key factor in cumulative R&D spending only increasing by about 3% that year, which reached US$907.46 million, another new record.

R&D spending trends in 2017

In 2017, with four companies (REC, Trina Solar, ReneSola and SolarWorld) no-longer tracked, due to stock market de-listings, it would be understandable that further R&D spending growth could be problematic.

However, R&D spending hit a new record of US$967.28 million in 2017, an increase of around 6.6%, year-on-year, more than double the relative small increase seen in 2016.

Interestingly, spending growth would seem to have been hampered by a total of 10 companies reducing R&D spending in 2017, compared with the previous year, a new record number.

In the 2017 analysis, Gintech had reduced R&D spending in five consecutive years, First Solar had reduced spending in three consecutive years, while only Hareon Solar had reduced spending in two consecutive years.

Four companies (SunPower, Hanhwa Q CELLS, Eging and JA Solar) had lowered spending in 2017, compared to 2016, when spending had reached record levels.

SunPower had only lowered annual R&D spending once before, in 2013, while in the case of JA Solar, 2017 was the first year its annual spending had declined.

In total, nine companies increase R&D spending

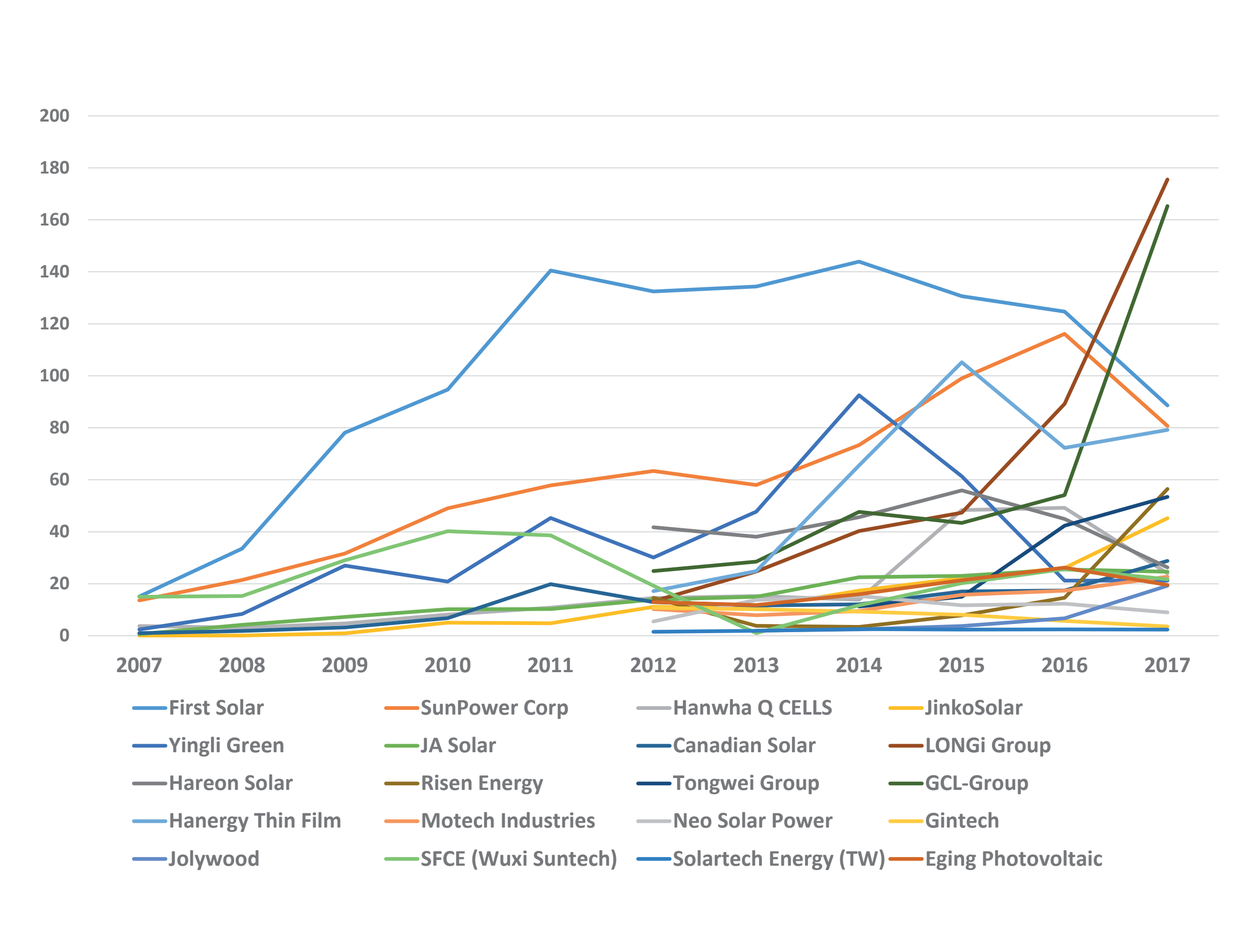

Figure 2. PV manufacturers (publicly listed) annual R&D expenditure, US$ millions, 2007 to 2017, flow chart.

year-on-year, while one (Yingli Green) spent exactly the same amount (US$21.2 million) as it did in the previous year. The first company to achieve that feat.

Spending pattern divergence

With the loss of the four companies previously tracked, coupled to an equal split of covered companies either reducing or increasing spending, year-on-year, there has been a marked divergence in spending behaviour, notably since the overall global solar market reached another year of record installations that almost reached the 100GW milestone.

Part of the divergence could be attributed to several of the 10 companies (First Solar, SunPower, Hanwha Q CELLS and Eging) that lowered spending in 2017, were near completing various significant R&D programmes that had led to peaks in annual spending in recent years.

Also contributing to the decline has been the financial condition of some of the companies, such as Hareon Solar, which drastically cut spending from a peak of US$55.9 million in 2015 to US$26.28 million in 2017. The company lost approximately US$707 million in 2017 and had been loss making for at least six years. The company is technically bankrupt in 2018.

This may also be a contributing factor in SunPower reducing spending as the company reported a GAAP net loss of US$851 million in 2017, its fifth consecutive year of losses.

In the case of First Solar, which is shifting production from its small form factor Series 4 modules to the large-area Series 6 modules and building three new plants, restricting overall spending could have been a factor in R&D spending declining to US$88.6 million in 2017, compared to US$124.7 million in 2016.

In contrast, a number of the nine companies in 2017 that increased spending (GCL, LONGi, JinkoSolar, Canadian Solar, Risen and Jolywood) did so at significantly higher levels than in the previous year. All of these companies had major R&D programmes in full swing in 2017, not least GCL and LONGi across materials, wafers, cells and modules.

High rollers

In the case of LONGi, R&D spending increased from US$89.23 million in 2016, to US$175.5 million in 2017, a year-on-year increase of 96.67% from US$89.2 million in 2016.

LONGi set a new solar industry record, not only by surpassing the two historical R&D spending leaders (First Solar and SunPower) but also

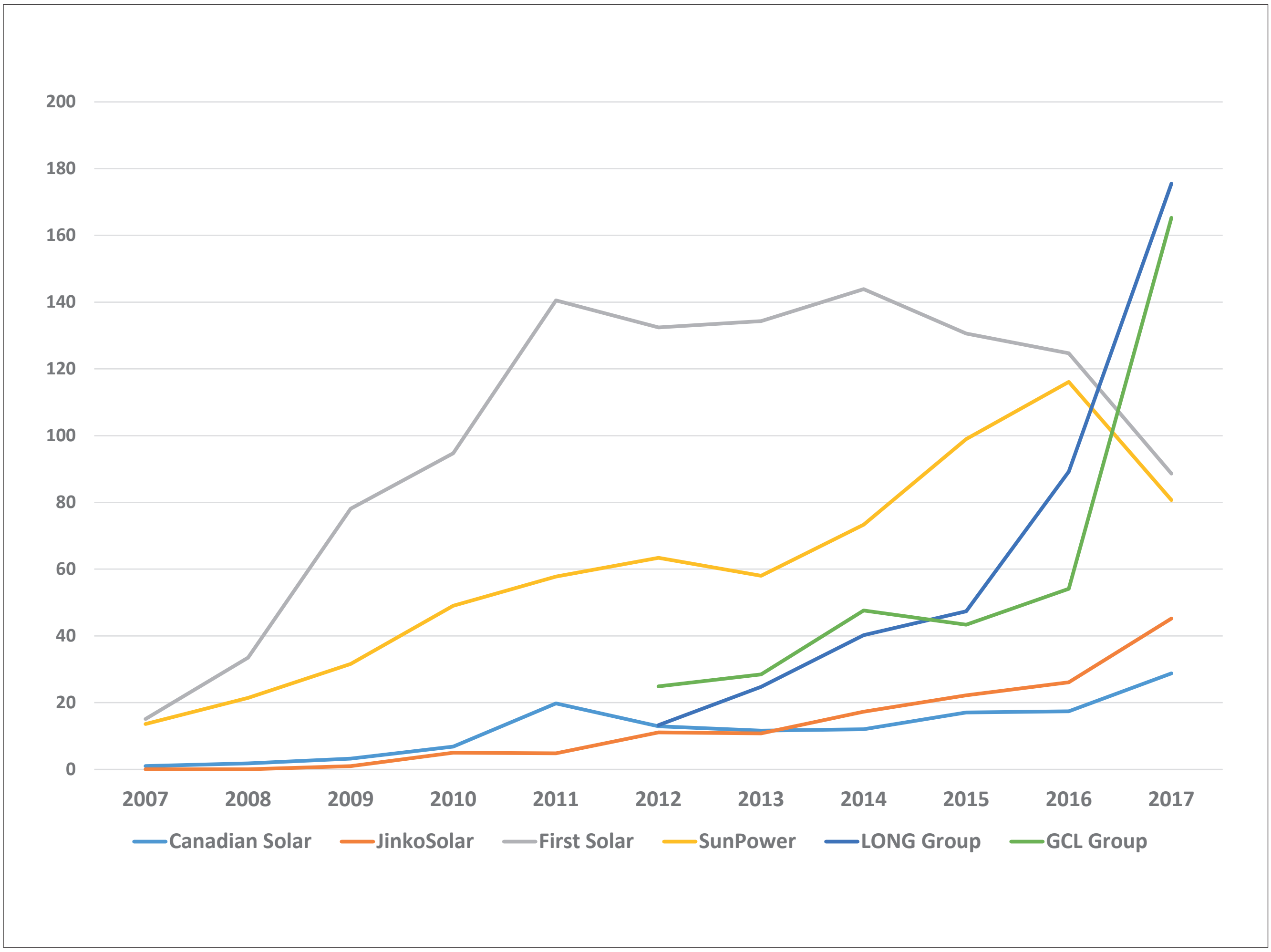

Figure 3. Annual R&D expenditure: historial leaders and laggards, (US$ millions.

spending more in one year than any other PV manufacturer to date.

LONGi reported total revenue of US$2.59 billion in 2017, up almost 42% from the previous year, with R&D spending accounting for 6.77% of revenue.

Only SunPower has come close to that ratio when in 2015, R&D spending accounted for 6% of revenue and First Solar's R&D spending ratio to revenue topped 5.1% in 2011.

LONGi has increased R&D spending for six years in row and has maintained a high-level of R&D investment over the last four years.

LONGi has been the largest monocrystalline wafer producer but notably since 2015, the company started production of monocrystalline solar cells and modules. Focused on high-efficiency PERC (Passivated Emitter Rear Cell) technology, R&D spending almost doubled each year since 2016.

Leading polysilicon and solar wafer producer GCL-Poly Energy Holdings, part of the GCL Group had also reported a massive increase in R&D spending in 2017.

The company developed new mono-silicon crystal growth techniques and FBR (Fluidized Bed Reactor) technology as well as advances in diamond wire saw cutting and 'Black Silicon' wafer texturing for multicrystalline wafers.

GCL-Poly's R&D expenditure increased from US$39.1 million in 2016 to US$151.22 million in 2017, an increase of 288%. When R&D spending is combined with GCL-SI (cell and module manufacturer and downstream project developer, GCL New Energy), total spending reached US$165.27 million in 2017. GCL group revenue topped US$6.66 billion in 2017.

Major China-based PV module and materials manufacturer Risen Energy, which entered PV Tech's Top 10 module manufacturer rankings (by module shipments) for the first time in 2017, increased R&D spending from US$14.6 million in 2016 to US$56.54 million in 2017, an increase of around 280%, compared to the previous year. The company had reported revenue of US$1.56 billion in 2017, a 63.21% increase from the prior year and new record for the company.

In 2017 the company launched a number of R&D programmes related to mono PERC high-efficiency solar cells as well as N-type mono bifacial solar cell manufacturing processes and multi-busbar technologies as part of a CTM (Cell to Module) loss reduction strategy, amongst other programmes to boost conversion efficiencies.

Risen also initiated R&D programmes related to

EVA module films, such as a 'super' anti-PID EVA film and work on enhanced POE-based backsheet film and production process as well as flexible cell lamination technology research.

Also of note in ramping R&D spending was two 'Silicon Module Super League' (SMSL) members, JinkoSolar and Canadian Solar, known historically for low-spending on R&D.

As the leading (by shipments) module manufacturer, JinkoSolar increased R&D spending to US$45.2 million in 2017, up from US$26.1 million in 2016, an increase of around 73%, year-on-year.

R&D activities had spanned thinner wafers, longer carrier lifetime of wafers, through to improved passivated emitter and rear cell processes and improved dielectric rear reflectors and interconnects.

The company recently reset the P-type monocrystalline cell conversion efficiency record at 23.95%, through a range of wafer to cell optimisation, notably its selective emitter (SE) formation.

JinkoSolar had said that a combination of enhancements and optimisation, which included highly doped and low defect mono wafers, which improves the bulk quality, coupled to further optimization of SE formation as well as silicon oxide passivation and the rear side passivation had added to conversion efficiency gains. JinkoSolar also used its proprietary light-capturing technology, which employs black silicon and multi-layer ARC (Anti-Reflective Coating) technology that reduces the front side reflectivity of cells, said to be lower than 0.5%, boosting the short-circuit current.

Additionally, JinkoSolar said it deployed an advanced grid design and a new type of screen-printing paste to reduce the series resistance and the metal/silicon interface compound, enabling improved cell fill factor (FF).

SMSL member Canadian Solar took R&D spending from US$17.4 million in 2016 to US$28.77 million in 2017, increasing by almost 69%, year-on-year. However, R&D development expenses as a percentage of total revenues were 0.6% in 2016 and 0.8% for 2017.

The company has focused R&D activities on n-type bifacial cells, PASSCon cells, heterojunction cells as well as IBC cells and other high efficiency cell designs in 2017.

The SMSL also finished commercializing its in-house developed 'black silicon' technology on multicrystalline wafers in 2017, which led to all cell capacity converted to using the technology by the end of the year. Improving PERC (passivated emitter and rear cell) technology for multi-c-Si cells is also an ongoing project.

Although the total spending figure is relatively

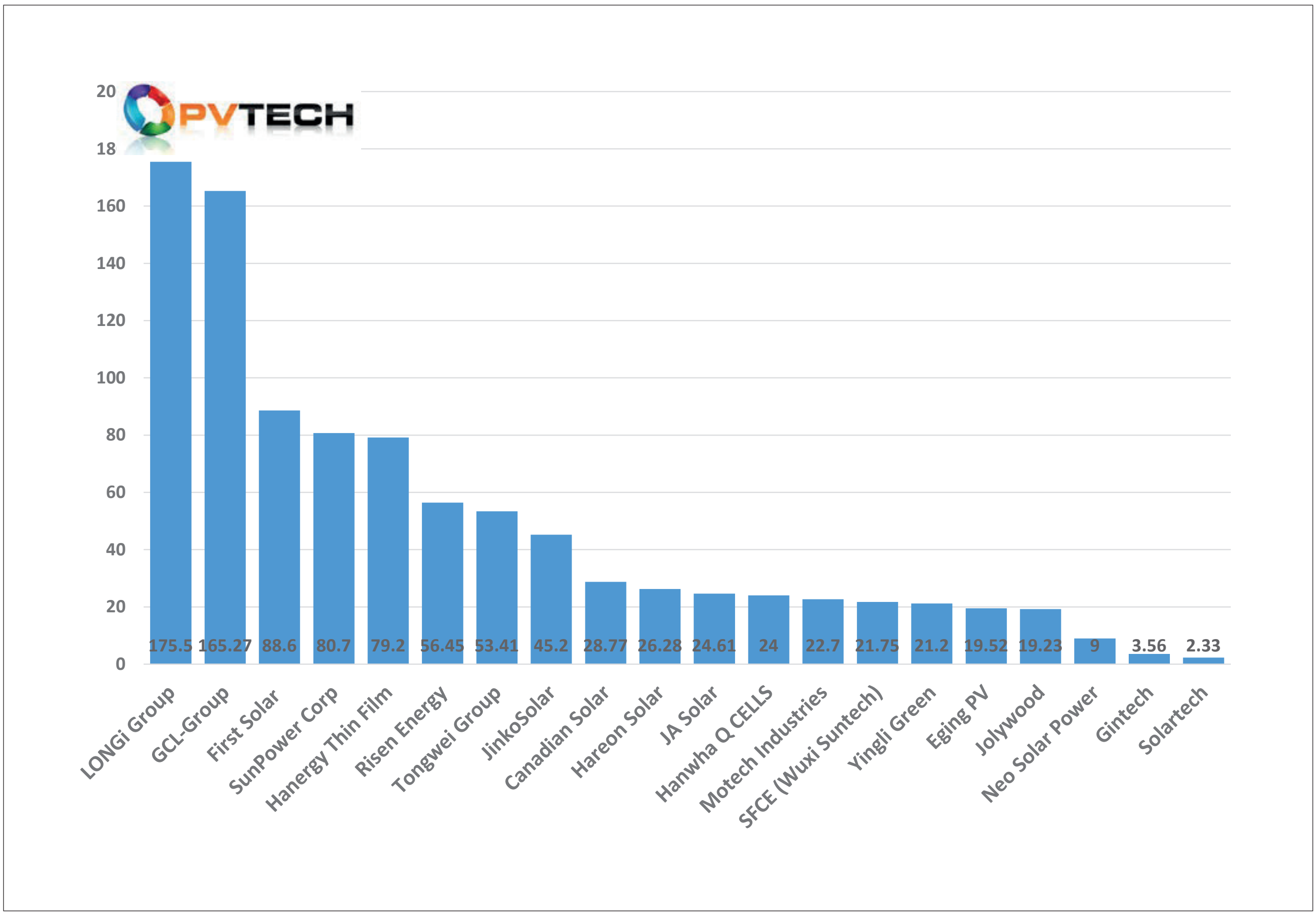

Figure 4. Annual R&D expenditure: 20-company sample ranked (publicly listed) in 2017, US$ millions.

low, Jolywood increased R&D spending from US$6.67 million in 2016 to US$19.23 million in 2017, around a 185% increase over the prior year and accounting for 3.47% of annual revenue.

On the materials front, Jolywood included inorganic Nano UV-resistant self-cleaning coating technology, micro-foam technology, and high water vapour barrier technology as key research and development projects in 2017.

In solar cells, Jolywood was active with N-PERT monocrystalline bifacial solar cell development, and continues to develop N-type mono bifacial TOPCon solar cells as well as N-type mono bifacial IBC solar cells in advance of mass production.

Spending clusters

The highest R&D senders in 2017 were LONGi and GCL, respectively. Both have significantly increased spending since 2015 and both spent in excess of US$160 million each in 2017.

Only two other companies had R&D spending over US$80 million each in 2017, First Solar and SunPower, respectively. Although thin-film firm Hanergy came close to that level at US$79.2 million.

Two companies are clustered in the US$50 million plus range (Risen and Tongwei), while JinkoSolar stands alone in spending in the mid-US$40 million range. There are no companies in the US$30 million spending range in 2017.

The largest cluster of seven companies is led by Canadian Solar, which spent US$28.77 million in 2017 and is held-up by Yingli Green at US$21.2 million.

Eging and Jolywood just skirt the US$20 million range at US$19.42 million and US$19.23 million, respectively.

The sub-US$10 million per annum spenders are Taiwan-based Neo Solar Power, Gintech and Solartech.

Conclusion

The year under review resulted in another record for solar industry R&D spending (selected 20 companies), despite the forced removal of four companies from historical analysis undertaken since 2007.

New record levels of absolute spending on a company basis were achieved as well as some on a year-on-year percentage basis.

However, a growing number of companies reduced R&D spending in 2017, only negated by a select number increasing spending, significantly.

Overall, the trends in R&D spending remain fluid as they can be positively impacted by the continued pace of new technology adoption as well as being impacted negatively by individual companies technology development cycles and financial condition. As seen in the 2012/13 period, industry overcapacity can stifle spending growth but the growth trajectory has remained consistent with global market installation growth.

News

India reduces 5GW solar manufacturing tender to 3GW

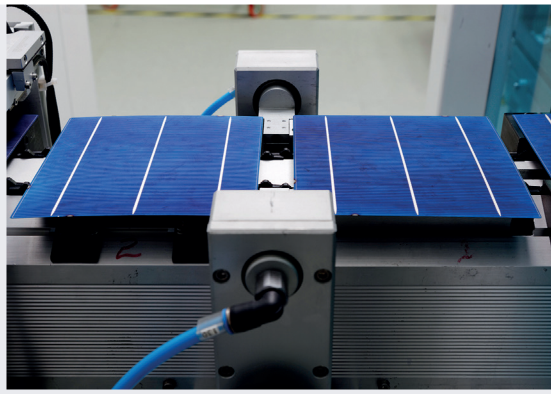
Credit: Tata Solar Power

Only a handful of companies were found to have the resources for both the scale of manufacturing and deployment involved in the tender.

The Solar Energy Corporation of India (SECI) has reduced the manufacturing component of its 5GW solar manufacturing / 10GW of solar deployment tender to just 3GW.

Media reports had cited officials suggesting that the manufacturing capacity could be reduced several weeks ago, but SECI has now confirmed the reduction and changed the title of its tender.

The original tender drew much interest at the EOI stage but after a pre-bid meeting, it became clear that interested parties wanted the manufacturing component reduced to make the prospect more viable and attractive. Indeed, consultancy firm Bridge to India had calculated that just four firms were capable of the capital outlay necessary for such a huge investment.

Analysts have also said that the 10GW of solar capacity would have been tendered in any case. The manufacturing addition was simply the latest attempt by the government to start cultivating a domestic PV manufacturing boom, ahead of its imposition of a safeguard duty on imports from China, Malaysia and developed countries, which is temporarily on hold.

Elsewhere, the Maharashtra State Power Generation Company (Mahagenco) invited expressions of interest (EOI) for setting up a solar manufacturing plant in the Indian state, using any type of cells and modules.

The integrated factory will be located on land provided by Mahagenco. The company wants the facility to provide solar equipment for at least 50-60% of its 2,500MW solar requirement.

The prospective manufacturers will be allowed to form joint ventures or consortiums with Mahagenco. Existing manufacturers of solar cells and modules, who intend to set up integrated facilities and are planning to expand their capacity, will also be eligible to bid under this scheme.

Mahagenco will shortlist bidders for the project based on technical and financial feasibility, the bidder's technical and financial capability, and the bidders' offered percentage in the project to Mahagenco.

The deadline for EOI submissions is 29 September this year.

EMERGING MANUFACTURING CENTRES

GCL Group adds Egypt to expanding manufacturing footprint plans

The largest solar PV manufacturer in the world, GCL Group, had its plans for a major 5GW manufacturing hub in Egypt approved by the National Authority for Military Production.

GCL Group, which includes publically listed subsidiaries such as leading polysilicon and multicrystalline wafer producer GCL-Poly Energy Holdings and 'Silicon Module Super League' (SMSL) member GCL System Integrated Technology Co and downstream project developer GCL New Energy Holdings, had combined annual revenue of over US$6.6 billion in 2017.

Reports in May 2018 had highlighted an MOU signed between the Egyptian ministry and GCL Group, highlighting plans for a 5GW module assembly plant at a cost of US$2 billion.

The level of investment would indicate GCL planned to build an integrated manufacturing hub that would include ingot/wafer, cell and module production. Details of the plans remain limited.

However, the news that the Chinese government is implementing major caps on the growth of PV deployments in the country indicates that major PV companies such as GCL and rival LONGi Green Energy have already determined that overseas growth would be required to meet ambitious goals over the coming years.

LONGi Group and GCL Group are expanding production into India, while GCL Group has previously touted the possibility to expand into Saudi Arabia.

LONGi already has cell and module production in Malaysia and GCL has the same in Vietnam.

Waaree launches 1GW 'fully automated' module assembly plant in Gujarat

Indian PV manufacturer Waaree has started commercial production at a 1GW solar module assembly factory in the state of Gujarat, with several large tenders soon coming to fruition expected to counter the lull in activity brought about by a lack of tenders in H2 2017, according to a company official.

Speaking to PV Tech at Intersolar Europe 2018 in Munich, Sunil Rathi, Waaree's director of sales and marketing, said the company is maintaining its targets of supplying 60-65% of its modules to the domestic market and 35-40% for export. Waaree assembles multi-crystalline, monocrystalline, and mono PERC modules among other technologies. Through its partnership with US-based firm Merlin, it also has 20MW of flexi module capacity.

Waaree already has a 500MW facility in Surat in Gujarat, inside a special economic zone (SEZ). The new facility is located on the border of Maharashtra outside the SEZ.

When asked if there has been any clarification on whether solar manufacturing plants in SEZs will be subjected to anti-dumping or safeguard duties, should they be brought in, Rathi, said: "A lot of uncertainty is there. Nothing is clear so far. That is not the reason why we shifted [location], but that can be advantage to us. If duty comes then it will be easy for us."

Waaree will be watching the market closely and plans to ramp up the facility to 1.5GW "very soon" if the conditions are favourable. For example, Rathi suggested that if a duty on imports is brought in, the 1GW capacity simply won't be enough to meet demand.

The fully automated plant will help to increase productivity and the facility is expected to generate around 350 jobs, said Rathi.

When asked about the impact of China's recent major solar cuts, Rathi said ASPs have started to decline, but he expects this to be a short-term trend with prices to stabilise again in 3-6 months' time, but added: "Currently there is a lot of distress happening."

Finally, Rathi said that India has begun to see significant demand for monocrystalline modules as the technology has started to become competitive with multi in the last year.

CHINESE ADVANCES

Trina bags US$30 million financing for Vietnam solar fab operations

Trina Solar (Vietnam) Science & Technology, part of China-based Silicon Module Super League (SMSL) member Trina Solar, has secured a US$30 million credit facility with one of Vietnam's four largest commercial banks, VietinBank.

The credit will be primarily used to fund and finance the production and operation of Trina Solar's PV manufacturing plant in Bac Giang, Vietnam, which went into operation at Van Trung Industrial Park in early 2017. It has 800MW of module assembly capacity and 1GW of cell capacity.

VietinBank head office deputy general manager and executive director Tran Minh Binh said: "We have witnessed Trina Solar plant's entire development journey from starting construction to going into mass production in Bac Giang. We at both the head office and the Bac Giang branch are confident in the partnership with Trina Solar, which is renowned for its operational efficiency and brand excellence. With the favourable new energy policies enacted by Vietnamese government, we have reasons to believe that Trina Solar will be a great success in Vietnam."

Tongwei to start heterojunction pilot production with migration to Industry 4.0 manufacturing

China-based integrated polysilicon and merchant cell manufacturer Tongwei Group expects to begin pilot production of heterojunction (HJ) solar cells by the end of 2018, while the success of its 200MW Industry 4.0 fully-automated solar cell production line will lead to a longer-term migration of all cell production to intelligent manufacturing.

Tongwei said that ongoing R&D activities as part of an advanced collaboration effort on next-generation HJ solar cells would lead to pilot volume production evaluations by the end of 2018.

The company said that many PV manufacturers considered HJ cell technology to be the most promising next-generation high-efficiency cell.

HJ cell production requires higher cleanroom contamination requirements and automated handling and processing, in-line with Industry 4.0 objectives. Contamination of a HJ cell before the deposition of the a-Si layer, degrades the conversion efficiency of the cell.

US CAPACITY

LG Electronics establishing a 500MW solar module manufacturing plant in US

LG Electronics will establish a 500MW solar module manufacturing plant in Alabama, US at a cost of around US$28 million.

LG Electronics is establishing solar module assembly facilities in the US as a result of the imposition of the Section 201 tariffs.

LG Electronics USA said that the facility would be co-located at an existing complex in Huntsville-Madison County, Alabama. LG has had operations in Huntsville in 1981 and became the home of LG's service division in 1987.

The company said that PV module production was expected to start at the beginning of 2019, producing its high-efficiency 'NeON' 2 series 60-cell N-type mono modules with 340Wp-plus output, primarily for the US residential rooftop market.

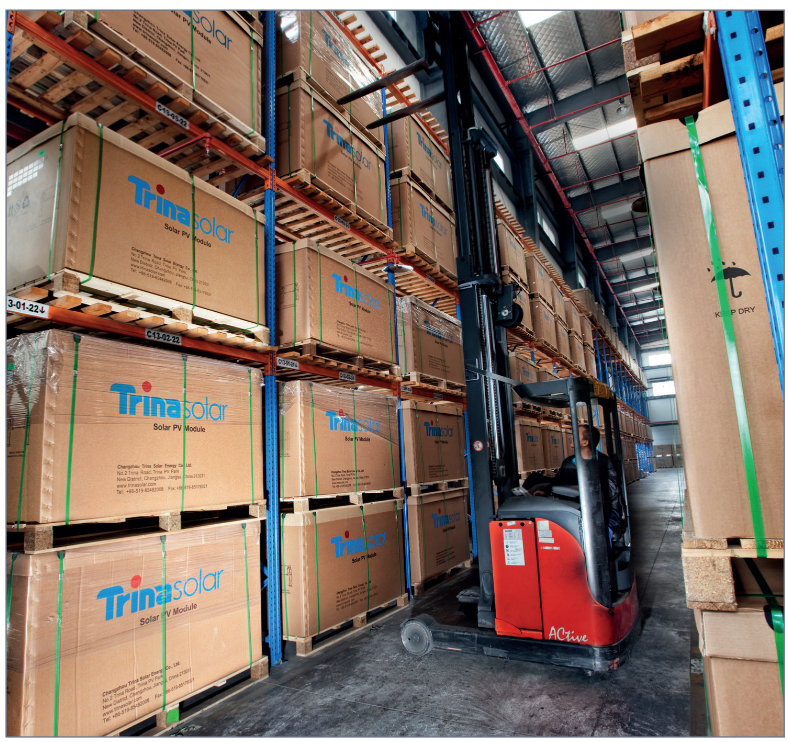

The funds will be used to back Trina's manufacturing operations in Vietnam.

Credit: Trina Solar

Credit: Hanwha Q CELLS

Hanwha Q CELLS will have 1.6GW of module assembly in place by February 2019.

Suniva plans partnership to restart manufacturing operations

US-based PV manufacturer Suniva has been released from bankruptcy proceedings and plans to restart manufacturing operations again with a partner, according to SQN Capital Management.

SQN Capital Management was a shareholder in Suniva since its start-up days and after its majority sale to China-based Shunfeng International Clean Energy in 2015.

SQN Capital said that it was "on the verge of determining which partner will provide the best path to revitalizing the company and meeting the overwhelming demand for Suniva's high-quality, high-efficiency products".

It also led the Suniva US Section 201 petition that ended with US President, Donald Trump imposing new import duties on not only Chinese PV manufacturer's imported solar cells and modules but effectively every country with the capability to import solar products into the US.

Jeremiah Silkowski, CEO of SQN Capital Management, commented: "It has been a long year but a fight worth fighting. We are pleased now to have multiple attractive options as we look toward [to] Suniva's future."

SQN Capital also noted that it had acquired Suniva's technology, licenses, and manufacturing capacity.

JinkoSolar and Hanwha Q CELLS update US manufacturing plans

'Silicon Module Super League' (SMSL) members JinkoSolar and Hanwha Q CELLS have both updated plans to start solar module assembly manufacturing in the US, post the US Section 201 trade case. Jinko said in its latest earnings call that shipments from the plant would begin in the fourth quarter of 2018. Back in March, the company stated that it would begin operations in October. This keeps in-line with JinkoSolar's key US customer for the Florida-made modules, NextEra Energy, which amended a previously unannounced supply deal with JinkoSolar that increased the deal to 2,750MW over a four year period starting in 2019. Hanwha Q CELLS said in its earnings call that Hanwha Q CELLS (Korea) would begin operations at its 1.6GW-plus module assembly plant in Whitfield County, Georgia in February 2019.

SERAPHIM

Seraphim establishes fully automated 300MW solar module assembly plant in South Africa

China-based PV module manufacturer Jiangsu Seraphim Solar System Co said it was in trial production at a new fully-automated 300MW Joint Venture (JV) solar module assembly plant in Eastern Cape, South Africa.

The 300MW module assembly plant in in East London IDZ, Eastern Cape was said to be a joint venture between Seraphim, ILB Helios Southern Africa and Industrial Development Corporation of South Africa, costing US$14 million.

"This isn't Seraphim's first overseas facility, but it signifies a critical milestone. Our South African initiative is symbolic of our commitment to global customers seeking reliable Tier-1 capacity to support their project pipeline," said Polaris Li, General Manager of Seraphim.

ILB Helios is a Spanish PV module manufacturer that has been active in the Southern African PV market since 2014, said to be supplying locally manufactured PV modules to the South African market.

TUV SUD certifies Seraphim Solar's module testing facility

Jiangsu Seraphim Solar System Co was accredited with a TUV SUD, IEC CTF (Customer Testing Facilities Certificate), which reduces time to market of new materials and modules under development.

Seraphim said that the IEC CTF was only the third such accreditation given globally by TUV SUD. As a result, Seraphim will be listed on the official website of the IEC, and its testing results can be directly used in 'Certification Body' ("CB") reports issued by TUV SUD.

To complete CTF qualification, an organization is required to meet strict regulations on personnel structure, environmental facilities, document control and sample management, amongst other practices.

Polaris Li, general manager of Seraphim said: "It's a great honour to be the third IEC-qualified CTF lab. It's the fifth world-class lab certification we've received after CSA, CNAS, CTC and TUV. Seraphim understands that innovation is a vital driver, so we devote ourselves to finding the best path forward. The CTF lab qualification further acknowledges Seraphim's strength in quality control and testing. In the meantime, the certifications offer immediate benefits to our customers."

Transition to Industry 4.0: Opportunities and challenges for the PV sector

Eszter Voroshazi[1], Kris Van de Voorde[1] & Jef Poortmans[1,2]
[1]imec, Leuven, Belgium; [2]imec/EnergyVille, Genk, Belgium

Abstract

After defining the term *Industry 4.0* according to the authors' interpretation, this paper elaborates on the opportunities and challenges that the Industry 4.0 transition will bring to the PV sector. The topic is approached from various angles. How can the PV industry and the related value chain itself progress to Industry 4.0? And how does this reflect in different application sectors, such as construction and automotive? This paper presents a future scenario towards which the industry could be heading; some of the steps already being taken and some of the main challenges ahead are described. The value of PV technology as an enabler for other sectors, such as edge versus cloud computing, to move into Industry 4.0 is also touched upon. Additionally, a number of enablers and boundary conditions are highlighted in the context of Industry 4.0 and their relevance to the PV industry (legislation, cyber security, etc.) The status of Industry 4.0 in PV compared with other sectors is also explored. Wherever appropriate and possible, examples of projects and activities that illustrate the described topics are given.

What is Industry 4.0?

Industry 4.0 is a term initially coined in Germany in 2011 [1]. Since then, it has become a bit of a catch-all for everything that has to do with advanced industrial digitization and process automation. In this paper, Industry 4.0 is interpreted as the transfer at a point in time of (significant quantities of) data, generated manually or automatically, between stakeholders across the production value chain in an automated and dynamic way. This means that relevant parameters are being monitored and exchanged from the design stage to the installation stage. Moreover, as soon as something changes, the data are automatically updated, and (artificial intelligence – AI) algorithms consider all the interlinked processes and consequences as well.

To illustrate the above concept as a hypothetical and oversimplified scenario for the PV sector, consider an architect designing a building requiring a specific set of building-integrated PV (BIPV) modules in terms of size and energy capacity. All relevant information is stored in a digital file, which is the central frame of reference for everyone downstream of the production and installation chains. Imagine that, during construction, the architect observes a deviation from the building plans, requiring adjustments to the BIPV modules. By simply entering this new information in the digital file, the BIPV manufacturer and its suppliers receive an automatic update of the new specifications. Or, vice versa, if in-line tests during PV production show a deviation from the electrical parameters, the architect gets an automatic alert, along with a suggestion from an AI application on how to compensate for this in the building information management (BIM). Possible suggestions could be to request a new production run, or to make adjustments elsewhere in the building design.

As will be discussed throughout this paper, Industry 4.0 is a multifaceted topic (Fig. 1). The scenario above is therefore merely used to underline the fact that the strategy goes beyond on-site automation. Furthermore, Industry 4.0 is more of a transition than an actual state or end goal: in an evolutionary way, the PV sector – as in the case of all the other sectors – will gradually move to Industry 4.0. It makes little or no sense to try to define whether 'you are already there'. For us, there are two important indicators for the value and maturity of Industry 4.0 in any given sector: first, the observation that it generates new revenue models; and, second (which is strongly linked to the first index), the changes seen in the value chain – mergers, new players entering or existing ones becoming obsolete, etc.

The PV sector's own transition to Industry 4.0

The success of today's PV industry is based on scaling up manufacturing capacity and on maximal standardization of current PV products to ensure maximal cost reduction of PV products for the PV power plant sector. This is a challenge in which the Asian players have demonstrated superior performance. The challenge in relation to the manufacturing of PV products for new markets such as BIPV is fundamentally different and requires a close link with local market players and customers. This opens up a real opportunity for new players in Europe, where extensive renovation of the existing building stock in an urban context will be necessary in order to achieve the goals set by the European Directive on near-zero-energy buildings (NZEB) [2] and local energy communities. In addition, the current practice of constructing near-zero-energy houses will be insufficient to reach the CO_2-

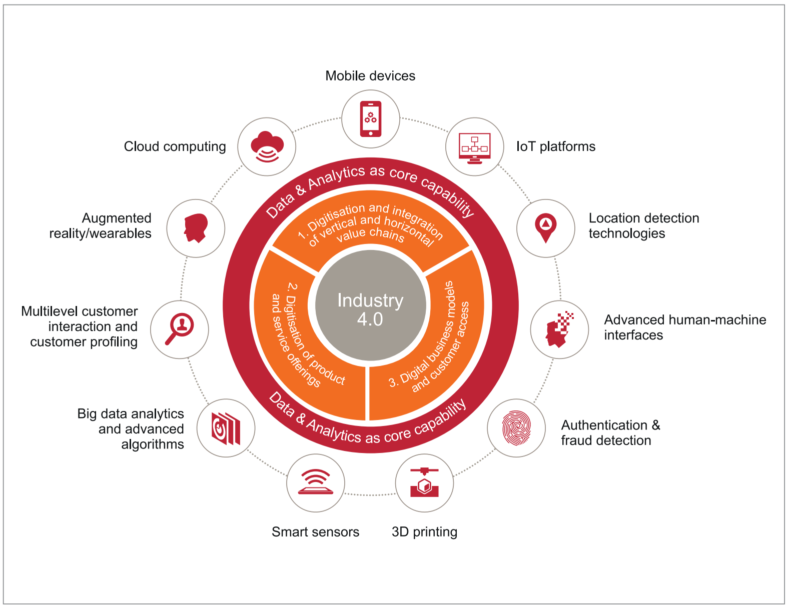

Figure 1. Industry 4.0 in all its facets, according to the 'Industry 4.0: hype or reality?' study by PWC and FlandersMake (©PWC).

emission-reduction targets for 2050. The authors see a need for further developing the concept of 'plus-energy houses', which produce more energy than they use. Buildings have relatively long life cycles before they need to be replaced, so it will be essential to speed up the development of the required technologies.

For ease of argument, the initial discussion of the transition of the PV sector to Industry 4.0 will focus on building applications, since this a rapidly growing market, specifically in the EU [3]; other application sectors will be explored in a later section. The scenarios described here will be built around crystalline PV, accounting for 95% of the global PV market [4].

In addition, module manufacturers will be given a central role in the build-up of this paper; they will assume a central role, in the authors' opinion, in the transition to Industry 4.0. Cell production is already largely standardized and automated, and has almost entirely shifted to Asia. For module manufacturers, the transition to Industry 4.0 could also be a golden opportunity to reclaim a European stake in the global PV value chain. The next aspect to be examined will be the variety of stakeholders who will be involved and how to make them part of the transition.

From design to module assembly

As mentioned, building architects are likely to be the ones furthest upstream in the chain. Typically, they mostly focus on a building's function and aesthetics; not to be neglected, of course, is the fact that they must consider legislative parameters regarding the energy performance of the buildings they design.

In an Industry 4.0 scenario, it will become increasingly possible to design buildings around their energy properties; probably the first example of such an approach is the Barcelona Forum, founded in 2004. Thanks to Industry 4.0, architects will have software at their disposal, assisting them in optimizing their designs in respect of the desired energy efficiency, and in translating the final design into CAD files (or something equivalent) to be used for module design, assembly and installation.

In the semiconductor industry, comparable systems are already commonplace; for example, the use of process design kits (PDKs) which include manufacturing specs provided by the foundry to the chip designer, ensuring a higher probability of getting the designs right the first time. Another example is the use of tools for design technology co-optimization (DTCO) – and more recently even system technology co-optimization (STCO) [5] – which include relevant specs from throughout the entire development chain, to allow the IC designer to make the optimal technology choices at the very start of the process. Once such solutions find their way into the PV production chain, this will immediately broaden the architect's scope and skillset and will create the first link with what happens downstream. Such assisted design in the building domain could lower the acceptance barrier to BIPV adaptation in the broader architect community. Architects could truly consider BIPV as 'smart or special glass', and design assistance could invisibly consider the electrical part of the design.

Now that the module supplier knows what to build, they can use the digital files to order their parts and plan their production runs, or even better still, their AI software will have already done all that for them. In this context, they will upgrade their partnerships with, for example, their glass manufacturer and their suppliers of cells, interconnections and lamination materials. At the cell level, no extreme customization is seen to be happening. It is the authors' current belief that cells might in the foreseeable future remain standardized products to be produced and ordered in large quantities. And, although the variety of shapes, colours and sizes might become increasingly diverse, it is felt that the catalogue of available cells will remain manageable and that customization will initially occur at the module level.

The possibility of working with a woven fabric-based foil [6] (Fig. 2) which functions as the lamination foil and has integrated interconnections is currently being examined at imec. Once in the production stage, this foil could be custom designed in the shape of the glass and module, significantly increasing the ease of customization. This means, however, that players from the textile industry will be introduced into the equation as new stakeholders. As a consequence, the digital file that is at the basis of the Industry 4.0 scenario might also need to include the necessary parameters for weaving, etc. Needless to say, a crucial role and a lot of opportunities for software developers are envisaged along this entire journey.

"Industry 4.0 is more of a transition than an actual state or end goal."

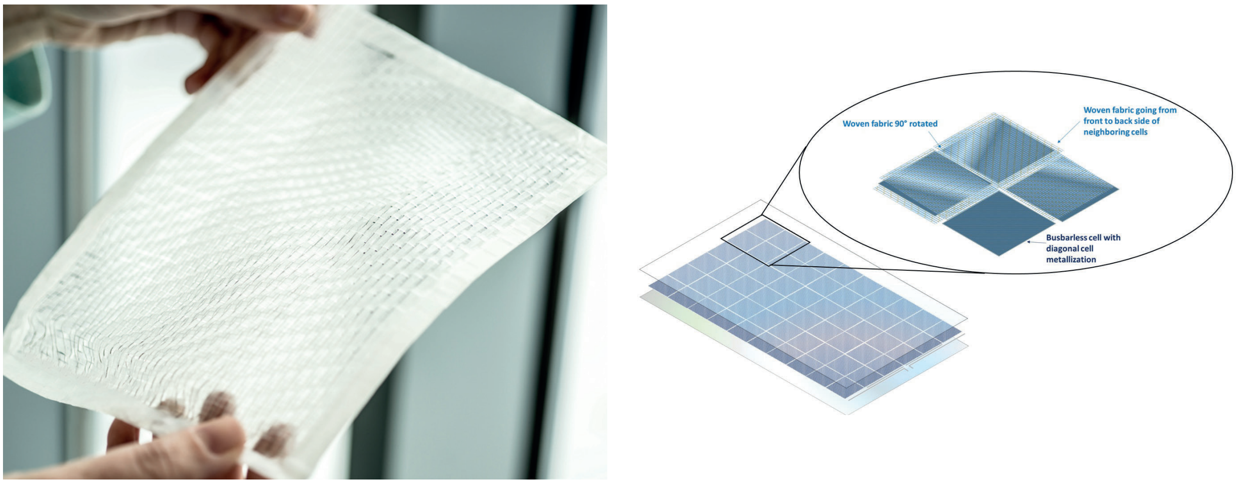

Figure 2. Innovations in interconnection and lamination technologies, such as this fabric-based foil (left), could ease customization and integration (right) in an Industry 4.0 scenario (©imec).

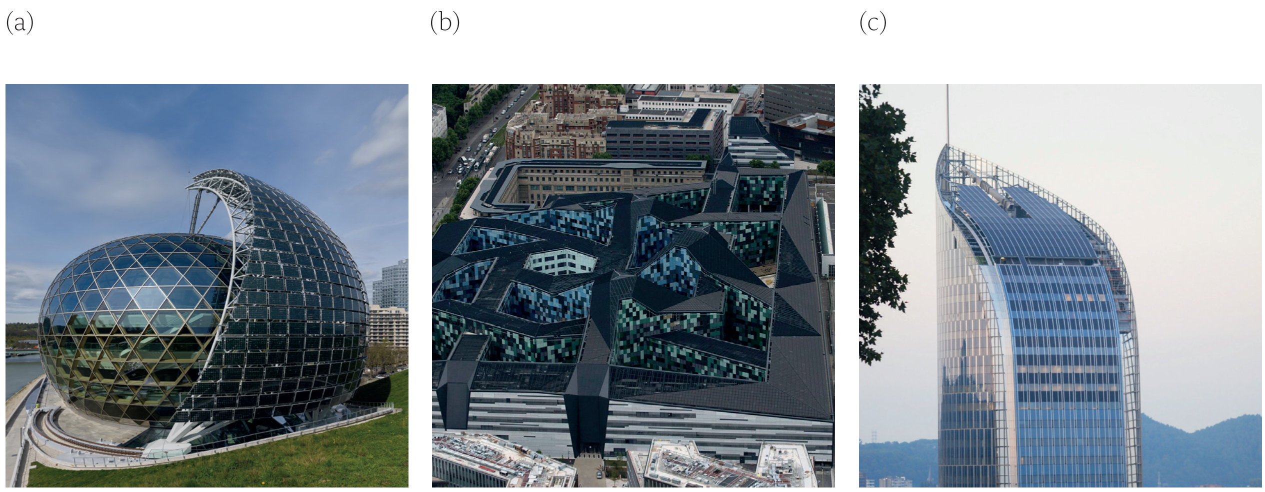

Pictures: Courtesy of ISSOL

Figure 3. Large-scale projects can kick off the market for customized BIPV and thereby justify the transition to automated production and assembly. (a) City of Music, Paris, Shigeru Ban architects, BIPV by ISSOL. (b) French Ministry of Defence, Paris, ANMA architects, BIPV by ISSOL (©Agence Nicolas Michelin & Associés). (c) Finance Tower, Liège, Belgium, Jaspers Eyers architects, BIPV by ISSOL (©P. Andrianopoli).

After all parts have been ordered and delivered, the assembly process can take place. At present, for custom-module designs, a lot of manual interventions are still needed; this is in contrast to standard cell and module manufacturing, in which highly automated production technologies are already mainstream. Once automated technologies have been implemented in custom-module manufacturing, they will allow (AI-supported) optimized process-flow management and execution, for example by smartly combining and planning batches in the light of the custom settings to be altered in the assembly line. Furthermore, automation will significantly improve quality. Cracks and other errors introduced by the handling of strings of cells, for example, can be avoided; similarly, better controlled and homogeneous pulling forces exerted while applying the lamination foils, etc. will minimize breakages, etc. Technically, there are no significant restrictions in automating customized module assembly.

At the moment, imec is ramping up its TWILL BIPV R&D project, which looks into precisely these aspects. Central to the project will be a 12-metre pilot line for the automated assembly of customized PV modules. However, because of the low production volumes, it is not yet economically viable for module manufacturers to proceed in this direction. A transition towards fully

"Once automated technologies have been implemented in custom-module manufacturing, they will allow (AI-supported) optimized process-flow management and execution."

automated assembly will become justified when one or more launching customers emerge; for example, a global project developer looking for complete design freedom might require a large number of customized PV modules (Fig. 3).

It should be noted that in view of the specific technological evolutions related to BIPV and printed electronics (e.g. organic PV – OPV), the module assembly scenario depicted above will of course have different consequences. For example, a recent R&D project undertaken by the Fraunhofer Institute for Solar Energy Systems ISE showed that customized manufacturing of BIPV even benefits from an average 35% reduction in production costs [7]. Nevertheless, the overall outcome of this step will largely be the same: at the end of the line there will be PV modules ready to be transported to the construction site.

From module to building integration

Moving on now to the construction site, one again encounters several relevant stakeholders. The shipment of large glass panels to the site within a tight framework has its own challenges, with manufacturing- and traffic-integrated planning being essential. First, the construction workers, such as builders and electricians, on site: radical changes as a consequence of Industry 4.0 might be seen at this level too. Will the electrician still be responsible for the electrical layout, or will the layout have already been generated and provided to him by one of the software modules being used in the building design phase? And will modules be installed manually, or will module installation be fully automated by cranes that are pre-programmed to do the job?

Second, at this point all the peripheral components, such as inverters and batteries, will need to be installed as well. In an Industry 4.0 scenario, these too will have been custom ordered to match the system requirements. Furthermore, technical evolutions in these domains will allow modular solutions that, during operational lifetime, can also flexibly adapt to the building's real-time energy demand and supply.

Finally, there is the maintenance aspect to be considered. Since downstream in the production chain Industry 4.0 ensures the logging of relevant data, these become an important input for the BIM. Aspects such as predictive maintenance and performance analysis will all become more efficient thanks to the data that will readily be available.

Related aspects

Now that the discussion has moved in a rather linear way through the chain from design to installation, some related elements to be considered in parallel will be examined.

Data is the main currency in any Industry 4.0 scenario; associated with this data are the aspects of ownership and security. In order to make Industry 4.0 a reality, stakeholders who are currently competitors with each other will be obligated to share data: for example, between equipment manufacturers the sharing of data relating to production runs almost implicitly means that information about the specific machine specifications or settings are included or can be extracted. The authors envisage that a new stakeholder will emerge who will hold an intermediate role in order to anonymize the data and manage the information flows extracted from it; legislative powers will also need to cater for this.

In the same way that data cannot be treated as an isolated entity, the building's energy forms part of a larger grid. At some point, Industry 4.0 scenarios will also have to look into the more holistic challenges and opportunities associated with this. On top of the localized energy optimization being performed in the building design phase (e.g. accounting for shadows), grid optimization will also be necessary. The upshot of all this is that protocols will need to be put in place to facilitate smart communication between multiple BIMs and grid management systems.

Partnerships

With regard to value-chain optimization in PV module assembly, it could be argued that there are quite a few similarities with the automotive industry. For decades, that sector has been adopting a highly integrated approach, involving car manufacturers, their tier suppliers and their distribution and dealer network to the customer. Before the PV sector starts mimicking those elements, however, one must be aware that this industry too is in a state of constant evolution. A recent presentation at the imec technology forum by Thomas Müller, Executive Vice President at Audi, illustrated the need to break through the rather linear hierarchy of tiers 1–4 suppliers and the collaborations and partnerships that come with it [8]. His argument was that car manufacturers need to interact more closely and directly with semiconductor companies. These companies are now typically in tier 4, and so are rarely, if ever, on the agenda of the manufacturer. Supporting his argument, Müller gave the example of an electronics component used in door handles, which – thanks to such direct interactions – was reduced to just 20% of its original size, allowing significantly increased design freedom for the car designer. As in the case of the car industry, the PV sector will also need to restructure and strengthen its partnerships with these and other sectors.

To gain a better understanding of these and other facets of the Industry 4.0 transition, imec is currently involved in several 'living labs' in Flanders, almost all of which are in close collaboration with Flanders Make, the strategic research centre for the manufacturing industry. The work at these living labs will also involve exploring aspects such as:

- Connectivity (tags, drones and other technologies for indoor localization and process optimization), co-bot operations (e.g. looking for an optimum in the operator's cognitive load during their cooperation with industrial robots).
- Energy (e.g. how to find a balance between the massive amounts of data that can be generated and the increasing energy demand of large data centres).
- Computing (e.g. clever selection of data and distribution over edge versus cloud computing).
- Challenges for smart maintenance and circular economy (e.g. recycling, reuse and other end-of-life scenarios).

Living lab settings such as these will become increasingly important in also prototyping the new collaboration and partnership structures that come hand in hand with the Industry 4.0 transition. They will also be useful for detecting and filtering out the directions that not only are sustainable but also bring economic value. To give just one example in the context of a circular economy, consider Atlas Copco, a world-leading provider of compressors, vacuum solutions, air treatment systems, etc.; this company has already for many years reclaimed used equipment from its clients and sells it on (after revision) to another client who might not necessarily be looking for state-of-the-art products. Why not introduce a similar business model into PV installation? Imec, jointly with the H2020 CIRCUSOL project partners, is exploring technical and business aspects of the circular economy in PV and batteries [9].

What 4.0 can bring to the PV sector

New business models, partnerships and progression in the construction sector are just some of the advantages Industry 4.0 can bring to the PV industry. It is also felt that Industry 4.0 can mean a definite breakthrough for PV into new markets, such as aviation, automotive and marine; there is an increasing tendency for all of these markets to shift to electric-powered vehicles [10–12]. However, for PV to fulfil its potential in these markets, some catching up needs to be done – first, at

"If appropriate action is taken, Industry 4.0 could also spark a revival of the European PV industry."

the PV-powered charging station level [13], and, second, at the vehicle-integration level itself. One of the main reasons why PV is trailing behind is its limitations regarding customization and integration. If, as argued, Industry 4.0 were to drastically increase the PV sector's capabilities with regard to these two aspects, one might finally see PV taking off in these new sectors as well, not to mention the possibilities created through the abundance of sensors for Internet of Things (IoT) and Industry 4.0 applications in all sectors imaginable. It is hard to believe that all these sensors will be battery powered, but not difficult to predict that they will also probably require advanced customization of PV modules in order for them to play a role.

Conclusion

In summary, it has been shown that the transition to Industry 4.0 is an evolution that, for the PV industry, brings an almost equal number of opportunities as it brings challenges. Grasping the entire complexity is an almost impossible mission, let alone trying to predict the sequence of events that will lead PV into Industry 4.0. What is possible, however, is to identify some of the guiding principles that one should keep in mind. One of these principles is that the choices to be made should always be weighed against the value that they will bring; this is to be accomplished within a framework comprising economic parameters (will the choice bring the company more, or new, business?) and sustainability ones (will the choice lead to a healthy planet with healthy people?). In support of the choices, a rethink of some of the fundamentals behind the partnerships will be necessary, and living lab environments could assist in this process. Moreover, if appropriate action is taken, Industry 4.0 could also spark a revival of the European PV industry, as it is likely that globally our ecosystem will be the best placed to tackle this holistic challenge.

References

[1] PWC and Flanders Make 2017, "Industry 4.0: Hype or reality?", Industry 4.0 Survey, p. 6.
[2] European Parliament and the Council of 19 May 2010, "Directive 2010/31/EU on the energy performance of buildings".
[3] Masson, G. 2017, "BIPV competitiveness and market potential", Presentation (Sep. 7), Becquerel Institute, pp. 5–6.
[4] Fraunhofer ISE 2018, "Photovoltaics Report", Report (Jun. 19), p. 4.
[5] Kim, R. et al. 2018, "IMEC N7, N5 and beyond: DTCO, STCO and EUV insertion strategy to maintain affordable scaling trend", *Proc. Des. Proc. Tech. Co-opt. Manufac. XII, SPIE Adv. Lith.,* Vol. 10588, San Jose, California, USA.
[6] Borgers, T. et al. 2017, "Combined interconnection and lamination of bifacial busbarless cells through woven wiring", *Proc. 33rd EU PVSEC*, Amsterdam, The Netherlands.
[7] Fraunhofer ISE 2018, "New production concept for building-integrated solar modules drastically reduces costs", Press Release (Apr. 16).
[8] Müller, T. 2018, "Mobility 2025", Video presentation [https://www.youtube.com/watch?v=5fNCNNAsoCs], 2'06"–3'00".
[9] CORDIS 2018, "Circular business models for the solar power industry", CIRCUSOL Project [https://cordis.europa.eu/project/rcn/216081_en.html].
[10] International Energy Agency (IEA) 2017, "Global EV Outlook 2017".
[11] Gonzalez, F. 2018, "Electric boats and ships 2017–2027. Technologies, markets, forecasts, key players and opportunities", IDTechEX Research.
[12] Harrop, P. 2018, "Manned electric aircraft 2018–2028. Hybrid & pure electric technology roadmap, market forecasts, companies, models, MEA convergence", IDTechEX Research.
[13] Chaouachi, A. et al. 2016, "Framework for electric vehicles and photovoltaic synergies: Perspective in the European Union", JRC Technical Reports.

About the Authors

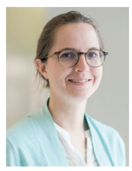

Dr. Eszter Voroshazi is the group leader of PV system activities at imec on the EnergyVille campus. This research group focuses on innovative PV-module and power-electronic technologies and energy-yield simulations for integrated PV systems. She received her engineer certification from INSA de Rennes (2008) and her Ph.D. from KU Leuven (2012).

Kris Van de Voorde is the innovation programme manager at imec. With a focus on clusters and transitions, he is initiating and supporting Industry 4.0 and circular-economy-related projects. He holds a master's in electrical engineering (UGent), a third degree in industrial management (KU Leuven) and an MBA (Vlerick Business School).

Dr. Jozef Poortmans is an imec Fellow and has been the scientific director of imec PV and energy activities since 2013. He is a part-time professor at KU Leuven and UHasselt, and is also the R&D strategy coordinator of EnergyVille, a partnership between imec, VITO, KU Leuven and UHasselt, which focuses on smart cities and smart grids.

Enquiries

Email: Eszter.voroshazi@imec.be

PV manufacturing capacity expansion announcements in Q2 2018

By Mark Osborne, senior news editor, Photovoltaics International

Abstract

PV manufacturing capacity expansion announcements in the second quarter of 2018 were slightly higher than the previous quarter, although activity slumped specifically in June, following China's decision to suddenly cap utility-scale and distributed generation projects. The quarter was also characterized by activity in India, partially driven by a major Chinese manufacturer. The report will also analyze first half year capacity expansion plans and targeted locations, globally.

April review

Total capacity expansion announcements in the month of April 2018 were 12,800MW, slightly higher than the total of 12,570MW announced in the previous month. In the last few years April had not been a particularly strong month for announcements but the plans announced were the highest on record for the month of April.

The strong month was supported by activity across thin film, solar cell and module assembly. Following on from an announcement in the previous month from Hanergy Thin film Power Group, primarily CIGS (Copper-Indium-Gallium-Selenide), which totalled 2,140MW, CdTe leader First Solar announced the building of a new 1.2GW manufacturing plant near its existing flagship facility in Perrysburg, Ohio.

The company said that the new production plant for its large-area Series 6 modules would require around US$400 million in capital expenditure and create around 500 new jobs.

The capacity expansion plan includes a one million square foot facility located in Lake Township, Ohio, a short distance from the Perrysburg facility, which started construction in mid-2018 and is expected to start full production ramp in late 2019.

As a result, First Solar will have a nameplate capacity in the US of 1.8GW of Series 6 modules and the largest PV manufacturing base of any PV company in the US.

Solar cell expansions announced in April were also strong, totalling 5,100MW, up from 3,810MW

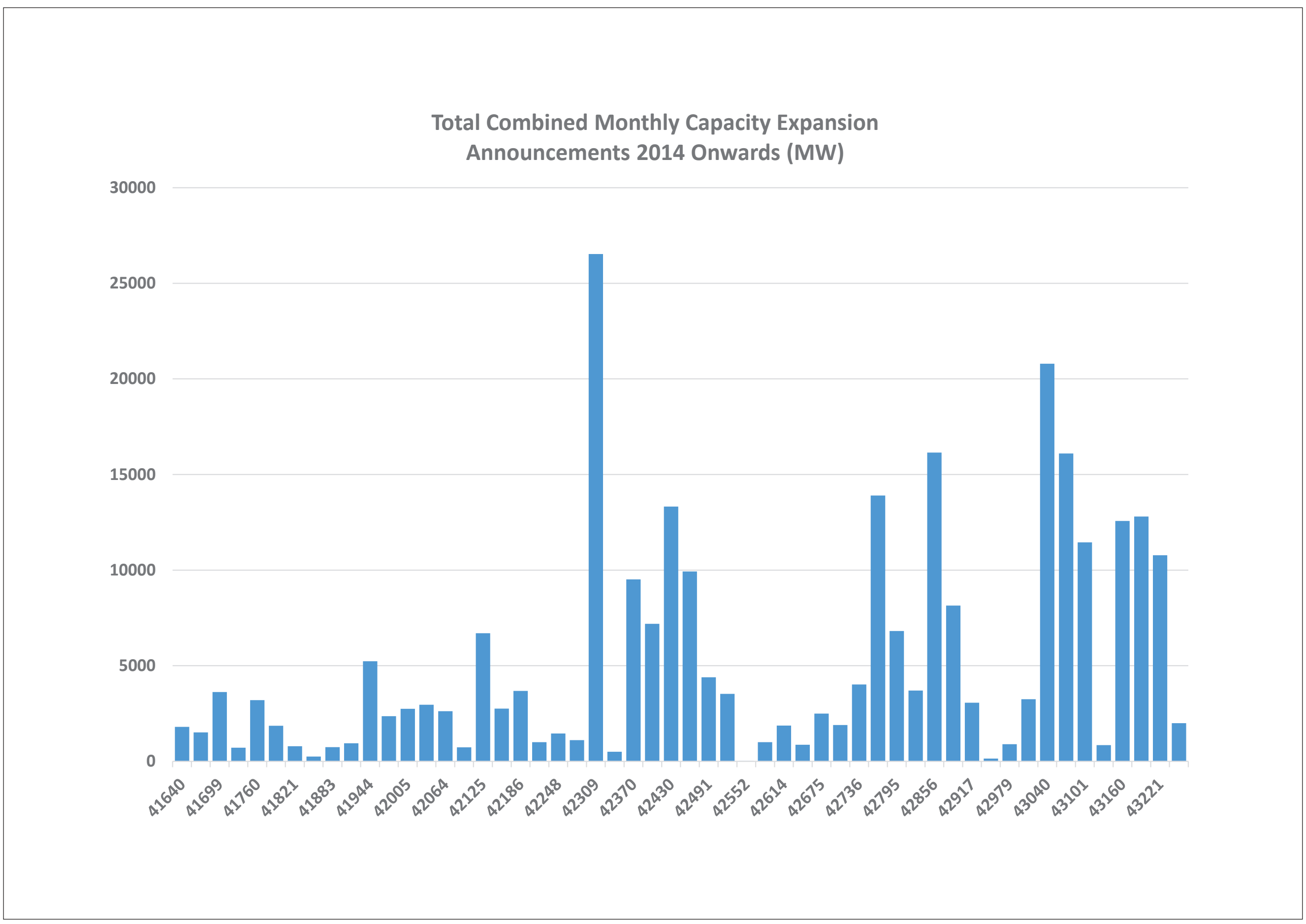

Total combined monthly capacity expansion announcements, 2014 onwards (MW).

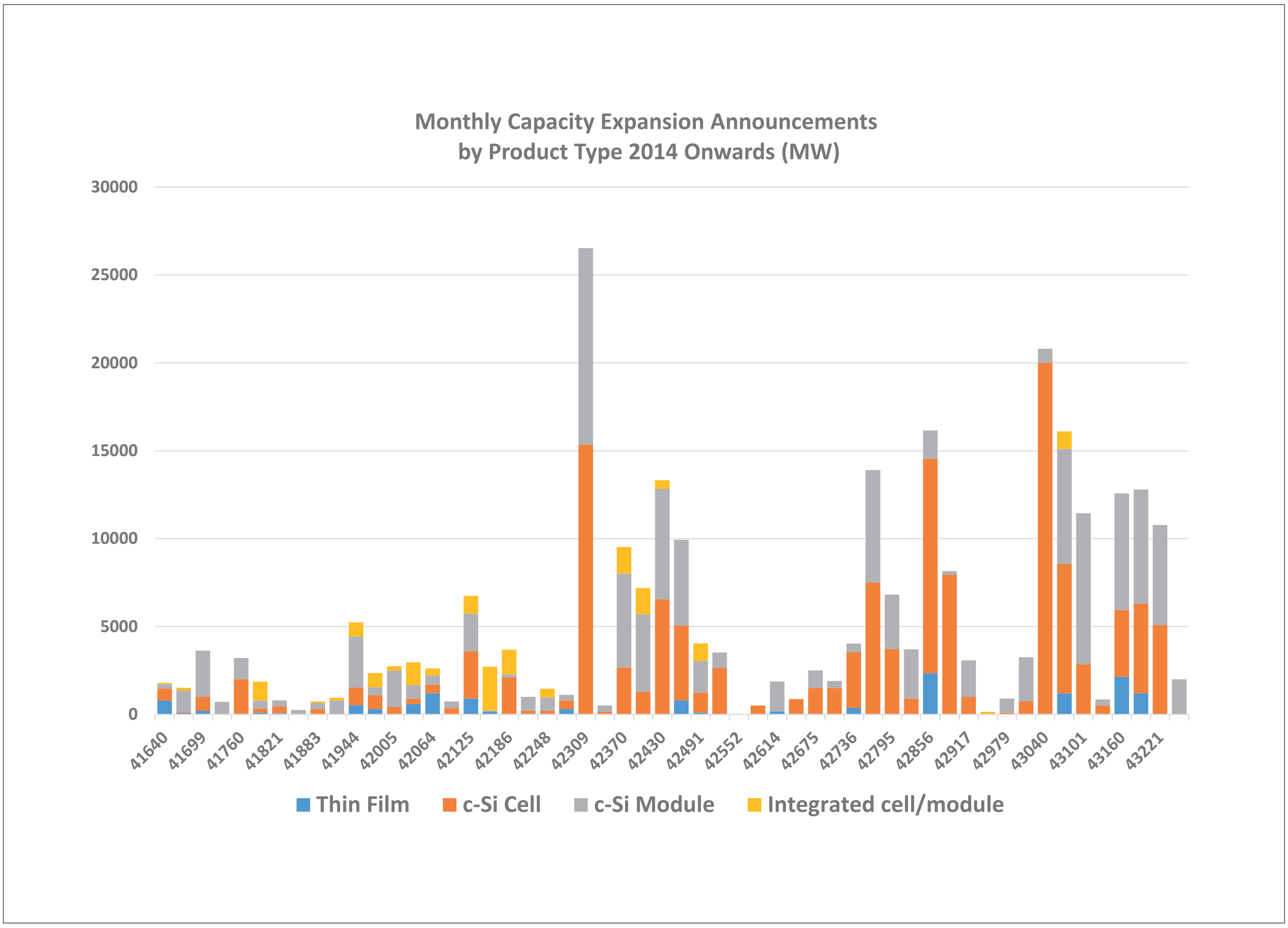

Monthly capacity expansion announcements by product type 2014 onwards (MW)

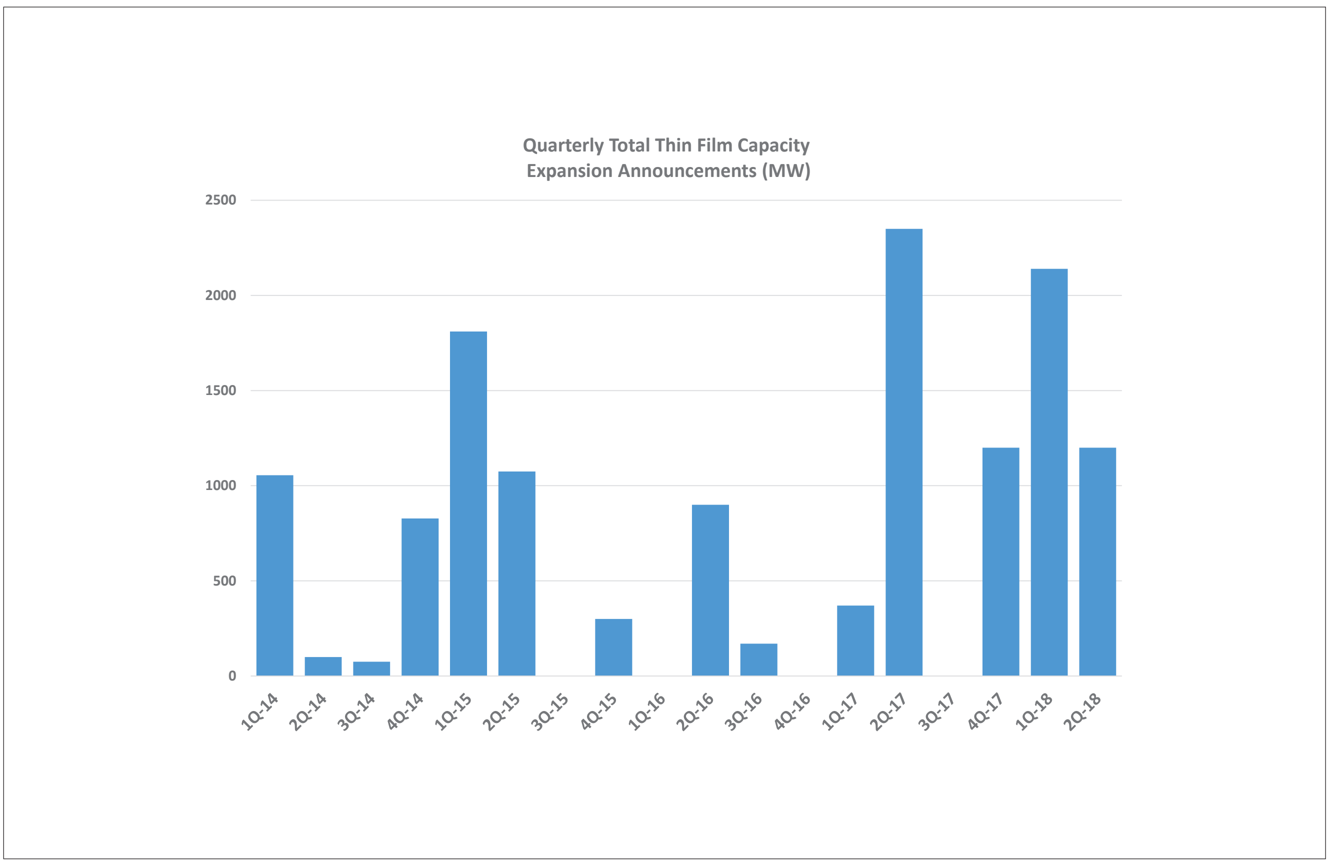

Quarterly capacity expansion announcements by product type, 2014 onwards (MW)

in the previous month and the highest level since December 2017 (7,350MW).

The solar cell announcements were dominated by Softbank Vision Fund (SBVF) and GCL Group, with the two parties signing a memorandum of understanding (MoU) to launch a US$930 million joint venture in the Indian state of Andhra Pradesh, primarily to manufacture PV ingots, wafers, solar cells and modules.

As with large capacity announcements, the companies said implementation would be carried out in two phases of 2GW each, should the plans be formalized. India has since placed a 'Safeguard Duty' on solar imports, making it more attractive to overseas PV manufacturers establishing local production.

At the opposite end of the scale, REC Group announced it had built a solar cell building at its integrated production plant in Tuas, Singapore, for its brand-new flagship module product, 'N-Peak'. The cell plant has adopted 'Industry 4.0' technologies and is expected to be highly automated. We have given this new plant an initial 100MW nameplate capacity as the company has yet to state the actual initial capacity or future nameplate capacity plans for the n-type mono half-cut cell facility.

Module assembly plans announced in April also trended strongly, reaching 6,500MW, slightly down from 6,620MW in the previous month, driven by the SBVF and GCL Group plans in India.

Other big news included plans by Turkish downstream EPC firm, Eko Yenilenebilir Enerjiler A.S. (EkoRE), which announced government support to build 1GW of wafer, cell and module assembly capacity in the Bor Organized Industrial Zone (OIZ) in Niğde.

'Silicon Module Super League' (SMSL) member JA Solar also released information on expanding mono wafer capacity in China by 4GW and expansions at module assembly plants in Fengxian, Shanghai (400MW), Hefei, Anhui (800MW) and 300MW at its facility in Xingtai, Hebei, China.

May review

Total capacity expansion announcements in May were 10,780MW, down from 12,800MW in April and 12,570MW in March.

Both cell and module assembly expansions plans were fairly balanced at over 5GW each. There were no new thin-film announcements in May.

Solar cell expansion plans (5,080MW) included 5GW from GCL Group, this time in Egypt and approved by the National Authority for Military Production. As with plans for India, GCL could be planning to build an integrated manufacturing hub that would include ingot/wafer, cell and module production. Details of the plans remain limited and very much at an early stage of evaluation, despite Egyptian government rubber stamp.

Turkey-based Suoz Energy Group (marSUN), a module manufacturer also announced plans for a 500MW module assembly plant expansion after also buying an 80MW cell line from Greece from a bankrupt company.

Total module assembly expansion announcements in May were 5,700MW, down from 6,500MW in April and 6,620MW announced in March 2018.

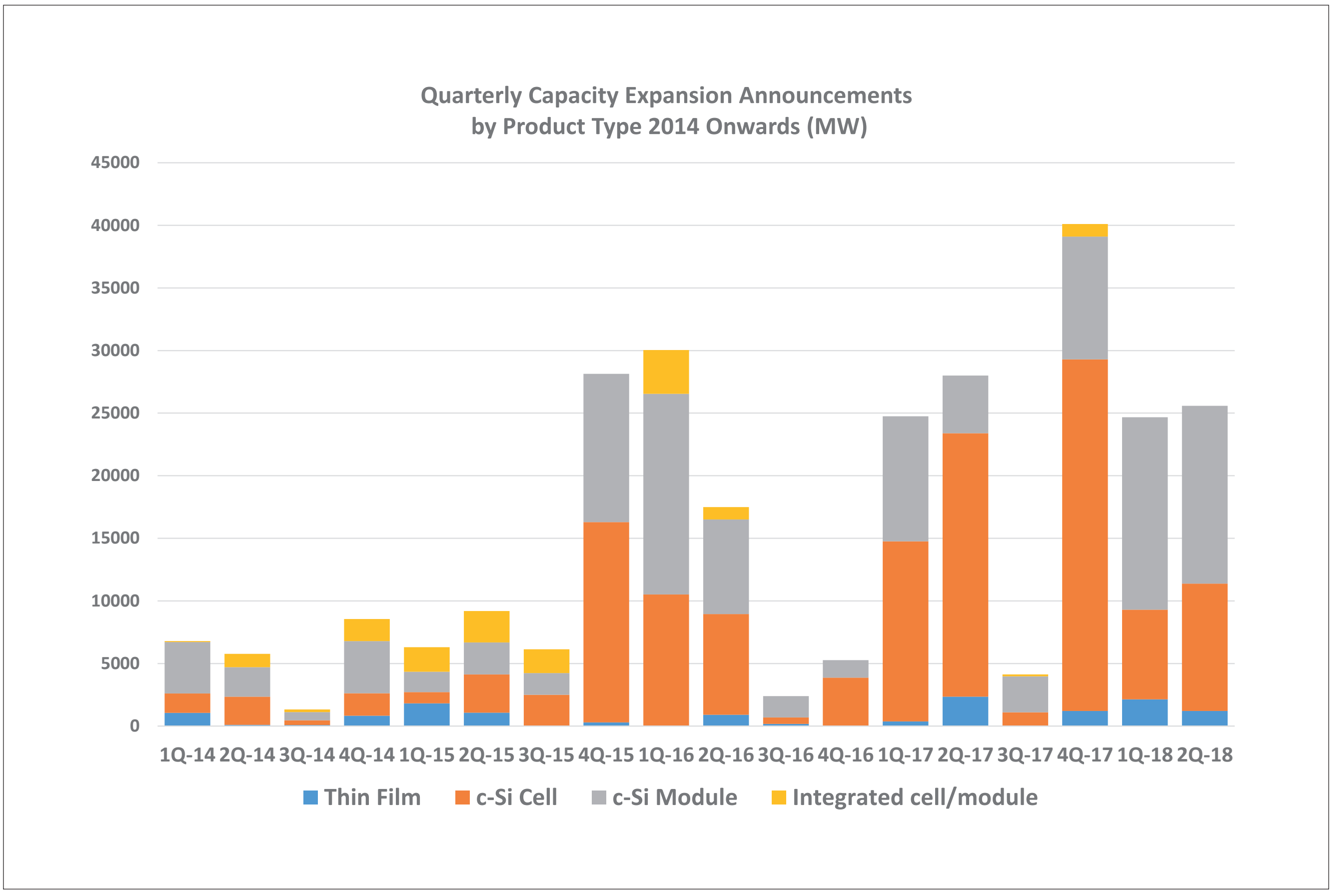

Total capacity expansion announcements by country in Q2 2018 (MW).

June review

Capacity announcements in June only related to module assembly plans, which totalled 2,000MW from only three companies.

Notably, following China's decision to suddenly cap utility-scale and distributed generation (DG) projects at the end of May, no China-based company announced new capacity expansion plans. Indeed, June stood out for being the only month so far in 2018 when a Chinese manufacturer did not announce new expansions.

India's Waaree Energies had started production at its new 500MW assembly plant in the month and said it would add a further 1GW in the future.

Goldi Green, also based in Gujarat, India announced plans for a 500MW module assembly expansion with the plant expected to be highly automated.

However, arguably the significant announcement in the month came from LG Electronics, which said it would establish a 500MW module assembly plant in Alabama, US at a cost of around US$28 million.

LG Electronics follows leading 'Silicon Module Super League' (SMSL) member, JinkoSolar, as well as Hanwha Q CELLS in establishing solar module assembly facilities in the US, post the Section 201 trade case.

LG Electronics USA said that the facility would be co-located at an existing complex in Huntsville-Madison County, Alabama. LG has had operations in Huntsville since 1981 and became the home of LG's service division in 1987. The company said that PV module production was expected to start at the beginning of 2019, producing its high-efficiency 'NeON' 2 series 60-cell n-type mono modules with 340Wp-plus output, primarily for the US residential rooftop market.

Second quarter review

Total combined second quarter 2018 capacity expansion announcements were 25,580MW, up from 24,870MW in the first quarter of 2018, despite the rapid decline in announcements in June.

Plans by GCL in India and Egypt significantly boosted totals in the quarter and both announcements remain highly speculative at the time of writing. Excluding the 9GW of MOUs from GCL, total announcements would have been around 16,500MW, considerably down quarter-on-quarter.

The biggest impact from excluding GCL would have related to solar cell expansions, which would have totalled just over 1GW, instead of over 10GW as reported.

Module assembly announcements in the quarter totalled 14,200MW and 5,200MW if GCL was excluded from the analysis. Thin-film was 1,200MW in the quarter, all contributed by First Solar.

Plans by GCL in India and Egypt also skewed capacity announcements on a geographical basis in the second quarter. The 10GW possible plans (5GW cell and 5GW module assembly) in Egypt meant it

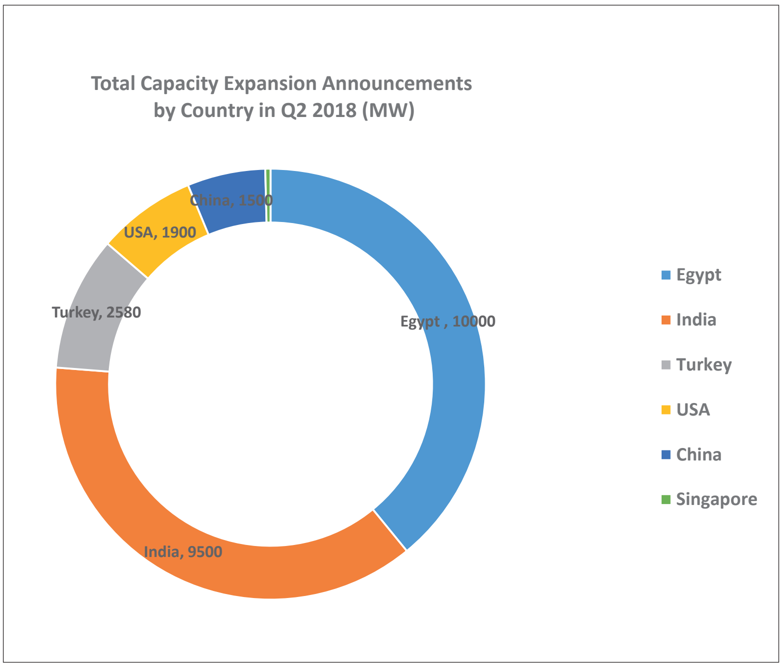

Quarterly total thin-film capacity expansion announcements (MW).

was the top location in the quarter.

However, GCL's potential plans in India were supported by planned expansions by two India-based companies, resulting in a total of 9.5GW announced in the quarter.

Turkey continues to attract potential capacity expansions. Having accounted for 3,950MW of announcements in 2017, the second quarter of 2018 accounted for 2,580MW, highlighting both the local content rules and growth in PV deployments in the country that continues to attract potential capital investments in manufacturing from both Turkey and overseas.

Also of note in the quarter was the impact of new import duties imposed on most of the rest of the world in the US. Led by First Solar and LG Electronics and adjustments by CSUN, the US attracted a total of 1,900MW of new capacity expansion announcements in the second quarter, up from 1,600MW in the previous quarter.

First half year review

In the first half of 2018 a total of just over 50.4GW of combined (cell, module and thin-film) capacity expansions were announced, down from over 52.7GW in the prior-year period, indicating very little change.

Thin-film planned expansions remained strong with announcements totalling over 3.3GW in the first half of 2018, compared to a total of over 3.9GW in all of 2017.

Solar cell announcements in the first half of 2018 topped 17.3GW, compared to over 30GW in the prior-year period. This figure drops to around 8.3GW if GCL plans in India and Egypt are excluded.

A total close to 30GW of new module assembly capacity expansion announcements were made in the first half of 2018. This compares to nearly 14.6GW in the prior year period. However, the key difference was the significant level of new investments in high-efficiency PERC and next-generation cell technologies, compared to module assembly expansions. Much of the existing module assembly capacity could be upgraded to meet the cell technology migration.

Again, decoupling GCL from the second quarter, lowers module assembly plans to just over 21GW.

When analysing expansion plans on a geographical basis in the first half of 2018, it would seem that its business as usual when total combined announcements for China topped 15.74GW. However, only 1.5GW was announced in the second quarter, all from JA Solar.

Almost identical was the 15.71GW of new capacity plans announced for India, which included over 6GW in the first quarter and 9.5GW in the second quarter. Again, GCL plans in India would have to be taken into account.

Interestingly, in 2016, India had over 16GW of combined capacity expansion announcements, the highest annual record for the country. This record could be exceeded in 2018.

The key catalyst behind the revival of the USA as a manufacturing location has been driven by the Section 201 case and subsequent import duties for the next four years. But due to the progressive reduction in tariffs that start at only 30%, non-domestic PV manufacturers have selected to build only module assembly plants, limiting capital expenditure and remaining flexible to any long-term manufacturing commitments as a result.

Finally, Turkey is proving to be an attractive location, not just for module assembly but in particular solar cells, with domestic PV manufacturers as well as overseas firms continuing to plan for manufacturing bases in the country, due to local content rules and government inward investment incentives.

In 2017, Turkey attracted almost 4GW of manufacturing expansion plans, ranked fourth for the first time. In the first half of 2018, Turkey attracted over 2.5GW of new expansion plans and has become an important downstream emerging market in the last two years.

In the first quarter of 2018, expansion plans were announced in 10 countries, while this declined to six in the second quarter with Egypt being a speculative bet at this time.

Conclusion

After record announcements in the fourth quarter of 2017, both first and second quarters of 2018 were stronger than expected, although a marked shift back to module assembly compared to cells in the fourth quarter of 2017. The revival in thin-film over the last nine months was supported in the second quarter of 2018 by the new First Solar facility for its Series 6 modules in the US, partially driven by the newly imposed import duties.

Government actions, whether positive (Turkey and Egypt, for example) or negative (USA, India and China), are influencing manufacturing decisions but in the first half of 2018, any major impact on announcements would not seem to be evident at this time.

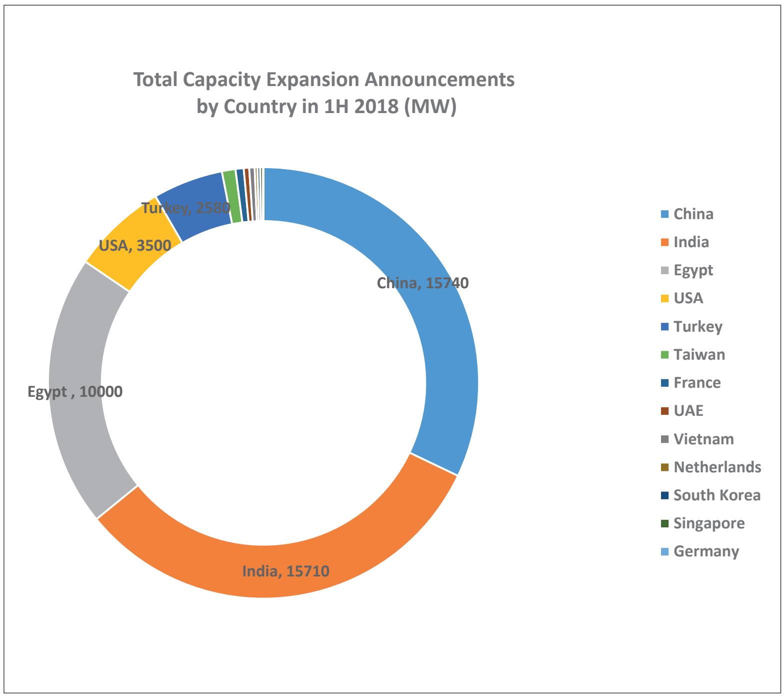

Total capacity expansion announcements by country in 1H 2018 (MW).

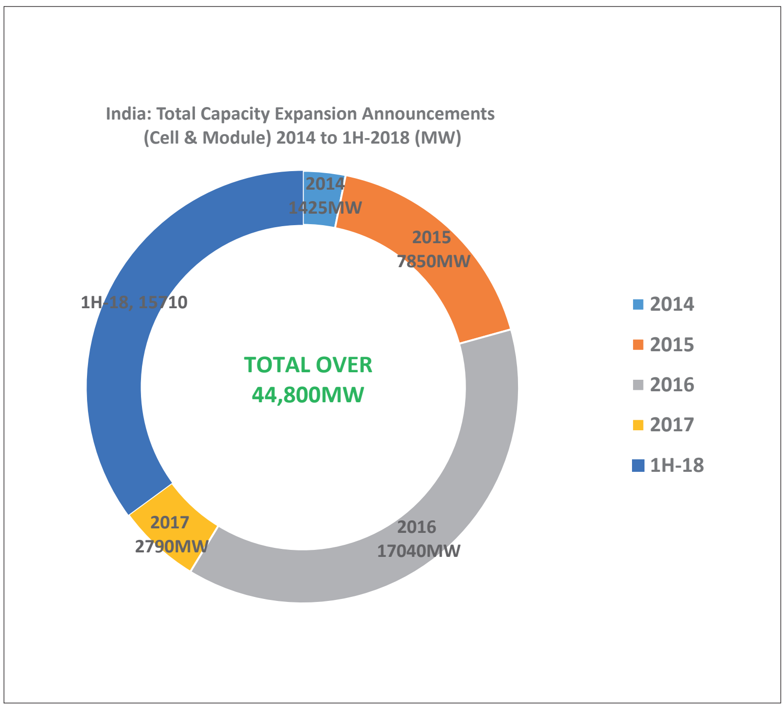

India: total capacity expansion announcements (cell & module), 2014 to 1H-2018 (MW)

News

N-type solar cell production to exceed 5GW in 2018 with 135% growth since 2013

As the solar industry has grown from a 50GW market to 100GW in just a few years, the desire to have differentiated production has increased, especially for companies entering the market or repositioning strategies.

Having a product offering that is either higher efficiency or lower cost is always a good way to extract funds to build new manufacturing capacity, and the solar industry has seen plenty of efforts in this regard.

Until a few years ago, the PV industry had just a few companies making n-type solar panels, with efforts spread across three 'different' approaches: back-contacted solar cells (or interdigitated back contact, IBC), front-contacted with doped/intrinsic thin a-Si (passivation) layers (heterojunction), and n-type designs that are more analogous to regular p-type solar cell processing but have rear passivation/diffusion.

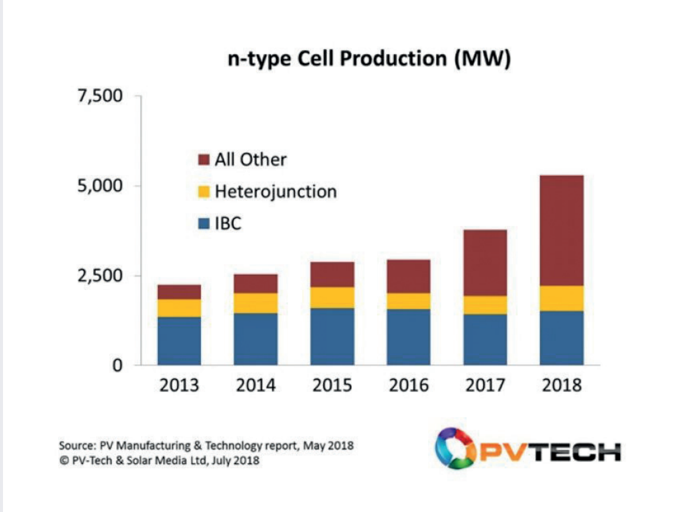

N-type cell production is projected to be over 5GW this year.

Heterojunction (or HJT) performance has slightly lower performance levels, compared to IBC, but offers higher powers than other n-type variants. The strengths of HJT can also be blended back-contacting of course, but as yet this is R&D only, and not close to mass production.

The 'other n-type' grouping has seen some pilot-line activity in the past, but saw its first real efforts to move into mass production about 10 years ago.

The net result of the new capital investments has seen the number of (meaningful) n-type cell producers grow to approximately 20, with many others engaged at the R&D level also, or working with research institutes on collaborative projects. Consequently, global cell production of n-type has grown from the 2GW-level in 2013 to what is projected to be more than 5GW this year.

BUSINESS

SunPower guides another year of massive losses

SunPower had previously guided a net GAAP loss for the second quarter to be in the range of US$125 million to US$100 million. Instead, the company decided to announce an impairment charge of approximately US$369.2 million related to all of its 800MW of E Series cell capacity at Fab 3 in Malaysia as it referred to it as its 'legacy manufacturing assets'.

The company didn't actually explain why it took the legacy manufacturing asset impairment charge in the second quarter of 2018, when a migration to the NGT cells in Malaysia was not expected to occur in 2019.

However, the Fab 3 in Malaysia will eventually be converted to its NGT (Next Generation Technology) IBC solar cell technology, which currently has a 100MW line installed and is expected to ramp sometime in the first quarter of 2019.

The company also took a gross margin hit, deciding to record US$355.1 million of the impairment charge in GAAP gross margin, resulting in a negative gross margin of 69.1%, compared to previous guidance of 2.5% to 4.5%.

Its full-year net GAAP loss for 2018 would be in the range of US$830 million to US$860 million, compared to a US$851 million loss posted in 2017.

SunPower reported better than expected revenue and deployments in the second quarter, as well as guiding further improvements in the third quarter of 2018. However, full-year revenue guidance remained unchanged at US$1.6 billion to US$2.0 billion on unchanged total deployments of 1.5GW to 1.9GW in 2018. SunPower had reported 2017 annual revenue of US$1.872 billion.

Meyer Burger turns profitable in 1H 2018 as new order intake dives

Leading PV manufacturing equipment supplier Meyer Burger reported first half year financial results, highlighting strong sales and a return to profitability but weak order intake, due to Chinese government solar policy changes and market uncertainties influenced by the USA-China trade conflict.

Meyer Burger reported first half 2018 sales of CHF 232.3 million (US$231.5 million), up 9.4% from CHF 212.3 million in the prior year period.

EBITDA more than quadrupled to CHF 29.2 million in the reporting period, while net earnings of CHF 8.3 million for the first half of 2018 meant a return to profitability.

However, its new orders plummeted to CHF 138 million, down from CHF 253 million in the second half of 2017 and down from its highest level since 2011 of CHF 308 million in the prior year period, a 55% decline.

The order backlog amounted to CHF 240.9 million, compared to CHF 343.8 million in the prior year period.

Meyer Burger said it was withdrawing guidance for 2018 net sales, which had expected to be in the range of CHF 400 million to CHF 440 million. The EBITDA margin guidance of around 10% would remain.

Amtech restructuring solar business as Chinese cell producers delay expansion plans

Specialist PV manufacturing equipment supplier Amtech Systems is restructuring its solar cell manufacturing equipment business with job losses after China-based customers have pushed out capacity expansion plans after government cuts were made to downstream solar installation targets as deployments far exceeded goals.

Fokko Pentinga, CEO of Amtech, said: "In our solar business, recent changes in China's domestic solar policies have slowed cell capacity expansion plans. However, we believe follow-on orders for the next phases of the large 1GW+ turnkey project will be received in the next few quarters and look to participate in other selective growth opportunities as we serve core customers over the long term."

The restructuring plan for Amtech's solar business segment included a reduction in its workforce of approximately 35-40 employees.

The restructuring was said to lead to approximately US$0.6 million to US$0.8 million of related costs that would be recorded in its fiscal the fourth quarter.

The company also announced that it had sold its remaining 15% stake in solar ion implant equipment manufacturer, Kingstone Technology Hong Kong Limited for approximately US$5.7 million.

GCL-Poly and Shanghai Electric US$2 billion polysilicon business deal collapses

Leading polysilicon and solar wafer producer GCL-Poly Energy Holdings has agreed with Shanghai Electric Group to terminate a framework agreement announced in early June 2018 with Shanghai Electric Group to sell a 51% stake in polysilicon production subsidiary Jiangsu Zhongneng Polysilicon.

GCL-Poly said that after multiple rounds of discussions and negotiations the size and complexity of the transaction meant it was difficult to reach a full agreement on the relevant acquisition terms and plans within a reasonable timeframe.

Both companies were said to have agreed that the timing and conditions for proceeding with the deal were "not mature enough."

Yingli Green Energy de-listed from NYSE

Struggling major China-based PV manufacturer Yingli Green Energy has said that it would not appeal a notification from the New York Stock Exchange (NYSE) on 28 June 2018 to de-list the company, due to non-compliance.

Yingli Green had failed to maintain an average global market capitalization of at least US$50 million, over a consecutive 30 trading-day period and its stockholders' equity was also less than US$50 million.

The company had previously reported a 2017 annual loss of US$510 million and a cash position of only US$58.1 million at the end of the year and had yet to report first quarter financial results.

Yingli Green's American Depositary Shares (ADS) were said to be listed instead on the OTC Pink marketplace on 2 July 2018, under the symbol 'YGEHY'. The company also noted that it would stop publishing regular quarterly earnings releases as it transitioned to the OTC market, although half-year and full-year results would be required for compliance.

Yingli Green reported total revenue of US$ 1,285.5 million in 2017, compared to US$1,206.4 million in 2016 on the back of PV module shipments of 2,953MW, compared to 2,170.4MW in 2016.

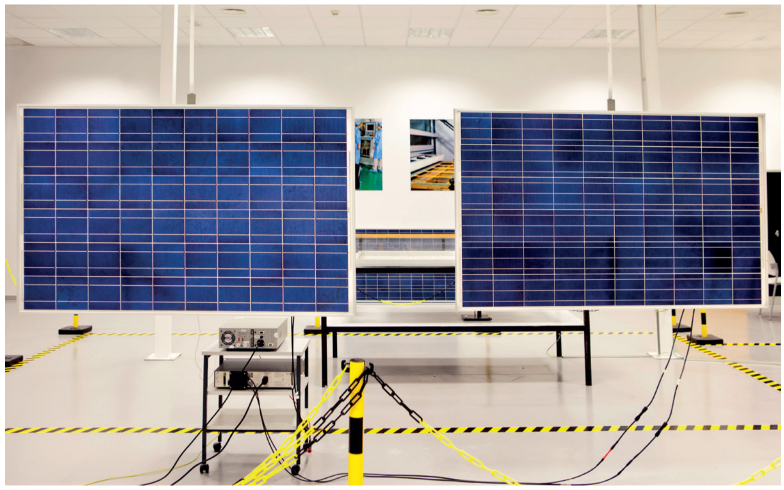

Credit: Yingli

Yingli Green reported total revenue of US$ 1,285.5 million in 2017.

Jolywood and Huanghe Hydropower establish n-type bifacial technology partnership

China-based PV module materials and n-type mono and IBC (Interdigitated Back Contact) bifacial module manufacturer, Jolywood, has solidified its business relationship with Qinghai province State Power Investment Corporation's Huanghe Hydropower Development Co., (SPIC) by establishing a joint laboratory to advance new materials, cells and module technology.

Jolywood said the technology partnership included such areas as n-type mono bifacial high-efficiency solar modules as well as mono N-type TOPCon and IBC solar cells and evaluating operating PV systems using these technologies in terms of efficiency, module encapsulation and backside efficiency, as well as on more in-depth studies on reliability and diversified application scenarios.

A few months ago, Jolywood entered into a 5GW 'framework agreement' with SPIC to further the adoption of advanced technology in utility-scale PV power plants in China. Emphasis was placed on deploying Jolywood's n-type mono 'TOPCon' modules to the tune of around 1GW in 2019.

SPIC also operates its own PV module manufacturing plants. The collaboration includes promoting high-efficiency technology for PV power plants to reach grid parity and beyond.

SPIC is responsible for operating the largest (100MW) grid connected PV power plant in the world designed to evaluate leading-edge technologies such as modules, trackers, inverters and O&M systems.

President of Heraeus Photovoltaics steps down from leadership role

PV metallization paste producer Heraeus Photovoltaics announced that its President, Andreas Liebheit, has stepped down from his position for personal reasons.

Liebheit had been responsible for shifting key operations of Heraeus Photovoltaics to Asia, establishing closer ties with customers and moved to Shanghai, China, to lead the company. In the last two years, Liebheit led the division into offering a broader product portfolio for the PV manufacturing sector, outside just metallization pastes.

Heraeus said that Liebheit stepped down from his position on 15 July, instead of leaving the company.

On a temporary basis, Raymund Chua, head of HPT in Singapore and head of Heraeus' Asia-Pacific Regional Centre, is taking charge of Heraeus PV Global Business Unit, while the company seeks a permanent replacement.

CELL EFFICIENCIES

Alta Devices sets new GaAs solar cell conversion efficiency record at 28.9%

Specialist gallium arsenide (GaAs) PV manufacturer Alta Devices, a subsidiary of Hanergy Group has achieved a new solar cell conversion efficiency record of 28.9%, which was certified by NREL (National Renewable Energy Laboratory).

Alta Devices has been a perennial world record holder for GaAs solar cell efficiency. The company uses a metalorganic chemical vapour deposition (MOCVD) process as well as an epitaxial lift-off (ELO) technique, which creates a thin, flexible, and lightweight solar cell for niche applications.

One of Alta Devices founders, professor Harry Atwater of Caltech said: "Achieving a new record for this class of devices is a landmark because a 1-sun, 1-junction cell is the archetypal solar cell. The fact that Alta is breaking its own record is also significant since many other teams have been actively attempting to break this record."

The new record cell was said to be the first based on 'Internal Luminescence Extraction', which has enabled Alta to set the new record. Luminescence extraction is the escape of internal photons out of the front surface of a solar cell and minimise the emission out of the back surface to boost conversion efficiency.

Oxford PV takes record perovskite tandem solar cell to 27.3% conversion efficiency

Perovskite solar cell developer Oxford Photovoltaics (PV) has reported a new perovskite tandem solar cell record, certified by Fraunhofer ISE at a conversion efficiency of 27.3%.

Oxford PV's latest record for a 1 cm2 perovskite-silicon tandem solar, exceeds the 26.7% efficiency world record for a single-junction silicon solar cell.

Recently, the company highlighted that it had produced a 1 cm2 perovskite-silicon two-terminal tandem solar cell with a verified conversion efficiency of 25.2%, through an ongoing collaboration with Helmholtz-Zentrum Berlin (HZB) and the Photovoltaics and Optoelectronics Device Group at the University of Oxford.

Oxford PV is currently scaling its perovskite-silicon solar cell technology from the lab to high-volume manufacturing capability as it bids to licence the technology to mainstream PV cell manufacturers.

The company is producing commercial sized 156 mm x 156 mm perovskite-silicon solar cells, at its 17,000 m2 industrial pilot line in Germany.

EPFL and CSEM use evaporation process to boost mono c-Si tandem perovskite cell to record efficiency

Researchers at EPFL's Photovoltaics Laboratory and the CSEM PV-centre have reported a record tandem junction solar cell with conversion efficiencies of 25.2%, using a standard monocrystalline cell and an evaporation and spin-on process to fully coat the structure.

The simple manufacturing technique could be directly integrated into existing production lines, and the cell conversion efficiency could eventually rise above 30%, according to new modelling.

In tandem cells, perovskite complements silicon cells as it converts blue and green light more efficiently, while silicon based cells are better at converting red and infra-red light.

"By combining the two materials, we can maximize the use of the solar spectrum and increase the amount of power generated. The calculations and work we have done show that a 30% efficiency should soon be possible," said the study's main authors Florent Sahli and Jérémie Werner.

"Silicon's surface consists of a series of pyramids measuring around 5 microns, which trap light and prevent it from being reflected. However, the surface texture makes it hard to deposit a homogeneous film of perovskite," added Quentin Jeangros, who co-authored the paper.

Oxford PV is currently scaling its perovskite-silicon solar cell technology.

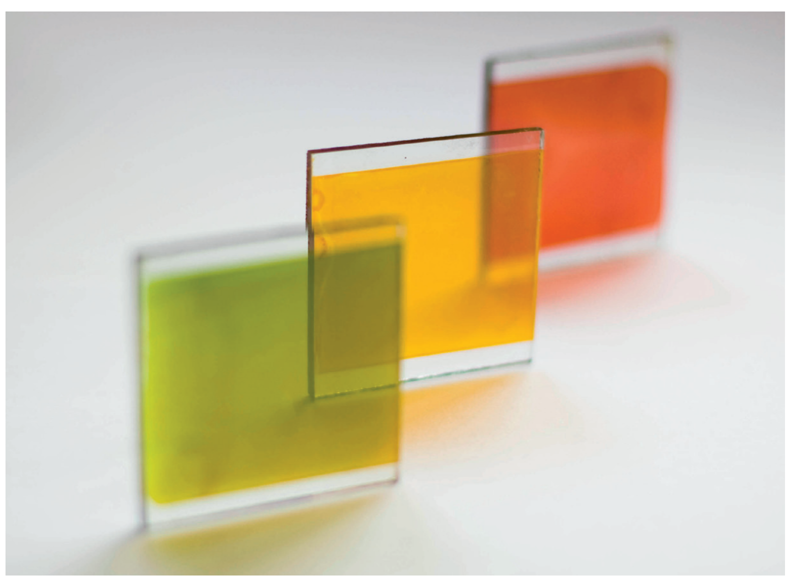

Credit: Oxford PV

On the fabrication of high-efficiency mc-Si PERC-based solar cells on diamond wire-sawn surfaces using industrially viable etching technologies

Bishal Kafle[1], Pierre Saint-Cast[1], Ahmed Ismail Ridoy[1], Sebastian Nold[1], Jonas Schön[1,2], Marc Hofmann[1], Jochen Rentsch[1],Laurent Clochard[3], Edward Duffy[3], Klaus Duncker[4], Kai Petter[4], Stefan Peters[4]
[1]Fraunhofer Institute for Solar Energy Systems ISE, Heidenhofstraße 2, 79110 Freiburg, Germany; [2]University of Freiburg, Department of Sustainable Systems Engineering, Emmy-Noether-Straße 2, 79110 Freiburg, Germany; [3]Nines Photovoltaics, IT Tallaght, Dublin 24, Ireland; [4]Hanwha Q Cells GmbH, Sonnenallee 17-21, 06766 Bitterfeld-Wolfen OT Thalheim, Germany

Abstract

Improving the texturing approach for diamond wire-sawn (DWS) multicrystalline silicon (mc-Si) wafers is one of the key steps to decrease its efficiency gap with monocrystalline silicon-based solar cells. In this regard, black silicon texturing has increasingly caught attention of both academia and industries as a potential approach towards mass production of high-efficiency mc-Si solar cells. In this paper, the challenges of implementing such a texture, with unique feature sizes, in mass production are discussed in detail, and the latest results are reviewed. Finally, results of the first trials at high volume manufacturer applying an alternative plasma-less dry-chemical etching (ADE) method are presented.

Introduction

A significant cost reduction in wafering is possible through the adoption of diamond wire (DW) sawing for monocrystalline (mono-Si) and multicrystalline (mc-Si)-based solar cells. The major advantages of using the DW-sawing method are its low Si kerf loss during sawing, and lower operational costs by avoiding the use and management of a complex slurry mixture [1]. However, in spite of the above mentioned benefits, the switch from standard multi wire slurry sawing to DW-sawing is slower for mc-Si wafers in comparison to mono-Si wafers. The reason for this slower transition for mc-Si is mainly because of the problem associated with the incompatibility of the conventional wet-chemical texturing process. Consequently, an easy adoption of diamond wire sawing aided with a gradually easing out supply constraint of the mono-Si wafer has significantly decreased its price gap with the mc-Si wafer.

Lately with the advent of additives, which can be added in the HNO_3/HF bath during the wet-chemical texturing process to form similar surface texture as in slurry-type wafers, conventional texturing processes can continue to be used for DW mc-Si. The cost increment in texturing by including additives has been reported to be non-significant by some industrial players. During the ongoing paradigm shift towards gigawatt deployment of photovoltaics (PV), however, the final cost per watt-peak of the module or system and eventually the levelized cost of electricity (LCOE) are becoming more important than just the price of a cell or module. This implies that increasing the conversion efficiency (η) and power output of mc-Si based cell technologies to reduce the efficiency gap with mono-Si based cell technologies is essential to keep its current market dominance.

The influence of the mono- and mc-Si based cell efficiency on watt-peak costs of the solar module and the system is summarized in Figure 1. In both cases, current capital and operational costs (CAPEX/OPEX) for a green-field investment were calculated for standard processing steps used in industrial manufacturing of passivated emitter and rear cell (PERC) concepts. Current spot market prices for DW-sawn wafers [2] are used for the calculation.

In Figure 1, cell efficiency-driven cost benefits are obvious for both mono- and mc-Si based PERC modules and systems. On the module level, a difference in cell conversion efficiency $\Delta\eta <$ 1.5% absolute is required for mc-Si PERC against mono-Si PERC in order to benefit through lower costs per watt-peak. On a system level, area-related costs per watt peak decrease with an increase in conversion efficiency, which means that the maximum allowed difference in cell efficiency for mc-Si will reduce to $\Delta\eta$ = 1.2%. For instance, mc-Si PERC solar cells with η > 20.8% would still compete on a system level in comparison to the mono-Si PERC cells with η = 22.0%. Going to the LCOE level, the allowed differences in the conversion efficiency are influenced by many other factors such as temperature coefficient and low-light performance of the modules that are not only technologically but also location specific, and therefore are not further discussed here.

In summary, achieving higher efficiency was never more important for mc-Si than in the current scenario in order to retain its competitive edge against mono-Si. Two of the major frontiers for increasing the conversion efficiency for mc-Si are: a) increasing the inherent bulk-material quality before and/or during the cell processing, and b) increasing the light absorption in the mc-Si wafer by surface texturing to achieve better anti-reflective and light trapping properties. In the former, researchers from both academia and industry are working on: a) improving crystallization and base-doping processes to produce high-quality wafers with low dislocation density, reduced impurity concentration, narrow bulk resistivity distribution [3,4]; and b) increasing the bulk lifetime during the solar cell processing by employing bulk-passivation schemes such as advanced phosphorous gettering and hydrogenation [5,6], and can be read in detail in above cited publications. In this article, the latter would be discussed more in detail.

Using additive-based wet-chemical texturing for DW-sawn mc-Si leads to a high surface reflection, and therefore no efficiency gain to the conventionally textured slurry-type mc-Si wafers is to be expected. In this regard, the adoption of DW sawing could be used as the disrupting technology that presents an opportunity to introduce novel texturing concepts promising J_{SC} improvement in comparison to the state-of-the-art techniques in solar cell production. Some of the widely promoted novel etching methods enabling high cell efficiencies of 20% on DW-sawn mc-Si wafers [7][8,9] are reactive ion etching (RIE), metal catalysed chemical etching (MCCE) and atmospheric pressure dry chemical etching (ADE). A previous article in Photovoltaics International has summarized the principle as well as the pros and cons of these methods [10]. Apart from these technologies, recently researchers from SERIS have also reported an alternative undisclosed method of nano-scale texturing, claimed to be low-cost, metal free and allowing high efficiencies [11].

Out of these technologies, RIE is typically considered to have high capital and operational costs and therefore is still not widely applied in large-scale production despite being a fairly proven and tested process to form surface texture in mc-Si. In contrast, MCCE has quickly developed to be one of the major technologies to drive the production of nanotextured high-efficiency solar cells on DW-sawn mc-Si surfaces, although there are still challenges to overcome for this technology such as: expensive consumables, a likelihood of presence of trace metal particles, and most notably a cumbersome waste management. In the meantime, ADE has evolved as a texturing method that promises the advantages of RIE and MCCE in a more cost-effective and ecological manner. The advantages are summarized as: a) high etching rate and inline modular nature of the etching tool allowing high volume production; b) low cost of ownership (COO) due to no vacuum in the process; c) easy abatement of waste gases (SiF_x, F_2) through standard wet scrubber systems; d) use of environmental friendly F_2 gas with zero global warming potential (GWP); and e) purely chemical etching without any ion-induced damage in Si. First trials with high-volume cell manufacturers have started applying the ADE technology [12].

All of the above mentioned methods are reported to form surface structures with dimensions that are either smaller or comparable to the wavelength range of the visible light.

Depending upon the feature sizes, such structures are either able to lower the overall surface reflection in a large wavelength spectrum and/or cause higher order scattering to increase the overall path length and absorption probability of the longer wavelengths in the Si wafer. Detailed studies on optical modelling of nanostructures with different structure geometry and feature sizes can be read elsewhere [13–15]. By controlling the aspect ratio of these nano-scale structures during the texturing process, very low weighted surface reflection values have been reached on both mono-Si and mc-Si wafers by using all of the above mentioned fabrication methods. Such a wafer appears black in colour, hence called as black silicon (B-Si). Especially for DW-sawn mc-Si wafer, the final surface reflection achieved by forming black silicon is much lower than what is achievable by applying HNO_3/HF based wet-chemical method with additives. The introduction of such novel textures, however, demands successive optimization of the subsequent cell processing steps like emitter diffusion, passivation and metallization in order to fulfil the promise of an improved electrical performance. Some of the major technological challenges are briefly discussed here.

Technological challenges of nanotexturing

The integration of such nano-scale texture in the standard cell processing sequence is not straightforward due to a significant difference in feature sizes compared to the structures that are formed by conventional wet-chemical texturing. Since texturing is one of the first steps in solar cell fabrication, each of the subsequent processes is significantly influenced by the introduction of nanotexture with unique surface features. Therefore, optimization of each of these process steps is required in order to fabricate efficient solar cells on nanotextured surfaces.

Optimal surface and emitter passivation

The application of a surface passivation layer reduces the minority carrier recombination in the surface. However, a large number of surface defects could remain un-passivated in the following conditions: i) the presence of surface structures that lead to a large surface area; ii) non conformality of the deposited dielectric layer; iii) higher stress-induced defects in the deposited passivation layer; and/or iv) crystal -orientation dependent recombination at the Si dielectric layer interface [16,17]. For such layers, the increase in recombination on nanotextured surfaces in comparison to the planar samples is accredited mostly to the difference in surface area ratio (S_f), which is experimentally calculated to be higher (S_f >2) in comparison to typical wet-chemical texture (for example $S_f \approx$ 1.5 1.7 for pyramid texture). However, an additional geometry dependent recombination component also has to be taken into consideration. Typical 'black' nanotextured surfaces show inverted conical geometry with a circular base radius in the range of 100-350 nm and depths in the range of 1 μm. In industrial facilities, plasma enhanced chemical vapour deposition (PECVD) is a preferred method of depositing dielectric passivation films, which, however, is not able to form a conformal coating on such structures. Meanwhile, excellently conformal coating of layers that are deposited by atomic layer deposition (ALD) allows reasonably low surface recombination velocities on rough surfaces like B-Si [18–20]. An example is shown in Figure 2 a) with the help of a cross sectional SEM image of ADE-formed black silicon that is deposited with a stack layer of ALD AlO_x/PECVD SiN_x.

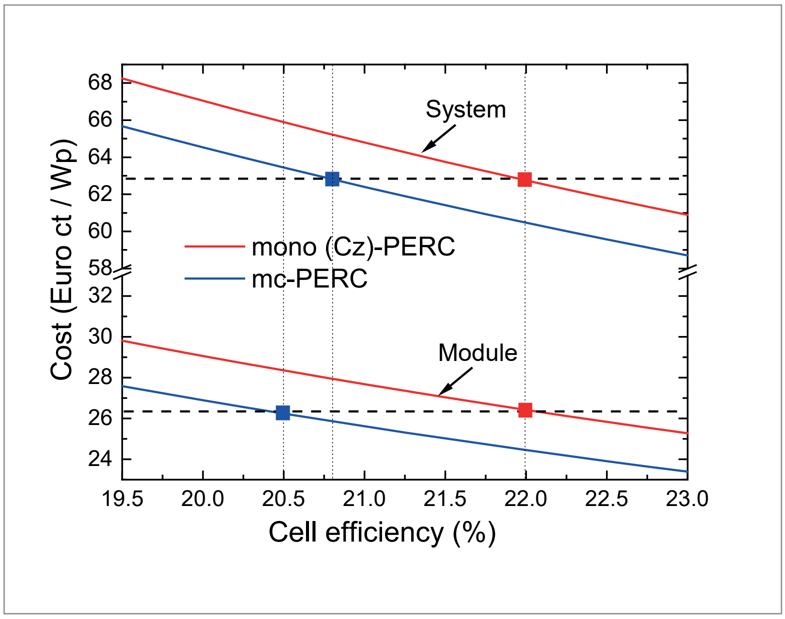

Figure 1. All-in PV module and system costs for mc PERC and Cz (mono-Si) PERC using standard PERC-process route for both types. One should note that the allowed efficiency gap $\Delta\eta$ between mc-Si and mono c-Si to reach equivalent costs decreases with increasing area-related costs. To reach a lower cost per watt-peak for mc-PERC in comparison to mono-PERC, $\Delta\eta$ <1.5% would be sufficient at the module level, whereas $\Delta\eta$ <1.2% is required on a system level.

However, industrial adoption of contemporary ALD tools is slow in PV. A quick work-around that is widely used to enhance the conformality of PECVD-layers on nanotexture is to perform a surface modification step either in alkaline or acidic solution to form modified nanotexture (M-Tex) with low S_f [21–28]. An example of such a modified nanotextured surface is shown in Figure 2 b), whereas the progression of etching and the consequent increase in weighted surface reflection (R_w) is shown in Figure 2 c). The weighted surface reflection (R_w) is calculated in the wavelength spectrum of 300-1,200 nm and a weighing function is applied using the internal quantum efficiency of a standard silicon solar cell and AM 1.5G illumination conditions [29].

Emitter diffusion process

Formation of nanotexture directly influences the emitter characteristics (total doping and emitter depth) and the homogeneity of the doping process. Insights on the nature of standard $POCl_3$-based tube diffusion on different nanotexture geometry can be obtained by performing 3-D predictive

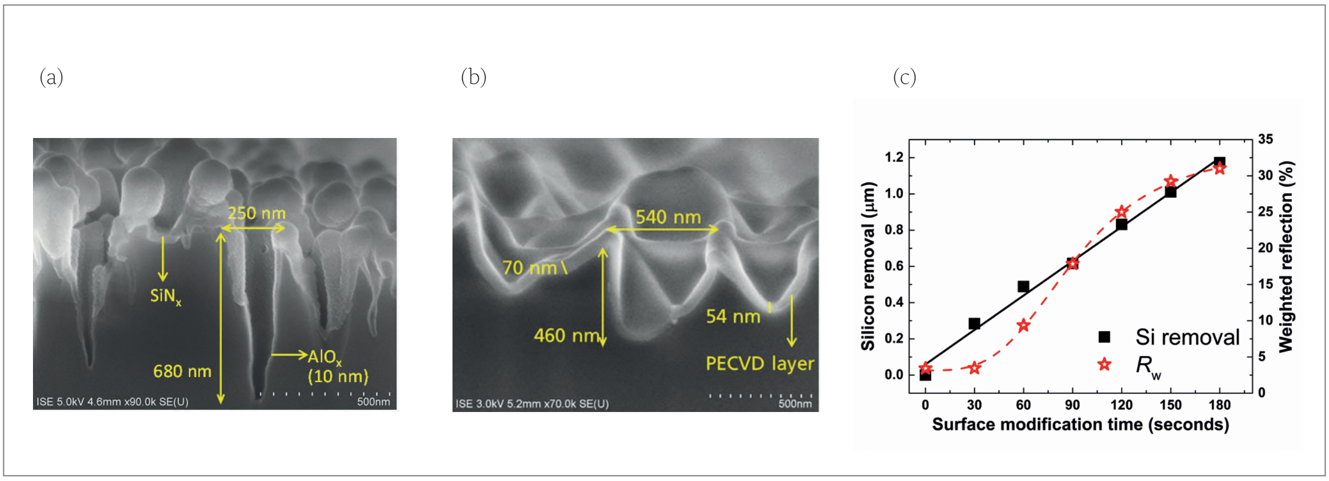

Figure 2. SEM cross sectional images of a) B Si after passivation with ALD AlO_x / PECVD SiN_x stack, and b) M Tex after passivation with PECVD SiriON/ SiN_x stack; c) plot showing increase in Si removal and surface reflection with an increasing duration of surface modification. In a) one should note that the thin ALD AlO_x forms very conformal layer in the nanostructure geometry, whereas conventional PECVD SiN_x layer is deposited mostly on the top-section of the texture and the valleys of the structures remain un passivated. In b), a conformal deposition of PECVD stack layers is achieved after surface modification.

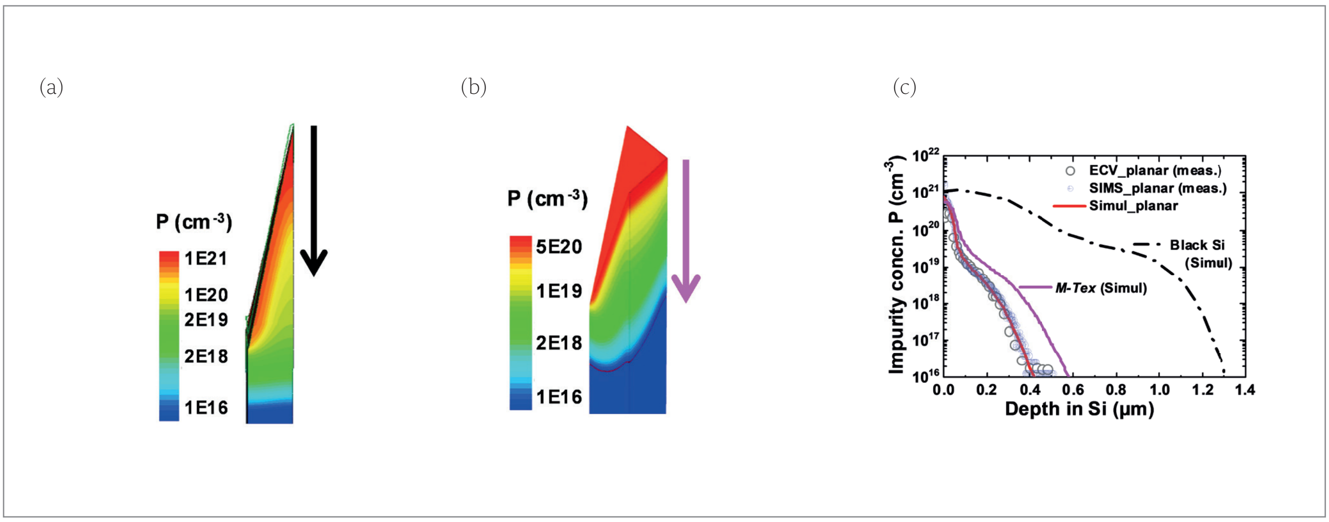

Figure 3. a) Process simulation of black silicon (B-Si) and modified texture (M Tex) showing a) cross section view of B-Si as (1/4th) nano pyramid, b) cross section view of M Tex as (1/4th) nano inverted pyramid; and c) a comparison of simulated active doping profiles of an identical emitter diffusion process on B-Si, M Tex and the planar surface. In c) 1D doping profiles are extracted for B-Si and M Tex from the 'peak' position in the direction perpendicular to the imagined planar surface, as shown by the arrows.

simulations of phosphorous in-diffusion in black-silicon (B-Si) and modified texture (M-Tex) using Sentaurus [30,31] and are presented in Figure 3. For the process simulations, M-Tex is considered to be an inverted pyramid structure with an aspect ratio of unity (width = 600 nm, depth =600 nm). Please note that B-Si has a width/height of 300 nm/1,000 nm. The dimensions are extracted from the SEM images of B-Si and M-Tex. Figure 3 a) and b) show the cross-sections of the symmetry elements of B-Si and M-Tex respectively, after the diffusion of an identical emitter. Here, different colours represent different doping regimes in the nanostructure. Figure 3 c) compares the simulated active P concentration profiles in B-Si and M-Tex surfaces that are extracted in 1 D from the peak position of nanostructures in the direction perpendicular to the imagined planar surface. For comparison, the total and active P doping profiles of the identical emitter in planar surface, which are respectively measured by using secondary ion mass spectrometry (SIMS) and electrochemical capacitance voltage (ECV) techniques, are also shown. Additionally, simulated active doping profile on planar surface is also plotted, which shows a good correlation between simulations and experiments.

In comparison to B-Si, surface modification (M-Tex surface) leads to a considerably lower active P concentration in the surface and bulk of the emitter, which means that the emitter optimization is less challenging for such surfaces. In the case of B-Si, the microscopic characterization and predictive process simulation suggest the formation of a relatively planar depletion region in comparison to the conventionally formed wet-chemical texture (acidic/pyramid) for an identical emitter diffusion. In contrast, after surface modification, the depletion region in M-Tex surface follows the nanostructure geometry very well. This indicates that an optimization of the emitter diffusion is needed for even a slight change in the surface morphology of nanostructures. In general, for all nanotextured surfaces, inclusion of an in situ oxidation process during the drive in step is found to be advantageous to avoid high doping in the emitter region. Meanwhile, the pre deposition process parameters (time, temperature, and $POCl_3$:N_2 flux) are very influential to lower the excess diffusion of both active and inactive dopants. Furthermore, it is observed that due to a large surface area, formation of nanotexture not only changes the degree of doping, but can also exacerbate the homogeneity of the emitter diffusion process. In this regard, adjustment of the pre deposition parameters is found to be crucial to improve the homogeneity of the diffusion processes.

Distribution of surface reflection on a mc-Si wafer

A mc Si wafer consists of grains of different crystal orientations. One of the challenges of the nano-scale texturing process is to maintain same etching properties in different crystal orientations. In the case of the dry etching method that uses ion-induced excitations such as in RIE, it is possible to etch all crystal orientation in the same way to leave a homogeneously etched surface with a low reflection [32,33]. The downside of such a process is the possible ion-induced damages in the crystal lattice of Si, which typically requires a defect-removal etching process before moving to further cell processing steps [33]. In other etching methods that are purely chemical in nature such as MCCE and ADE, process conditions have to be tuned to find a right balance between: a) differences in grain-grain etching, b) low surface reflection, and c) ease of integration in the subsequent cell processing steps. Especially in case of ADE, it has been observed that the starting surface before texturing plays a huge role in the grain-grain difference in reflection. An example of sister mc-Si wafers etched by applying two different ADE-based etching processes that differ mainly by process temperatures is shown in Figure 4. The corresponding weighted surface reflection measurements performed in six different grain orientations are also plotted. It can be observed that a more homogeneous texturing in different grain orientations can be achieved at a higher process temperature.

In case of MCCE, Ag nanoparticles are mostly used due to its high catalytic nature and cost-effectiveness in comparison to other noble metals such as Au and Pt [25]. However, Ag-MCCE process is also known to have crystal-orientation dependency in etching that results in some degree of etching inhomogeneity in the mc-Si wafer. In the meantime, Cu based MCCE process is shown to lack a preferential etching direction, which leads to less notable differences in morphology of nanostructures formed in different mc-Si grains [34]. Nevertheless, such a process is likely to be difficult to gain acceptance in large-scale PV manufacturing due to the likelihood of trace Cu nanoparticles in the wafer even after the cleaning process.

Meanwhile, for a less challenging integration of B-Si texture in emitter formation and PECVD deposition processes, typically the etched surfaces are further processed in an alkaline wet-chemical solution for a short duration as previously discussed (see Figure 2 b) and c)) [21,26,35,36]. In case of RIE-etched B-Si, such a post-treatment can also be used for defect-removal etching, i.e. etching of ion-induced defects and to modify the structures [33], or to remove the polymer layer formed during RIE [37]. The anisotropic etching behaviour of alkaline solution, however, leads to the formation of different surface morphologies in the grains with different orientations. Figure 5 b) shows a scan image of a typical B-Si textured mc-Si surface after post-treatment in the alkaline solution, showing a large distribution of reflection in the full-wafer area. SEM images of the darkest and the lightest grains of the mc-Si wafer, respectively in Figure 5 c) and d), show the formation of pseudo-pyramid-like structures with substantial differences in the aspect ratios, and hence the surface reflection values.

This large distribution of reflection not only directly limits the external quantum efficiency (EQE) and therefore the short circuit current density (J_{SC}) of the solar cell, but also cause concerns about the aesthetic appeal of the fabricated cell and module. Apart from optics, the optimization of emitter and PECVD deposition processes becomes challenging due to the difference in aspect ratio of nanostructures formed in different grains. The effect of such a large reflection distribution on electrical properties of the mc-Si solar cell is discussed more in detail in the later section of the article. In the meantime, applying acidic solution (HF/HNO_3) for post-treatment is being investigated to minimize the differences in morphology of nanostructures in different grains and thereby increase the J_{SC}. Apart from that, efforts on completely avoiding the post-etching steps are also being investigated for all of the above mentioned etching technologies.

Current status of high-efficiency mc-Si solar cells with nanotexture

The first step towards the application of nanotextured surfaces in high-efficiency PERC-type cells was to adapt them on conventional aluminium back-surface field (Al-BSF) architectures. The first investigations focused on understanding the challenges of integrating nano-scale structures in the subsequent cell processing steps date back as early as 2001 [38]. Extensive research into the fabrication of nanotexture on mc-Si surface and its

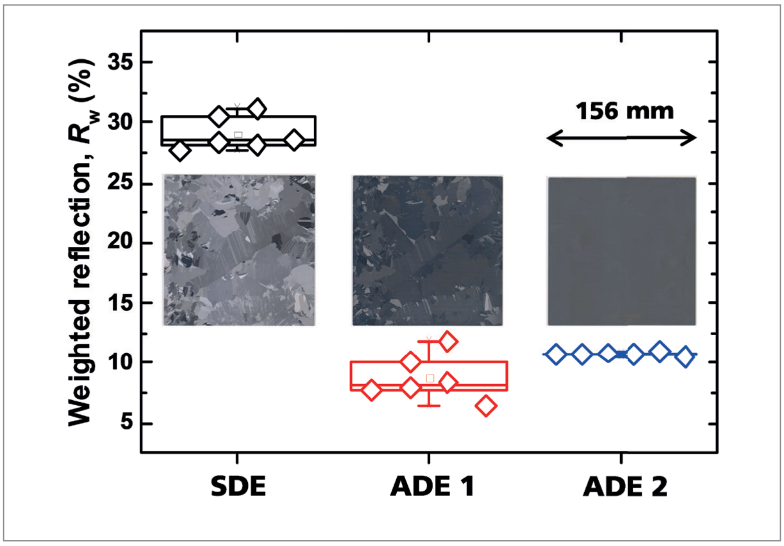

Figure 4. Plot comparing R_w measured in six different grains of the non-textured (saw-damage etched) and ADE textured mc-Si sister wafers, with inset showing scans of the wafers.

adaptation in standard solar cell process steps has since led to a steady increase in their conversion efficiencies [22,24,39][32,33,40]. Consequently, there exists a fairly large volume of literature dedicated to this topic, which cannot be covered in this article. Here, a brief review on the development towards mass production of nanotexture-based high efficiency DW-sawn mc-Si solar cells is presented.

First nanotextured mc-Si Al-BSF cells with η >18.0% and $\Delta\eta$ = 0.2-0.5% gain compared to iso textured surface were fabricated already in 2015 by employing all the above mentioned fabrication methods, namely MCCE, RIE and ADE [21,25–27,35,41]. In most of these studies, a post-etching step was applied after the black silicon texturing that is based on either alkaline or acidic solutions. Meanwhile, some studies also pointed out the possibility of avoiding this post-etching step completely and still reach comparable performances with MCCE [42] and RIE [37]. Promising results of black silicon-based Al-BSF cells paved the way to implement them in high efficiency PERC architectures and it coincided with the beginning of the phase where the PV industry needed solutions to texture diamond wire-sawn mc-Si wafers. Industrial-type high-efficiency mc-Si PERC solar cells with black silicon with efficiencies of 20% are announced by academia [8] and industry alike, culminating in the announcement of an mc-Si cell efficiency higher than 21.0% by Trina Solar with RIE [43], GCL with MCCE and RIE texture [44], and beyond 22% by JinkoSolar [45] by applying an undisclosed method of black silicon texturing. Although the details of the process steps and the associated cost-performance ratios are not disclosed, it definitely proves that mc-Si wafers would remain competitive to mono Si wafers in short and medium run. Mass production of MCCE-based mc-Si PERC cells with average efficiencies ≥ 20.5% are announced by some of the Tier 1 PV manufacturers citing a lower LCOE to that of commercially produced mono-Si-based modules [3,46]. The key towards mass production of black silicon textured cells has been the gradual adaptation of standard cell processing steps used in production facilities such as $POCl_3$ diffusion, PECVD passivation and screen-printing metallization with a strategy of making modest but continuous improvements in performance; rather than focussing only on novel disruptive technologies such as atomic layer deposition that might take some more time to become industrial standard. Two of the next steps to push the production efficiency beyond 21% are outlined as: a) lowering recombination and resistive losses in emitter and bulk, and b) use of advanced passivation schemes for texture with lower reflectivity. Recently, Fraunhofer ISE demonstrated η = 22.3% on small area using high quality n-type mc-Si material, black silicon texture and TOPCon cell concept [47] to further assert the case of mc-Si wafers to be considered with high efficiency cell architectures beyond PERC.

Figure 5: a) Typically used process flow for applying nanotextured surfaces in cell processing, b) scanned image of Gen.1 ADE-textured DW-sawn wafer and corresponding SEM images of pseudo-pyramid like structures formed in two grains – c) Grain 1 (G1) with lowest reflection and d) Grain 2 (G2) with highest reflection properties in the mc-Si wafer shown in b).

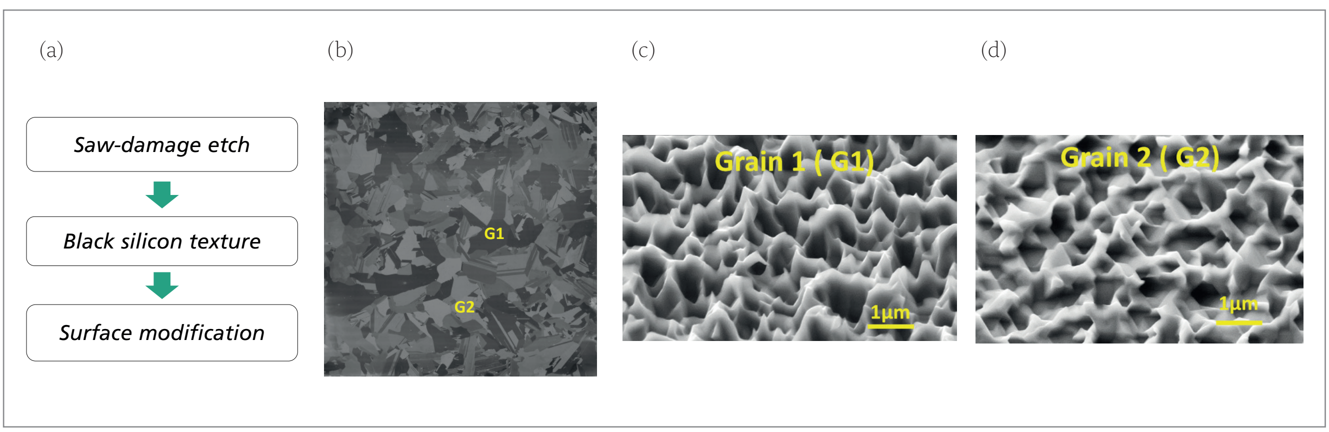

ADE-based mc-Si PERC solar cells

Formation of nano-scale structures on mc-Si surfaces by using ADE and their successful integration in Al-BSF type mc Si solar cells is already achieved and discussed in past publications [27,48]. Here, we briefly discuss the integration of different generations of ADE textured p-type mc-Si wafers in passivated emitter and rear cell (PERC)-type architectures [9]. ADE-based texturing does not distinguish between slurry and DW-sawn mc-Si surfaces and show comparable etching results. In the first generation, slurry-sawn high performance (HP) mc-Si wafers are chosen to see the potential of ADE-texture in terms of achievable V_{OC} and J_{SC} values. The process plan for first-generation mc-Si solar cells is shown in Figure 6 a).

The reference group of wafers is acidically textured in an HF/HNO_3 solution to reach typical weighted reflection values (R_w) of 26-27%. The test group of wafers is first saw-damage etched and then textured using the ADE process, during which the wafers are dynamically transported in an inline mode through the reaction chamber of the ADE tool with the process described elsewhere in detail [48]. After formation of B-Si, a short post-treatment in an alkaline solution is performed in the process described in Figure 2 c) to reach the average weighted surface reflection of 18%. The ADE-textured and the reference groups are subjected to $POCl_3$-based tube diffusion to form an n-type emitter. No significant differences in the emitter sheet resistance (R_{SH}) values are observed between the test and reference groups. Afterwards, the rear side emitter is removed. It has to be mentioned that since ADE is a single-sided process, the rear side is essentially flat. Therefore, typically used rear-sided polishing can be modified to just remove the rear-side emitter. Afterwards, the Q.ANTUM process [49] of Hanwha Q-Cells is applied to prepare PERC solar cells. Illuminated I-V measurements are performed under the standard test conditions using an in-house solar simulator that is calibrated with the Fraunhofer ISE CalLab reference. The results are presented in the table in Figure 6. The best solar cells of both test and reference groups are measured independently by Fraunhofer ISE CalLab and are also listed.

ADE-textured solar cells show an average conversion efficiency η = 20.0%, which is +0.2% absolute higher than the reference iso-textured solar cells fabricated on same material in this batch. The champion solar cell reaches 20.1%. The gain in η is solely because of a higher J_{SC} value of ADE textured solar cell pertaining to a lower surface reflection and an improved light trapping in comparison to the reference solar cell. An equivalent V_{OC} of test and reference groups suggests no significant electrical losses on test cells due to the surface and emitter recombination of the charge carriers. Furthermore, the nanotextured surface facilitates a low contact resistance between the emitter and screen-printed Ag grid [50], thus leading to an equivalent FF to the reference groups in this batch. Figure 7 shows the high resolution (200 µm) surface reflection mapping at 405 nm wavelength of an ADE textured solar cell, which is measured using a light beam-induced current (LBIC) method using a PV Tools Loana system.

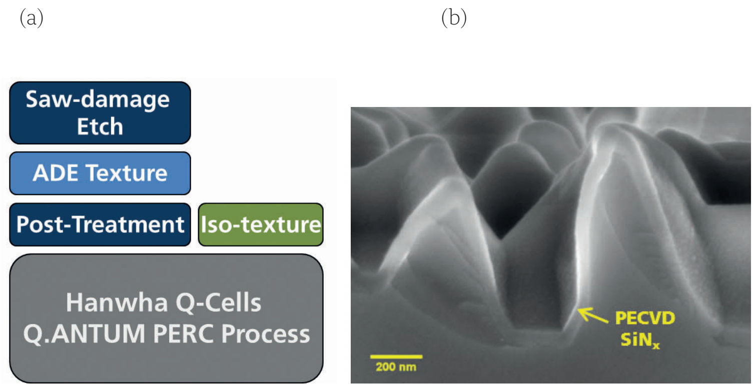

(c)

Texture type	Value (# cells)	V_{oc} (mV)	J_{sc} (mA/cm²)	*FF* (%)	η (%)
ADE	Avg. (12)	659	38.2	79.5	20.0
ADE	Best*)	660	38.4	79.4	20.1
Reference	Avg. (15)	658	37.9	79.5	19.8
Reference	Best*)	660	37.9	79.4	19.9

Figure 6. a) Process plan for mc-Si PERC solar cells, b) SEM image showing example of a conformal deposition of PECVD SiNx on nanostructures formed in a mc-Si wafer after applying ADE etching and surface-modification step, c) table showing I-V parameters of the ADE and reference iso-textured groups with base resistivity $\rho_b \approx 1.8\ \Omega$ cm. Cell area is A_{cell} = 15.6×15.6 cm² and all cells feature solder pads, *) independently measured by Fraunhofer ISE CalLab.

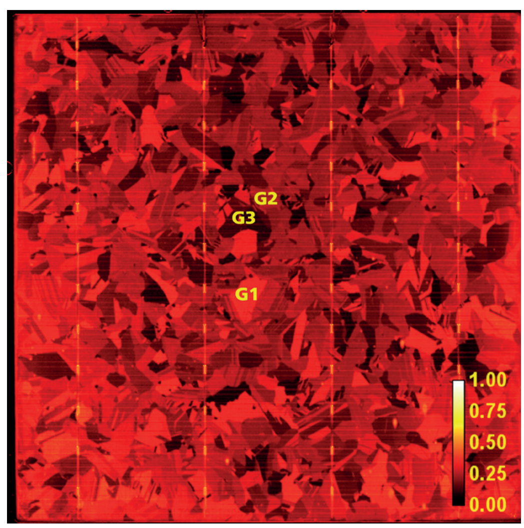

Figure 7. Reflection scan at 405 nm for ADE textured solar cell, with inset showing reflection and three different grains – G1,G2,G3; where local quantum efficiency measurements are also performed using PV-tools Loana system for the wavelength spectrum of 300-1200 nm.

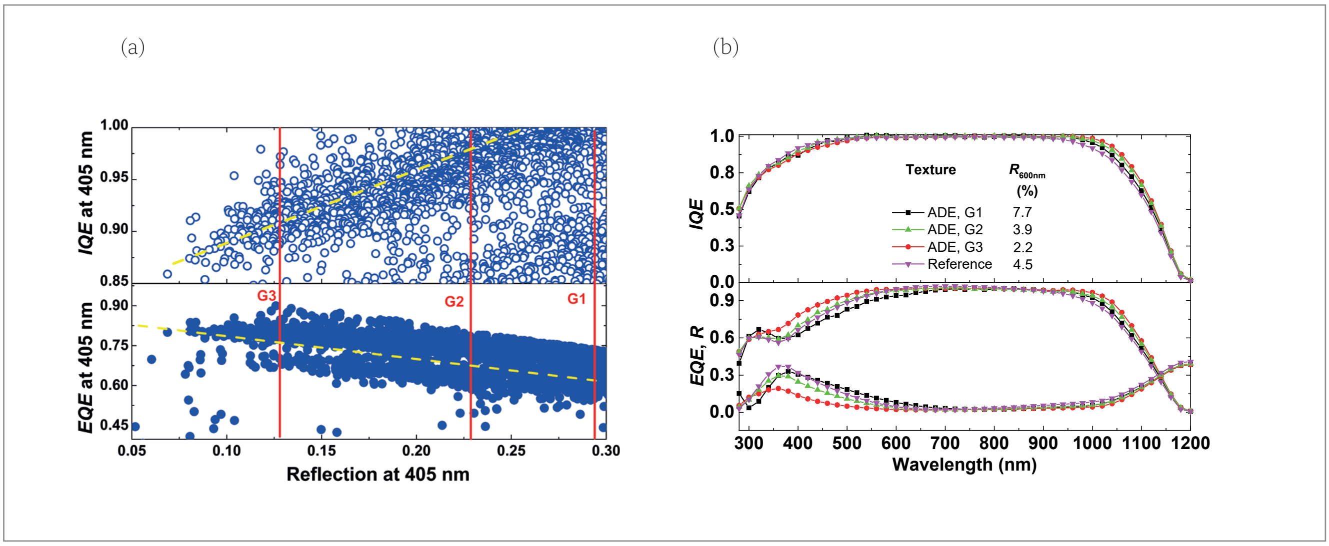

Figure 8. a) plot showing IQE and EQE of ADE-textured solar cell against corresponding reflection values at 405 nm, and b) locally measured IQE, EQE and R for three different grains G1,G2,G3 in a), showing reflection values at 600 nm. In a), the full red lines show the positions of G1, G2 and G3; whereas the dashed yellow lines serve as guides for eye.

A large distribution of reflection values can be observed in ADE textured solar cell, mainly due to the problems associated to the anisotropic nature of the post-etching process.

The influence of surface reflection on EQE and IQE of the ADE textured solar cell at 405 nm is depicted in Figure 8 a).

Here, lower reflection values correspond to higher EQE values, following a noisy but an overall linear relationship. The plot also suggests that lowering the reflection, however, still negatively impacts the IQE of the solar cell at short wavelengths until a certain value of surface reflection is reached after which the IQE saturates to its highest value. In order to have a more detailed understanding of this matter, local measurements of IQE/EQE/R are performed in three different mc-Si grains. Based on the LBIC reflection mapping in Figure 8 b), grain 1 (G1), grain 2 (G2) and grain 3 (G3) were chosen as the areas representing highest, moderate and lowest reflection values respectively in the full-area of an ADE textured solar cell with measured reflection values R_{600nm} of 7.7%, 3.9% and 2.2% respectively at 600 nm. In comparison, R_{600nm} of 4.5% is measured for the reference textured solar cell. Please note that the reflection of Ag is not subtracted during the estimation of reflection values. It can be seen that only G2 and G3 EQE values predict a gain in J_{SC} value to the reference texture in the wavelength spectrum of 300-700 nm and 900-1100 nm. Meanwhile, G1 predicts a loss in J_{SC} value due to a higher reflection than the reference texture. No significant losses in IQE are observed at short wavelengths for ADE texture of all types in comparison to the reference texture. Therefore, it can be maintained that the surface and emitter recombination are not significantly limiting the electrical parameters of the ADE textured solar cells that are fabricated in the current batch. In fact, a higher IQE for ADE-texture in comparison to the reference texture is

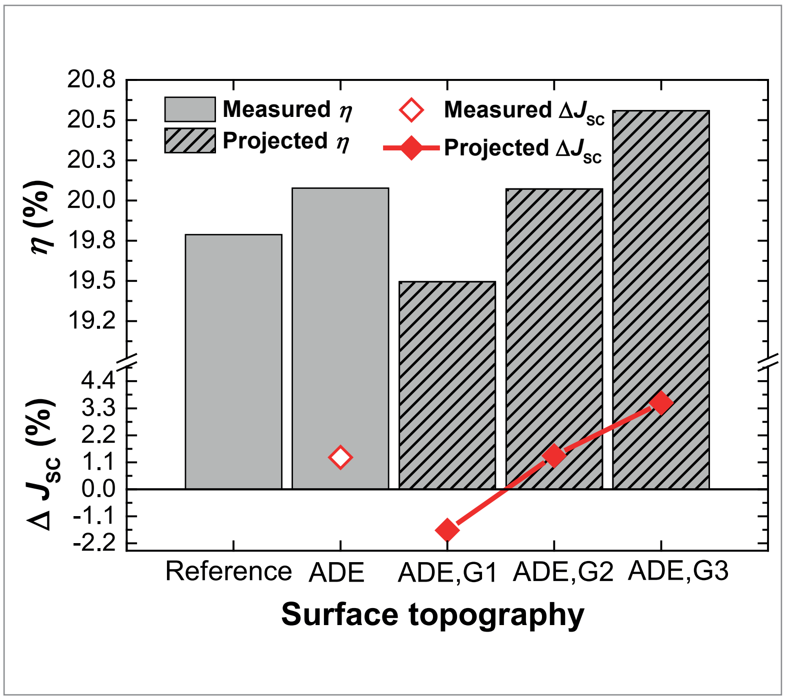

Caption Figure 9. Plot showing projected percentage change in J_{SC} (ΔJ_{SC}) and corresponding in comparison to the reference texture, considering a homogeneous ADE texture of either of type G1, G2 or G3 respectively along the full area of the solar cell. In addition, measured of best reference and ADE textured solar cells and measured ΔJ_{SC} (%) of best ADE-textured solar cell are also shown.

observed at longer wavelengths (λ >950 nm) possibly due to higher scattering of these wavelengths at front-texture. This phenomenon is subject to further investigations.

We estimate the relative percentage change in J_{SC} value of ADE textured solar cell in comparison to the reference, assuming a homogeneous texture G1, G2 or G3 across the whole wafer area, with the following equation:

$$J_{SC} = q \int_{\lambda=280}^{\lambda=1200} \phi(\lambda) \times EQE(\lambda)\, d\lambda,$$

where q is the elementary charge of an electron and $\phi(\lambda)$ is the incident photon flux.

Figure 9 plots the measured and projected percentage change in J_{SC} (ΔJ_{SC}) of ADE texture to that of best reference textured solar cell based on this calculation.

The measured ΔJ_{SC} for the best ADE textured surface is +1.3% higher in comparison to the best reference textured solar cell. Grain 3 (G3) is found to have the maximum difference between measured and calculated values of ΔJ_{SC} in ADE-textured wafer (ΔJ_{SC}=+3.5%). This corresponds to an absolute enhancement potential of up to +0.8% in conversion efficiency to the reference texture without any further optimizations in emitter diffusion and surface passivation.

By evaluating Gen.1 ADE-textured mc-Si PERC solar cells, it became evident that the next steps required in further increasing the J_{SC} of ADE-textured cells should focus both on lowering an overall reflection as well as to narrow the spatial distribution of reflectivity. This requires evaluating the ADE-texturing process, and most importantly the impact of the post-treatment step on different mc-Si grains. In the next generations (Gen.2 and Gen.3), collective optimization of ADE and post-etching processes is performed on DW-sawn mc-Si wafers in order to achieve best optical and electrical performances in the cell-level. Figure 10 a) shows the scan image of Gen.3 ADE-textured DW-sawn mc-Si wafer, which shows a narrow distribution of reflection in the whole wafer-area. The etching process is developed to obtain spherical cap-like structures with dimensions of 1 µm. Such characteristic dimensions are expected to cause high scattering of the middle and long wavelengths of visible light, leading to an improved light trapping in comparison to sub-micron wavelength structures. In Figure 10 b), an SEM image of a boundary region of three grains in the Gen.3 ADE-textured surface is shown. The etching process developed for Gen.3 ADE texture leads to the formation of spherical cap-like structures homogeneously in all crystal orientations of the mc-Si wafer. In this particular wafer, the weighted surface reflection measured along the full-wafer area is in the range of 14-17% after the texturing process.

Figure 11 depicts histograms comparing the distribution of reflection values at 405 nm for the full wafer area of ADE textured samples of different generations after PECVD SiN_x anti-reflective coating, which are extracted from the Loana tool. For comparison, reflection data of industrially applied additive-based texture after SiN_x coating is also included.

One should note a significantly smaller reflection distribution for Gen.3 ADE texture in comparison to previous generations. This improvement in reflection distribution is achieved in just two iterations of process optimization. In comparison to the additive-based wet-chemical texture on DW-sawn wafers, Gen.3 ADE texture shows both lower average reflection values as well as a comparable reflection distribution in the full wafer area. Using Gen. 3 texture, we expect to further increase the conversion efficiency ($\eta \approx 20.5\%$) for DW-sawn mc-Si PERC in upcoming cell batches.

Summary

DW-sawn mc-Si wafers can now be textured to a satisfying level by using additives in conventional wet-chemical processing, leading to similar reflection as the isotexturing process used for slurry-type mc-Si wafers. However, increasing the efficiency of mc-Si-based solar cells is essential to keep it competitive against the mono-Si based technologies in system and LCOE levels. Black silicon texturing has received an increased attention from academia and industries alike due to its promise to boost the current and conversion efficiency of DW-sawn mc-Si solar cell. Some technologies that are getting mature for large scale production are MCCE, RIE and ADE, although RIE method is considered to have higher capital and operational costs. Due to their unique feature sizes, nano-scale texturing poses major challenges in standard cell fabrication steps, mainly in surface passivation and emitter diffusion. These challenges are met by modifying the surface in a post-treatment step after formation of black silicon that, however, could lead to a large reflection and colour distribution in a mc-Si wafer. To mitigate this problem, strategies are being implemented in the direction of either applying a more isotropic post-etching step or to completely avoid this additional step altogether. Stepping on the massive research in this area, black silicon based mc-Si PERC solar cells with efficiencies >20.0% are beginning to be mass produced by solar cell manufacturers. ADE method of black silicon texturing is presented to be an alternative to MCCE and RIE due to its technological and ecological advantages. Already in the first trials in the industrial pilot-line of high-volume manufacturer, efficiencies of 20% are achieved on ADE-textured mc-Si PERC architecture.

Acknowledgements

This work is partly funded by the federal ministry for economic affairs and energy (BMWi) of Germany within the project APPI under the contract number 0325895A. Project APPI is supported under the umbrella of SOLAR-ERA.NET Cofund by Agence de l'Environnement et de la Maîtrise de l'Energie, Project management Jülich, Technology Strategy Board and Centro para el desarollo tecnológico. SOLAR-ERA.NET is supported by the European Commission within the EU Framework Programme for Research and Innovation HORIZON 2020 (Cofund ERA-NET Action, N° 691664). The authors would like to thank all co-workers at photovoltaics department of Fraunhofer ISE, especially Elisabeth Schaeffer and Felix Martin for their help in solar cell characterization.

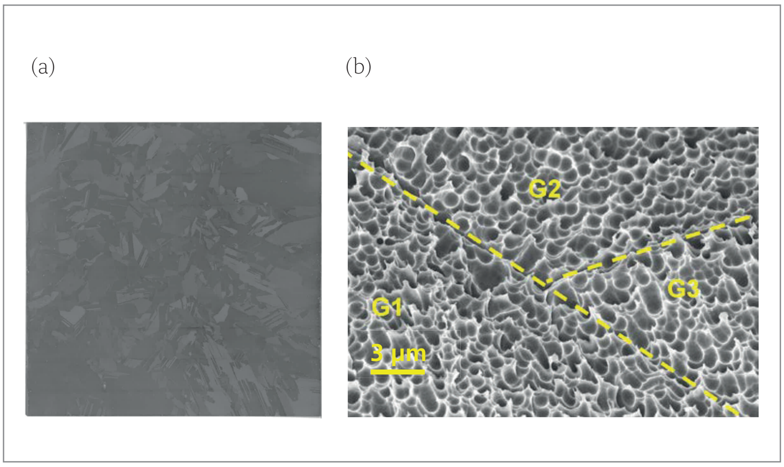

Figure 10. a) Scan image of Gen.3 ADE-textured DW-sawn wafer, b) SEM image showing tilted cross-section view of the boundary region of three grains (G1,G2,G3) in a).

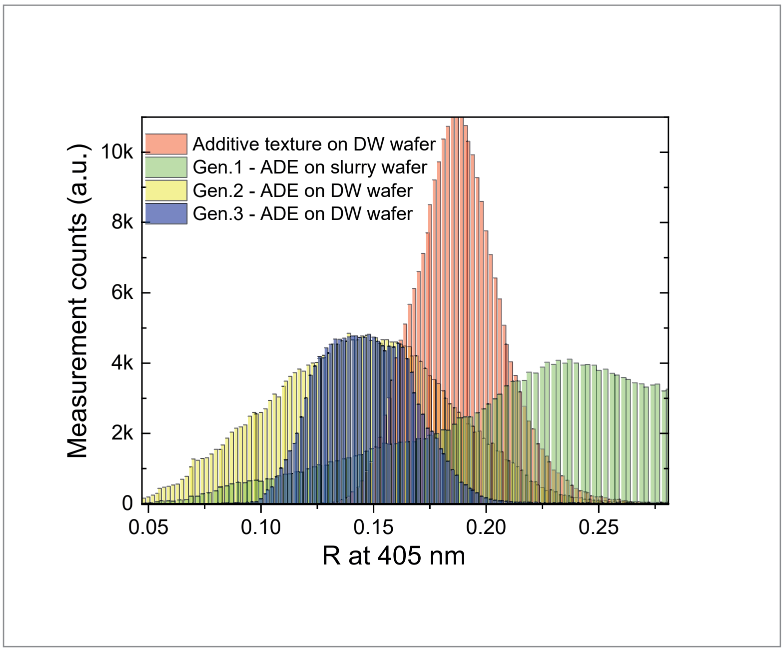

Figure 11. Histograms showing distribution of reflection at 405 nm in the full wafer area for different generations of ADE texture, in comparison to the additive-based acidic texture on DW-sawn wafer. Please note that, for all samples, reflection measurements are performed after applying PECVD SiN_x ARC layer on textured surfaces.

References

[1] B. Meinel, T. Koschwitz, C. Blocks, J. Acker, Comparison of diamond wire cut and silicon carbide slurry processed silicon wafer surfaces after acidic texturisation, Materials Science in Semiconductor Processing 26 (2014) 93–100.

[2] http://pvinsights.com/ (accessed on August 3, 2018).

[3] Yuepeng Wan, Differentiated High Performance Silicon Materials for High Efficiency Solar Cell and Modules, in 12th SNEC PV Power Expo (2018).

[4] C.W. Lan et al., in International PVSEC-25, Busan, South Korea (2015).

[5] H.C. Sio, S.P. Phang, P. Zheng, Q. Wang, W. Chen, H. Jin, D. Macdonald, Recombination sources in p-type high performance multicrystalline silicon, Jpn. J. Appl. Phys. 56 (8S2) (2017) 08MB16.

[6] B. Hallam, D. Chen, M. Kim, B. Stefani, B. Hoex, M. Abbott, S. Wenham, The role of hydrogenation and gettering in enhancing the efficiency of next-generation Si solar cells: An industrial perspective, Phys. Status Solidi A 214 (7) (2017) 1700305.

[7] Shu Zhang, Yang Yang, Daming Chen, Weiwei Deng, Hongwei Huang, Pietro P. Altermatt, Jianmei Xu, Zhiqiang Feng and Pierre J. Verlinden, 19.86% Aperture Efficient World Record P-type Multi-crystalline Module with 20.59% Efficient PERC Solar Cells, in 44th IEEE Photovoltaic Specialists Con-ference, Wahington D.C., United States (2017).
[8] J. Jin, H. Shen, P. Zheng, K.S. Chan, X. Zhang, H. Jin, >20.5% Diamond Wire Sawn Multicrystalline Sili-con Solar Cells With Maskless Inverted Pyramid Like Texturing, IEEE J. Photovoltaics 7 (5) (2017) 1264–1269.
[9] B. Kafle, A. I. Ridoy, P. Saint-Cast, L. Clochard, E. Duffy, K. Duncker, K. Petter, M. Hofmann, J. Rentsch, Atmospheric Pressure Dry Texturing Enabling 20% Conversion Efficiency on Multicrystalline Silicon PERC Solar Cells, in Silicon PV, Lausanne (2018).
[10] J. Rentsch, B. Kafle, M. Hofmann, K. Krieg, M. Zimmer, Texture etching technologies for diamond-wire-sawn mc-Si solar cells, Photovoltaics International 38 (2018).
[11] Armin Aberle, Global trends in crystalline silicon photovoltaics, in SNEC PV Power Expo (2018).
[12] Press release, Nines Photovoltaics, May 25th 2018.
[13] Hitoshi Sai, Homare Fujii, Koji Arafune, Yoshio Ohshita, Yoshiaki Kanamori, Hiroo Yugami, and Masa-fumi Yamaguchi, Wide-Angle Antireflection Effect of Subwavelength Structures for Solar Cells, Jpn. J. Appl. Phys. 46 (6A) (2007).
[14] H. Sai, Y. Kanamori, K. Arafune, Y. Ohshita, M. Yamaguchi, Light trapping effect of submicron sur-face textures in crystalline Si solar cells, Prog. Photovolt: Res. Appl. 15 (5) (2007) 415–423.
[15] A.J. Bett, J. Eisenlohr, O. Hohn, P. Repo, H. Savin, B. Blasi, J.C. Goldschmidt, Wave optical simulation of the light trapping properties of black silicon surface textures, Optics express 24 (6) (2016) A434-45.
[16] K.R. McIntosh, L.P. Johnson, Recombination at textured silicon surfaces passivated with silicon diox-ide, J. Appl. Phys. 105 (12) (2009) 124520.
[17] C. Schwab, A. Wolf, M. Graf, N. Wöhrle, S. Kühnhold, J. Greulich, G. Kästner, D. Biro, R. Preu, Re-combination and Optical Properties of Wet Chemically Polished Thermal Oxide Passivated Si Surfac-es, IEEE J. Photovoltaics 3 (2) (2013) 613–620.
[18] G. von Gastrow, R. Alcubilla, P. Ortega, M. Yli-Koski, S. Conesa-Boj, Fontcuberta i Morral, Anna, H. Savin, Analysis of the Atomic Layer Deposited Al2O3 field-effect passivation in black silicon, Solar Energy Materials and Solar Cells 142 (2015) 29–33.
[19] M. Otto, M. Kroll, T. Käsebier, R. Salzer, A. Tünnermann, R.B. Wehrspohn, Extremely low surface recombination velocities in black silicon passivated by atomic layer deposition, Appl. Phys. Lett. 100 (19) (2012) 191603.
[20] P. Repo, A. Haarahiltunen, L. Sainiemi, M. Yli-Koski, H. Talvitie, M.C. Schubert, H. Savin, Effective Passivation of Black Silicon Surfaces by Atomic Layer Deposition, IEEE J. Photovoltaics 3 (1) (2013) 90–94.
[21] F. Cao, K. Chen, J. Zhang, X. Ye, J. Li, S. Zou, X. Su, Next-generation multi-crystalline silicon solar cells: Diamond-wire sawing, nano-texture and high efficiency, Solar Energy Materials and Solar Cells 141 (2015) 132–138.
[22] D.Z. Dimitrov, C.-H. Lin, C.-H. Du, C.-W. Lan, Nanotextured crystalline silicon solar cells, Phys. Status Solidi A 208 (12) (2011) 2926–2933.
[23] X.X. Lin, Y. Zeng, S.H. Zhong, Z.G. Huang, H.Q. Qian, J. Ling, J.B. Zhu, W.Z. Shen, Realization of im-proved efficiency on nanostructured multicrystalline silicon solar cells for mass production, Nano-technology 26 (12) (2015) 125401.
[24] J. Oh, H.-C. Yuan, H.M. Branz, An 18.2%-efficient black-silicon solar cell achieved through control of carrier recombination in nanostructures, Nat Nano 7 (11) (2012) 743–748.
[25] X. Ye, S. Zou, K. Chen, J. Li, J. Huang, F. Cao, X. Wang, L. Zhang, X.-F. Wang, M. Shen, X. Su, 18.45%-Efficient Multi-Crystalline Silicon Solar Cells with Novel Nanoscale Pseudo-Pyramid Texture, Adv. Funct. Mater. 24 (42) (2014) 6708–6716.
[26] Z. Yue, H. Shen, Y. Jiang, W. Chen, Q. Tang, J. Jin, T. Pu, J. Luo, F. Kong, C. Rui, J. Cai, Large-scale black multi-crystalline silicon solar cell with conversion efficiency over 18 %, Appl. Phys. A 116 (2) (2014) 683–688.
[27] B. Kafle, A. Mannan, T. Freund, L. Clochard, E. Duffy, M. Hofmann, J. Rentsch, and R. Preu, Nanotex-tured multicrystalline Al-BSF solar cells reaching 18% conversion efficiency using industrially viable solar cell processes, Phys. Status Solidi RRL 9 (8) (2015) 448–452.
[28] B. Kafle, T. Freund, A. Mannan, L. Clochard, E. Duffy, S. Werner, P. Saint-Cast, M. Hofmann, J. Rentsch, and R. Preu, Plasma-free dry-chemical texturing process for high-efficiency multicrystalline silicon solar cells, Energy Procedia 92 (2016) 359–368.
[29] J. Zhao, M.A. Green, Optimized antireflection coatings for high-efficiency silicon solar cells, IEEE Trans. Electron Devices 38 (8) (1991) 1925–1934.
[30] B. Kafle, J. Schön, C. Fleischmann, S. Werner, A. Wolf, L. Clochard, E. Duffy, M. Hofmann, J. Rentsch, On the emitter formation in nanotextured silicon solar cells to achieve improved electrical perfor-mances, Solar Energy Materials and Solar Cells 152 (2016) 94–102.
[31] J. Schön, A. Abdollahinia, R. Müller, J. Benick, M. Hermle, W. Warta, M.C. Schubert, Predictive Simu-lation of Doping Processes for Silicon Solar Cells, Energy Procedia 38 (2013) 312–320.
[32] J. Yoo, J.-S. Cho, S. Ahn, J. Gwak, A. Cho, Y.-J. Eo, J.-H. Yun, K. Yoon, J. Yi, Random reactive ion etching texturing techniques for application of multicrystalline silicon solar cells, Thin Solid Films

546 (2013) 275–278.
[33] G. Xiao, B. Liu, J. Liu, Z. Xu, The study of defect removal etching of black silicon for solar cells, Mate-rials Science in Semiconductor Processing 22 (2014) 64–68.
[34]J. Zha, T. Wang, C. Pan, K. Chen, F. Hu, X. Pi, X. Su, Constructing submicron textures on mc-Si solar cells via copper-catalyzed chemical etching, Appl. Phys. Lett. 110 (9) (2017) 93901.
[35] Y.F. Zhuang, S.H. Zhong, Z.G. Huang, W.Z. Shen, Versatile strategies for improving the performance of diamond wire sawn mc-Si solar cells, Solar Energy Materials and Solar Cells 153 (2016) 18–24.
[36]B. Kafle, T. Freund, A. Mannan, L. Clochard, E. Duffy, S. Werner, P. Saint-Cast, M. Hofmann, J. Rentsch, R. Preu, Plasma-free Dry-chemical Texturing Process for High-efficiency Multicrystalline Silicon Solar Cells, Energy Procedia 92 (2016) 359–368.
[37] S. Liu, X. Niu, W. Shan, W. Lu, J. Zheng, Y. Li, H. Duan, W. Quan, W. Han, C.R. Wronski, D. Yang, Im-provement of conversion efficiency of multicrystalline silicon solar cells by incorporating reactive ion etching texturing, Solar Energy Materials and Solar Cells 127 (2014) 21–26.
[38]S.H. Zaidi, D.S. Ruby, J.M. Gee, Characterization of random reactive ion etched-textured silicon solar cells, IEEE Trans. Electron Devices 48 (6) (2001) 1200–1206.
[39]B.T. Chan, E. Kunnen, M. Uhlig, J.-F.d. Marneffe, K. Xu, W. Boullart, B. Rau, J. Poortmans, Study of SF6/N2O Microwave Plasma for Surface Texturing of Multicrystalline (150 mu m) Solar Substrates, Jpn. J. Appl. Phys. 51 (2012) 10.
[40] Y. Liu, T. Lai, H. Li, Y. Wang, Z. Mei, H. Liang, Z. Li, F. Zhang, W. Wang, A.Y. Kuznetsov, X. Du, Nanostructure Formation and Passivation of Large-Area Black Silicon for Solar Cell Applications, Small 8 (9) (2012) 1392–1397.
[41] Y. Jiang, H. Shen, T. Pu, C. Zheng, Q. Tang, K. Gao, J. Wu, C. Rui, Y. Li, Y. Liu, High efficiency multi-crystalline silicon solar cell with inverted pyramid nanostructure, Solar Energy 142 (2017) 91–96.
[42]Z. Ying, M. Liao, X. Yang, C. Han, J. Li, J. Li, Y. Li, P. Gao, J. Ye, High-Performance Black Multicrystal-line Silicon Solar Cells by a Highly Simplified Metal-Catalyzed Chemical Etching Method, IEEE J. Pho-tovoltaics 6 (4) (2016) 888–893.
[43]Trina Solar Press Release, 2015.
[44] GCL System Integration Technology Co., Ltd. Solar MBU, GCL roadmap to mass production with 21% efficient multicrystalline PERC cells and 300W+ modules, in SNEC PV Power Expo (2018).
[45]JinkoSolar Press release, 2017.
[46] Guoqiang Xing, CELL AND MODULE TECHNOLOGIES FOR MULTI C-SI TO KEEP THE WINNING EDGE, in SNEC PV Power Expo (2018).
[47]J. Benick, R. Müller, F. Schindler, A. Richter, H. Hauser, F. Feldmann, P. Krenckel, S. Riepe, M. C. Schubert, M. Hermle, S. W. Glunz, APPROACHING 22% EFFICIENCY WITH MULTICRYSTALLINE N-TYPE SILICON SOLAR CELLS, in 33rd European PV Solar Energy Conference and Exhibition, Amsterdam, The Netherlands (2017).
[48]B. Kafle, J. Seiffe, M. Hofmann, L. Clochard, E. Duffy, J. Rentsch, Nanostructuring of c-Si surface by F2 -based atmospheric pressure dry texturing process, Phys. Status Solidi A 212 (2) (2015) 307–311.
[49] P. Engelhart, D. Manger, B. Klöter, S. Hermann, A.A. Stekolnikov, S. Peters, H.-C. Ploigt, A. Eifler, C. Klenke, A. Mohr, G. Zimmermann, B. Barkenfelt, K. Suva, J. Wendt, T. Kaden, S. Rupp, D. Rychtarik, M. Fischer, J.W. Müller, P. Wawer, Q.ANTUM – Q-CELLS NEXT GENERATION HIGH-POWER SILICON CELL & MODULE CONCEPT, in 26th European PV Solar Energy Conference and Exhibition, Hamburg, Germany (2012).
[50]B. Kafle, T. Freund, S. Werner, J. Schön, A. Lorenz, A. Wolf, L. Clochard, E. Duffy, P. Saint-Cast, M. Hofmann, J. Rentsch, On the Nature of Emitter Diffusion and Screen-Printing Contact Formation on Nanostructured Silicon Surfaces, IEEE Journal of Photovoltaics 7 (1) (2017) 136–143.

About the Authors

Bishal Kafle completed his MSc and PhD degree in microsystems engineering from Albert-Ludwigs University of Freiburg, Germany in 2011 and 2017 respectively. His PhD degree was related to developing novel texture for mono-and multi-crystalline Si wafers and integrating them into the further solar cell processing steps. At Fraunhofer ISE, his current research focusses on integration of novel textures on cell and module level, and optimizing processing steps for rear passivated solar cells.

Pierre Saint-Cast received an MSc degree in micro-and nanoelectronics from Joseph Fourier University, Grenoble, France, and an engineering degree from the Polytechnic Institute of Grenoble, both in 2007. In 2012, he received his PhD from the University of Konstanz, in Germany. Since 2008 he has been with Fraunhofer Institute for Solar Energy Systems, Freiburg, Germany. His research interests include the development of passivation layers for solar cell applications, the processing, analysis and analytical modelling of PERC solar cells.

Ahmed Ismail Ridoy received his MSc degree in optics and photonics from the Karlsruhe Institute of Technology (KIT) in 2014. Currently he is conducting his doctoral research at the Fraunhofer ISE. His doctoral research focuses on the development of novel non-plasma dry texturing technique alternative to the industrially-standard texturing technique for passivated emitter and rear multicrystalline silicon solar cells.

Sebastian Nold studied industrial engineering at the University of Karlsruhe, Germany, and the University of Dunedin, New Zealand, and earned his diploma in industrial engineering at Karlsruhe in 2009. He has been working at the Fraunhofer ISE since 2008 in the field of cost calculation, technology assessment and economic evaluation of new concepts in the production of silicon solar cells. Sebastian is currently completing his doctoral thesis at the ISE on the economic assessment of silicon solar cell production along the PV value chain.

Jonas Schön received a diploma in physics from the University of Hamburg, Germany, in 2006 and a PhD degree from the University of Constance in collaboration with Fraunhofer ISE in 2011. Currently, he is a scientist in the department of sustainable systems engineering (INATECH) of the University of Freiburg and the Fraunhofer ISE. His research interests include simulation of impurities in silicon, cell processing and novel solar cells.

Marc Hofmann is Head of the Plasma Technology group at Fraunhofer ISE. In 2003, he received a diploma degree in electrical engineering from the University of Applied Sciences Koblenz, Germany, and a Ph.D. degree in physics from the University of Konstanz, Germany in 2008. His research is focussing on thin film and etching processes for high-efficiency crystalline silicon solar cells.

Jochen Rentsch is head of department production technologies – Surfaces and Interfaces at Fraunhofer ISE. He received his PhD degree in physics in 2005 from the Albert-Ludwigs University of Freiburg, Germany. He studied physics at the Technical University of Braunschweig and obtained his diploma degree in 2002. At Fraunhofer ISE, his research focuses on the development of rear passivated solar cells, new wet and dry chemical processing technologies and the coordination of cell technology transfer projects.

Laurent Clochard is the chief technical officer (CTO) at NINES PHOTOVOLTAICS since 2010, with a focus on developing a novel industrial dry etching tool and process (ADE), specifically designed for the solar industry. Prior to that, Laurent held positions in equipment companies (TEL Magnetic Solutions, Alyxan) where he was in charge of the product R&D and transition from research to industrial product, as well has CNRS. Laurent holds a B.Sc. of Thermal & Energy science from IUT Poitiers (France), an MSc in Physics from University La Rochelle (France), an MSc research in applied physics from Trinity College Dublin (Ireland), and a DEES Post-Master degree from Joseph Fourier University Grenoble (France).

Edward Duffy is the founder and CEO of NINES PHOTOVOLTAICS. He has been involved in semiconductor capital equipment business since 1996, at companies including TEL Magnetic Solutions and Applied Materials, where he held a number of senior positions both at their installed base at Intel Fab Operation (IFO) in Ireland and other facilities in Israel and the US. These positions included senior equipment engineer in the metal etch cluster and Installation and Qualification (I/Q) Lead Engineer/System Expert for HDP CVD (High Density Plasma Chemical Vapour Deposition) cluster. Edward holds a bachelors of science degree in engineering from Trinity College Dublin (TCD) and a diploma in mechanical engineering from the Dublin Institute of technology (DIT).

Klaus Duncker is senior expert in the department R&D Processes Frontend at Hanwha Q CELLS. He is responsible for the deposition processes of dielectric passivation layers on front and rear side. Klaus studied physics at the Universities of Kiel and Marburg and received a Ph.D. degree from the University of Halle in 2008.

Kai Petter is senior manager of the department R&D Silicon at Hanwha Q CELLS' headquarter for technology and innovation in Germany. He is responsible for testing new silicon wafer technologies. Kai studied physics at the University of Hamburg and received a PhD degree from the University of Marburg in 2006.

Stefan Peters is director of the department R&D Processes Frontend at Hanwha Q CELLS´ headquarter for technology and innovation in Germany. He is in charge of the development of solar cell processes for texturing, cleaning, doping and layer deposition. Stefan studied physics at the University of Bielefeld and received a PhD degree from University of Constance in 2004.

Enquiries

Bishal Kafle | Phone: +49 (0)761 4588 5499 | e-mail: bishal.kafle@ise.fraunhofer.de

Riding the workhorse of the industry: PERC

Pietro P. Altermatt, Yifeng Chen, Yang Yang, Zhiqiang Feng
State Key Laboratory of PV Science and Technology (SKL), Trina Solar, Changzhou, Jiangsu, PR China

Abstract

Improving PERC cells requires rather different strategies than standard cells have required, demanding concrete improvements in materials, manufacturing procedures and fabrication tools. Highlights of this paper include:

Highlights

- In recent years, PERC cell efficiencies have increased by about 0.4%$_{abs}$ per year in mass production. This paper discusses how the industry's median efficiency can be increased to 24% within about seven years while fabrication cost may drop to about half.
- A simulated roadmap shows that, presently, efficiency is either limited by a homogeneous emitter, or in case of a selective emitter by wafer lifetime. The next improvements are cleaner fabrication, Ga doping of wafers to reach 2 ms lifetime, better emitter profiles and emitter passivation, finer metallization, and improved hydrogenation.
- 24% efficiency will not be reached by solely optimising existing technology, but by steadily improving existing technologies further, which requires continuous R&D efforts and the further development of some specific manufacturing tools.

The present PERC cell efficiencies of large Chinese manufacturers are typically up to 21.4% with homogeneous emitters, and from 21.5% to 22.2% for selective emitters. The selective emitters are mostly fabricated with laser doping of the n^{++} part; some use selective etch-back, which offers greater flexibility. The highest efficiencies are obtained with both wafers near the seed end of the ingot and clean processing, so the bulk lifetime in the finished cells is high. Manufacturers tend to buy wafers that are thinner (mostly 170 μm), larger (mostly M2 with 156.75 mm side length and 210 mm diameter), and with lower resistivity, typically 0.5-1.5 Ωcm. We have monitored [1] the evolution of PERC module efficiency over recent years by consulting the main manufacturer's websites, taking their median module power divided by module area, see Fig. 1.

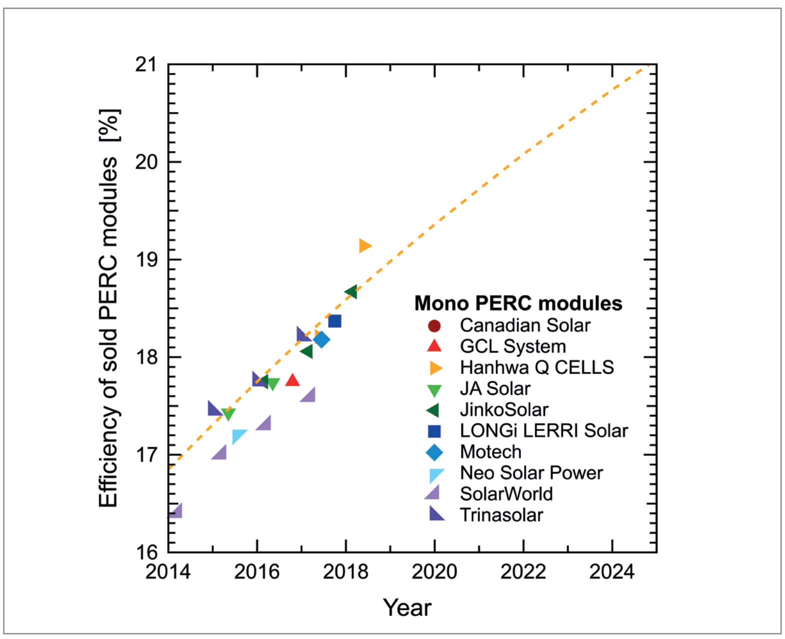

Figure 1. Efficiency of sold monocrystalline PERC modules, calculated from the module's power and area listed on manufacturers' websites. The date is the latest update of each web page, which may lag behind fabrication by up to one year. Adapted from [1].

The date in the graph is the latest update of each web page, which may lag behind fabrication by up to one year. The graph does not aim at completeness but to reveal the trend. We fit the efficiency trend over the years with the Goetzberger function [2] (dashed line):

$$\eta(t) = \eta_{\text{limit}} \left[1 - \exp\left(\frac{t_0 - t}{c} \right) \right],$$

because it considers that efficiency saturates towards a practical efficiency limit η_{limit}. In our data fitting, the development speed c turns out to be 21 years, meaning that the curve is still rather close to linear (the starting time t_0 at zero efficiency has no practical meaning). Presently, PERC module efficiency increases by about 0.4%$_{abs}$ per year, and this trend can continue for the coming years under conditions discussed in this paper. Part of this steady progress in China is fostered by a high staff turnover, where skills and knowledge is exchanged between manufacturers. Another part is an ongoing optimization of PV tools and screen-printing pastes, which have played an important role.

Roadmap for PERC cell efficiency improvements

Two detailed roadmaps for PERC cell efficiency improvements were published in [3] and [4,5]. The latter was obtained with detailed Sentaurus device modelling, and an updated version is depicted in Fig. 2.

The roadmap started in 2015 with a bulk SRH lifetime of 350 μs and a rather poor emitter. Meanwhile, most manufacturers have at least an advanced homogeneous emitter (advEm on the x-axis of Fig. 2) or a selective emitter (selEm1) with a sheet resistivity near $\rho_{sh} \approx 160$ Ω/sq. Additionally, they shape their local BSF with segments instead of lines (BSFseg), they add boron to their Al-paste (Al-B-BSF), and have five

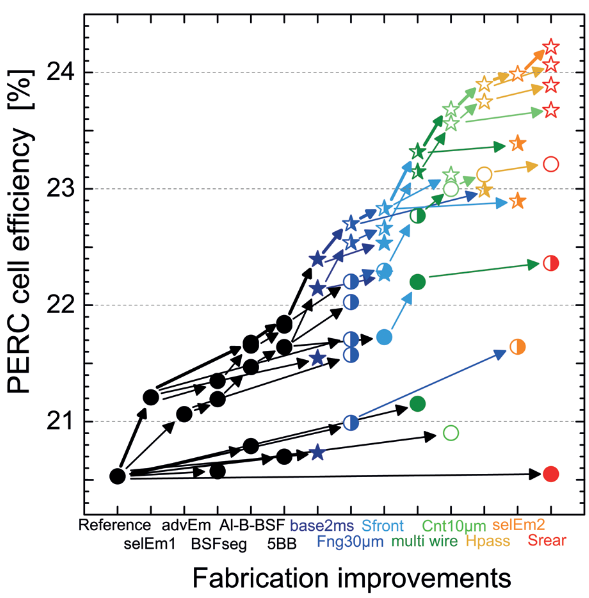

Figure 2. Roadmap of monocrystalline PERC cells, simulated with Sentaurus assuming present materials and technology being steadily developed further (no break-through technologies). Black: task fulfilled since 2015 by most manufacturers. Stars: wafer materials with 2ms lifetime; filling of symbols: various front metal finger designs with 91 fingers/60 µm wide (filled), 155/30 (half-filled), 155/21 (empty). Updated from [4,5].

busbars (5BB), some already multi-busbars. Their present-day cell efficiencies are predicted by this study very precisely, considering that such a study cannot take manufacturers' individual details into account. This gives trust that the predictions for further cell efficiency improvements are reliable.

For improving PERC cell efficiency further, this graph shows two important features: firstly, with already existing technology continuously improved further, about 24% PERC cell efficiency can be reached in mass production (no passivated contacts or other emerging technologies like hetero-emitters have been considered). Secondly, each technology needs to be improved at its right time, as becomes obvious for example with the last improvement in the graph: the rear passivation (Srear). The arrow from the starting reference pointing to this improved rear passivation is practically horizontal, while the arrows above 23% efficiency increase steeply. This has the following reason: at the reference point, recombination at the rear passivated surface is small compared to recombination in the emitter and the base region. Hence, reducing recombination at the rear does not lead to a noticeable reduction of recombination. However, once the emitter and base regions are improved so the cell reaches 23%, reducing recombination at the rear has its impact. Hence, reducing the dominant recombination losses increases cell efficiency far more than reducing smaller recombination losses. Thus, knowing the dominating recombination losses [6] indicates where to improve the cell next.

This implies that the rear Al_2O_3-passivated surface is currently too good [5] and its further improvement would hardly influence efficiency. Some manufacturers therefore currently use an oxynitride [7]. However, with improving other losses in the cell in coming years, finally rear passivation will become important and oxynitrides are expected to become efficiency limiting. Hence, investing in Al_2O_3 passivation is not wrong, but it is an investment mainly for the coming years. The roadmap in Fig. 2 may guide manufacturers to buy tools to avoid a 'legacy lag' in the near future.

The fact stated at the beginning of this article – that, presently, changing from a homogeneous to a selective emitter improves efficiency considerably – shows that a homogeneous emitter is currently limiting efficiency. This is so although inactive phosphorus [8,9] has been largely reduced, contributing greatly to efficiency improvements also of standard cells in recent years. With a selective emitter, usually the wafer lifetime causes the dominant losses. There is still some uncertainty about how the lifetime in p-type wafers may improve. The stars in Fig. 2 can only be reached with 2 milliseconds (ms) final bulk lifetime at MPP, demonstrating how important high lifetimes will be. Two ms has been reached with boron doping in the laboratory at ISFH, Germany, since 2016 for 2 Ωm Cz material after re-generation [10]. It was also nearly achieved with Ga-doped wafers 30 years ago [11] and with an industrial Cz puller 20 years ago [12]. Although iron reduces lifetime more in Ga-doped than in B-doped material [13], it looks like that 2 ms final lifetimes with Ga-doping will soon be on the market on a large scale, because the Ga doping patent from Shin-Etsu is going to expire soon. Ga does not cause light-induced degradation as long as there are no large amounts of Cu in the material [14]. Hence, the regeneration tools will soon not be necessary anymore (but they may be useful one day again for hydrogenation of passivated contacts).

Important is not only the initial wafer lifetime; the final bulk lifetime after fabrication determines cell efficiency, and it may be limited by the degree of cleanliness in many production facilities. This is particularly the case in lines that were upgraded from old standard to PERC manufacturing or in lines where mono and multi materials are used alternatingly, despite standard cleaning procedures between material changes.

For cleaner fabrication, factories may adopt changes including the following:

- Purer quartz tubes. Purer ones cost about five-fold than the standard fittings, but the cheap ones tend to cause a clearly noticeable degree of contamination.
- Clean air. An air class 1000 throughout the manufacturing line won't be sufficient for higher efficiencies.
- Avoiding impurity drag into the line from saw-damage/texturing. If the materials used in the machines for saw-damage etch become porous or brittle, they store and release old impurities into the new chemical bath. Also, it is important that these chemicals are renewed in a way that no old liquids stay in the system.
- Carefully monitored deionized water having high resistivity is also important.
- Impurities may travel from saw-damage down to the firing furnace via conveyor belts, roller bearings, and handling systems (originating also from lubricants and mechanical wear). Contactless wafer handling may seem costly at the moment, but if the PV industry adapts it on a large scale, it should be affordable and will enable higher efficiencies.
- Automation may help. But before that, simple procedures may help sooner, like removing metallic door handles as well as metal lids on the floor, not allowing fork lifts to enter the premises, protecting the operators' mobile phones, etc.

If cell efficiencies well above 22% should be reached, the cleanliness procedures in production facilities may look rather different from how they look now, regardless of whether n-type or p-type material will be used.

Apart from cleaner production, an improvement of hydrogenation may increase the final lifetime as well. Presently, hydrogenation takes place during

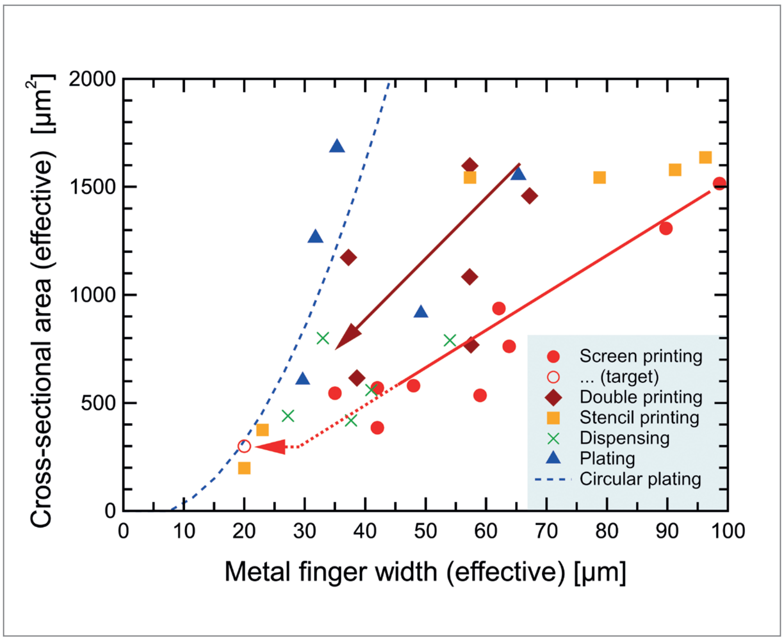

Figure 3. Evolution of front metal fingers: their width (causing shading) and cross-sectional area (causing resistive losses). Literature values (symbols) with the indicated printing techniques, arrows indicate trends. The width (and area) of other printing techniques are slightly adjusted to the optical factor (and resistivity) of screen-printed fingers for direct comparison. Adapted from [21].

DKEM Industry Leading Supplier of PV Silver Paste

Stronger. Together.

Embrace the Advanced PERC & Interconnection Era

DKEM™ *When Performance Matters*™ offers
High Performance PV Silver Paste

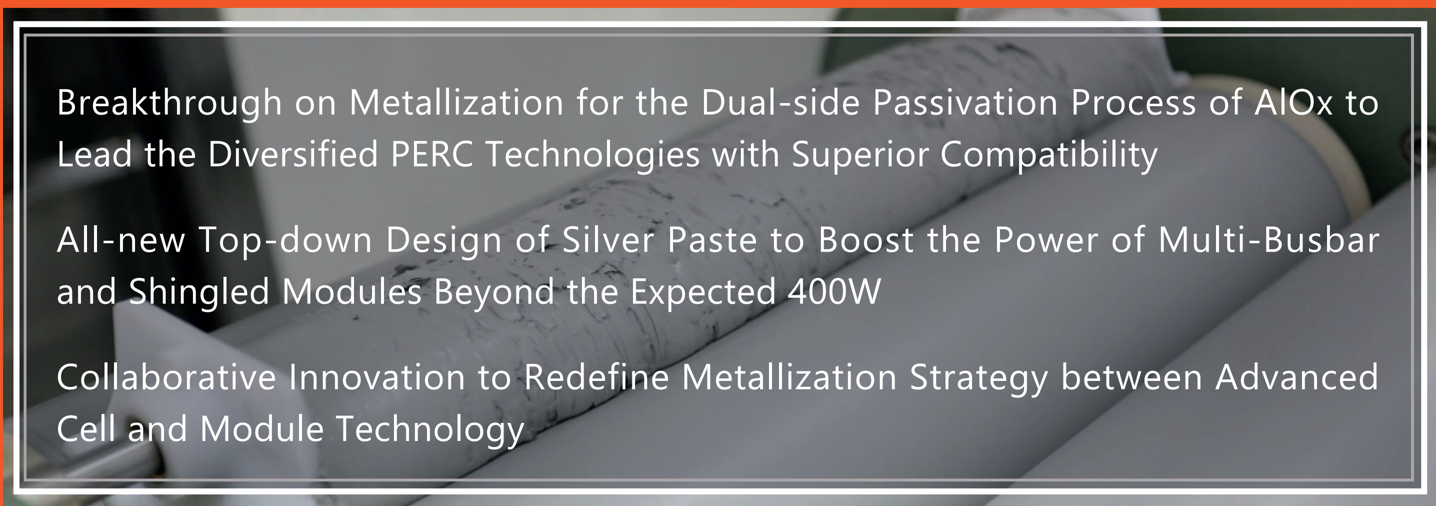

DK Electronic Materials, Inc.
www.dkem.cn | info@dkem.cn

the firing step and during re-generation, where the hydrogen stored in the SiN_x layers readily diffuses into the cell. The transport of hydrogen at medium temperatures is being better understood thanks to progress in research and models [15]. Also, it is not completely clarified yet whether, sometimes, too much hydrogen is left in the final device, creating more defects than passivating. More research into hydrogenation may help to improve the final bulk lifetime in PERC cells considerably.

Presently, some recombination loss may occur at the rear metal contacts if the BSF depth is smaller than about 4 µm at locations sideways very close to the rear surface. Recombination in the Al-B-doped region is dominated by the Al-O complex [16] so a BSF depth of about 4 µm is optimum [17]. If the BSF is sub-optimal, recombination at the rear contacts can easily become a major contribution to efficiency variations, and it is important to distinguish this from failures or contamination in rear surface polishing or passivation.

In case manufacturers succeed in fabricating a good BSF, further improvements in the emitter may help next. There are various ways to do this in parallel. One possibility is improving the alignment of screen-printing so the n^{++} region can be narrower. The selective emitters fabricated by laser-doping may be improved by reducing the phosphorus dopant density in both n^{++} and n^+ regions by further process tuning. Certainly, a better front passivation beyond the usual SiN_x is beneficial (Sfront in Fig. 2). This creates possibilities to further reduce the dopant density at the surface by etching the lased-doped, selective emitter homogeneously back (selEm2). This reduces mainly Auger losses in the n^{++} region and, if the front surface passivation is good enough, also the recombination losses in the n+ region. Provided that a good front surface passivation is achieved, a 0.4 µm deep n+ emitter with a phosphorus concentration near 1×10^{19} cm^{-3} at the surface would be optimum, because its sheet resistivity stays below 350 Ω/sq and its J_o reaches 10 fA/cm^2 [18]. This is expected to be achievable with POCl3 diffusion and etch-back.

Of course, a considerably larger sheet resistivity ρ_{sh} may increase the resistive losses. Increasing the number of metal fingers only helps reducing these resistive losses if the fingers are sufficiently thin so they don't cause too much shading (finger30um). There are two effects helpful in optimization: (i) in the module, the shading losses due to the front metal fingers are reduced compared to air due to back-reflection at the front glass, quantified by a reduction of the 'optical shading factor' from 0.69 in air [19] to 0.42 in the module [19,20]. (ii) At low ρ_{sh}, the electrons flow from the base region straight up to the emitter and then flow sideways along the emitter to the contacts; but with increasing ρ_{sh}, an increasing proportion of electrons flows along a curved path in the base. The front finger distance and ρ_{sh} of the emitter should therefore be optimized taking all these influence factors into account, not just a few.

In this context, the question arises which further improvements in metallization are necessary and most beneficial. Not now, but once the emitter is improved and has a lower n^{++} doping, introducing a narrower front contact opening of about 10 µm (Cont10um) instead of the whole finger width will improve cell efficiency. This was already achieved in the Pluto cell (at that time with plating). Fig. 3 shows the evolution of the front finger width (determining shading) and the finger's cross-sectional area (determining series resistance) over time [21], collected from literature.

In order to plot Ag or Cu plating in the same graph, its area was adjusted by ρ_{SP}/ρ_{Ag} and its width by the reduced shading factor to 0.32 (hence, by 0.42/0.32). The graph shows that it has been too early to adopt plating (dashed lines), but with reaching multi-wire/multi-busbar designs, plating can become a more serious competitor to screen printing, although screen printing is poised to arrive at 30 µm finger width with knotless printing rather soon, enabling great flexibility in emitter optimization. If silver price rises considerably, silver consumption needs to be reduced from presently below 100 mg/cell with five busbars and below about 50 mg/cell with multi-busbars or multi-wires. Twenty mg are doable [22]. Only if this is still too much silver, Cu fingers may become the solution. To avoid Cu diffusion into Si over 30 years of module lifetime, an initial 200 nm thick Ni or NiSi layer is necessary [23], and to avoid yellowing of the EVA, a very thin layer of Ag on top of the Cu helps. All in all, the desired finger width and cross-sectional area are near the bottom of the left corner in Fig. 3. For example, the 25% efficient PERL cells at UNSW in the 1990s had $\rho_{sh} \approx 200$ Ω/sq, a finger distance of 0.8 mm and an optimum finger width of 20 µm in 2 × 2 cm^2 cells [24]. Also calculations and laboratory experiments show [22] that for multi-wire/multi-busbar designs, the metal finger width does not need to go below 20 µm. The roadmap for the front fingers does neither ask for high aspect ratios, offered by some alternative printing methods, nor for geometries narrower than 20 µm, and most benefits are already obtained with 30-25 µm.

For module power, improvements in cell efficiency have the strongest impact because most of the module area is covered by the cells, not by the white spaces. Apart from efficiency improvements, some other measures at the cell level may additionally foster improvements in the module. For example, using officially calibrated cells for precise tuning of the IV tester, and carefully adjusting the operating parameters of the IV tester may help. It can easily happen that cell efficiency is measured about $0.5\%_{abs}$ too high. An overestimated cell efficiency implies an underestimated cell-to-module (C2M) ratio, making it difficult to evaluate where to improve the module. And it makes also OEM fabrication more difficult, which has become a considerable factor in the PV industry. Establishing a Chinese ISO-17025 accredited IV Test laboratory would certainly improve the current situation in the Chinese PV industry. Even the gratifying row of latest world record efficiencies of industrial-type PERC cells were not officially calibrated and, hence, these efficiency levels should be taken with some caution so long as these manufacturers do not compare themselves with certified measurements. The efficiencies of these champion cells fit into the roadmap of Fig. 2, though.

Not all improvements on the cell level can be transported to the module level. An example occurred when the industry moved to double AR-coatings at the front to prevent potential-induced degradation (PID): the higher refractive index of EVA made the double ARC ineffective. We will see a present-day example of black silicon texturing below: it may improve the cells in air, but not as much in the module. Doing a detailed optical analysis [25,26] helps to quantify the benefit of the optical improvements in the cell for the module, and it avoids possible mutual blaming between the cell and module manufacturing departments for delays.

Timeframe for improvements and production cost

The expected timeframe of efficiency improvement can be estimated by combining Fig. 1 with Fig. 2: it may take about seven years to reach 24% PERC cell efficiency in the industry's median. This is assuming that neither major interruptions nor breakthroughs will occur. Fig. 4 shows the fabrication cost decay [27] (not only the sales price). An extrapolation [1] suggests that, by then, module cost may drop down to about half of today's cost, which is at the present overcapacity cycle near RMB 2.5/W.

Main contributions to cost reduction have come from cheaper PV tool manufacturing in China, standardization all along the value chain, and a fierce fight for gigawatts. Recently, a very swift change from slurry-saw wafers to diamond-sawn wafers has reduced CAPEX for poly silicon (before, it caused over 30% of CAPEX required for the value chain up to the module). Now, only four grams of poly-Si are required per watt. A reduction in CAPEX is very beneficial for the further scaling up of the Si PV industry. If solar cells should contribute significantly to reducing CO$_2$, the global cumulative installed capacity needs to go beyond 10 TW [28], compared to about 0.4 TW installed now, and hence the production capacity needs to grow about 10-fold. This implies that silver consumption per cell eventually needs to be reduced [29].

Reducing wafer thickness can further reduce CAPEX. This may occur rather slowly from the present 180-170 µm to, say, 140 µm, not because of yield problems but because J_{sc} gets smaller. The J_{sc} losses depend on texturing and light trapping. We should keep in mind that, with standard texturing and AR coating, cells can look already black in the module (although many manufacturers adjust the AR coating thickness such that the cells look blue). Overall, the main reflection loss comes from light escape in the infrared [24], followed by absorption losses in the module glass and by EVA. Different texturing, often coined as black silicon, can therefore increase a 60-cells module's power only by maximally 1 W by reduced front surface reflection alone. However, improved texturing may distribute the sun rays, entering the wafer, more evenly so more light gets absorbed and less escapes in the infrared, by an amount that depends strongly on the reflectance at the rear cell surface: about 3 W may be realistic, 4 W is absolute maximum, as ray tracing simulations show [30] (if higher gains are observed, they come from an accompanying reduction of emitter J_o and an increase in collection efficiency due to changes in the front surface topology).

A further important cost reduction will continue to come from higher throughput. Fig. 5 shows how throughput has increased over recent years. The data of texturing and PECVD tools are from S.C New Energy Technology Corp. having 50-60% market share in China; the other tools are averages from various manufacturers. Increasing throughput is very effective because it reduces many different cost aspects.

Also, the margin may continue to shrink, and may continue to force either large manufacturers to become larger, or smaller manufacturers to find their own ways of keeping their cost and overhead very low. By how much a further automation of manufacturing lines will reduce cost in China is too early to judge.

In maturing industries other than PV, increasing process control tends to be a cost saver when margins get small and competition more subtle, and this may also be the case in PV. In many factories, underperformance of cells discovered by the IV tester cannot be traced back directly to the tools because it is not monitored at what time the cells went through which tools in batch processing; on the way, cells may be on differently sized boats and carriers and get spontaneously diverted when a piece of equipment is down. In PERC fabrication, quite some time may pass from saw-damage etching to firing and re-generation. Basically, this is a lack of information that hampers a concrete feedback. Information can be seen as entropy, and the state of the fabrication system becomes better defined by either maximising or reducing

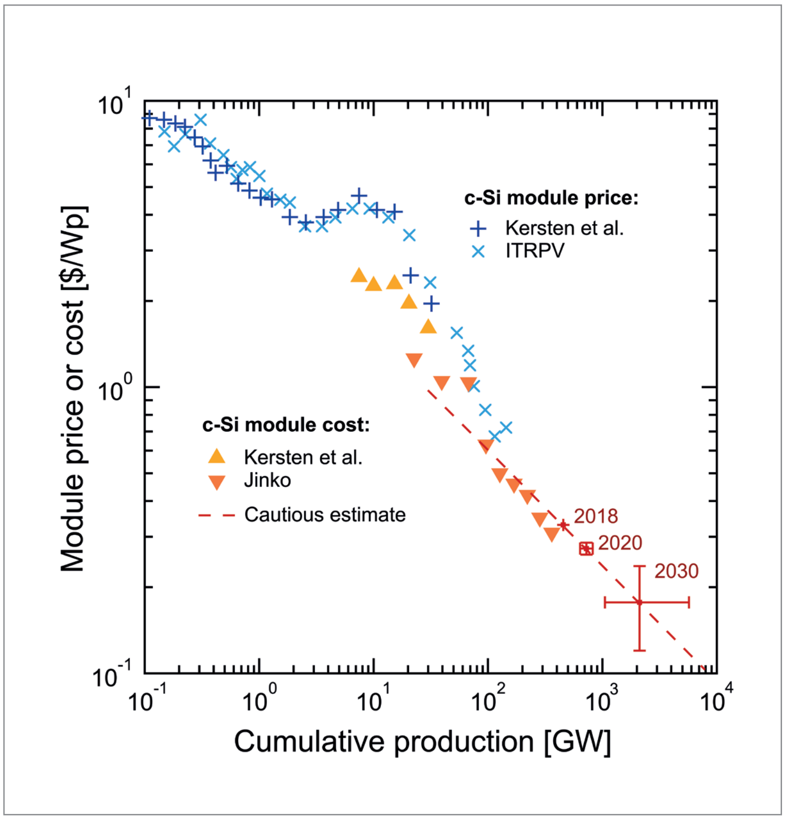

Figure 4. Crystalline silicon module cost [26] and future estimate [1], compared to module price.

entropy. Maximising entropy means shuffling a large amount of wafers before feeding them to the lines so all the tools get the same statistical mix of wafers – making any underperforming tool stand out after some time. Reducing entropy means either improving traceability of the wafers or closer monitoring of the tools, or both. It is not necessary to trace every single wafer, but helpful can be for example RFID coding of boats and carriages, designing smart handling systems, or real-time monitoring of the tools that cause most of the efficiency variation. Statistical methods help to pin down these tools [31,32,33], and if statistics is combined with device physics, efficiency can be improved even better. Because bulk lifetime tends to be limited by cleanliness, tracing bulk lifetime though the production process is advantageous. Etching back some cell precursors from various stages of fabrication and (re)passivating them is an option. As Al_2O_3 passivation is done at elevated temperature, superacid passivation [34] can be done at room temperature, so the lifetime is not influenced by an additional thermal budget. A further possibility for enhanced process control is to go beyond monitoring the IV parameters alone, which is mostly just efficiency. Some brands of IV testers may measure more cell parameters including the pseudo fill factor (pFF), a reliable R_s, wafer doping concentration, the sum of back and front J_o, and bulk lifetime [35]. These parameters are very helpful in tracking down short-term or long-term problems. Last but not least, the cell's capacitance increases strongly with increasing V_{mpp}

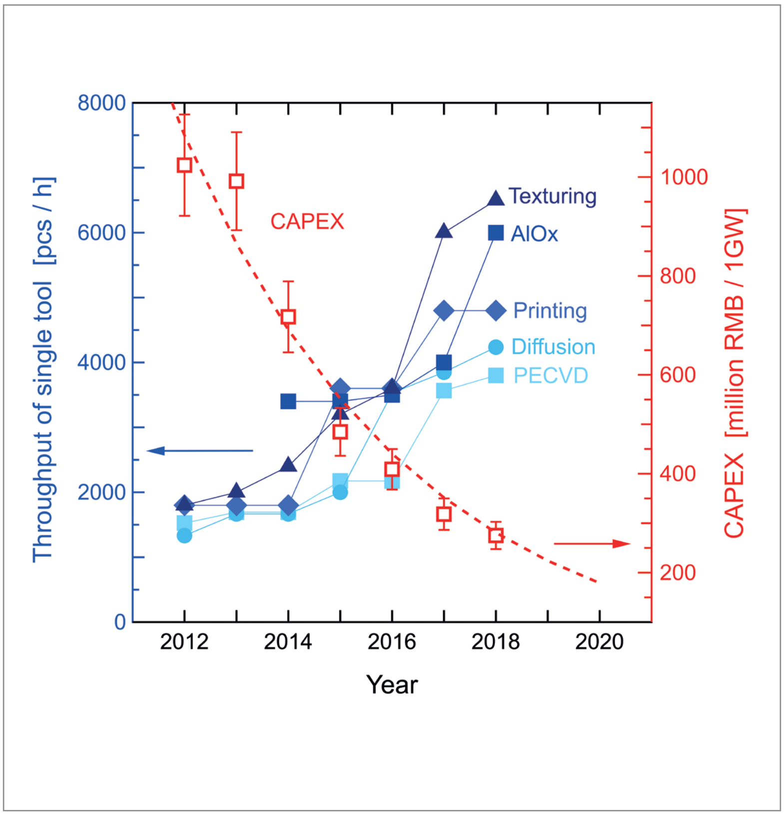

Figure 5. Historical development of throughput of tools made, as well as the typical CAPEX required for 1 GW of PERC cell manufacturing capacity built in China. Adapted from [1].

[36], making special procedures necessary in most IV testers to avoid hysteresis. If such IV testers are not updated, IV parameters may become unreliable (e.g. overrating efficiency).

Process control is expected not only to narrow down the cell efficiency distribution, but also to increase efficiency. Over the years, standard, full-area BSF cells could be optimized partly with 'trial and error' because the variation of process parameters has impacted cell efficiency in a quite straight-forward manner. And the high numbers of cells produced made small increments statistically significant. PERC cells, however, have considerably more process parameters, and parameter alterations interact in a complex manner with other parameters. This complexity restricts optimization by 'trial and error' to the point that other approaches need be developed to optimize PERC cells swiftly, like the statistical methods mentioned above.

It is important to realize that optimization alone is not sufficient to arrive at 24% PERC cell efficiency. The simulations of the roadmap assume that existing technology is steadily being improved, not just optimized, hence R&D is important for further technological improvements of tools, materials and processes. Questions to answer include:

"In maturing industries other than PV, increasing process control tends to be a cost saver, and this may also be the case in PV"

- What needs to be changed in cell manufacturing so 2 ms bulk lifetime can be achieved in the final cell on large scale?
- Which is the next tool? Does improved front surface passivation require new or adjusted tools or only new materials and processes with existing tools?
- Should tools and pastes be developed already now to enable smaller contact openings than metal finger width? These tools need to be ready to be bought and sold on a large scale only once the emitter is so good that the front contact contributes significantly to the overall recombination losses.
- Can hydrogenation be significantly improved and, if so, how?
- Silver contributes considerably to the manufacturing cost and will increasingly do so. What will be the tools and material requirements for reducing silver consumption below 40 mg/cell?
- While seed ends of ingots reach 2 ms lifetime, how can the lifetime in the rest of the ingot be improved?

Table 1 lists the eight main processing steps of PERC cells and their supposed origins. It is striking how many of these processing steps originated from universities and other public institutions. However, PV tool manufacturers were necessary for implementation, sometimes in close collaboration with these institutions and aided by government grants. When considering the PERC road map, we should ask questions like: where are new and improved process steps being invented today? Where is collaboration between inventors and PV tool manufacturers happening? Is there enough government funding for this? Which tool manufacturers actively develop equipment for implementing such new process steps? Besides having the 'Top Runner' programme in China fostering high-efficiency cells, it may be beneficial to also have a 'Top Tools' programme for actively fostering new types of tools.

N-type or p-type?

Most PV tool manufacturers do a great job at optimizing tools, as for example seen in the throughput in Fig. 5. However, because PERC is still in a rather early stage of manufacturing, most PV tool manufacturers do not yet seem to know concretely how to improve PERC cell efficiency beyond optimization and do not seem to prepare new tools particularly for this. Most Chinese PV tool manufacturers undertake hardly any R&D activities beyond optimising existing tools, with some notable exceptions like Laplace, Leadmicro, Maxwell, DR Laser (and surely some others we missed out). Instead, some tool manufacturers hope that switching to n-type wafers will deliver the necessary further efficiency improvement and will foster the sales of new equipment like LPCVD, new screen-printing pastes, etc.

Some large cell manufacturers invest more R&D in n-type than in p-type cell development, although they mainly produce p-type cells, and do this although their calculations mostly indicate that n-type is rather unlikely to compete with p-type in the near term. This may be partly caused by insecurity about how to improve PERC cells beyond 22% efficiency, and partly by a "we do so because the others do so" effect (which is important for minimizing risk of missing new trends). Both these aspects may become a self-fulfilling prophecy: because manufacturers focus more on n-type R&D, PERC development may get partly neglected over time and indeed may not go far above 22% – and because many manufacturers build n-type lines the same time, prices for manufacturing of n-type cells may significantly drop.

Let's play the devil's advocate. Here are some aspects for staying with p-type:

- Manufacturing both a local, deep Al-BSF and rear local metal contacts in one firing step is hard to beat. We are very lucky that Al is both a dopant and reduces the melting point of silicon, while Ag pastes work excellently on n-type emitters (in contrast, pastes don't work as well on p-type emitters in n-type cells).
- The p-type community has PERC as a clear and single target and concentrates its efforts and supply chain standardization on that, while the roadmap for n-type seems unclear so the n-type community disperses its efforts and power among n-PERT, n-type passivated contacts, HIT, and IBC.
- All well-developed cell types like PERC, PERT, IBC, and HIT, be it on p-type or n-type, move towards a similar practical efficiency limit in mass fabrication, which is between 25% and 26% [37]. Hence, differences in manufacturing cost will become even more important than they are now, favouring PERC.
- Research in lifetime-limiting defects for p-type is well established and well on the way, while many n-type advocates think that n-type won't be affected by defects. However, both material types contain oxygen and other impurities. While oxygen decreases FF in PERC cells, it increases FF in n-type cells by reducing Voc, an often overseen effect [38].
- Phosphorus diffusion is the cheapest way to getter the material efficiently, boron diffusion does not getter as much [39].
- The phosphorus-rich layer (PSG) has a more negative formation enthalpy than the boron-rich layer (BSG), hence PSG collects and removes significantly more impurities from the process than does BSG. Considering the issues with clean cell production, discussed above, PERC efficiency will be easier to maintain on high levels than n-type cells over the long term.

Process step	Origin and year
Texturing	General Electric Ltd 1969
P diffusion	US Army 1962
Rear side polish	RHENA, imec 2008
Selective emitter	Laser doping via PSG: University of Stuttgart, 2009; Etch-back: University of Konstanz, 2008
Passivation by SiN_x; by Al_2O_3	University of Erlangen 1989, ISFH 1995; imec, TU Eindhoven 2006
Rear laser opening	ISE Freiburg 2000
Screen printing	Spectrolab Inc. 1973
Firing	BSF: ARCO Solar 1988; Firing through: Mobil/Schott Solar 1997 and imec, University of Konstanz 2000

Table 1. The eight main processing steps of PERC production and their supposed origins (not aimed at completeness, but to show the deep involvement of universities and other public institutions).

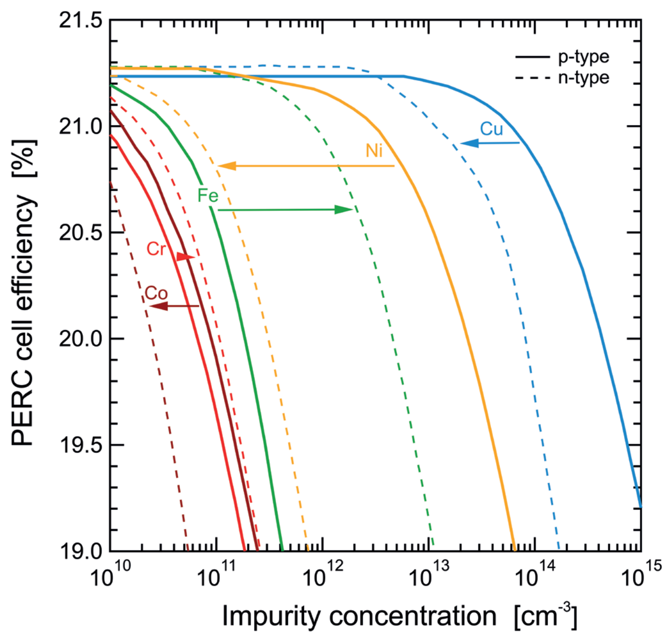

Figure 6. Simulated monocrystalline PERC cell efficiency with increasing homogeneous concentration of a single contaminant as indicated. This suggests that p-type (solid lines) is less sensitive to these contaminants than an equivalent cell structure on n-type (dashed lines) if Fe is under control. Adapted from [37].

- The Sentaurus simulations [40] in Fig. 6 suggest that n-type cells are more sensitive to metal impurities than p-type cells – once Fe contamination is under control.
- For development beyond PERC, cells on p-type wafers offer better opportunities for passivated contacts than on n-type wafers. This is so because a hole-conducting contact is more difficult to achieve than an electron-conducting contact (due to differences in tunnelling mass and required work functions). Hence, electron-conducting contacts can be used locally at the front (making a conducting oxide for lateral

"The PERC cell may be developed into a PERC+ cell by incorporating features such as passivated contacts, hetero-emitters and hetero-BSFs"

conduction obsolete), and the hole-contact can be spread across the entire rear surface, allowing its contact resistivity to be as high as 30 mΩcm^2 [41] and its J_0 as high as 20 fA/cm^2.

- Tools for n-type cells are difficult to maintain (for example dust in LPCVD, furnace tubes for boron diffusion, etc.), and there is considerable absorption of light in both a-Si of HIC concepts and poly-Si front passivated contacts.

And now comes the devil's advocate with aspects favouring a change to n-type:

- Many cells made of n-type wafers have always had higher efficiency than on p-type, this is a well-established fact, and there are no signs why they should not continue to do so.
- The defect engineering of p-type material should not be trusted; the stars in Fig. 2 show what will happen to PERC cells if final lifetime cannot reach 2 ms in the whole p-type ingot. Lifetime in Cz n-type mono wafers can easily achieve milliseconds, while most of p-type mono wafers are a few 100 µs.
- There is less light-induced degradation in n-type than in p-type, even with the current deactivation procedures for p-type.
- Boron diffusions reach lower J_0 values than phosphorus diffusions and are not significantly more expensive in 24/7 fabrication if BBr_3 is avoided.
- PERT designs have significantly better bifaciality than PERC. Improving bifaciality in PERC is possible but is not done.
- From a materials production point of view, switching to n-type can be easily done with little additional cost, and is technologically mature, so it is likely to happen.
- N-type cells require mostly the identical manufacturing tools as PERC cells; given the efficiency advantage over PERC, manufacturers are likely to switch.
- Dominance of p-type has historical reasons: when Si cells were used for satellites in the 50s and 60s, p-type cells degraded less quickly in space than n-type cells, so processes on p-type wafers were developed. Now it is time to overcome this historical development and take advantage of n-type.

Watching out for these various aspects and how they develop in the coming years will be important for recognizing trends sufficiently early. And, above all, the PERC cell may be developed into a PERC+ cell by incorporating features from n-type cells such as passivated contacts, hetero-emitters and hetero-BSFs.

Instead of one main workhorse, will we have more cell concepts coexisting? If so, they would need to converge to very similar efficiencies and fabrication cost to coexist, otherwise one cell concept will be the main workhorse and push out the others to emerging niche markets. The race is on.

Acknowledgements

We would like to thank Byungsul Min from ISFH for updating Fig. 2.

References

We do not aim giving a broad and neutral overview on PERC literature and cite often our own contributions:

[1] Chen, Y. et al. 2018, "From laboratory to production: Learning models of efficiency and manufacturing cost of industrial crystalline silicon and thin film photovoltaic technologies", Proc. 7th WCPEC, Waikaloa, HI, (to appear).

[2] Goetzberger, A. et al. 2002, "Solar cells: past, present, future", Sol. Energy Mater. Sol. Cells, Vol. 74, pp. 1–11.

[3] Huang, H. et al. 2017, "20.8% industrial PERC solar cell: ALD Al_2O_3 rear surface passivation, efficiency loss mechanisms analysis and roadmap to 24%", Sol. Energy Mater. Sol. Cells, Vol. 161, pp. 14–30.

[4] Min, B. et al. 2015, "Incremental efficiency improvements of mass-produced PERC cells up to 24%, predicted solely with continuous development of existing technologies and wafer materials", Proc. 31st EUPVSEC, pp. 473–476.

[5] Min, B. et al. 2017, "A Roadmap Toward 24% Efficient PERC Solar Cells in Industrial Mass Production", IEEE J. Photovolt., Vol. 7, pp. 1541–1550.

[6] Deng, W. et al. 2017, "22.61% efficient fully screen printed PERC solar cell", Proc. 44th IEEE PVSC, Portland, OR, paper no. 486.

[7] Kimmerle, A. et al. 2016, „Precise parameterization of the recombination velocity at passivated phosphorus doped surfaces", J. Appl. Phys., Vol. 119, 025706.

[8] Dastgheib-Shirazi, A. et al. 2013, "Relation between diffusion parameters and phosphorus precipitation during the POCl3-diffusion process", Energy Procedia, Vol. 38, pp. 254–262.

[9] Min, B et al. 2014, "Heavily doped Si:P emitters of crystalline Si solar cells: recombination due to phosphorus precipitation", Phys. Stat. Solidi RRL, Vol. 8, pp. 680–684.

[10] Walter, D.C. et al. 2016, "Realistic efficiency potential of next-generation industrial Czochralski-grown silicon solar cells after deactivation of the boron-oxygen-related defect center", Prog. Photovolt., Vol. 24, pp. 920–928. (the simulations in that work are not a broad optimization study and hence limited to 22% efficiency).

[11] Pang, S.K. et al. 1988, "Doping dependence of

minority carrier lifetime in Ga-doped silicon", Proc. 20th IEEE PVSC, Las Vegas, pp. 435–440.
[12] Glunz, S.W. et al. 2000, "Stable Czochralski silicon solar cells using gallium-doped base material", Proc. 16th EUPVSEC, Glasgow, pp. 1070–1076.
[13] Schmidt, J. & Macdonald, D., 2005, "Recombination activity of iron-gallium and iron-indium pairs in silicon", J. Appl. Phys., Vol. 97, 113712.
[14] Lindroos, J. et al. 2013, "Light-induced degradation in copper contaminated gallium-doped silicon", Phys. Stat. Solidi RRL, Vol. 7, pp. 262–264.
[15] Hamer, P. et al. 2018, "Modelling of hydrogen transport in silicon solar cell structures under equilibrium conditions", J. Appl. Phys., Vol. 123, 043108.
[16] Bock R. et al. 2010, "Formation of aluminium-oxygen complexes in highly aluminum-doped silicon", Sem. Sc. Tech., Vol. 25, 105007.
[17] Chen, Y. et al. 2013, "Analysis of recombination losses in screen-printed aluminum-alloyed back surface fields of silicon solar cells by numerical device simulation", Sol. Energy Mater. Sol. Cells, Vol. 120, pp. 356–362.
[18] Wagner H. et al. 2016, "Optimizing phosphorus diffusion for photovoltaic applications: Peak doping, inactive phosphorus, gettering, and contact formation", J. Appl. Phys., Vol. 119, 185704.
[19] Woehl, R. et al. 2008, "Analysis of the Optical Properties of Screen-Printed and Aerosol-Printed and Plated Fingers of Silicon Solar Cells", Adv. OptoElectronics, Vol. 2008, Article ID 759340.
[20] Witteck R, et al. 2016, "Optimizing the solar cell front side metallization and the cell interconnection for high module power output", Energy Procedia, Vol. 92, pp. 531–539.
[21] Chen, Y. et al. 2016, "Front metal finger inhomogeneity: its influence on optimization and on the cell efficiency distribution in production lines", Energy Procedia, Vol. 98, pp. 30–39.
[22] Braun, S. et al. 2014, "High Efficiency Multi-busbar Solar Cells and Modules", IEEE J. Photovol., Vol. 4, pp. 148–153.
[23] Jung, V. & Köntges, M., 2013, "Al/Ni:V/Ag metal stacks as rear-side metallization for crystalline silicon solar cells", Prog. Photovolt., Vol. 21, pp. 876–883.
[24] Altermatt, P.P. et al. 1996, "Spatially resolved analysis and minimization of resistive losses in high-efficiency Si solar cells", Prog. Photovolt., Vol. 4, pp. 399–414.
[25] Yang, Y. et al. 2017, "Combining ray tracing with device modeling to evaluate experiments for an optical analysis of crystalline Si solar cells and modules", Energy Procedia, Vol. 124, pp. 240–249.
[26] Winter, M. et al. 2015, "Combining structures on different length scales in ray tracing: analysis of optical losses in solar cell modules", Opt. and Quant. Electr., Vol. 47, pp. 1373–1379.
[27] Kersten, F. et al. 2011, "PV learning curves: past and future drivers of cost reduction", Proc. 26th EUPVSEC, Hamburg, pp. 4697–4702.
[28] Needleman, D.B. et al. 2016, "Economically sustainable scaling of photovoltaics to meet climate targets", Energy Environ. Sci., Vol. 9, pp. 2122–2129.
[29] Kavlak, G. et al. 2015, "Metal production requirements for rapid photovoltaics deployment", Energy and Env., Vol. 8, pp. 1651–1659 (for silver, see supplemental information of this paper).
[30] Module Ray Tracer, PV Lighthouse, Keith R. McIntosh, Coledale, NSW. Australia.
[31] Wasmer, S. et al. 2017, "Impact of Material and Process Variations on the Distribution of Multicrystalline Silicon PERC Cell Efficiencies", IEEE J. Photovolt., Vol. 7, pp. 118–128.
[32] Evans R. & Boreland, M., 2018, "Multivariate Data Analytics in PV Manufacturing—Four Case Studies Using Manufacturing Datasets", IEEE J. Photovolt., Vol. 8, pp. 38–47.
[33] Altermatt, P.P. et al. 2018, "A Method for Optimizing PERC Cells in Industrial Production Lines Using Final IV Parameters, Statistical Procedures and Numerical Device Modeling", AIP Conference Proceedings, Vol. 1999, pp. 110001.
[34] Pointon, A.I. et al. 2018, "Superacid-derived surface passivation for measurement of ultra-long lifetimes in silicon photovoltaic materials", Sol. Energy Mater. Sol. Cells, Vol. 183, pp. 164–172.
[35] Blum, A. & Sinton R.A., 2016, "Lifetime and Substrate Doping Measurements of Solar Cells and Application to In-Line Process Control", Proc. 43rd IEEE PVSC, Portland, OR, pp. 3534–3537.
[36] Sinton, R.A., 2006, "A solution to the problem of accurate flash-testing of high-efficiency modules", Proc. 21st EUPVSEC, Dresden, pp. 634–638.
[37] Steinkemper, H. et al. 2016, "Comprehensive simulation study of industrially relevant silicon solar cell architectures for an optimal material parameter choice", Prog. Photovolt., Vol. 24, pp. 1319–1331.
[38] Duan W. et al. 2016, "A route towards high efficiency n-type PERT solar cells", Proc. 32nd EUPVSEC, Munich, pp. 399–402.
[39] Weber T. et al. 2006, "Numerical simulations of gettering and recombination in iron-contaminated boron emitters", Proc. 21st EUPVSEC, Dresden, pp. 1486–1489.
[40] Schmidt, J. et al. 2012, "Impurity-related limitations of next-generation industrial silicon solar cells", IEEE J. Photovolt., Vol. 3, pp. 114–118.
[41] Melskens , J. et al. 2018, „Passivating Contacts for Crystalline Silicon Solar Cells: From Concepts and Materials to Prospects", IEEE J. Photovolt., Vol. 8, pp. 373–388.

Enquiries
Pietro P. Altermatt, Trina Solar,
pietro.altermatt@trinasolar.com

Metallization and interconnection for high-efficiency bifacial silicon heterojunction solar cells and modules

Antonin Faes[1], Agata Lachowicz[1], Armand Bettinelli[2], Pierre-Jean Ribeyron[2], Jean-François Lerat[2], Delfina Munoz[2], Jonas Geissbühler[1], Heng-Yu Li[1], Christophe Ballif[1] & Matthieu Despeisse[1]
[1]CSEM, PV-Centre, CH-2002 Neuchâtel, Switzerland; [2]CEA, INES, Le Bourget du Lac, France

Abstract

Silicon heterojunction (SHJ) solar cells demonstrate a high conversion efficiency, reaching up to 25.1% using a simple and lean process flow for both-sides-contacted devices, and achieving a record silicon solar cell efficiency of 26.7% in back-contacted configuration. In addition, the field advantages of SHJ cell technology are a native bifaciality and low thermal coefficient providing impressive energy yield. Finally, the technology demonstrates potential cost reduction as it is perfectly suited for thin wafers integration. The SHJ technology is therefore today triggering strong interest in the PV industry, appearing on the roadmap of different cell manufacturers, with several production lines and pilot lines being installed worldwide. One limiting factor of the technology is related to the metallization: due to temperature restrictions on hetero-contacts, the standard firing through silver paste needs to be replaced by low curing temperature paste. This type of pastes yield fingers with higher bulk resistivity (two to three times the one obtained with high temperature cured silver pastes) and lower adhesion after soldering. In this paper, materials, processes and costs figures will be reviewed for the metallization and module integration of SHJ solar cells, with a focus on copper plating benchmarked to silver screen-printing, for varying module interconnection technologies.

Introduction

The first publications of silicon heterojunction (SHJ) solar cells emerged at the end of the 1980s and beginning of the 1990s by Sanyo in a Japanese and a British patent relating to their HIT (heterojunction intrinsic thin-layer) cell technology [1,2]. Already in 1992, the HIT cell conversion efficiency was above 18% [3]. Important milestones for the technology were the two world record conversion efficiencies for Si-based solar cells obtained on interdigitated back-contacted (IBC) SHJ configuration, with 25.6% and 26.7% in 2014 and 2017, respectively [4,5].

SHJ technology are bifacial by nature and present a low temperature coefficient in the range of -0.23% to -0.3%/°C [6,7]; these two elements improve the energy yield and reduce the levelized cost of electricity (LCOE) [8]. The reliability of SHJ is confirmed in the field as the first HIT modules were produced in 1997 and data show no degradation of SHJ module after 14 years [9].

Today, even if SHJ module technology is still a niche market, the production level is promisingly increasing as several companies around the world have chosen this technology to differentiate from the mainstream. These companies are usually new comers that want to use a new technology with expected higher potential than mainstream. Thus, in 2018, about 2 GW of capacity was reported to be SHJ technology with the main player still being Panasonic, the founder of the technology in the 90s. Panasonic has about 1 GW capacity in Japan and Malaysia and has established an agreement with TESLA for the implementation of a Gigafactory in Buffalo based on SHJ cells, allowing it to at least double its production capacity.

In Europe, several players have chosen SHJ technology: in Russia, HEVEL, formerly producing thin film silicon modules, has shifted its production facility to SHJ with a capacity of about 200 MW [10]. In Italy, ENEL Green Power, one of the biggest renewable electricity companies, decided to invest in the technology in Catania (Sicilia) at a level of about 200 MW. One of the main reasons for this choice is the capacity of SHJ to reduce LCOE to a level that can't reach mainstream technologies.

In Asia, more and more players are considering SHJ. Among them, NSP (Neo Solar Power) has implemented a 50 MW line in Taiwan to evaluate properly the potential and cost reduction capabilities of SHJ. In China, Hanergy and Jinergy are true believers of the technology, investing at a level of hundreds of MW each. Recently, Tongwei has announced its intention to invest in the manufacturing of the technology to a level of 500 MW with Three Gorges Capital Holding.

These announcements are creating an ecosystem that will be able to bring cost down on the material as well as the equipment side, enabling SHJ to hold an increasing part of the PV market.

The process steps of the SHJ cells are simple and require temperatures below 250°C (Figure 1). Initial steps consist of n-type monocrystalline silicon wafer texturing and cleaning (with wafer as thin as 120 microns); followed by PECVD of intrinsic hydrogenated amorphous Si (a-Si:H) deposition

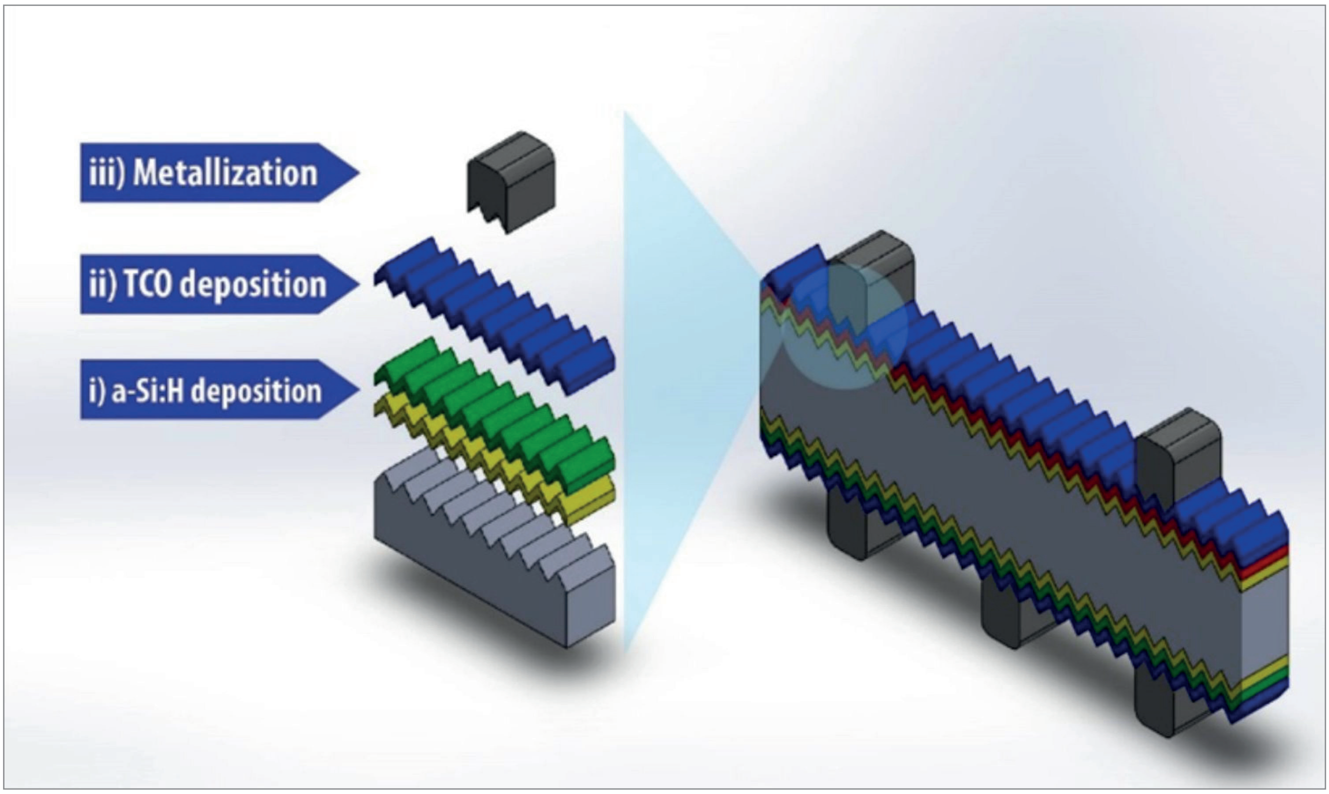

Figure 1. Manufacturing steps and schematic cross-section of a finished bifacial silicon heterojunction solar cell.

on both sides. On respective sides, phosphorus and boron-doped a-Si:H layers are deposited. Then the wafer is coated on both sides by sputtering with a transparent conductive oxide (TCO) that acts as an anti-reflective coating (ARC) and lateral electrical transport layer. To improve conductivity, metal grids are deposited on the TCO usually by screen-printing [11], and specific silver paste needs to be used as the curing temperature should be below 250°C. The bulk resistivity of the fingers printed with low curing temperature (LCT) silver paste is strongly improving with the years but is still about two times higher than firing through silver paste (figure 2). For standard soldered ribbons interconnection, relatively thick busbars (between 25 and 35 microns) need to be printed for reaching the requirement of ribbon peel test (usually 1 N/mm). Finally, as a similar TCO contact is done at both the front and back sides, LCT silver paste is screen-printed on both sides, which steps up again the silver consumption compared to Al backside metallization of p-type cells. These three reasons increase the silver consumption for standard metallization and interconnection (M&I) applied for SHJ solar cells technology, limiting the cost effectiveness of the technology [12]. Thus, innovative approaches avoiding excessive amount of silver are welcomed. The M&I cost for SHJ cells technology is the topic of the presented paper.

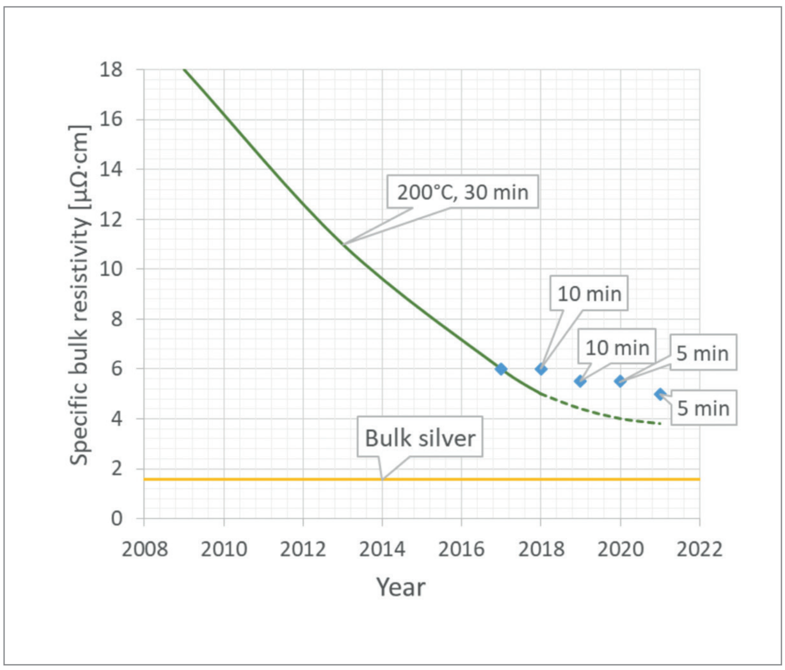

Figure 2. Specific bulk resistivity of low curing temperature silver paste evolution compared to pure silver (horizontal line). Continuous line is from paste measurement after 30 minutes curing at 200°C, dashed line is the forecast for curing 30 minutes at 200°C and diamond are curing at 200°C for shorter time also with forecast (data courtesy of Namics Corporation).

Metallization

In the PV market end of 2017, industrial metallization designs were the following: about 40% with four busbars (4BB), 40 % as well with 5BB, only 10% with 3BB and the last 10% shared between 6BB and wire interconnection. In seven years from now, predictions from [13] indicate that 5BB could have about 50% of the market share, 6BB and more could have about 30% and the rest could be covered by busbar-less design: meaning that three and 4BB will have disappeared from the market. Today, 97% of the metallization is done by screen-printing in

	Soldering			ECA-gluing			Wire interconnection	
	4BB	5BB	6BB	4BB	5BB	6BB	Certified	Optimized
Front mg	165	155	145	75	70	65	40	20
Back mg	255	220	190	170	135	110	60	40
Total mg	420	375	335	245	205	175	100	60

Table 1. Screen-printed silver paste deposited mass at front and backside for 4, 5, 6 busbars for soldering, electrical conductive adhesive (ECA) gluing and wire interconnection grid design ("certified" can pass five times IEC reliability test and "optimized" for lower silver usage).

the PV industry, most of the rest is plating. Copper electroplating could grow from 3% today to about 8% in seven years [13].

Screen-printing

As discussed in the introduction, screen-printing for SHJ solar cells consumes more silver compared to standard cells due to three reasons. Indeed, the bulk resistivity of the printed material is still higher than the one achieved with standard firing through paste, even though the evolution in low temperature cured material is impressive, as shown in Figure 2. Today, the best silver paste has specific bulk resistivity (ρc) of 6 and 5 µΩ.cm after 10 and 30 minutes of curing at 200°C, respectively. In four years, ρc could be at 5 and 3.8 µΩ.cm for 5 and 30 min of curing at 200°C, respectively. In literature, some pastes have shown already today bulk resistivity from 4 to 4.5 µΩ.cm after only 5 to 10 min at 200°C [14]. The future ρc perspectives extrapolate the value down to 3.5 µΩ.cm in 2020 and 3.0 µΩ.cm in 2022 [14]. As the bulk resistivity is higher, more silver or more busbars are needed on the cells for similar performance. The second limitation is the soldering on LCT silver paste; adhesion can reach 1 N/mm with a minimum BB thickness between 25 and 35 µm. This induces also a higher silver consumption compared to standard paste. The final reason is clearly observed in Table 1: as LCT paste is printed on both sides, consumption of LCT silver paste is important and reaches 420 mg in total for 4BB design. This consumption is reduced to 375 mg and 335 mg for 5BB and 6BB, respectively.

Front side laydown of high temperature silver paste is about 90 mg; in the case of SHJ, the front side laydown for soldering interconnection is about 50% to 80% higher depending on the number of BB due to higher ρc and thicker BB as shown in Table 1 [13]. If the interconnection is done via

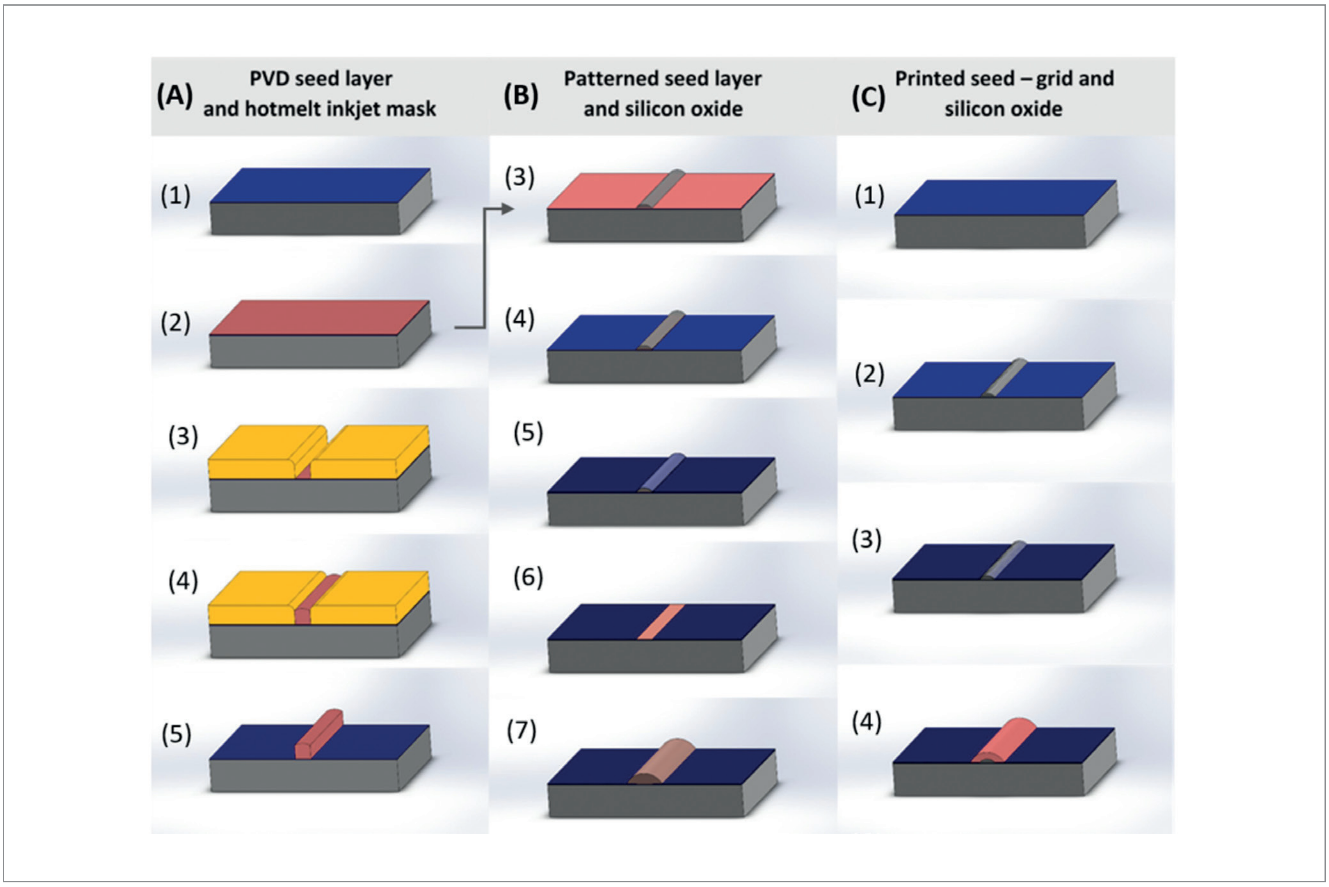

Figure 3. Comparison of process steps for fabrication of seed-layer and masking before copper electro-plating: (A) seed layer + organic mask, (B) patterned seed layer + dielectric and (C) printed seed-grid + dielectric.

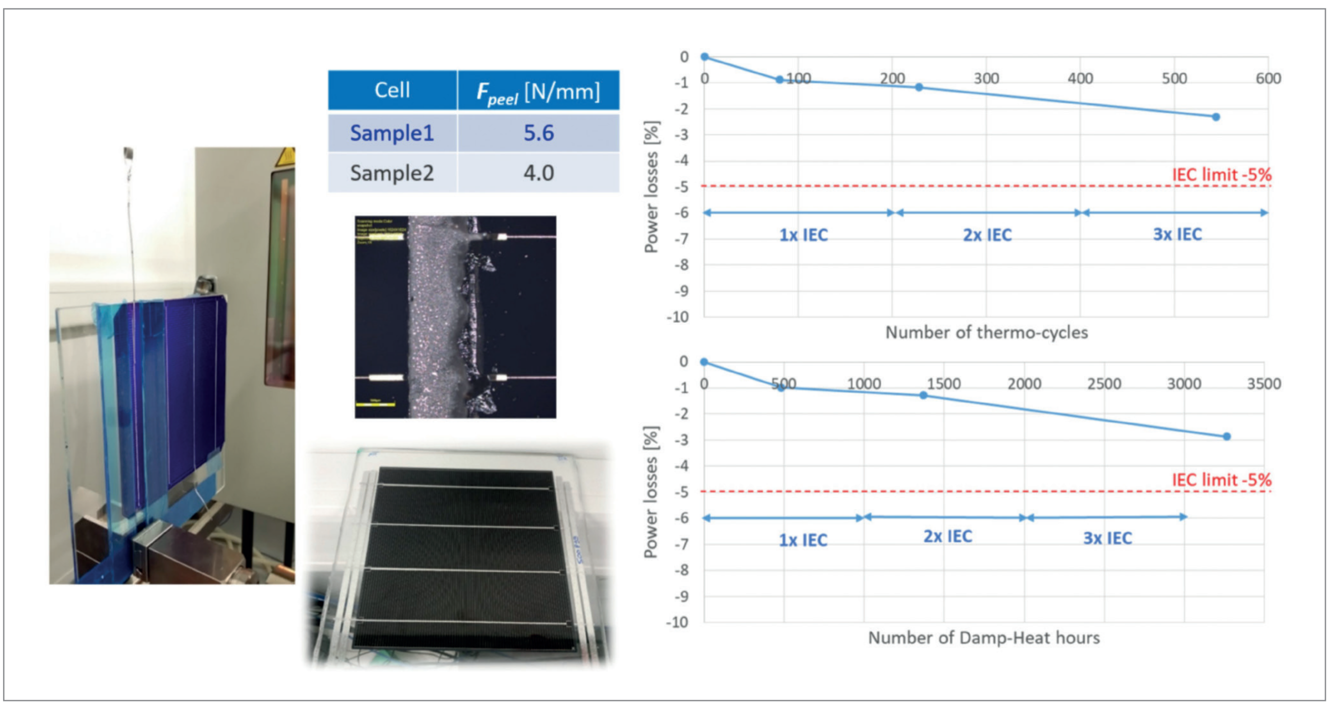

Cell	F_{peel} [N/mm]
Sample1	5.6
Sample2	4.0

Figure 4. Cells plated with sputtered seed layer and hotmelt inkjet mask and interconnected with soldered ribbons: Peel force test at 180° and thermo-cycles and damp-heat reliability test of small R&D module. Source: CSEM.

gluing the LCT silver paste mass at the front side drops by more than 50% to values as low as 65 mg for 6BB. This saving in paste is possible as busbars are drastically reduced; the gluing using electrical conductive adhesive (ECA) can be done directly on TCO surface and on optimized BB design.

In the case of wire interconnection, busbar-less (BB-less) design is used with ultra-fine fingers (silver line) dropping the laydown to 40 or 20 mg. The wire interconnection uses 12 or more wires, which strongly reduces the power loss in the finger due to charge transportation as compared to 4 to 6BB [15]. As the ohmic loss in the finger is heavily reduced, the silver mass can be strongly decreased. The laydown of 20 mg gives module with high performance but the reliability might be affected with today's paste and wire interconnection.

The silver mass at the backside is always higher compared to the front side because the number of fingers is higher to reduce the power loss in the backside TCO to optimize the cell fill factor (FF).

Copper electroplating

Owing to the impressive improvements in screen printing and the reduction of silver price the share of plating in production is much lower than originally predicted [13,16], with Sunpower and IBC cells being the main contributor. Plating activities for SHJ solar cells (or similar) have been reported by several companies such as Panasonic [4], Kaneka [17], Choshu Industry Co. LTD [18], Tetrasun [19, 20], Silevo and Sunpreme [21].

Having the advantage of the intrinsic bifaciality of heterojunction cells and taking into account the fast increasing market share of bifacial cells [13] we focus on processing routes enabling simultaneous plating on both sides. This implies sufficient lateral conductivity along the wafer surface. Basically three processing routes are conceivable: first (3A), the deposition of a seed layer over the entire wafer surface and an organic plating mask (figure 3A) or a conductive "seed-grid" and a dielectric layer to prevent metal deposition on the TCO, where the conductive seed-grid is formed either through patterning of a sputtered seed layer (figure 3B) or by printing of a metal paste (figure 3C).

For the first processing route (figure 3A), the seed layer is usually deposited by PVD (A2) and consists of a stack comprising a barrier or adhesion layer and a conductive layer [22]. The type of masking (A3) determines the shape and dimensions of plated lines. The simplest is a screen-printed mask (non-photosensitive organic resist) with rather wide openings, usually above 70 µm [23] and with bevel edges leading to increasing finger width as the thickness of plated copper increases. This method is applicable to cells without constraints for shadowing by metallization, like for IBC cells. With photolithography, narrow and rectangular fingers (~20 µm) can be defined. However, even though photolithography is used for mass production of (low-cost) printed circuit boards, for solar cells photoimaging-free alternatives are needed for further cost reduction. A non-photosensitive liquid photoresist, applied by spraying and patterned by inkjet printing of a functional liquid, has been described for metallization of busbar-less cells for SmartWire interconnection [24], with finger width 20-25 µm and finger height 5-10 µm. Another photoimaging-free method is inkjet printing of a hotmelt ink [25]. It requires only one process step for patterning, with geometries of plated lines comparable to photolithography [26]. After copper and finish layer (for example silver or tin) plating (A4), the organic mask is removed and the seed layer is etched back (A5). CSEM has develop further this process sequence to obtain up to a 24.1% record 4BB cell efficiency [26], high peel force of standard PbSn coated ribbon soldering and good coupon module reliability even after three times IEC (see Figure 4).

In the second processing route (Figure 3B), the processing sequence can start with a blanket seed layer. Onto the seed layer a grid pattern is deposited by inkjet printing of an UV-curable ink (B3) and the seed layer blanket in between the grid is etched away (B4). Subsequently a dielectric layer like silicon oxide or silicon nitride is deposited for instance by PECVD over the entire surface (B5), including also the UV-ink. The dielectric serves at the same time as an additional antireflective coating, giving the possibility for TCO thickness reduction. The openings in the dielectric are formed through removal of the UV-ink (B6), simultaneously exposing the seed layer grid for the plating of copper and finish layer (B7).

The third processing route (figure 3C), is based on a seed-grid formed by simple screen printing or inkjet printing of a metal paste or respectively a metal ink (C2). Because of the rough surface of the printed metal the subsequently deposited dielectric layer (C3) is non-continuous on the seed-grid. Plating selectively occurs (C4) where the printed grid is present underneath the dielectric. The industrial feasibility of this process sequence has been confirmed by Kaneka, moreover the module stability during damp-heat ageing has been significantly improved through the dielectric, a PECVD-SiOx layer [17].

Numerous variations of the processes described above have been reported and new processes are being developed with the aim to further simplify the process sequence and to reduce cost [27].

Cell interconnection

Interconnection of SHJ cells was for a long time the critical point as standard soldering is not well adapted on LCT silver paste. Due to this limitation new approaches of cell interconnection were tested and developed for SHJ cells like gluing of ribbon using electrical conductive adhesive (ECA) or wire interconnection well adapted to SHJ cells proposed by Meyer Burger and called SmartWire Connection Technology (SWCT).

Soldering

Usually, the silver busbar peels off the TCO surface after standard soldering with force bellow 1 N/mm. To reduce the stress between the cell and the ribbon, solder based on BiSnAg can be used as shown by Isofoton 10 years ago for standard c-Si solar cell [28, 29]. As the melting temperature of BiSnAg is about 40°C lower compared to PbSn, the stress between cell and ribbon is reduced as well as the silver leaching from the busbar into the solder. Nowadays some companies are proposing bismuth based solder and dedicated flux for PV application [30, 31]. Paste manufacturers also improved the paste formulation to enable standard PbSn soldering on the LCT busbar paste.

	ECA screen-printing process		
	4BB	5BB	6BB
ECA deposit (mg 2 sides) - reliable	80	100	120
ECA deposit (mg 2 sides) - optimized	32	40	48

Table 2. Electrical conductive adhesive deposit done by screen-printing process for 4, 5 and 6 busbars ("reliable" pass two time IEC reliability test).

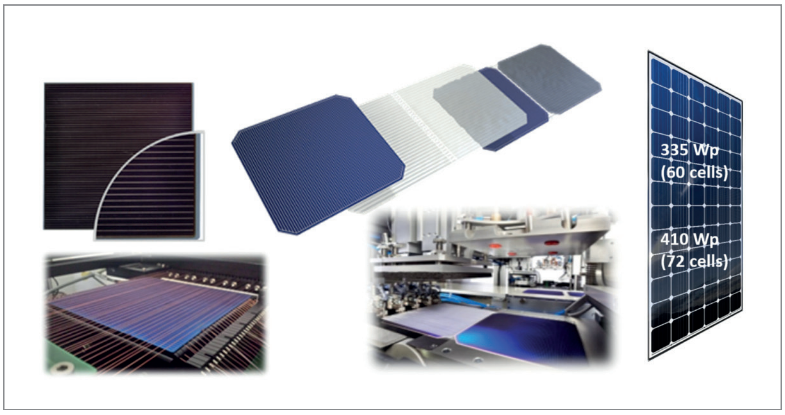

Figure 5. Busbarless cells and the GridTouch measurement, the SWCT concept and bifacial record module for 60 and 72 SHJ cells at 1 Sun.

Ribbon gluing

Nowadays the ribbon interconnection can be attached with electrical conductive adhesives (ECA) or conductive films using production tools while keeping the same reliability as for the soldered ones [32-36]. ECA is a conductive glue composed normally by silver particles; for cost reduction other metals are used like Ni, Cu or Sn based alloys [37, 38]. ECA can be applied by screen-printing, dispensing or valve jetting. The conductive films are composed of preformed conductive adhesive in foil shape. Beside silver screen-printing paste saving, the second advantage of ribbon gluing is the possibility of using textured ribbons (like the light-capturing ribbons from Ulbrich), which allows the recycling of the light falling on the ribbon and increases the module power up to 2% relative [39, 40]. The silver paste saving is balanced by the use of ECA, that has a similar price, as shown in Table 2. For reliable process, 10 mg of ECA per ribbon are needed to date, whereas only 4 mg can be used after

	Print + Soldering			Print + ECA-gluing			Print + SWCT		Plating + soldering		
Cell Efficiency (%)	4BB	5BB	6BB	4BB	5BB	6BB	Certified	Optimized	4BB	5BB	6BB
	22.4	22.5	22.7	23.0	23.1	23.2	22.8	23.0	22.7	22.7	22.7
CTM performance	1.01	1.01	1.01	1.00	1.00	1.00	1.01	1.01	1.01	1.01	1.01
Module power (Wp)	398	400	403	404	406	408	405	408	403	403	403
Module power Bifi20 (Wp)	470	472	476	477	479	482	478	482	476	476	476

Table 3. Performance of the cells done by screen-printing and plating with different grid design, module with 72 cells in glass/glass configuration and the respective cell-to-module (CTM) factor. Module power is calculated for a bifacial module with 20% power from the backside due to the albedo (Bifi20). Module bifaciality is 90%.

important process optimization (module reliability under investigation).

Wire interconnection

Wire interconnection has been implemented by different major solar manufacturers such as LG and Hanwa Q CELLS. The major gains are reduction of power loss in the metallization grid, reduced interconnection shadowing, improved module reliability against cell cracks and increased power output by more than 3% relative [8, 41]. SWCT from Meyer Burger is composed of low melting temperature alloys coated on copper wire that are supported by a polymer foil, which was initially developed by day4 Energy [42] (see Figure 5). In the last years, an important development has been done to reduce the cost of the wire and adapt the foil-wire assembly to improve the performance as well as the reliability, enabling power output higher than 335 Wp for 60 cells and 410 Wp for 72 cells and module passing five times IEC for thermo-cycles (1,000 cycles between -40°C and +85°C) without noticeable degradation and five times IEC for damp-heat (5,000 hours at 85°C and 85% relative humidity) [43, 44]. As a validation of the strong improvement in the Meyer Burger interconnection technology, SWCT equipment was ordered last May by Panasonic in Osaka for interconnection of its HIT cell technology [45].

Cell and module power

The cell efficiencies and module power shown in Table 3 have been measured experimentally on R&D runs of a few hundred cells from paired wafers in the case of printed cells. In the case of plated cells, the values are based on a few dozen cells based on paired wafers with printed cells. The module power is based on a smaller size module and extrapolated to 72-cell modules in the case of plated cells. Cell efficiencies are increasing with busbar numbers for printed cells as the power loss in the fingers is reduced; this is not the case for plated cells as the finger line resistance is lower. For the ECA-gluing case, the cell efficiency is higher thanks to reduced shadowing from fine busbars. In the case of busbar-less cells (SWCT), the contacting for cell measurement is done with GridTOUCH from Meyer Burger: the efficiency is then corrected as effective efficiency to account for wire shadowing in the module [46]. Thanks to light reflection inside the module, shadowing of textured ribbons and wire is reduced by 40% and 30%, respectively.

Cost methodology

The cost calculation is done for seven years of amortization for the equipment price and includes standard consumables such as silver paste, screen and squeegee for screen-printing. In the case of plating, the cost depreciation and consumables for all processing steps have been considered, including seed layer deposition, patterning, plating chemistry and waste treatment. Most of the country-dependent costs such as manpower, land, electricity and interest rate are being excluded.

The costs of both metallization and interconnection are in the range of €0.022/Wp to €0.049/Wp (see Figure 6). These values are between 7 and 16% of the module price if one considers standard modules. Today's price for modules based on multi-Si cells is about €0.3/Wp; as modules based on SHJ cells can be considered as high-efficiency bifacial module (about 18% relative higher efficiency compared to multi-Si) the price can be increased due to higher energy yield and reduced surface and balance-of-system (BOS) costs of the PV installation [13].

By using standard soldering about 90% of the costs is due to the LCT silver paste. With ECA-gluing the silver paste cost is nearly divided by two but some of the reduced costs are transferred to the ECA glue and textured ribbon coated with silver. Finally the cost reduction of passing from standard soldering to ECA-gluing is in the range of -8 to -15% for 6 to 4BB, respectively. By optimizing the process of ECA deposition and using silver-free textured ribbons, the metal and interconnection cost will be reduced again by about -20% (figure 7).

SmartWire Connection Technology enables the silver cost to be divided by four or by seven in the case of a certified bill-of-materials (passing five times IEC reliability test) and optimized processes still at R&D stage, respectively. Compared to standard soldering the absolute cost saving for the metallization and interconnection (M&I) is about €-0.02/Wp or about -10 eurocents/wafer or €-7/module. The second interesting point with SWCT is that the silver cost represents less than half (or less than a third with the light process) of the M&I total

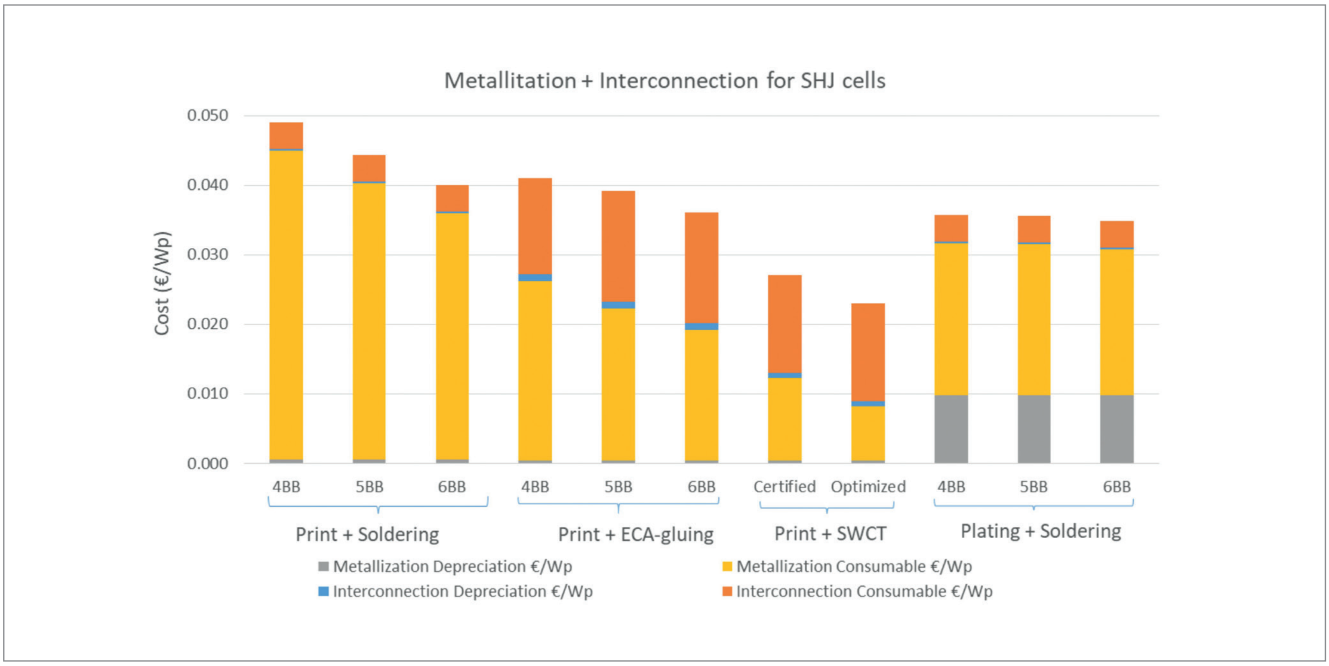

Figure 6. Metallization and interconnection (M&I) cost comparison for the different technologies for bifacial modules. First group is for low curing temperature silver paste screen-printing (SP) and standard soldering, then SP + electrically conductive adhesive (ECA) gluing of textured ribbons, third group SP + SmartWire ConnectionTechnology (SWCT) and finally copper plating using PVD seed layer with hotmelt inkjet mask process.

cost, so the silver price variability on the PV module cost will be reduced.

To remove totally the silver variability of the PV module, copper electroplating will be the solution. A plating process with sputtered seed layer and hotmelt inkjet mask is included for comparison. Today's price for this process is better than standard soldering and competitive with screen-printing and ECA-gluing of textured ribbons. Alternative processing routes are described in the plating section.

Cost comparison for three plating sequences

The calculation is based on cost figures provided by equipment and chemistry suppliers, partially on literature values [12] and on calculations implementing experience from our R&D pilot line. As already mentioned for screen printing, only depreciation for equipment (over seven years) and costs for materials, consumables and waste water treatment are included.

The considered processes are:

A. first a PVD seed layer with hotmelt inkjet mask (figure 3A)
B. a patterned PVD seed with a silicon oxide layer deposited by PECVD (figure 3B)
C. an inkjet-printed seed-grid, also with silicon oxide (figure 3C).

First, it is worth commenting that the depreciation cost is significantly higher than for screen printing mainly due to several process steps being involved: PVD, inkjet-printing and plating and chemical steps (figure 6 and 8). Additionally, the actual production volumes for these equipment types are small and the price consequently higher compared to screen printers.

For the A process the biggest portion of the consumables is the price for hotmelt-ink. The ink

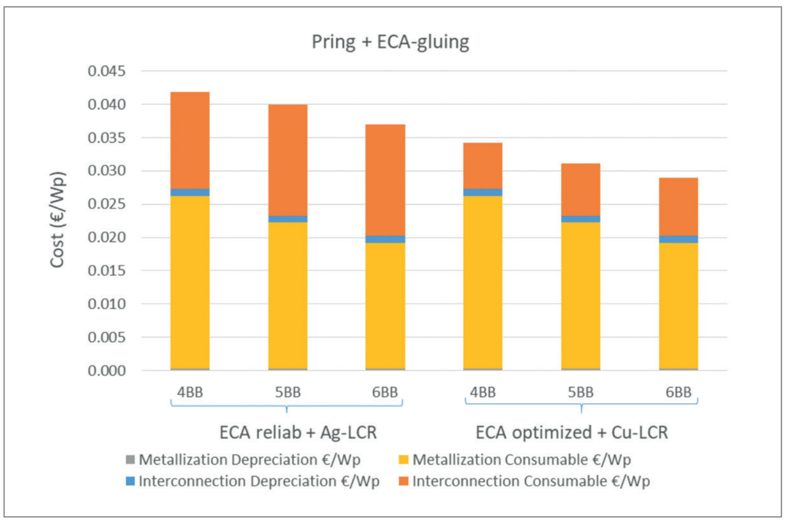

Figure 7. Metallization and interconnection (M&I) cost of screen-printing + ECA-gluing of light capturing (LCR) silver-coated ribbons passing two times IEC (ECA-reliab) versus optimized deposition of ECA and silver-free LCR ribbons.

consists mainly of commonly available waxes and a huge potential for cost reduction with increasing production volumes and more competition in the market may be assumed.

For the second process with patterned PVD seed, one more piece of equipment is required – PECVD for the dielectric layer – further increasing the capex. On the other side the cost for consumables is reduced, still with potential for reduction by volume effects e.g. for UV-curable ink.

For the last process also inkjet-printing of silver nanoparticles ink is considered for the sake of comparability with the other two processes utilizing an inkjet printer. The consumption of

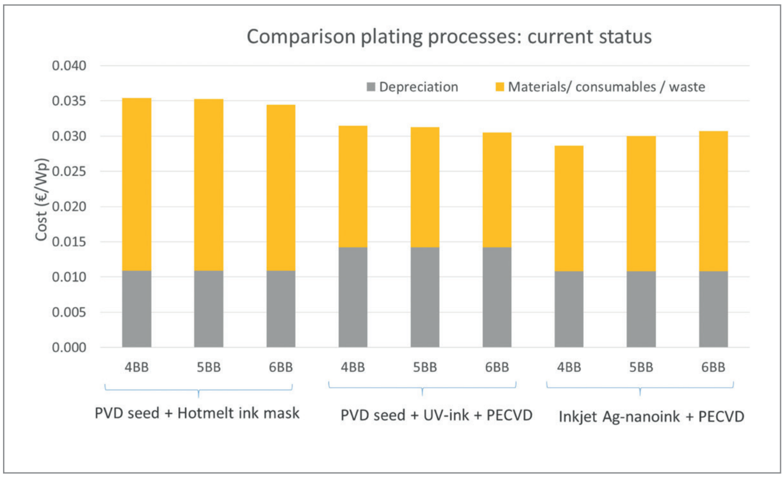

Figure 8. Metallization only cost comparison of three different masking processes for copper-plating (current status).

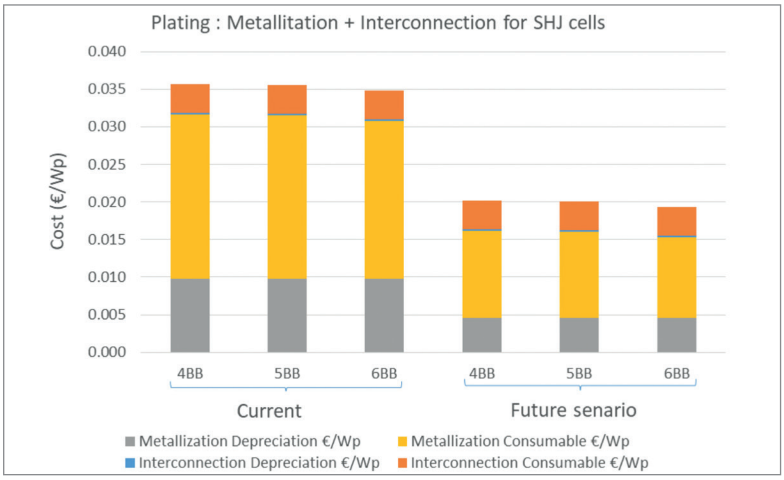

Figure 9. Future scenario with 50% average cost/Wp reduction for copper plating equipment and process using PVD seed layer with hotmelt inkjet mask process.

the nano-ink is extremely low, even below 10 mg for the front side of a busbar-less cell [25], but the price of the nano-ink is at the R&D stage. Here the processing cost increases for 5 or 6 busbars because of higher ink consumption, contrary to the other two processes with a slightly lower price for 5 or 6 busbars, because of thinner required copper plated fingers and consequently slightly shorter plating line.

As demonstrated by Kaneka, screen-printed silver paste can be used in spite of nano-ink, with paste consumption at 20 mg for the entire seed-grid on the front [17], which entails not only lower paste cost but also cheaper equipment. The value for efficiency has been kept constant for all processes at 22.5%. A small gain in Jsc is achievable with plated fingers defined by hotmelt ink; the difference with screen printing depends on the layout and achievable printed line width for the given layout (number of busbars). On the other side, the round shape of the plated line done over a thin dialectric mask (Figure 3 B and C) reduces the optical finger width in the module, similar to screen-printed fingers [47].

In Figure 9, an optimistic future scenario is shown, supposing average price/Wp (which includes cell efficiency and throughput increase with equipment and consumable price reduction) reduction by 50% for equipment as well as for materials and consumables simply by volume effects and continuous process improvement, once the implementation of plating in production has gained a bit more momentum. Such evolution has been seen for screen printing during the last seven years, with savings even higher than 50% taking into account the reduction in silver paste consumption (-60%), the equipment throughput increase (+50%), cell efficiency improvement (+18% relative) and the silver price decrease between 2011 and 2018 (-60%). [13, 48-50]. This supposed cost reduction places the plating + standard soldering as the cheapest M&I option for SHJ PV bifacial module. Nevertheless, as plating is not already implemented for metallization in SHJ cell production, some more R&D work needs to be done on the topic, to improve and develop the best option in term of efficiency, reliability and cost approach. But the conclusions of this work show the cost reduction potential of this metallization technology to make it competitive for high efficiency SHJ cells and modules.

Conclusion

When new technologies enter the market, like silicon-heterojunction (SHJ) solar cells and modules for the PV market, new opportunities and challenges are present. In the aforementioned case, the metallization and interconnection (M&I) combined processes could be a nice opportunity for new technologies – in particular for the light-capturing (LCR) ribbons attached with electrical conductive adhesive (ECA) interconnection that can save today 10% of cost for 5BB cell design with 6 Wp gain on a 72-cell module and up to 30% with process optimization.

SmartWire Connection Technology was developed with a strong emphasis for the SHJ technology in the last years, and this technology reduces the cost of M&I by 50% thanks to silver consumption divided by four in the case of reliable modules and by seven in the case of the light-silver approach. The power gain for a 72-cell module is 5 and 8 Wp in the case of the reliable module and light-silver approach, respectively.

In spite of the high complexity of plating there are processing routes available already today with costs comparable to screen printing for ribbon interconnection. Further cost savings are possible simply by volume effects and continuous process improvements, provided the implementation of plating in production would finally start. But the hurdle is high: different technologies, high investment, only small amounts of data on reliability. A technological need will be necessary to make the decision for plating like in case of IBC cells. The high conductivity of copper lines would also enable a reduction in the number of cell segments for shingling, and thus a reduction in laser cutting steps.

The silver consumption for PV accounts for 7.5% of the world silver supply and the production capacity is supposed to be at least three times higher in 2025 [13]. The higher demand may lead to a higher silver price and give an additional stimulus for copper plating.

Acknowledgment

This work was supported by the EU with projects NEXTBASE, DISC and AMPERE. The authors would like to acknowledge Mark Francis from EMS, Marco Galiazzo and Giorgio Cellere from Baccini Cell System/Applied Materials, Christian Prischmann from Ulbrich, Tero Horttana from Luvata, Dmitriy Andronikov from Hevel Solar, Martijn Zweegers from Meco, Joost Hermans from Meyer Burger (Netherlands) B.V. and Bruce Lee from MacDermid-Enthone.

References

[1] H. Kuriyama, S. Nakano, S. Okamoto, T. Takahama, "Photovoltaic Device", JP2846651B2, March 1989.

[2] S. Nakano, S. Okamoto, T. Takahama, M. Nishikuni, "Photovoltaic Device", GB2230138, Oct. 1990.

[3] M. Tanaka, M. Taguchi, T. Matsuyama, T. Sawada, S. Tsuda, S. Nakano, H. Hanafusa and Y. Kuwano, "Development of New a-Si/c-Si Heterojunction Solar Cells: ACJ-HIT (Artificially Constructed Junction-Heterojunction with Intrinsic Thin-Layer)", Japanese Journal of Applied Physics, Volume 31, Part 1, Number 11, (1992)

[4] K. Masuko, M. Shigematsu, T. Hashiguchi, D. Fujishima, M. Kai, N. Yoshimura, T. Yamaguchi, Y. Ichihashi, T. Mishima, N. Matsubara, T. Yamanishi, T. Takahama, M. Taguchi, E. Maruyama and S. Okamoto. "Achievement of More Than 25%; Conversion Efficiency With Crystalline Silicon Heterojunction Solar Cell", Journal of Photovoltaics, IEEE, vol. 4, no. 6, pages 1433–1435, (2014)

[5] K. Yoshikawa, H. Kawasaki, W. Yoshida, T. Irie, K. Konishi, K. Nakano, T. Uto, D. Adachi, M. Kanematsu, H. Uzu and K. Yamamoto, "Silicon heterojunction solar cell with interdigitated back contacts for a photoconversion efficiency over 26%", NATURE ENERGY 2, 17032, (2017)

[6] T. Mishima, M. Taguchi, H. Sakata and E. Maruyama, "Development status of high-efficiency HIT solar cells", Solar Energy Materials & Solar Cells, (2011)

[7] J. Haschke, J. P. Seif, Y. Riesen, A. Tomasi, J. Cattin, L. Tous, P. Choulat, M. Aleman, E. Cornagliotti, A. Uruena, R. Russell, F. Duerinckx, J. Champliaud, J. Levrat, A. A. Abdallah, B. Aissa, N. Tabet, N. Wyrsch, M. Despeisse, J. Szlufcik, S. De Wolf and C. Ballif, "The impact of silicon solar cell architecture and cell interconnection on energy yield in hot & sunny climates", Energy & Environmental Science, DOI: 10.1039/c7ee00286f, (2017)

[8] T. Söderström, et al., "Low cost high energy yield solar module lines and its applications", Proc. 42nd IEEE PVSC, New Orleans, Louisiana, USA. (2015)

[9] Panasonic Solar: HIT, Mai 2017, https://panasonic.net/ecosolutions/solar/

[10] D. Andronikov, A. Abramov, S. Abolmasov, K. Emtsev, G. Ivanov, A. Kukin, I. Nyapshaev, D. Orekhov, A. Semenov, G. Shelopin, E. Terukova, E. Terukov, N. Belkova, A. Dubrovskiy, P. Ishmuratov, A. Ivanov, D. Saykin, I. Shakhray, A. Smirnov, V. Tarasov, V. Timakov, A. Tomchinskiy, G. Kekelidze, "A Successful Conversion of Silicon Thin-Film Solar Module Production to High Efficiency Heterojunction Technology" 33rd European Photovoltaic Solar Energy Conference and Exhibition, p. 732 – 735.

[11] S. DeWolf, A. Descoeudres, Z. C. Holman and C. Ballif, "High-efficiency Silicon Heterojunction Solar Cells: A Review", Green, Vol. 2 (2012), pp. 7–24, (2012)

[12] A. Louwen, W. van Sark, R. Schropp and A. Faaij, "A cost roadmap for silicon heterojunction solar cells" Solar Energy Materials and Solar Cells, Vol. 147, pp. 295-314. (2016)

[13] International Technology Roadmap for Photovoltaic (ITRPV) 9th Edition report, March 2018, itrpv.net

[14] A. Bettinelli, et al., "Busbar and busbar-less heterojunction cell printing on CEA-INES pilot line ribbons and SWCT module performance", Metallization and Interconnection Workshop, Konstanz, 24 October 2017.

[15] A. Faes, M. Despeisse, J. Levrat et al., "SmartWire Solar Cell Interconnection Technology", Proc. 29th EU PVSEC, Amsterdam, The Netherlands, (2014)

[16] ITRPV International Technology Roadmap for Photovoltaic, 5th Edition, 2014

[17] D. Adachi, T. Terashita, T. Uto, J. L. Hernández and K. Yamamoto, "Effect of SiOx barrier layer prepared by plasma-enchanced chemical vapor deposition on improvement of long-term reliability and production coast for Cu-plated amorphous Si/crystalline Si heterojunction solar cells", Solar Energy Material and Solar Cells, 2017

[18] F. Ishimura, W. Li, E. Kobayashi, K. Hashimoto, S. Sato, Y. Watabe,E. Bende, and G. Coletti, "Metal Wrap Through Heterojunction Solar Cell with Plated Electrode", 32nd European Photovoltaic Solar Energy Conference and Exhibition (2016)

[19] https://phys.org/news/2013-11-solar-cell-efficient-costly.html

[20] Luca Pavani, Adrian Turner, Oliver Schultz-Wittmann, "Silicon Cracking in Plated c-Si Solar Cells", Reliability Workshop, NREL, 2012.

[21] B. Li "Industrial bifacial silicon heterojunction technology that improves system LCOE", Hercules Workshop, Berlin, 2016

[22] S. Singh, B. O'Sullivan, M. Kyuzo, S. Jambaldinni, L. Tous, R. Russel, M. Debucquoy, J. Szlufcik and J. Poortmans, "Application of seed and plate

metallization to 15.6cm x 15.6cm IBC cells", Photovoltaics International, Vol. 29 (2015)
[23] A. Khanna et al., "Screen-printed masking of transparent conductive oxide layers for copper plating of silicon heterojunction cells", Applied Surface Science, 2015
[24] Z. Li, P.-C. Hsiao, W. Zhang, R. Chen, Y. Yao, P. Papet, A. Lennon, "Patterning for Plated Heterojunction Cells", Energy Procedia, Volume 67, Pages 76-83, (2015)
[25] J.P. Hermans, R. von Knippenberg, E. Kamp, W.J.M Brok, P. Papet, B. Legradic, B. Strahm, "Inkjet Printing for Solar Cell Mass Production on the PIXDRO JETX Platform", 28th European Photovoltaic Solar Energy Conference and Exhibition, Paris, 2013
[26] A. Lachowicz, J. Geissbühler, A. Faes, J. Champliaud, F. Debrot, E. Kobayashi, J. Horzel, C. Ballif, M. Despeisse, "Copper Plating Process for Bifacial Heterojunction Cells", 33rd European Photovoltaic Solar Energy Conference and Exhibition, Amsterdam, 2017
[27] A. Rodofili, W. Wolke, L. Kroely, M. Bivour, G. Cimiotti, J. Bartsch, M. Glathaar, J. Nekarda, "Laser-transferred Ni-seed for the Metallization of Silicon Heterojunction Solar Cells by Cu Plating", 33rd European Photovoltaic Solar Energy Conference and Exhibition, Amsterdam, 2017
[28] B. Lalaguna, P. Sánchez-Friera, I.J. Bennett, D. Sánchez, L. J. Caballero, J. Alonso, EVALUATION OF BISMUTH-BASED SOLDER ALLOYS FOR LOW-STRESS INTERCONNECTION OF INDUSTRIAL CRYSTALLINE SILICON PV CELLS, 22nd European Photovoltaic Solar Energy Conference, 3-7 September 2007, Milan, Italy.
[29] B. Lalaguna, P. Sánchez-Friera, H. Mäckel, D. Sánchez, J. Alonso (Isofoton), EVALUATION OF STRESS ON CELLS DURING DIFFERENT INTERCONNECTION PROCESSES, 23rd European Photovoltaic Solar Energy Conference, 1-5 September 2008, Valencia, Spain
[30] https://alphaassembly.com/Products/Photovoltaic, 28.08.2018
[31] http://www.indium.com/solar-assembly-materials/, 28.08.2018
[32] Teamtechnik, https://www.teamtechnik.com/en/news/major-contract-for-teamtechnik-italian-pv-manufacturer-orders-stringers-for-pro-duction-of-high-efficiency-modules-with-hjt-cells/
[33] A. Schneider, R. Harney, S. Aulehla, E. Lemp, S. Koch, "Progress in interconnection of busbar-less solar cells by means of conductive gluing" Energy Procedia Vol. 38, pp. 387 – 394, (2013)
[34] T. Geipel, Z. Huq and U. Eitner, "Reliable interconnection of the front side grid fingers using silver-reduced conductive adhesives", Energy Procedia Vol. 55, pp. 336 – 341, (2014)
[35] Engineered Materials Systems, Inc., Nagase Group, http://nagaseamerica.com/product/conductive-ribbonstringer-attach-adhesives/
[36] A. De Rose, et al., "Challenges for the interconnection of crystalline silicon heterojunction solar cells", Photovoltaics International, Volume 40, 2018.
[37] M. Yoshidaa, H. Tokuhisaa, U. Itoha, T. Kamataa, I. Sumitab, S. Sekinec, "Novel Low-Temperature-Sintering Type Cu-Alloy Pastes for Silicon Solar Cells" Energy Procedia Vol. 21, pp. 66 – 74, (2012)
[38] G. Beaucarne, I. Kuzma-Filipek, F. Campeol, et al. "Innovative cell interconnection based on ribbon bonding of busbarless cells using silicone-based electrically conductive adhesives", Energy Procedia Vol. 67, pp. 185 – 193., (2015)
[39] W. Muehleisen, L. Neumaier, C. Hirschl et al., "Comparison of output power for solar cells with standard and structured ribbons", EPJ Photovoltaics Vol. 7, pp. 70701, (2016)
[40] H. Holst, H. Schulte-Huxel, M. Winter et al. "Increased light harvesting by structured cell interconnection ribbons: an optical ray tracing study using a realistic daylight model" Energy Procedia, Vol. 92, Pages 505-514, (2016)
[41] S. Braun, G. Micard and G. Hahn, "Solar cell improvement by using a multi busbar design as front electrode" Energy Procedia Vol. 27, pp. 227 – 233, (2012)
[42] A. Schneider, L. Rubin, & G. Rubin, "Solar cell improvement by new metallization techniques – The DAY4TM electrode concept", Proc. 4th WCPEC, Waikoloa, Hawaii, USA, p. 1095, (2006).
[43] C. Ballif et al., "Novel designs and materials for durable PV modules: applications on the ground, in cities and in the air" IEEE PVSC-44, Washinton, (2017)
[44] CEA, Meyer Burger, "Record 410 watt module with photovoltaic heterojunction cell technology", 28.04.2018, http://liten.cea.fr/cea-tech/liten/en/Pages/News/record-photovoltaic-heterojunction.aspx
[45] Meyer Burger, Panasonic, "Meyer Burger's SmartWire Connection Technology selected by Panasonic Solar for evaluation in the manufacture of its innovative high efficiency solar modules", 28.05.2018, https://www.meyerburger.com/jp/en/meyer-burger/media/news-detail/article/meyer-burgers-smartwire-connection-technology-selected-by-panasonic-solar-for-evaluation-in-the-man/
[46] P. Papet, et al., "Effective Efficiency of Busbarless solar cells", Metallization and Interconnection Workshop, Konstanz, 24 October 2017.
[47] Y.Chen, Y. Yang, W. Deng, A. Ali, P.P. Altermatt, and P.J. Verlinden, "Shape and homogeneity of front metal fingers – impact on cell efficiency and its distribution in production lines", 6th Metallization Workshop, Konstanz, (2016)
[48] ITRPV International Technology Roadmap for Photovoltaic, 2nd Edition, 2011
[49] ITRPV International Technology Roadmap for Photovoltaic, 4th Edition, 2014
[50] https://silverprice.org/silver-price-history.html, 31.08.2018.

About the Authors

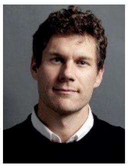

Antonin Faes received his PhD in 2010 for his work on solid oxide fuel cells at the Interdisciplinary Centre for Electron Microscopy (CIME) and the Industrial Energy System Laboratory (LENI) at EPFL. In 2012 he joined the CSEM PV-center in Neuchâtel, where he is responsible for c-Si solar cell metallization and interconnection activities, with a particular focus on silicon heterojunction solar cells.

Agata Lachowicz studied chemistry at Heinrich Heine University Düsseldorf and worked initially on processes for printed circuit boards, followed by development of etching and plating processes for solar cells at Schott Solar and optimization of PERC cells at Meyer Burger Germany. She joined CSEM PV-centre in 2014 for development of plating processes for silicon heterojunction cells.

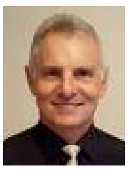

Armand Bettinelli received his PhD in 1987 for his work on cofiring of alumina and tungsten at the Strasburg University. He worked in the industry as Process or Technical manager in the field of High and Low T° Cofired Ceramics then Plasma Display Panels. In 2005 he joined the CEA-INES centre, where he works as senior expert for c-Si solar cell metallization and interconnection, for both homo and heterojunction c-Si solar cells.

Pierre-Jean Ribeyron has been involved in photovoltaic energy since 1994. He received his PhD from Grenoble University in 1998 on the crystallization of multicrystalline silicon for PV applications. In 2000, he joined CEA to build a first photovoltaic solar cell platform and moved in 2007 to CEA-INES as silicon solar cell lab manager. Since 2014, he has been a member of the executive board at CEA-INES. His research interest cover the whole value chain of PV, from silicon material to modules and systems as well as related technological transfer to industry.

Jean-François Lerat studied engineering in materials science & nanotechnologies at INSA Rennes (France) and at RWTH Aachen (Germany). He developed applications for a laser equipment manufacturer for four years in the semiconductor industry before joining CEA-INES. Since 2016, his work has focused on development in silicon heterojunction solar cells and advanced metallization.

Delfina Muñoz is a senior researcher in photovoltaic technology. She got her PhD in the Technical University of Catalunya on heterojunction solar cell development. She joined CEA-INES in 2008 in the heterojunction solar cell team. Since then, she has been actively working in material, device and integration improvement. She has been coordinating the successful FP7 HERCULES project.

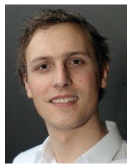

Jonas Geissbühler received his PhD from EPFL, Switzerland in 2015, writing his thesis on high-efficiency silicon heterojunction solar cells. He joined the CSEM PV-Centre in 2016. His research interests include the metallization of silicon heterojunction solar cells, inkjet printing and high efficiency silicon heterojunction solar cells.

Heng-Yu Li received his PhD from EPFL, Switzerland in 2013 on c-Si PV module technology. He joined the CSEM PV-Centre in 2014 and since then has been developing functional encapsulation materials and innovative module designs for BIPV, PIPV, advanced interconnection technology, etc. Since 2018, he has also been working towards ultra-long module lifetime and module lifetime modelling.

Christophe Ballif received his PhD from EPFL, Switzerland, in 1998. In 2004 he became a full professor with the Institute of Microengineering at the University of Neuchâtel, where he directs the Photovoltaics and Thin-Film Electronics Laboratory, which is now part of EPFL. Since 2013 he has also been the director of the CSEM PV-centre. His research interests include materials for PV, high-efficiency c-Si solar cells, module technology, BIPV and energy systems.

Matthieu Despeisse received his PhD in 2006 for his work on advanced detectors at CERN in Geneva, Switzerland. He then joined EPFL in 2009 as head of the thin-film silicon photovoltaics research team. Since 2013 he has led research activities at CSEM concerning crystalline silicon photovoltaics and metallization, with a special focus on silicon heterojunction technology, passivating contacts, metallization and interconnection.

Enquiries

Antonin Faes
Email: antonin.faes@csem.ch
Tel: +41 32 720 51 11,
Website: www.csem.ch

News

First Solar breaks ground on largest thin-film solar manufacturing plant in the US

Leading CdTe thin-film PV module manufacturer First Solar held a ground-breaking ceremony on 8 June 2018 for the construction of its new 1.2GW manufacturing plant near its existing flagship facility in Perrysburg, Ohio.

The planned annual nameplate capacity of the Ohio 2 facility makes it the largest single thin-film solar module manufacturing facility in the US and combined with the Ohio 1 flagship facility, creates the largest solar thin-film manufacturing hub in the US at 1.8GW.

Both facilities are dedicated to First Solar's large-area Series 6 modules (3x size) of its previous Series 4 modules.

Initial module production is expected in late 2019 and is expected to cost around US$400 million, while creating around 500 new jobs.

"Strong demand in the US for advanced solar technology, along with recent changes in US corporate tax policies, have encouraged our decision to grow First Solar's US production operations," said Mike Koralewski, First Solar's senior vice president of global manufacturing.

Credit: First Solar

First Solar's Initial module production is expected in late 2019.

MANUFACTURING

Manz gets further €67 million for major CIGS turnkey thin-film order

PV and electronics equipment manufacturing and automation specialist Manz AG has secured another advanced payment for CIGS (Copper, Indium, Gallium, DiSelenide) thin-film manufacturing equipment, which is part of a major production order with Chinese partners, the Shanghai Electric Group and the Shenhua Group.

The payment meant Manz had received almost €197 million (US$227.76 million) from the order worth around €263 million when it won the order at the beginning of 2017.

Eckhard Hörner-Marass, CEO of Manz AG said: "We are very optimistic that we will be able to continue moving forward on this challenging major order with determination and complete it successfully as planned. Our whole team is working ambitiously to complete the next upcoming milestones – if the project continues successfully, we expect follow-up orders from the first half of 2019 onwards."

The orders include a 44MW CIGS research line (CIGSlab) as well as a 306MW CIGS turnkey system (CIGSfab) for series production of CIGS thin-film solar modules. The CIGSfab was already launched with the ground-breaking in early 2018 in China.

Completion and acceptance of the CIGSlab and CIGSfab are scheduled for the middle of 2019.

First Solar's Series 6 module production starts in Malaysia as almost 900MW of new orders booked

Leading CdTe thin-film module manufacturer First Solar has started production of its large-area Series 6 modules at its first manufacturing plant in Malaysia and said it was nearing the start of production at a third facility as new orders in the second quarter almost reached 900MW.

First Solar had already started production of the Series 6 modules at its lead fab in Ohio, US late last year and the first production plant in Malaysia was said to have just started production late in the second quarter of 2018.

The 600MW Ohio fab was said to be at around 60% nameplate capacity and the Malaysia S6 Factory 1 at over 40% nameplate capacity, which is 1,200MW. However, this is slightly below expectations, due to backend line bottlenecks, partially due to tool availability but also process yield related issues.

The third Series 6 manufacturing plant, its first in Vietnam (Vietnam S6 Factory 1) was said to be fully-staffed and undergoing factory acceptance with the first modules through the production lines expected late in the third quarter of 2018. The planned nameplate capacity of the Vietnam S6 Factory 1 is 1,200MW.

The construction of Vietnam S6 Factory 2 (1,200MW) nameplate capacity was noted to be on schedule and initial tools had arrived onsite. Vietnam S6 Factory 2 is still expected to start production in late 2019.

LPKF secures further orders from solar thin-film module customer

German laser systems specialist LPKF Laser & Electronics has secured new follow-on orders from a

Manz expects follow-up orders from the first half of 2019 onwards for its CIGS tool.

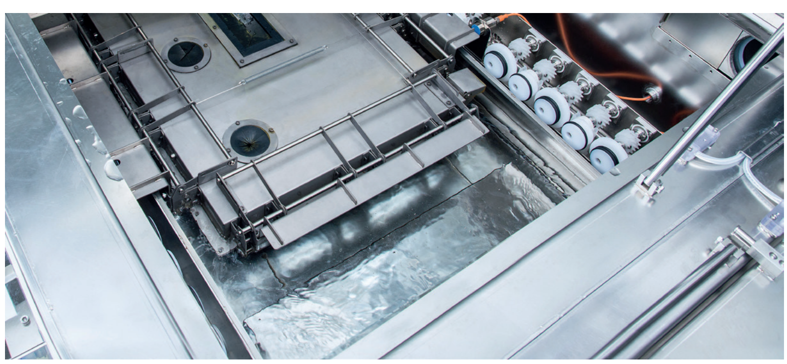

Credit: Manz

thin-film PV module manufacturer.

LPKF did not disclose the value of the orders or delivery schedules but noted that follow-on orders from customers could be placed at short notice. The company is known for its thin-film laser scribing technology.

Based on PV Tech's ongoing analysis of global PV manufacturing capacity announcements and possible expansion plans, several thin-film producers such as Avancis (CIGS) and First Solar (CdTe) are the likely customers, due to ongoing capacity expansions.

The company experienced strong demand for its laser structuring and scribing systems from the thin-film solar sector in 2017, achieving sales growth of 48% and forcing the company to add manufacturing capacity to meet demand.

PEROVSKITE

Oxford PV awarded €2.8 million German grant to ready perovskite-silicon solar cell production

Perovskite solar cell developer Oxford PV has been awarded a €2.8 million grant from the German Ministry of Economic Affairs and Energy to prepare perovskite-silicon solar cells for high-volume manufacturing.

The technology consortium is by headed by Oxford PV and includes specialist PV equipment manufacturer VON ARDENNE and three German institutes, Fraunhofer Institute for Solar Energy Systems, Helmholtz-Zentrum Berlin (HZB) and the Technical University of Berlin.

Oxford PV recently announced that it had achieved a world record certified efficiency of 27.3% for its perovskite solar cell. This exceeded the 26.7% efficiency world record for a single junction silicon solar cell.

Chris Case, CTO at Oxford PV, said: "The consortium partners bring together the perfect balance of expertise. Refining the manufacturing process of our perovskite solar cell technology will ensure the highest performing tandem solar cell in the field and the easy transfer of our technology into silicon solar cell and module production lines."

Imec pushes 4-terminal perovskite/silicon tandem solar cell to record 27.1%

Nanoelectronics R&D organisation imec has reported a record 4-terminal Perovskite/silicon tandem photovoltaic cell with a conversion efficiency of 27.1%, while claiming further microcrystal engineering leads a path of efficiencies of over 30%.

Key to the new record cell was the use of perovskite microcrystals.

Manoj Jaysankar, doctoral researcher at imec/EnergyVille noted: "We have been working on this tandem technology for two years now, and the biggest difference with previous versions is in the engineering and processing of the perovskite absorber, tuning its bandgap to optimize the efficiency for tandem configuration with silicon."

Imec noted that carefully engineered perovskite microcrystals minimizes the thermal losses that occur in the silicon cell, boosting efficiency.

The latest record tandem cell was said to deploy a 0.13 cm^2 spin-coated perovskite cell developed within the Solliance cooperation and stacked on top of a 4 cm^2 industrial interdigitated back-contact (IBC) silicon cell in a 4-terminal configuration.

Scaling up the tandem device by using a 4 cm2 perovskite module on a 4 cm2 IBC silicon cell, a tandem efficiency of 25.3% was achieved, surpassing the stand-alone efficiency of the silicon cell.

Recently, perovskite solar cell developer Oxford PV reported a perovskite tandem solar cell record, certified by Fraunhofer ISE at a conversion efficiency of 27.3%.

COMPANY NEWS

German CdTe manufacturer Calyxo to restart production

German CdTe thin-film module manufacturer Calyxo will resume production after finding a buyer for the business.

The way is now clear for the company to come out of insolvency after being bought by TS Group, which manufactures industrial equipment. It plans to retain the 150-strong workforce and restart operations immediately.

"By selling the company, we have managed to secure Calyxo's future here at the Bitterfeld-Wolfen site and to provide the employees with a perspective," said insolvency administrator Lucas F. Flöther. "In the TS Group we have found an investor who has recognized the potential of Calyxo and is prepared to lead the former German market leader back to the top again," he added.

All patents are transferred and the Calyxo brand will be retained.

Calyxo's managing director Michael Bauer will stay in post under the new owner.

"I am relieved that with the TS Group we have found an investor who knows and understands the industry; this will allow us to further extend our lead in research and development," said Bauer.

The firm ran into trouble in April after the loss of a major order.

Singulus and Avancis partner on next-gen CIGS process

Specialist PV manufacturing equipment supplier Singulus Technologies has signed an agreement with a key CIGS thin-film module customer, Avancis, which is part of China National Building Materials (CNBM) to develop the next generation of manufacturing equipment.

Singulus said that it would work with Avancis on the development and optimization of its CISARIS selenization equipment, which the companies have collaborated on since 2008.

Stefan Rinck, chairman of Singulus Technologies, said: "Our CISARIS selenization plants are at an important stage in the entire production process. CNBM's CIGS thin-film technology will meet even greater demands in the future through the use of new equipment."

Towards the next generation of high-efficiency $Cu(In,Ga)Se_2$ thin-film solar cells – Sharc25

Wolfram Witte[1], Philip Jackson[1], Stephan Buecheler[2], Romain Carron[2], Susanne Siebentritt[3], Florian Werner[3], Sébastien Duguay[4], Arantxa Vilalta-Clemente[4], Roberto Menozzi[5], Giovanna Sozzi[5], Emilie Bourgeois[6], Giedrius Degutis[6], Marcus Bär [7,8], Thomas Kunze[7], Sascha Sadewasser[9], Nicoleta Nicoara[9], Martti J. Puska[10], Maria Malitckaya[10], and Ayodhya N. Tiwari[2]

[1]Zentrum für Sonnenenergie- und Wasserstoff-Forschung Baden-Württemberg (ZSW), Stuttgart, Germany; [2]Laboratory for Thin Films and Photovoltaics, Empa-Swiss Federal Laboratories for Materials Science and Technology, Dübendorf, Switzerland; [3]Laboratory for Photovoltaics, University of Luxembourg, Belvaux, Luxembourg; [4]Groupe de Physique des Matériaux, Normandie Univ, UNIROUEN, INSA Rouen, UMR CNRS 6634, Rouen, France; [5]Department of Engineering and Architecture, University of Parma, Parma, Italy; [6]IMOMEC division, IMEC, Diepenbeek, Belgium; [7]Renewable Energy, Helmholtz-Zentrum Berlin für Materialien und Energie GmbH (HZB), Berlin, Germany; [8]Energy Materials In-Situ Laboratory Berlin (EMIL), Helmholtz-Zentrum Berlin für Materialien und Energie GmbH, Berlin, Germany; [9]INL - International Iberian Nanotechnology Laboratory, Braga, Portugal; [10]Aalto University, Department of Applied Physics, Aalto, Finland

Abstract

The EU Horizon Sharc25 project has provided deep insights into highly efficient $Cu(In,Ga)Se_2$ (CIGSe) thin-film solar cells fabricated by low- and high-temperature co-evaporation using advanced characterization methods, analytical tools, device simulation, and density functional theory modelling. This complementary approach led to a continuous knowledge-driven development and improvement of the CIGSe absorber. Based on optimized chemical composition, profiles, and alkali metal post-deposition treatments (PDT) using KF, RbF, and CsF, the CIGSe cell efficiency could be substantially increased to a record value of 22.6%. Due to additional modifications at the absorber/emitter (replacement of standard buffer system by a combination of thin CdS and TiO_2) and back contact/absorber (introduction of Al back reflector in combination with InZnO diffusion barrier) interfaces, in particular the short-circuit current could be increased. Furthermore, passivation layers in combination with point contact schemes at the CIGSe front and back side were developed and are still under investigation.

Introduction

Over the last five years, many research institutes and companies have increased their efficiency values for chalcopyrite-type thin-film solar cells to a level of close to 20% or even above, as listed in Table 1. These high values could be reached with $Cu(In,Ga)Se_2$ (CIGSe), $(Ag,Cu)(In,Ga)Se_2$ (AgCIGSe), and $Cu(In,Ga)(S,Se)_2$ (CIGSSe) absorber layers grown by the co-evaporation (simultaneous evaporation of all elements) or sequential deposition process (deposition of metallic precursors and subsequent selenization and/or sulfurization).

The Sharc25 project: an overview

Comparing the high efficiencies for chalcopyrite-based solar cells achieved by several groups worldwide, as described in Table 1, with the theoretical Shockley-Queisser limit of 33% for single-junction solar cells, there is still a large gap of >10% (absolute) between the experimental results and the maximum theoretical efficiency. The efficiency gap is a result of differences between all experimental solar cell parameters such as open-circuit voltage (V_{OC}), short-circuit current density (J_{SC}), and fill factor (*FF*) compared to their maximum theoretical counterparts. This difference was the main reason why the project "Sharc25" was initiated in 2014 and started in 2015 within the EU Horizon 2020 programme. The goal of Sharc25 is to challenge the key limiting factors in state-of-the-art CIGSe solar cells, namely non-radiative carrier recombination and light absorption losses in emitter layers. Electronic losses like recombination at the absorber/buffer interface and at the back contact are addressed. Different kinds of fluctuations and defects within the absorber are identified and addressed as well as optical losses such as reflection at and absorption in the transparent conductive oxide (TCO) emitter, reflection and absorption in the buffer layer, and insufficient absorption/recombination in the CIGSe absorber. The acronym "Sharc25" stands for "Super high efficiency $Cu(In,Ga)Se_2$ thin-film solar cells approaching 25%".

The Sharc25 project is coordinated by the Centre for Solar Energy and Hydrogen Research Baden-Württemberg (ZSW) and the consortium consists of 11 partners from eight European countries including R&D partners, universities, national laboratories, and two companies (Flisom AG and NICE Solar Energy GmbH). The task of the companies is to assess the experimental and theoretical results of the consortium with respect to their relevance to and compatibility with industrial large-scale mass production. The idea behind the project is to pool the complementary multidisciplinary skills of the involved research groups in a bid to push the CIGSe single junction solar cell performance towards the theoretical limit, as illustrated in Figure 1. The Sharc25 project started in May 2015 and will run until the end of October 2018.

η (%)	Institute/Company	Absorber	Year	Comment
22.9*	Solar Frontier (JAP)	CIGSSe	2017	1 cm^2 cell, with S, sequ. process
22.6*	ZSW (GER)	CIGSe	2016	
22.2[1]	Solibro (SWE/GER)	CIGSe	2018	1 cm^2 cell
22.0[2]	AIST (JAP)	CIGSe	2018	after 25 h heat-light soaking
20.9[3]	ÅSC (SWE)	AgCIGSe	2017	1 cm^2 cell, CIGSe with Ag
20.8*	NREL (USA)	CIGSe	2014	
20.7	Toshiba (JAP)	CIGSe	2016	
20.4*	Empa (CH)	CIGSe	2013	on flexible polyimide foil
19.9	IEC Delaware (USA)	AgCIGSe	2015	CIGSe with Ag
19.7*	AGU (JAP)	CIGSSe	2013	with S, sequential process

**) independently certified efficiency*
1) O. Lundberg, presented at IW-CIGSTech 9 in Stuttgart, Germany (2018).
2) J. Nishinaga, T. Koida, S. Ishizuka, Y. Kamikawa, H. Shibata, and S. Niki, presented at E-MRS Spring Meeting 2018 in Strasbourg, France.
3) M. Edoff, T. Jarmar, N. S. Nilsson, E. Wallin, D. Högström, O. Stolt, O. Lundberg, W. Shafarman, and L. Stolt, IEEE J. Photovolt. 7 (2017) 1789-1794.

Table 1. Power conversion efficiency η values of small-area $Cu(In,Ga)Se_2$ (CIGSe), $(Ag,Cu)(In,Ga)Se_2$ (AgCIGSe), and $Cu(In,Ga)(S,Se)_2$ (CIGSSe) chalcopyrite-type thin-film solar cells (see [1,2] and references therein; list is not complete).

CIGSe absorber modifications

Integral chemical composition and compositional gradings within the CIGSe absorber could have a significant influence on device performance. This relation is also relevant for different kinds of treatments of the absorber layer affecting bulk and surface properties of CIGSe prior to formation of the important CIGSe/buffer interface.

Improved Ga grading and increased Cu content

A method to increase J_{SC}, mainly by increasing the absorption coefficient in the near-infrared (NIR) region, was described by Avancini et al. [3]. With the low-temperature CIGSe growth process established at Sharc25 partner Empa the [Ga]/([Ga]+[In]) (GGI) double gradient can be precisely controlled within the absorber, i.e. the increase of GGI to front and back side of the absorber. If the notch, the minimum of the GGI double grading, is widened and the Cu content is simultaneously increased, i.e. the [Cu]/([Ga]+[In]) ratio (CGI) raised to a maximum above a value of 0.90, a gain of approx. 1.1 mA/cm^2 could be achieved in J_{SC} [3].

Numerical device simulations with the Sentaurus TCAD suite for different CGI and GGI profiles by the Sharc25 partner University of Parma support these experimental findings [4]. In addition, the increased light absorption in the NIR region by widening the notch could exactly be described by optical simulations developed at Empa calculating reflectance and external quantum efficiency (EQE) on the basis of experimental GGI depth profiles. The important dielectric functions of CIGSe and of the windows and back contact layers were determined experimentally by a combination of ellipsometry, reflectance, and transmittance measurements [5].

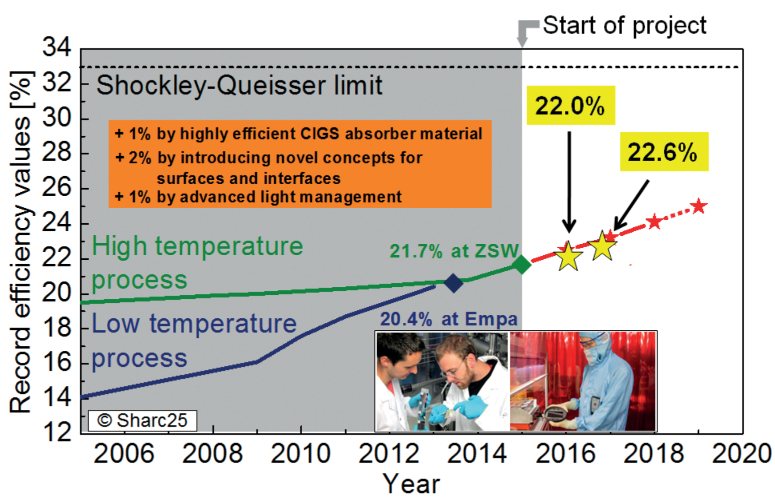

Figure 1. Sharc25 project roadmap with efficiency values of 20.4% (by Empa with low-temperature co-evaporation process) and 21.7% (by ZSW with high-temperature process) at start of project and values of 22.0% and 22.6% achieved during the Sharc25 project (all efficiencies with ARC).

Post-deposition treatment (PDT) with alkali metals

Originally, the PDT of the CIGSe absorber with alkali metal salts was introduced by Rudmann et al. in 2004 [6]. NaF was thermally evaporated on the CIGSe front side after the CIGSe growth and afterwards annealed at 400°C to diffuse Na into the CIGSe absorber prior to CdS buffer growth by chemical bath deposition (CBD). This procedure is crucially required to provide the necessary Na content for high-efficiency solar cells if the CIGSe

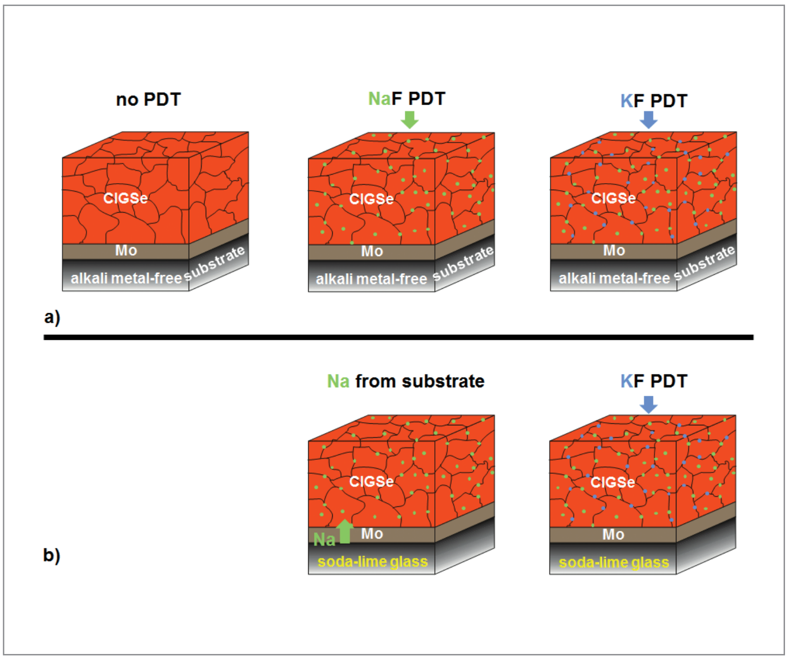

Figure 2. Post deposition treatment (PDT) of CIGSe absorbers prior to buffer growth. a) Low-temperature processed CIGSe on alkali metal-free substrates: First NaF- and in a second step KF-PDT is applied. b) High-temperature CIGSe growth on alkali-containing glass substrates: Only one PDT process is applied – KF-PDT (alternatively RbF- or CsF-PDT).

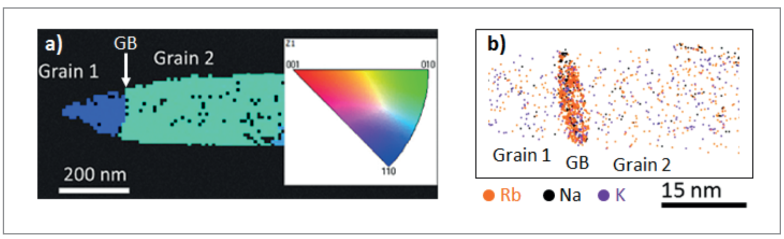

Figure 3. a) High-angle grain boundary (GB) at the atom probe tip prepared from a RbF-PDT treated high-temperature CIGSe absorber as revealed by transmission Kikuchi diffraction. b) Reconstruction of the same atom probe tip shows a Rb (K and Na) accumulation at the GB [14].

absorber is deposited on a Na-free substrate – since Na usually inherently diffuses into the absorber during absorber formation at elevated temperatures when Na-containing substrates are used.

A major step to push the CIGSe cell performance further was the discovery of the beneficial effect of potassium and the application to the front side of the CIGSe absorber in 2013 [7,8]. In this case the PDT was performed in-situ with KF (without breaking the vacuum) under a selenium atmosphere at temperatures typically around 350°C. This KF-PDT is applied after an initial NaF-PDT if an alkali-metal free substrate like polyimide, stainless steel foil or soda-lime glass with SiO_x diffusion barrier is used as illustrated in Figure 2a. With this combined NaF-PDT + KF-PDT process, Empa was able to achieve a cell efficiency of 20.4% on polymer film using a low-temperature CIGSe process [7].

In the case of the high-temperature growth process, CIGSe is deposited onto Na- and K-containing glass substrate (soda-lime glass or alkali-aluminosilicate glass). These alkali metals diffuse from the glass substrates into the CIGSe absorber at elevated temperatures during the CIGSe process. In order to ensure the optimal amount of K in the CIGSe, a KF-PDT is performed in a selenium atmosphere prior to CdS buffer growth by CBD (see Figure 2b).

The PDT method with alkali metals (or variations) was successfully adapted and applied by several research groups and companies worldwide leading to efficiency improvements on cell and module level. With the application of K on their chalcopyrite-based absorber layers, Solibro with a co-evaporation process and Solar Frontier with a sequential process, for example, have reported efficiencies of 21.0% [9] and 22.3% [10] (both with ARC) for chalcopyrite-based solar cells, respectively. Interestingly the K treatment works also for the penternary $Cu(In,Ga)(S,Se)_2$ absorbers with sulfur at the front side [11].

In 2016 a next step was taken by ZSW by introducing even heavier alkali metals like Rb and Cs in the PDT procedure. As a consequence, a new independently certified cell record efficiency of 22.6% with ARC was achieved. It should be noted that at ZSW CIGSe cell efficiencies above 20% with ARC could be achieved with all three PDT methods: KF-, RbF-, and CsF-PDT [12]. Many single cells were fabricated at ZSW during the Sharc25 project with high reproducibility and an efficiency level around 22% (with ARC). Also Empa improved their cell efficiencies for the low-temperature process during the project duration approaching 21% efficiency using the double-PDT processes with RbF-PDT or KF-PDT after an initial NaF-PDT on both flexible polyimide foils and glass substrates with alkali diffusion barrier. Successful PDT treatment processes with higher alkali metal atoms like Cs was reported by Solar Frontier for sulfur-containing CIGSSe absorbers [13].

Location of Rb in CIGSe, formation of defects, and alkali indium selenide phases

A statistical number of secondary ion mass spectroscopy depth profiles of CIGSe absorbers exposed to RbF- or CsF-PDT, showed that the intentionally introduced Rb (or Cs) was not only found at the CIGSe surface but was completely distributed inside the CIGSe absorber and was even observed at the Mo/CIGSe back side interface [12]. To investigate the location and distribution of Rb within the CIGSe absorber, highly spatially-resolved atom probe tomography (APT) measurements were performed by Sharc25 partner University of Rouen. Figure 3 shows an Rb accumulation on a nanometer scale at a high-angle grain boundary (GB) in a CIGSe absorber grown by the high-temperature process after RbF-PDT [14]. In addition, Na and K stemming from the alkali-containing glass are also enriched at the GB. The Rb concentration within the grain bulk is below the detection limit of the APT (10 ppm) whereas Na could be detected within the CIGSe grain bulk as well. The accumulation of Na at GBs in CIGSe was reported previously by Cadel et al. [15] and this property was suggested to passivate the GBs, which could be beneficial for the cell

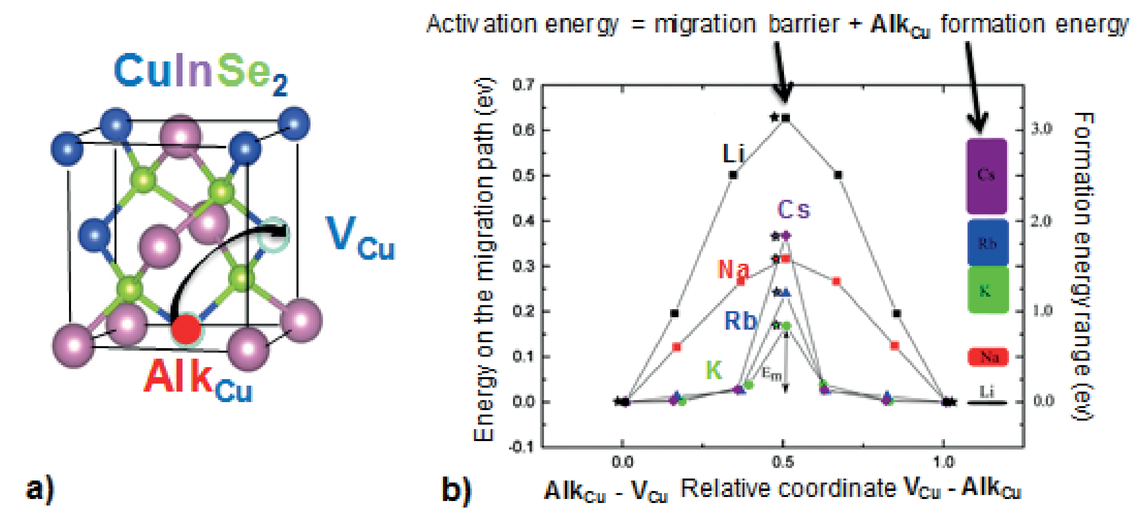

Figure 4. a) Bottom part of $CuInSe_2$ unit cell (Cu atoms in blue, In in purple, and Se in green) illustrating the mechanism of an alkali metal atom on a Cu site (Alk_{Cu} in red) exchanging to a Cu vacancy site (V_{Cu} in white). b) Formation energy of alkali metals Li to Cs on Cu site in $CuInSe_2$ (right vertical axis) and migration barrier for Alk_{Cu} - V_{Cu} and V_{Cu} – Alk_{Cu} mechanism (left vertical axis) after Malickaya et al. [17] (Adapted with permission from Ref. [17], ACS Publications, 2017).

performance. A comparison between an untreated sample without RbF-PDT and with RbF-PDT revealed that after Rb segregation at the GBs the Na concentration is reduced, suggesting that the lighter alkali element Na is replaced by the heavier element Rb at the GB [14].

The above described experimental finding (Rb at GBs in CIGSe measured by APT) is supported by the density functional theory (DFT) calculations performed by Sharc25 partner Aalto University. Based on a model for ternary $CuInSe_2$ with intrinsic bulk point defects and complexes [16] they theoretically investigated the insertion of alkali metal atoms from Li to Cs on different defect sites (interstitials, vacancies etc.) and the ensuing impurity migration in $CuInSe_2$ [17]. The formation energies and the vacancy mechanism migration barriers for alkali metal atoms on Cu sites are depicted in Figure 4. Li and Na in contrast to Rb and Cs have distinct effects on the structure of the $CuInSe_2$ absorber whereas K represents an interesting borderline case. Briefly, Li and Na could energetically be incorporated into $CuInSe_2$ grains, whereas Rb and Cs are more likely to accumulate at GBs and surfaces.

The stability of alkali metal phases was also studied, suggesting that metal phases $Li_xCu_{1-x}InSe_2$ or $Na_xCu_{1-x}InSe_2$, i.e. Li and Na as impurities, might form at typical PDT substrate temperatures of 350°C and alkali metal concentrations <0.1 at.% in $CuInSe_2$. In contrast for heavier alkali metals like K, Rb, and Cs separated ordered $AlkInSe_2$ and $CuInSe_2$ phases are more probable to form [17]. Such a K-In-Se compound was experimentally evidenced using a combination of different surface sensitive techniques by Sharc25 partner Helmholtz-Zentrum Berlin for Materialien und Energie GmbH (HZB) for low-temperature processed CIGSe surfaces fabricated at Empa using various KF-PDT methods [18].

Defects and barriers in high-efficiency CIGSe absorbers

In general, the CIGSe absorbers fabricated at Empa and ZSW exhibit no signatures of detrimental deep defects as measured with photoluminescence (PL) recorded at 10 K by Sharc25 partner University of Luxembourg [19], which were often reported by other groups. PL spectra of high-efficiency CIGSe absorbers often reveal interference fringes which negatively affect the detailed analysis of the PL spectra. These interferences can be overcome by angle-resolved PL measurements [20] and important parameters such as the quasi-Fermi level splitting could be extracted [21].

Admittance spectroscopy with an additional applied bias voltage by Empa revealed that at the interface-near CIGSe absorber region an additional capacitance step was observed which could be a result of the RbF-PDT procedure [22]. This new capacitance step at positive bias voltages is very likely caused by the PDT process (also with different types of alkali metals), which might form a transport barrier at the CIGSe front side for excessive alkali concentrations [23]. In contrast, the dominant capacitance step in conventional zero-bias admittance spectroscopy measured at University of Luxembourg appears to be independent of the alkali PDT and is best explained by an electron injection barrier located fully within the buffer/window stack [19].

Numerical simulations performed by Sharc25 partner University of Parma also explored the effect of several cell features and parameters on the capacitance-voltage characteristics and the apparent doping profiles extracted from them: these features and parameters include n-side doping densities, buffer thickness, and absorber/buffer conduction band offset [24].

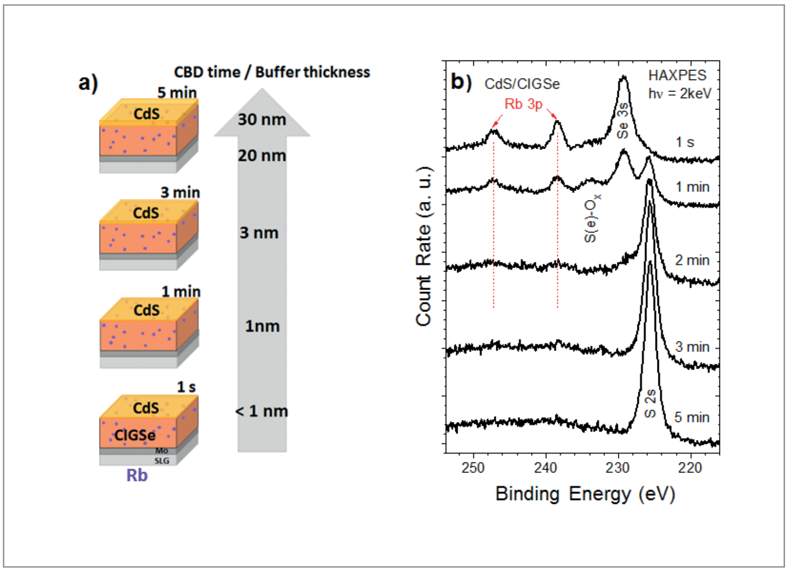

Figure 5. Junction formation of CBD-CdS buffer layer on CIGSe subjected to RbF-PDT. a) Scheme of CBD-CdS buffer growth with different deposition times and estimated thicknesses on CIGSe after RbF-PDT. b) 2 keV hard X-ray photoelectron spectroscopy (HAXPES) measurement of CIGSe with RbF-PDT and solution-grown CdS on top. Different deposition times of CdS in CBD are indicated and the Rb-related HAXPES signals are highlighted by red arrows/dashed lines [25]. (Reproduced with permission from [25], ACS Publications, 2018).

Influence of RbF-PDT on CIGSe surface and buffer growth by CBD

Na typically accumulates at the CIGSe surface after the CIGSe growth process and completely dissolves from the surface during the subsequent ammonia-based CBD of CdS. To investigate the situation in the case of RbF-PDT, CIGSe surfaces fabricated at high-temperature were analyzed at HZB after different deposition times of CdS (see Figure 5a) with synchrotron-based hard X-ray photoelectron spectroscopy (HAXPES) at 2 keV (corresponding to a maximal inelastic mean free path of approximately 4 nm). The HAXPES spectra depicted in Figure 5b clearly exhibit the Rb-related peaks which attenuate similar to the CIGSe-related Se 3s line with the growing buffer layer, i.e. the Rb is not dissolved by the CBD-CdS process [25]. The presence of a Rb-enriched surface was confirmed by lab-based X-ray photoelectron spectroscopy measurements performed at Empa on low-temperature CIGSe absorbers treated with RbF-PDT after different rinsing and etching procedures, similarly as observed for KF-PDT [26].

The RbF-PDT of CIGSe has also an influence on the growth of CdS buffer layer by CBD. Kelvin probe force microscopy (KPFM) measurements performed at Sharc25 partner INL revealed that the initial growth of CdS during the first few minutes leads to inhomogeneities in the surface and interface electronic properties. After about two to three minutes of CdS deposition a pn-junction forms, which was probed by a small surface photovoltage in some sample areas. After more than three minutes the surface photovoltage signal is large and homogeneous, indicating a complete junction formation [25].

New approaches and concepts at CIGSe front side

The widely used CdS buffer layer in combination with the high resistive (HR) i-ZnO layer for CIGSe or CIGSSe solar cells and modules both absorb part of the short wavelength spectrum due to their bandgap energies of 2.4 and 3.2 eV, respectively, thus limiting J_{SC}. In the last decades there were many efforts to substitute these layers with more transparent alternatives such as ZnS-based buffers or (Zn,Mg)O as HR layer. In addition, recombination losses at the CIGSe/buffer interface might occur, which can impair the device performance. Such losses could be mitigated by an optimization route borrowed from silicon solar cells. Employing a passivation layer in combination with point contacts at the front side of the CIGSe absorbers seems feasible and promising as discussed below.

Thinning of solution-grown CdS buffer layer

Within the Sharc25 project alternative buffer materials to the widely used CBD-CdS are under investigation, like solution-grown Zn(O,S) and mixed buffer layers like (Cd,Zn)S or ZnInS to increase transparency in the short-wavelength region. In addition, the consortium is working to thin the CBD-CdS down (i.e., decreasing its thickness) to a minimum to reduce detrimental absorption due to the CdS bandgap energy of 2.4 eV. This approach can be realized with different high resistive (HR) layers as alternatives to i-ZnO.

Figure 6 illustrates a CIGSe stacking sequence with the standard CBD CdS/i-ZnO buffer system on top of a CIGSe absorber without alkali metal PDT. The thickness of the CdS buffer layer is approximately 50 nm. Just reducing this thickness and still using i-ZnO would result in a decrease of the efficiency mainly due to reduced values of V_{OC} and FF. If CIGSe with alkali PDT is used, the CBD-CdS buffer can be thinned down to 30 nm without any V_{OC} losses. A further thickness reduction of CdS down to 20 nm is possible if sputtered (Zn,Mg)O is used as HR layer instead of i-ZnO. The CdS thickness can even be thinned down to 10 nm by using TiO_2 grown by atomic layer deposition (ALD) as alternative HR layer, resulting in an improved collection in the short wavelength region and thus increase in J_{SC} [27]. The standard TCO ZnO:Al was used for all stacking sequences described here. A further potential to increase efficiency is the combination with a TCO that offers higher mobility and thus enabling lower carrier concentrations and an improved IR transmittance. Such candidates could be hydrogen-doped In_2O_3 or InZnO which were successfully tested with different stacking sequences including CBD-Zn(O,S) buffers in combination with sputtered (Zn,Mg)O as HR layer [28].

Passivation layers and point openings at CIGSe front side

The high cell efficiencies presented in Table 1 could be further improved by reducing recombination at the CIGSe/buffer interface. Typical approaches

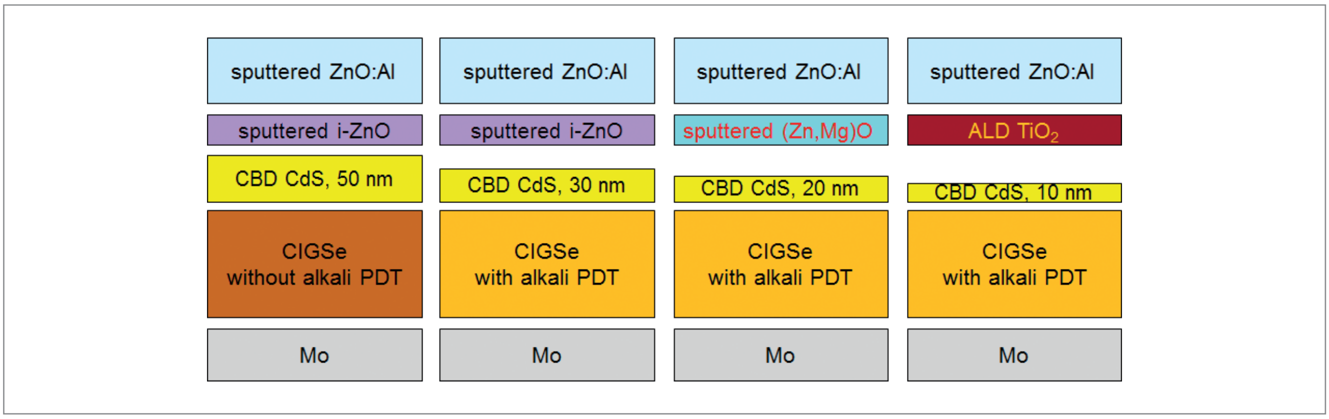

Figure 6. Approach to thin the CBD-CdS buffer layer (from left to right) including the application of alkali metal PDT after CIGSe growth and the use of different HR layers like sputtered (Zn,Mg)O or ALD TiO_2 as an alternative for the commonly used sputtered i-ZnO.

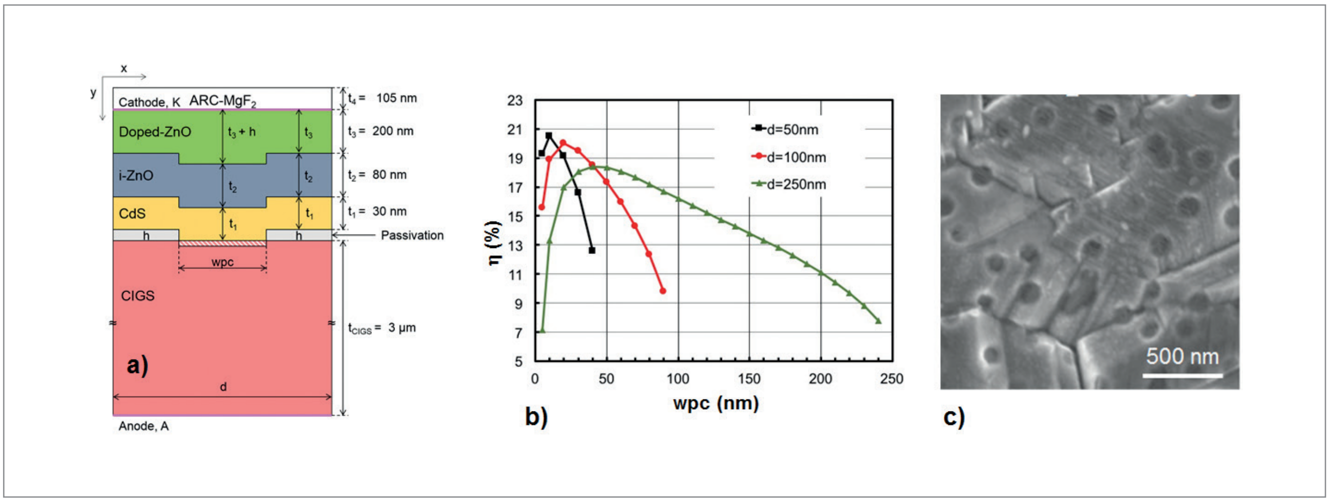

Figure 7. a) Scheme of a CIGSe solar cell cross-section with an insulating passivation layer and a point contact opening between CIGSe absorber and CdS buffer layer. b) Calculated power conversion efficiencies *η* with 3D device simulation (Sentaurus TCAD) in dependence on point contact size (wpc) and pitch (d) [29]. c) SEM top view of point contact openings experimentally realized with hole-mask colloidal lithography on 14 nm thick ALD HfO_x grown on polycrystalline CIGSe.

adopted from silicon solar cells are passivation layers applied to HIT (Heterojuntion with Intrinsic Thin layer) solar cells and structured point or line openings as they are implemented on the rear side of PERCs (Passivated Emitter and Rear Cell).

Figure 7a illustrates a CIGSe cross-section with an insulating passivation layer on top of CIGSe with point contact openings of a certain size and pitch, where CIGSe is in direct contact with the CdS buffer layer. Figure 7b shows the optimum size and pitch of point contacts on the CIGSe front side as calculated by 3D device simulations at the University Parma. To achieve a beneficial effect with a passivation layer and point contact openings at the CIGSe front side the size of the point contact should be in the range of several tens of nanometers, more or less independently of the pitch size [29].

Realizing such small openings on the relatively rough CIGSe surface (RMS roughness is typically around 100 nm) is a major challenge. Figure 7c shows a scanning electron microscope (SEM) top view image of polycrystalline CIGSe with typical grain sizes in the range of 1-2 μm and a 14 nm thick ALD HfO_x passivation layer on top. The openings were made with hole-mask colloidal lithography (HCL) by Sharc25 partner imec. The standard HCL method was specially optimized to CIGSe, but the opening sizes are in the range of 100- 200 nm, larger than the ideal simulated values of several tens of nanometers. Another challenge is the complete removal of the ALD passivation layer inside the holes to ensure optimum contact between the CIGSe absorber and buffer/TCO. Due to the large point contact openings applied to high-efficiency CIGSe cells, no increase in efficiency could be achieved with the passivation layers. Nevertheless, the successful application of the HCL method on the rough CIGSe front side could also be useful for other polycrystalline thin-film materials suffering from interface recombination losses, such as kesterite-type solar cells.

Modifications at CIGSe back side and Mo/CIGSe interface

Similar to the CIGSe absorber front side, recombination losses can also occur at the Mo/CIGSe back side interface. One solution could again be the application of a passivation layer in combination with point contacts, which were successfully employed for very thin CIGSe

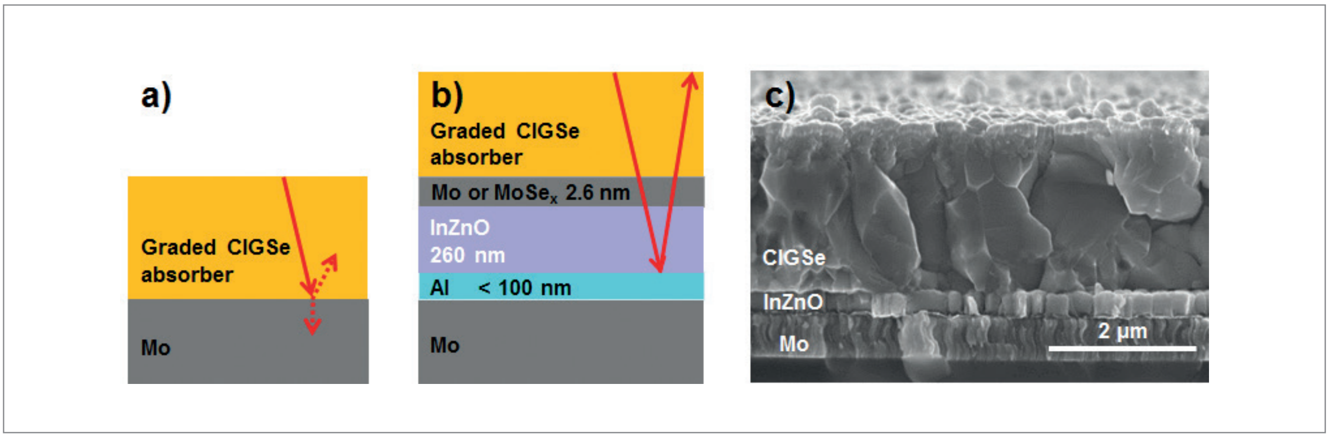

Figure 8 a) Scheme of CIGSe absorber with GGI grading and standard Mo back contact. b) Scheme. of stacking sequence of CIGSe with Al back contact reflector with InZnO spacer and a very thin Mo or MoSe$_x$ layer on top. c) SEM cross-section image with InZnO spacer between Mo and CIGSe.

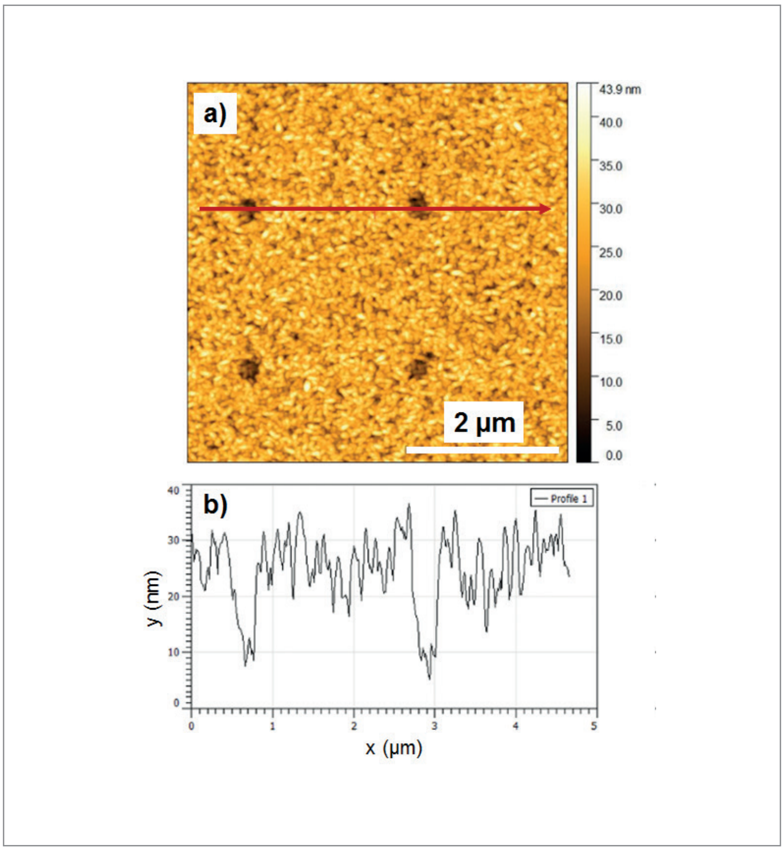

Figure 9: a) Atomic force microscopy (AFM) image of 10 nm thick ALD Al_2O_3 with point contact openings with pitch size of around 2 μm and point contact opening size of 200 nm realized by nano-imprint lithography on top of sputtered Mo back contact. b) AFM line profile extracted along red arrow in Figure 9a.

layers [30]. With a non-graded CIGSe layer with thicknesses of 2-3 μm, these concepts can also increase efficiency. For point contact openings at the back side, calculations show that the size can be in the range of 200 nm and a typical pitch of around 2 μm would have a beneficial effect. Another approach to further enhance efficiency is to increase the optical path of photons within the CIGSe absorber layer with a back contact reflector or a mirror on top of the Mo contact. An advanced concept is a combination of such a reflector with a passivation layer and point contact openings.

Back contact reflector

An experimentally feasible approach to increase J_{SC} in CIGSe solar cells by the use of a back contact reflector is illustrated in Figure 8. In this case a <100 nm thick Al reflector is directly deposited on top of a standard substrate. To prevent diffusion of Al into CIGSe, which has a detrimental effect on cell performance, a 260 nm thick InZnO spacer is positioned between Al and CIGSe absorber as diffusion barrier. Even in the case of a 3 μm-thick CIGSe absorber grown by a low-temperature co-evaporation process at Empa there is an increase in NIR EQE and a pronounced subgap reflectance. The gain in J_{SC} from reflection alone is around 0.3-0.7 mA/cm^2 and the best cell with reflector showed an efficiency of 19.9% compared to the best reference cell with 19.5% from the same CIGSe deposition run without reflector (both cells with MgF_2 ARC) [31].

Back side passivation layer with point contacts

The atomic force microscopy (AFM) image in Figure 9a shows the realization of a 10 nm thick ALD Al_2O_3 passivation layer with point contact openings on top of a sputtered Mo back contact. The passivation layer and point contact openings were fabricated by nano-imprint lithography (NIL) at imec and typical pitch between the openings is 2 μm as shown in Figure 9b. So far, however, there has been no increase in efficiency through the use of the combination of a passivation layer and point contacts on the CIGSe back side for standard CIGSe thicknesses of 2-3 μm and standard double grading of GGI ratio. Nevertheless, the passivation effect could be proved by time-resolved PL measurements and the beneficial effect could be demonstrated for thin CIGSe films, similar to results reported by other groups.

Conclusion

The EU H2020 Sharc25 project has provided deep insights into highly efficient CIGSe thin-film solar cells using advanced characterization methods, analytical tools, device simulation, and DFT modelling. This approach led to a continuous development and improvement of the CIGSe absorber, additional functional layers, and important interfaces. With optimized GGI gradient, CGI ratios, and alkali metal PDT with K, Rb, and Cs the efficiency of CIGSe thin-film solar cells prepared by the co-evaporation process (low- and high-temperature) could be significantly enhanced. The Rb intentionally inserted by PDT after the CIGSe growth accumulates at grain boundaries and is still present at the CIGSe front interface after the CBD process. It is very likely that $AlkInSe_2$ phases like $RbInSe_2$ form during the PDT process as calculated by ab-initio modelling. The J_{SC} of CIGSe cells could be increased by thinning down the CBD-CdS buffer layer in combination with a TiO_2 HR layer grown by ALD to reduce detrimental absorption in the UV. Another successful approach to enhance J_{SC} significantly was the implementation of an Al back reflector in combination with an InZnO spacer as diffusion barrier. Passivation layers grown by ALD on the front and back of the CIGSe absorber in combination with point contact openings were developed, but could not yet increase cell efficiency for CIGSe absorbers with standard thicknesses of 2-3 µm, as predicted by device simulations. Often an increase in one solar cell parameter is accompanied by a decrease in others. Nevertheless, during the Sharc25 project the efficiency values at Empa and ZSW were substantially increased and a value of 22.6% was achieved for a solar cell composed of a CIGSe absorber layer that underwent a RbF-PDT and featured a thinned CBD-CdS buffer layer, and a sputtered (Zn,Mg)O HR layer.

Acknowledgements

This project has received funding from the European Union's Horizon 2020 research and innovation programme under grant agreement No 641004, project Sharc25. This work was also supported by the Swiss State Secretariat for Education, Research and Innovation (SERI) under contract number 15.0158. The authors thank Dimitrios Hariskos, Ruben Hünig, Friedrich Kessler, and Michael Powalla, ZSW; Benjamin Bissig, Enrico Avancini, Thomas Feurer, Johannes Löckinger, and Thomas P. Weiss, Empa; Max H. Wolter, University of Luxembourg; Mohit Raghuwanshi, Celia Castro, Emmanuel Cadel, and Philippe Pareige, University of Rouen; Simone Di Napoli and Martina Carrisi, University of Parma; Robert Gehlhaar, Yinghuan Kuang, Tom Aernouts, An Hardy, Marlies K. Van Bael, and Milos Nesladek, imec; Evelyn Handick, Ting Xiao, Penghui Yang, Jakob Bombsch, Roberto Félix and Regan G. Wilks, HZB; Ville Havu and Hannu-Pekka Komsa, Aalto University; Patrick Reinhard, Flisom AG; and Rolf Wächter and Bernhard Dimmler, NICE Solar Energy GmbH for their contributions and discussions.

References

[1] T. Feurer, P. Reinhard, E. Avancini, B. Bissig, J. Löckinger, P. Fuchs, R. Carron, T. P. Weiss, J. Perrenoud, S. Stutterheim, S. Buecheler, and A. N. Tiwari, 2017, "Progress in thin film CIGS photovoltaics – Research and development, manufacturing, and applications", Prog. Photovolt. Res. Appl., Vol. 25, pp. 645-667.

[2] M. A. Green, Y. Hishikawa, E. D. Dunlop, D. H. Levi, J. Hohl-Ebinger, and A. W. Y. Ho-Baillie, 2018, "Solar cell efficiency tables (version 52)", Prog. Photovolt: Res. Appl., Vol. 26, pp. 427-436.

[3] E. Avancini, R. Carron, B. Bissig, P. Reinhard, R. Menozzi, G. Sozzi, S. Di Napoli, T. Feurer, S. Nishiwaki, S. Buecheler, and A. N. Tiwari, 2017, "Impact of compositional grading and overall Cu deficiency on the near-infrared response in $Cu(In,Ga)Se_2$ solar cells", Prog. Photovolt. Res. Appl., Vol. 25, pp. 233-241.

[4] G. Sozzi, S. Di Napoli, R. Menozzi, R. Carron, E. Avancini, B. Bissig, S. Buecheler, and A. N. Tiwari, "Analysis of Ga grading in CIGS absorbers with different Cu content", Proc. 43rd IEEE Photovoltaics Specialists Conference (PVSC), Portland, OR, USA, June 5 – 10, 2016, pp. 2279-2282.

[5] R. Carron, E. Avancini, T. Feurer, B. Bissig, P. A. Losio, R. Figi, C. Schreiner, M. Bürki, E. Bourgeois, Z. Remes, M. Nesladek, S. Buecheler, and A. N. Tiwari, 2018, "Refractive indices of layers and optical simulations of $Cu(In,Ga)Se_2$ solar cells", Sci. Technol. Adv. Mater., Vol. 19, pp. 396-410.

[6] D. Rudmann, A. F. da Cunha, M. Kaelin, F. Kurdesau, H. Zogg, A. N. Tiwari and G. Bilger, 2004, "Efficiency enhancement of $Cu(In,Ga)Se_2$ solar cells due to post-deposition Na incorporation", Appl. Phys. Lett., Vol. 84, pp. 1129-1131.

[7] A. Chirila, P. Reinhard, F. Pianezzi, P. Bloesch, A. R. Uhl, C. Fella, L. Kranz, D. Keller, C. Gretener, H. Hagendorfer, D. Jaeger, R. Erni, S. Nishiwaki, S. Buecheler, and A. N. Tiwari, 2013, "Potassium-induced surface modification of $Cu(In,Ga)Se_2$ thin films for high-efficiency solar cells", Nat. Mater., Vol. 12, pp. 1107-1111.

[8] A. Laemmle, R. Wuerz, and M. Powalla, 2013, "Efficiency enhancement of $Cu(In,Ga)Se_2$ thin-film solar cells by a post-deposition treatment with potassium fluoride", Phys. Stat. Sol. RRL, Vol. 7, pp. 631-634.

[9] O. Lundberg, E. Wallin, V. Gusak, S. Södergren, S. Chen, S. Lotfi, F. Chalvet, U. Malm, N. Kaihovirta, P. Mende, G. Jaschke, P. Kratzert, J. Joel, M. Skupinski, P. Lindberg, T. Jarmar, J. Lundberg, J. Mathiasson, and L. Stolt, "Improved CIGS Modules by KF Post Deposition Treatment and Reduced Cell-to-Module Losses", Proc. 43rd IEEE Photovoltaics Specialists Conference (PVSC), Portland, OR, USA, June 5 – 10, 2016, pp. 1293-1296.

[10] R. Kamada, T. Yagioka, S. Adachi, A. Handa, K. F. Tai, T. Kato, and H. Sugimoto, "New World Record $Cu(In,Ga)(Se,S)_2$ Thin Film Solar Cell Efficiency Beyond 22%", Proc. 43rd IEEE Photovoltaic Specialists Conference (PVSC), Portland, OR, USA, June 5 – 10, 2016, pp. 1287-1291.

[11] T. Kato, 2017, "$Cu(In,Ga)(Se,S)_2$ solar cell research in Solar Frontier: Progress and current status", Jpn. J. Appl. Phys., Vol. 56, 04CA02.

[12] P. Jackson, R. Wuerz, D. Hariskos, E. Lotter, W.

Witte, and M. Powalla, 2016, "Effects of heavy alkali elements in Cu(In,Ga)Se_2 solar cells with efficiencies up to 22.6%", Phys. Stat. Sol. RRL, Vol. 10, pp. 583-586.
[13] T. Aramoto, "Solar Frontier: Past Present and Future", presented at 9th International Workshop on CIGS Solar Cell Technology (IW-CIGSTech 9), Stuttgart, Germany, June 18, 2018.
[14] A. Vilalta-Clemente, M. Raghuwanshi, S. Duguay, C. Castro, E. Cadel, P. Pareige, P. Jackson, R. Wuerz, D. Hariskos, and W. Witte, 2018, "Rubidium distribution at atomic scale in high efficient Cu(In,Ga)Se_2 thin-film solar cells", Appl. Phys. Lett., Vol. 112, 103105.
[15] E. Cadel, N. Barreau, J. Kessler, and P. Pareige, 2010, "Atom probe study of sodium distribution in polycrystalline Cu(In,Ga)Se_2 thin film", Acta Mater., Vol. 58, pp. 2634-2637.
[16] M. Malitckaya, H.-P. Komsa, V. Havu, and M. J. Puska, 2017, "First-principles modeling of point defects and complexes in thin-film solar-cell absorber $CuInSe_2$", Adv. Electron. Mater., Vol. 3, 1600353.
[17] M. Malitckaya, H.-P. Komsa, V. Havu, and M. J. Puska, 2017, "Effect of alkali metal atom doping on the $CuInSe_2$-based solar cell absorber", J. Phys. Chem. C, Vol. 121, pp. 15516-15528
https://pubs.acs.org/doi/abs/10.1021%2Facs.jpcc.7b03083
[18] E. Handick, P. Reinhard, R. G. Wilks, F. Pianezzi, T. Kunze, D. Kreikemeyer-Lorenzo, L. Weinhardt, M. Blum, W. Yang, M. Gorgoi, E. Ikenaga, D. Gerlach, S. Ueda, Y. Yamashita, T. Chikyow, C. Heske, S. Buecheler, A. N. Tiwari, and M. Bär, 2017, "Formation of a K-In-Se Surface Species by NaF/KF Postdeposition Treatment of Cu(In,Ga)Se_2 Thin-Film Solar Cell Absorbers", ACS Appl. Mater. Interfaces, Vol. 9, pp. 3581-3589.
[19] F. Werner, M. H. Wolter, S. Siebentritt, G. Sozzi, S. Di Napoli, R. Menozzi, P. Jackson, W. Witte, R. Carron, E. Avancini, T. P. Weiss, and S. Buecheler, 2018, "Alkali treatments of Cu(In,Ga)Se_2 thin-film absorbers and their impact on transport barriers", Prog. Photovolt. Res. Appl., pp. 1-13.
https://doi.org/10.1002/pip.3032
[20] M. H. Wolter, B. Bissig, P. Reinhard, S. Buecheler, P. Jackson, and S. Siebentritt, 2017, "Correcting for interference effects in the photoluminescence of Cu(In,Ga)Se_2 thin films", Phys. Stat. Sol. C, Vol. 14, 1600189.
[21] M. H. Wolter, B. Bissig, E. Avancini, R. Carron, S. Buecheler, P. Jackson, and S. Siebentritt, 2018, "Influence of Sodium and Rubidium Postdeposition Treatment on the Quasi-Fermi Level Splitting of Cu(In,Ga)Se_2 Thin Films", IEEE J. Photovolt., Vol. 8, pp. 1320-1325.
[22] T. P. Weiss, S. Nishiwaki, B. Bissig, S. Buecheler, and A. N. Tiwari, 2017, "Voltage dependent admittance spectroscopy for the detection of near interface defect states for thin film solar cells", Phys. Chem. Chem. Phys., Vol. 19, pp. 30410-30417.
[23] T. P. Weiss, S. Nishiwaki, B. Bissig, R. Carron, E. Avancini, J. Löckinger, S. Buecheler, and A. N. Tiwari, 2018, "Injection Current Barrier Formation for RbF Postdeposition-Treated Cu(In,Ga)Se_2-Based Solar Cells", Adv. Mater. Interfaces, Vol. 5, 1701007.
[24] G. Sozzi, M. Lazzarini, R. Menozzi, R. Carron, E. Avancini, B. Bissig, S. Buecheler, and A. N. Tiwari, "A numerical study of the use of C-V characteristics to extract the doping density of CIGS absorbers", Proc. 43rd IEEE Photovoltaics Specialists Conference (PVSC), Portland, OR, USA, June 5 – 10, 2016, pp. 2283-2288.
[25] N. Nicoara, T. Kunze, P. Jackson, D. Hariskos, R. Félix Duarte, R. G. Wilks, W. Witte, M. Bär, and S. Sadewasser, 2017, "Evidence for Chemical and Electronic Nonuniformities in the Formation of the Interface of RbF-Treated Cu(In,Ga)Se_2 with CdS", ACS Appl. Mater. Interfaces, Vol. 9, pp. 44173-44180.
https://pubs.acs.org/doi/10.1021/acsami.7b12448
[26] E. Avancini, R. Carron, T. P. Weiss, C. Andres, M. Bürki, C. Schreiner, R. Figi, Y. E. Romanyuk, S. Buecheler, and A. N. Tiwari, 2017, "Effects of Rubidium Fluoride and Potassium Fluoride Postdeposition Treatments on Cu(In,Ga)Se_2 Thin Films and Solar Cell Performance", Chem. Mater, Vol. 29, pp. 9695-9704.
[27] J. Löckinger, S. Nishiwaki, T. P. Weiss, B. Bissig, Y. E. Romanyuk, S. Buecheler, A. N. Tiwari, 2018, "TiO_2 as intermediate buffer layer in Cu(In,Ga)Se_2 solar cells", Sol. Energy Mater. Sol. Cells, Vol. 174, pp. 397-404.
[28] W. Witte, R. Carron, D. Hariskos, F. Fu, R. Menner, and S. Buecheler, 2017, "IZO or IOH window layers combined with Zn(O,S) and CdS buffers for Cu(In,Ga)Se_2 solar cells", Phys. Stat. Sol. A, Vol. 214, 1700688.
[29] G. Sozzi, S. Di Napoli, R. Menozzi, B. Bissig, S. Buecheler, and A. N. Tiwari, 2017, "Impact of front-side point contact/passivation geometry on thin-film solar cell performance", Sol. Energy Mater. Sol. Cells, Vol. 165, pp. 94-102.
[30] B. Vermang, V. Fjällström, J. Pettersson, P. Salomé, and M. Edoff, 2013, "Development of rear surface passivated Cu(In,Ga)Se_2 thin film solar cells with nano-sized local rear point contacts", Sol. Energy Sol. Cells, Vol. 117, pp. 505-511.
[31] B. Bissig, R. Carron, L. Greuter, S. Nishiwaki, E. Avancini, C. Andres, T. Feurer, S. Buecheler, and A. N. Tiwari, 2018, "Novel back contact reflector for high efficiency and double-graded Cu(In,Ga)Se_2 thin film solar cells", Prog. Photovolt. Res. Appl., pp. 1-7.
https://doi.org/10.1002/pip.3029

About the authors

Wolfram Witte gained a diploma degree from the University of Freiburg (Germany) in 2003 and in 2010 he earned his doctoral degree in materials science from the University of Erlangen-Nürnberg

(Germany). He has 14 years of experience concerning CIGS growth, interface design as well as thin-film and device characterization. Currently he works at ZSW as a scientist with a focus on high-efficiency CIGS solar cells and CIGS/buffer interface design. He is the coordinator of EU H2020 project Sharc25.

Philip Jackson studied physics at the University of Tuebingen and has for the past 16 years worked as a research scientist on Cu(In,Ga)Se_2 solar cells, both at the Institute for Physical Electronics (ipe), University of Stuttgart, and at the Centre for Solar Energy and Hydrogen Research (ZSW).

Stephan Buecheler received his PhD degree from the Swiss Federal Institute of Technology in Zurich (ETH Zürich) in 2010. He is currently group leader in the Laboratory for Thin Films and Photovoltaics at the Swiss Federal Laboratories for Materials Science and Technology (Empa) with a main research focus on the materials science and device physics of different thin-film photovoltaic and solid state battery technologies.

Romain Carron received his PhD from EPFL in the field of GaAs-based quantum nanostructures in 2013 after a master degree in physics at the Swiss Federal Institute of Technology in Lausanne (EPFL), Switzerland. Since 2015 he has been a scientist in the Laboratory for Thin Films and Photovoltaics at Empa, Switzerland. His research interests centre on the fabrication and characterization of CIGS solar cells and related materials.

Susanne Siebentritt is a physics professor and heads the laboratory for photovoltaics at the University of Luxembourg. Her research interest is twofold: the development of new thin film solar cells and the semiconductor physics of the materials used in these cells. She studied physics at the University of Erlangen and received her doctoral degree from the University of Hannover. After several postdoc positions at the University of Los Angeles, the Free University of Berlin and the Hahn-Meitner-Institute (now Helmholtz-Zentrum Berlin), she led a group at Hahn-Meitner-Institute for nearly 10 years, which focused on the physics of chalcopyrite solar cells. In 2007 she moved to Luxembourg and built up the laboratory for photovoltaics.

Florian Werner received his Ph.D. degree in 2014 from the University Hanover, where he developed a novel surface passivation for silicon photovoltaics. His current research at the University of Luxembourg focuses on the development of electrical characterization techniques for thin-film photovoltaic devices and the development and evaluation of surface passivation methods for Cu(In,Ga)Se_2 and related materials.

Sébastien Duguay is an assistant professor at the GPM laboratory, University of Rouen, in France, which he joined in 2007. He is a specialist in atom probe tomography related to semiconductors. He graduated from INSA of Rennes (France), an engineering school, in 2002. He then joined the University of Strasbourg and the ICUBE laboratory to carry out his master and obtain his PhD thesis in the field of microelectronics in 2006.

Arantxa Vilalta-Clemente received her PhD in Material Science from University of Caen Normandy in 2012. From 2012-2016, she was a postdoctoral researcher with the Materials Department in Oxford. She focused on applying the electron backscatter diffraction (EBSD) and transmission Kikuchi diffraction (TKD) to several materials. From 2016, she was postdoc with the "Group Physique des Matériaux" at University of Rouen Normandy. Her research work is mainly focused on the preparation and characterization of thin-film semiconductors by different techniques.

Roberto Menozzi received the Laurea degree in electronic engineering from the University of Bologna, Italy, in 1987, and in 1994 a PhD degree in information technology from the University of Parma, Italy, where he is currently full professor of electronics with the Department of Engineering and Architecture. His research has covered different aspects of the physics, reliability, and modeling of semiconductor devices. He is a senior member of the IEEE.

Giovanna Sozzi received the M.S. (cum laude) degree in electronic engineering from the University of Parma, Parma, Italy, in 1997. She is currently an assistant professor of electronics with the University of Parma. Her current research interests include the design and modelling of thin-film solar cells and the characterization and electrothermal modelling of silicon carbide devices.

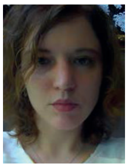

Emilie Bourgeois has been working as a researcher in IMEC and Hasselt University since 2013, in the field of optical and electro-optical characterizations of materials for photovoltaic and photonics applications. She received her master in engineering from the Paris School of Mines (2006) and completed her PhD studies at the Laboratory of Gas and Plasma Physics (University of Paris XI) from 2007 to 2010.

Giedrius Degutis obtained a PhD degree in chemistry from the University of Hasselt in 2015 in the group of Inorganic & Physical Chemistry. Since 2015 he has worked at IMEC as a researcher, where he investigated and developed nanofabrication methods for the facile point contact fabrication.

Marcus Bär graduated in environmental engineering/renewable energies from the University of Applied Sciences (FHTW) Berlin in 1999. In 2004, he acquired a PhD degree in electrical engineering from the Technische Universität Berlin. After a short postdoc at the Hahn-Meitner-Institut Berlin, in 2005 he became an Emmy-Noether Fellow and went abroad to the University of Nevada, Las Vegas. From 2011-2017, he was a W1-Professor for Photovoltaics at the Brandenburg Technical University Cottbus-Senftenberg. In 2018, he became a department head at the HZB and accepted a W2-Professorship at the Friedrich-Alexander-Universität Erlangen-Nürnberg.

Thomas Kunze graduated in physics from the University of Rostock in 2009. In 2014, he acquired a PhD degree in physics from the Freie Universität Berlin. From 2015-2018, he was a postdoc in the "Interface Design" Group of Marcus Bär at the Helmholtz-Zentrum Berlin für Materialien und Energie GmbH (HZB).

Sascha Sadewasser holds a diploma (1995) in physics from the RWTH Aachen, Germany and a PhD (1999) from the Washington University, St. Louis, USA. From 1999-2011 he worked at HZB, interrupted by a Ramón y Cajal fellowship at the Centro Nacional de Microelectónica in Barcelona, Spain from 2003 to 2004. He was also the deputy head of the Department for Heterogeneous Materialsystems at HZB from 2008-2011. In 2011, he accepted a principal investigator position at the INL - International Iberian Nanotechnology Laboratory, Braga, Portugal, where he still leads the Laboratory for Nanostructured Solar Cells (LaNaSC). Since 2018 he has also been the head of the Department for Quantum and Energy Materials at INL.

Nicoleta Nicoara received a diploma degree in physics from the Babes-Bolyai University, Cluj-Napoca (Romania) in 2000 and the PhD degree in condensed matter physics from Universidad Autónoma de Madrid (Spain), in 2007. During her PhD and postdoc until 2011, she worked on the nanoscale tronic devices and also on the development of advanced scanning probe microscopy techniques. Since 2012, when she joined INL, her research has been dedicated to the SPM characterization of the optoelectronic properties of chalcopyrite $Cu(In,Ga)Se_2$ semiconductor materials used in high efficiency solar cells.

Martti J. Puska is a Professor in the Department of Applied Physics at Aalto University in Helsinki since 1999. His interests include the modelling of materials and nanostructures using the first principles (time-dependent) density functional methods. The most recent works comprise studies of materials properties of CIGS thin-film photovoltaics, electron injection in dye-sensitized solar cells, plasmonic harvesting of light by nanoparticles, and electron transport in carbon nanotube networks aimed at transparent electrodes.

Maria Malitckaya is a PhD student at the Department of Applied Physics in Aalto University. She obtained her MSc degree at NRNU "MEPhI" in Moscow, Russia. She will defend her PhD thesis in 2019 at Aalto University. Her research interest is DFT modelling, mainly applied for the materials for solar cell application.

Ayodhya Nath Tiwari is the head of the Laboratory for Thin Films and Photovoltaics, Empa, and a Professor at ETH Zürich, Switzerland. He is the chairman and founder of Flisom Ltd. producing flexible CIGS thin film solar modules. He received his PhD degree from Indian Institute of Technology, Delhi, India in 1986. His research interests include thin films for energy conversion and storage including thin film solar cells based on chalcogenides, kesterites and perovskites.

Enquiries

Wolfram Witte
Zentrum für Sonnenenergie- und Wasserstoff-Forschung Baden-Württemberg (ZSW)
Meitnerstraße 1
70563 Stuttgart (Germany)
Email: wolfram.witte@zsw-bw.de
www.zsw-bw.de
www.sharc25.eu

News

Credit: Canadian Solar

Canadian Solar, LG and Risen are among the biggest providers of PV modules for projects outside of China.

Leading GW-plus module suppliers to non-China PV global markets - market insight by Finlay Colville

As module suppliers adapt to the slowdown of Chinese module demand in 2018 and 2019, global EPCs and developers are likely to see new Asia-produced panels being offered for both rooftop and ground-mount installations.

This issue forms a key theme of the forthcoming PV ModuleTech 2018 event, on 23-24 October 2018, in Penang, Malaysia.

This article reveals who the GW-plus module suppliers are to the global end-market, once we remove module supply to the domestic Chinese market, and identifies some of the chasing pack that are hoping to increase global brand awareness going into 2019.

While there remain hundreds of companies producing modules today, from regional single-production-line start-ups, to the multi-GW capacities of the Silicon Module Super League players, once we remove China market supply channels and all the low-volume suppliers (typically into a small subset of non-China markets), we are left with 12 major global suppliers. They are, in alphabetical order:

Canadian Solar, First Solar, GCL-SI, Hanwha Q CELLS, JA Solar, JinkoSolar, LG Electronics, LONGi, REC Solar, Risen, SunPower and Trina Solar.

In fact, collectively these companies are likely to account for about two-thirds of global PV module installation capacity (excluding China) during 2018, with much of the supply being to utility-scale projects where company and technology are two critical issues that undergo various forms of risk-mitigation, auditing and bankability.

The list of 12 companies can be grouped to illustrate the different profiles and strategies for non-Chinese global module supply. This is discussed more on PV-Tech.org and will form a major part of the discussion at PV ModuleTech in October.

AFTER CHINA MAY DAY

JinkoSolar claims immunity from industry woes as 2018 shipment guidance remains unchanged

JinkoSolar reported higher than guided second quarter PV module shipments and reiterated total shipments guidance to be in the range of 11.5GW to 12GW in 2018.

It reported total PV module shipments of 2,794MW, up from 2,015MW in the previous quarter and the second highest quarterly record, which was set (2,884MW) in the prior year quarter. The company had previously guided shipments for the second quarter of 2018 to be in the range of 2.4GW to 2.5GW.

Kangping Chen, JinkoSolar's CEO commented: "We delivered a strong quarter with module shipments hitting 2,794 MW while generating total revenue of US$915.9 million. Leveraging our cutting-edge technologies, strong global sales network, and industry leading cost structure, I'm confident in our ability to generate sustainable profits and growth going forward."

"Growth during the quarter was strong and we expect this momentum to continue into the second half of the year despite the impact from the new policies issued by the Chinese government on May 31 as shipments to overseas markets are expected to continue growing and account for an increasing proportion of our shipments," he added. "We believe these new policies will have a relatively limited impact on our operations over the short-term and are optimistic about our future prospects. We expect demand from Top Runner Programme, poverty alleviation projects, local government subsidies, and self-contained DG projects to continue to drive the growth in the Chinese market, especially in regions with ample sunlight and high commercial power prices."

Asia's module makers 'must' look abroad as consolidation looms

China's solar deployment caps will not have as profound an impact on the global industry as many fear, according to the president of LONGi Group, but consolidation on the manufacturing side is expected.

The shifts are expected to cut 10GW from demand in China leaving many companies looking overseas.

"The new policy in China will not have as big an impact as people think. The policy is not as different," said Li Zhenguo, president of LONGi Group. "It will make the industry develop in a faster and [more efficient] way for solar adoption. China might be reduced by 10GW but the resulting price declines will stimulate other markets. What we don't have is detailed numbers that tell us whether this will be enough to offset the decrease in China," he said during an interview with PV Tech.

It is also anticipated that the fall in prices, oversupply of some module formats and the increasing importance of overseas markets, could squeeze some companies out. Consolidation of the Chinese PV ecosystem has failed to materialise in the past, however.

"The government would prefer a policy that

Caption: Credit: LONGi

supports industry growth," said Li. "The space for cost reduction is limited but there is scope for better performance. We believe that consolidation will happen. It doesn't make sense to let companies that are behind in terms of their technology, to stay in the industry."

FINANCES REVEAL MIXED FORTUNES

Hareon Solar's sales collapse as company struggles to survive

China-based PV module manufacturer Hareon Solar Technology Co, reported unaudited first half 2018 financial results, highlighting the collapse in the company in 2017, as losses mounted and was forced into major restructuring in 2018.

Hareon Solar had suffered major financial issues before reporting a net loss in 2017 of approximately US$707 million after losses were reported every year since 2012. Its PV manufacturing subsidiary was forced into bankruptcy proceedings, senior management left including its CTO and the company has been fending off delisting.

It would also seem that Huajun International Group Limited, an investment holding company has acquired a major stake in the company and started a major restructuring of Hareon Solar, including the closure of some of the PV manufacturing operations and disposal of 'inefficient loss-making assets' and idled assets that are not required for production and current business operations, which also include some PV power plant projects, in order to reduce the company's management costs.

Hareon Solar reported unaudited first half 2018 sales of RMB 581.99 million (US$85.3 million approx.), down 66.2% from the prior year period.

Canadian Solar feels the pinch: key guidance figures for 2018 lowered

Canadian Solar lowered its full-year shipment, sales and capacity expansion plans for 2018, citing a number of global market and policy changes impacting its business.

The company noted that it had lowered full-year PV module shipments to 6GW to 6.2GW, compared to previous guidance of 6.6GW to 7.1GW.

Full-year revenue was lowered to US$4.0billion to US$4.2 billion, down from US$4.4 billion to US$4.6 billion, previously guided.

The impact would really start in the third quarter as the company guided total solar module shipments to be in the range of 1.5GW to 1.6GW, compared to second quarter 2018 shipments of 1.7GW. The third quarter shipments would also include approximately 210MW of shipments to its utility-scale PV power plant projects. Shipments in the third quarter of 2017 were 1.87GW.

Total revenue for the third quarter of 2018 is expected to be in the range of US$790 million to US$840 million, compared to US$912.2 million in the prior year period.

Dr. Shawn Qu, chairman and CEO of Canadian Solar, commented: "The revision of our annual guidance is in-line with the boarder industry and mainly reflects the expected reduction of shipment volumes to the Chinese market in the second half of the year, as well as the expected lower solar module average selling price. In the near-term, we will focus on maintaining our market share and protecting a reasonable profit margin."

LONGi sets new quarterly shipments, sales and R&D spending records

LONGi Green Energy Technology, the world's largest dedicated manufacturer of monocrystalline wafers and its subsidiary, LONGi Solar, a member of the 'Silicon Module Super League' (SMSL) has reported first half year results that included record quarterly shipments, operating income and R&D spending.

LONGi Group reported first half 2018 operating income of approximately RMB 10.02 billion (US$1.49 billion approx.), compared to US$995.2 million approx.), in the prior year period, an increase of 59.36%.

On a quarterly basis, LONGi reported second quarter operating income of US$956.1 million, compared to approximately US$569.1 million in second quarter of 2017, a 68% increase year-on-year.

The second quarter income exceeded LONGi's previous quarterly record set in the fourth quarter of 2017, when the company reported an operating income of approximately US$874.8 million.

Although the company mirrored many competitors in reporting relatively soft first quarter results, due to seasonality in key markets, including China, LONGi's significant increase in shipments of mono wafers and mono PV modules were behind the operating income growth.

The company reported first half year 2018 mono c-Si wafer production of 1.544 billion pieces, with 758 million pieces old externally and 786 million pieces were used in-house, compared to the first half of 2017 when external sales volume was 449 million pieces, and in-house consumption was 419 million pieces

In the first half of 2018, PV module shipments reached 3,232MW, including sales of 2,637MW and 375MW of modules used for its downstream PV project business, which included a number of poverty alleviation projects in China.

However, the major change in module shipments came from international sales, which accounted for 687MW in the first half of 2018, 18 times higher than the prior year period.

US NEWS

Tesla's solar panel suppliers have changed rapidly

In the hotly contested Californian residential solar market, new data compiled by ROTH Capital Partners highlights that Tesla's solar panel supply base is undergoing a major transition and that it has been changing for several years.

Back in 2016, Kyocera and REC Group had been the main panel suppliers to the company, accounting for 31% and 35% of supply to California installs, respectively. A much smaller share came from Trina Solar and Canadian Solar with 7% and 6%, respectively.

In that year, the company also sourced panels from Hanwha Q CELLS and LG Electronics, 1% and 3%, respectively. Unspecified 'other' suppliers accounted for 7% of the total through 2016.

In 2017, the company increased its use of Canadian Solar, Trina Solar and LG Electronics considerably. By year-end Canadian Solar's share was 15%, while Trina Solar's totalled 28%. Trina accounted for only 3% of supply in January 2017 and ended with a share of 33% by December.

In the case of LG Electronics the supply would seem to have been a short partnership, having mainly started strongly in the fourth quarter of 2016, it peaked in February, 2017 (30% of supply) and leaned out significantly by December (2%) and accounted for 14% of supply in 2017.

Long-term trusted suppliers, Kyocera and REC Group, lost out in 2017 as their shares declined to 4% and 10%, respectively.

But the supplier base has changed again in 2018. Although data is only available through May, the chart highlights that Canadian Solar's erratic share through 2017, ended abruptly at the beginning of 2018 and only recovered to 2% of the total by May. Trina Solar, which had been the largest supplier to Tesla from the second quarter of 2017 saw its share fall from a peak of 45% in October, 2017 to 28% by May, 2018.

Although Hanwha Q CELLS' share started relatively strongly in the first quarter of 2017, the chart shows an erratic pattern, similar to that of Canadian Solar. The only difference here is that Hanwha Q CELLS' share suddenly bounced back from zero in April, 2018 to 17% in May this year. This is the only supplier to have gained meaningful share through the first five months of 2018.

Hanwha Q CELLS to build new US factory in excess of 1.6GW

Hanwha Q CELLS will build a PV module manufacturing plant in the US with a capacity that "will exceed 1.6GW".

The company said construction in Whitfield County, Georgia will begin this year and is expected to be completed in 2019. The PERC modules will be used to supply the US solar rooftop and ground-mount segments.

"The new manufacturing fab is testament to Hanwha Q CELLS Korea's commitment to the US market, in spite of the recently imposed trade barriers," it said in a press statement.

The company has confirmed to PV Tech that the new facility will be module assembly only.

TESTING

Indian government issues guidelines on lab testing of solar modules

India's Ministry of New and Renewable Energy (MNRE) has issued guidelines on how to conduct testing on solar PV modules in test labs.

This comes as part of the implementation of Solar Photovoltaics Systems, Devices and Component Goods Order 2017, which imposes standards on certain PV equipment across India, and more recently energy storage products.

The guidelines cover testing crystalline and thin-film, including bifacial technology.

For a quantitative selection of samples, MNRE suggests taking a total of eight modules at random from production batches. Among a range of instructions, MNRE said that modules should contain the bypass diode wherever applicable, but in the case of the modules having a sealed junction box the client should provide one extra module with access to the diode for conducting the bypass diode test.

Modules should be clearly marked with details such as model number and nominal wattage, while module suppliers must also provide details such as maximum system voltage or the module will not be accepted by the testing house.

For module safety qualifications, a total of seven modules should be tested with the module manufacturer supplying its bill of materials and fabrication.

Tesla's module suppliers that were used for installations in California since the beginning of 2017 through to May 2018.

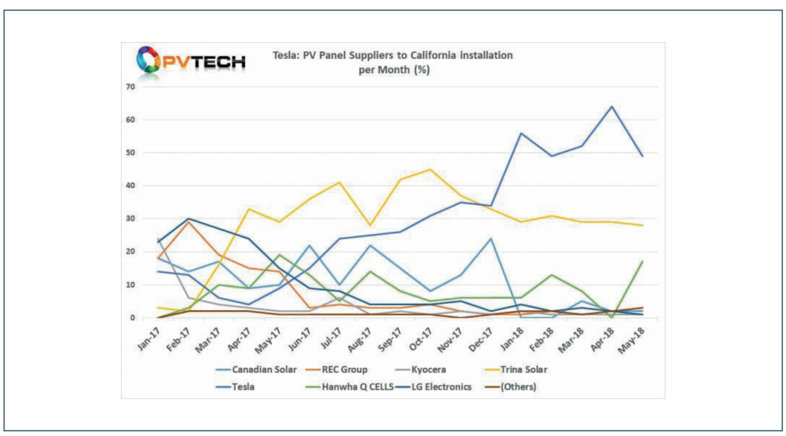

Credit: PV Tech

Advances in module interconnection technologies for crystalline silicon solar cells

J.M. Kroon[1], B.R. Newman[1], J. Govaerts[2], E. Voroshazi[2] & T. Borgers[2]
[1]ECN Part of TNO, PO Box 15, 1755 ZG Petten, The Netherlands; [2]imec/EnergyVille, Thor Park 8320, 3600 Genk, Belgium

Abstract

In the evolution towards higher cell efficiencies, new cell concepts (two-sided and back contacted) have been introduced and for each of these concepts, new module materials and interconnection technologies have to be developed to fulfil all the demands of a good end product in terms of lowest costs, highest yield and power and above all superior quality (reliability and durability). There is no single module concept that fits all cell concepts or module application type so existing module concepts need to be adapted or innovative module technologies are required to fit the aforementioned requirements. This paper provides an overview summarizing the recent developments of integrated cell to module manufacturing approaches such as multi-busbar, multi-wire, half-cell and shingling technologies for two-side contacted cells and advanced soldering, woven fabric and foil based module technologies for back contacted cells aiming for the highest power outputs, lowest costs and longest lifetimes.

Introduction

The current market is dominated (>95%) by crystalline-Si (x-Si) technology; and predominantly by the traditional Al-BSF p-type cell technology that has already been the standard technology for several decades. The cell efficiencies range from 18% for multi- to >20% for the best performing mono-variants.

In the race towards the highest efficiencies for single junction x-Si cells, the trend is from multi to mono, from p- to n-type wafers and from two-side-contacted towards back-contacted cell concepts. At the same time an increasing number of cells will become light sensitive on both sides, so-called bifacial cells. The anticipated evolution, according to the insights of the PV community, of the average stabilized cell efficiency in mass production for all cell concepts on different wafer materials is reflected in the annual recurring ITRPV roadmap predictions [1]. Figure 1 shows the expected trend as published in the most recent edition of 2018.

The present insights confirm that the market will be dominated by the two-side-contacted cell types with an increasing share of PERC/PERT/PERL concepts to become mainstream after 2020. Despite the fact that heterojunction (HJT) and back-contact (MWT, IBC) cell concepts have proven a very high efficiency potential by module producers such as Panasonic, SunPower and Kaneka, their market share is expected to grow slower with expected shares of 15 and 10% in 2028 respectively.

As the solar cells are the basic units of the final PV system and not the final product, these individual cells are integrated into a module where cells are connected in series to add up voltage and generate the power characteristics that are useful for a practical application. The basic design of solar modules has not changed for many decades and most improvements have mainly relied on innovations at the cell level. However, the introduction of advanced and high-efficiency cell concepts revealed the limits of standard module technology and therefore highlighted the need for novel approaches towards module integration. Each cell concept has to be individually evaluated for the optimal module interconnection in terms of:

- Cell-to-module (CtM) power ratio
- Optimized production costs reflected by high yields and low investment costs
- Optimized bill of materials (BoM) at the lowest costs
- Best energy yield reflected by temperature, low light and incident angle behaviour
- Application fit: monofacial versus bifacial
- Reliability and durability guaranteeing more than 30 years' product lifetime under various climate conditions
- Sustainability and recycling potential as an emerging metric

This combination of requirements in terms of maximum module power optimization, long-term reliability and low-cost pressure has resulted in growing research efforts from R&D institutes and module manufacturers to improve PV panel output power independent of the cell efficiency developments [2]. The research progress translates into an increased CtM power ratio which is an acceptable metric to assess developments at the module level. Two complementary approaches that are followed to influence CtM power ratio can be summarized as:

1. Applying light management strategies using innovative module materials e.g. anti-reflection coatings, reflective busbars and backsheets
2. Reducing the resistive losses by increasing ribbon cross section, number of busbars, multi-wires, downsized cells, and conductive backsheets

Combining Figure 1 with the predicted increase of the CtM power ratio leads to Figure 2 and shows the trend curve as depicted by ITRPV for a typical 60 module with 156 x 156 mm^2 cells [1].

In this paper, we provide an overview of the current research and development trends in module interconnection technologies for (p- and n-type) two-side-contacted and back-contacted x-Si cell concepts that could be retrieved via the public channels. We are fully aware that this overview is not exhaustive as there are certainly module technologies under investigation by companies that have not disclosed their approaches in the public domain.

Standard interconnection of two-side-contacted cells into modules

Today, the most common PV module fabrication technology involves stringing of two-side-contacted photovoltaic cells. The generated electrical current is collected through distributed metal fingers across the cell into typically two or more busbars. By soldering of tinned copper ribbons to these busbars, cells are electrically connected in series to form cell strings, as illustrated in Figure 3. The size of these ribbons is a compromise between shadowing on the illuminated surface of the cells and resistive losses. The individual cell strings are connected with string connection ribbons and laminated into a module.

Evolving into more and more distributed stringing interconnection...

For both improving electrical performance and reducing optical losses, a trend towards an increasing amount of busbars is materializing [1]. Indeed, for the same amount of material, a lower resistive loss can be obtained by decreasing the finger losses or alternatively for the same loss, less material is needed. In terms of optics, more narrow ribbons will result in a reduced reflection out of the module and thus enhance light recycling, yielding a higher current. Culminating this trend are multi-wire interconnection technologies, with the additional advantage that busbars are no longer needed on the cells and the conductivity of the fingers can be strongly reduced, decreasing the cost of the silver metallization on cell level. This is illustrated in Figure 4.

- Increasing the amount of busbars (2-5-15) reduces the resistive losses in the fingers: the current is collected closer to where it has been generated in the cell, resulting in lower finger currents and thus lower resistive losses
- Switching from rectangular ribbons to round wires (while keeping the same total cross-section) yields reduces optical (reflection) losses due to the enhanced light trapping within the module [3]
- Using thicker wires, the total cross-section is increased and the resistive losses in the ribbons are reduced, though the thicker wires induce an additional optical (reflective) loss

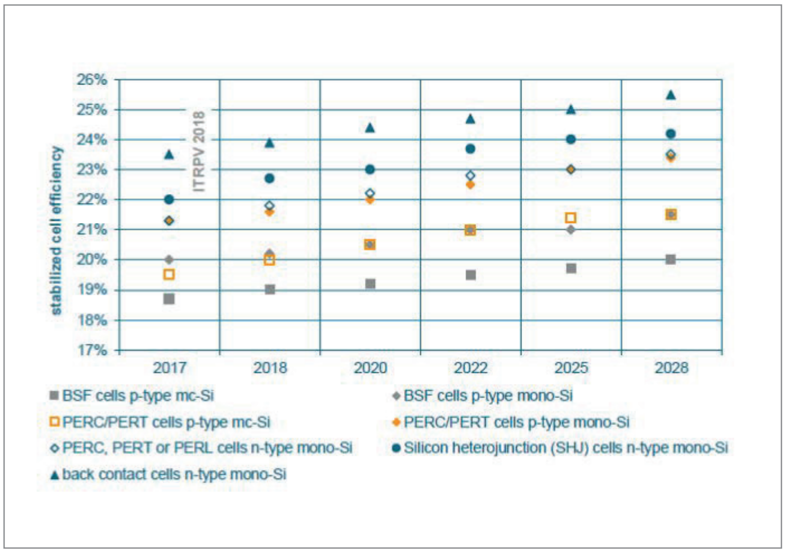

Figure 1. The projected development of average stabilized efficiency values for various x-Si cell types from the ITRPV roadmap 2018 edition [1].

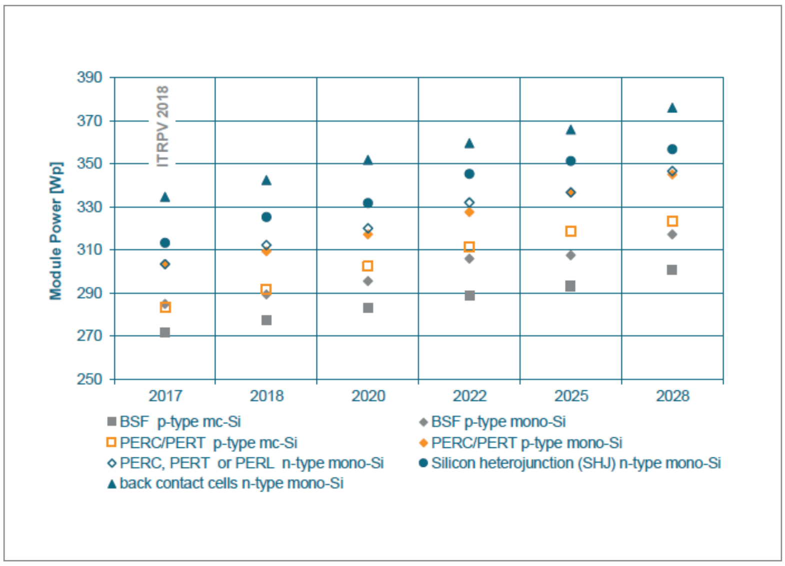

Figure 2. The projected development of module power values of 60-cell modules for different x-Si cell types in the ITRPV roadmap 2018 edition [1].

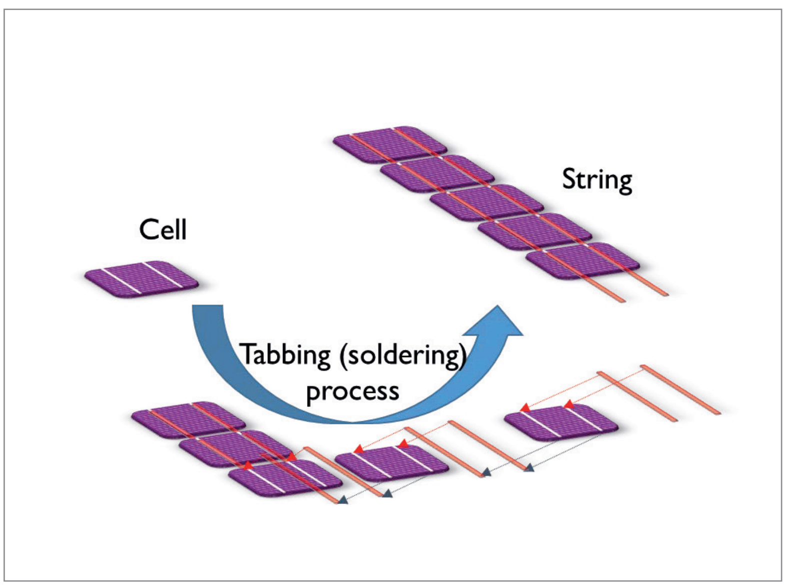

Figure 3. Standard interconnection of two-side-contacted cells into strings is achieved through alternatingly laying down and soldering of cells and ribbons in the so-called tabbing process.

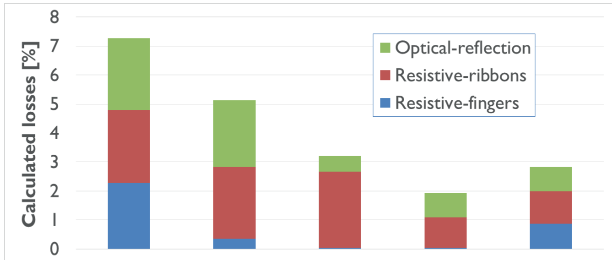

# busbars	2	5	15	15	15
Ribbon/wire section	2x0.3 mm²	0.8x0.3 mm²	0.16 mmØ	0.25 mmØ	0.25 mmØ
Finger section [mm²]	0.1x0.02	0.1x0.02	0.1x0.02	0.1x0.02	0.02x0.005

Figure 4. The relative impact of amount and cross-section of ribbons/wires, and cross-section of fingers in (calculated) resistive and optical losses due to interconnection (illustrative numbers, assuming fixed amount of fingers and finger and ribbon conductivity).

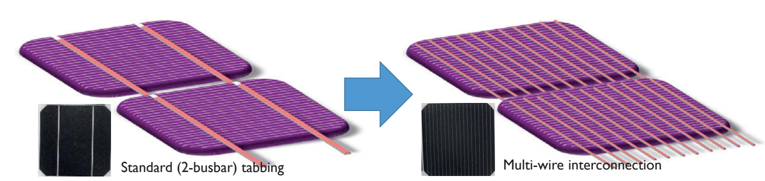

Figure 5. Illustrating the evolution in appearance (small insets) and interconnection scheme from standard (two-busbar) tabbing (left) to multi-wire interconnection (right).

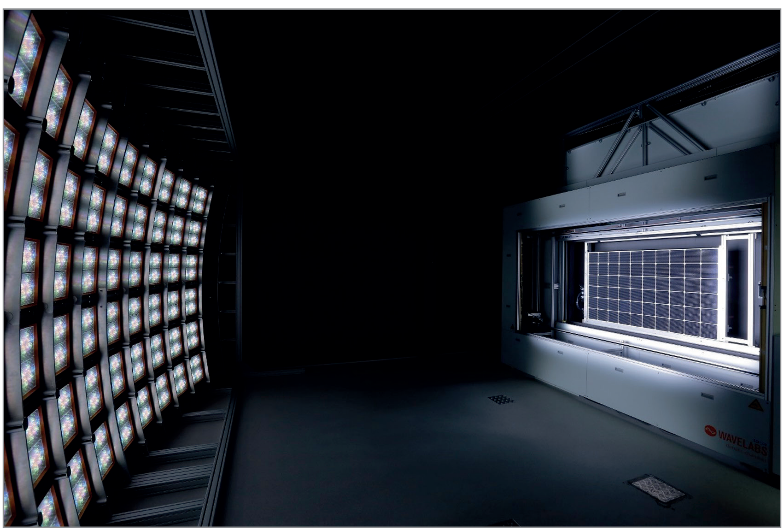

Figure 6. A commercial multi-wire soldered Neon module from LG acting as a reference module during flashing.

- Making the trade-off with cost, the finger metallization could be reduced, though at the expense of additional resistive losses

Apart from the electrical and optical benefits, also the aesthetics are improved, yielding a darker (cf. reduced optical losses) and more uniform module surface, as indicated in Figure 5.

Two such multi-wire interconnection technologies are in a very advanced stage of development. One approach effectively mimics the standard technology by soldering on finger solder pads, replacing the busbar [4]. As in standard production, this step is then followed by a separate encapsulation process through vacuum lamination. Such an approach requires controlling wire expansion during the soldering process and alignment of the wires to the finger pads. High performance and reliability has been demonstrated with this approach, and is already in volume production by LG [5], reaching 340Wp and 20% module efficiency.

... and merging with module-level encapsulation

A second approach applies a contact foil directly onto the metallized cell followed by a lamination process; this is the so-called Smart Wire Connection Technology (SWCT) [6]. The contact foil integrates low-temperature-solder-coated copper wires on an optically transparent supporting film with an adhesive layer. During the lamination the wires of the contact foil are soldered directly to the metal fingers of the cell. The use of low-temperature solder reduces stress between the wire-to-finger contact points on the cell. The contact foil is produced with the wires alternating on opposite sides of the supporting film, to allow the wires to contact neighbouring two-side-contacted cells to realize a series interconnection. Similarly as for the first approach, stress considerations may require some attention for compensating differences in thermal expansion between the cells and the wires, and an additional layer of encapsulant material is used for the subsequent module lamination step.

In its latest version, Meyer Burger has demonstrated 60-cell modules with heterojunction (HJ) cells reaching 335Wp, based on In-free soldering and UV-transparent encapsulation (white tiger foils) [7]. It also publishes good reliability results up to 2-3 times IEC testing for damp heat and thermal cycling, for both glass-glass and glass-backsheet modules. Commercialization of this HJ cell and module technology is gradually starting up.

Building further on these evolutions, and bringing in weaving knowhow, imec is looking into the replacement of the contact foil with a woven interconnection sheet allowing to similarly combine interconnection and encapsulation in the lamination step, though without introducing additional materials. Such a woven sheet can be manufactured by weaving metal wires perpendicularly into encapsulant ribbons. The weaving process immediately allows the metal wires to protrude on both sides of the fabric and thus can be also contacted electrically on either side.

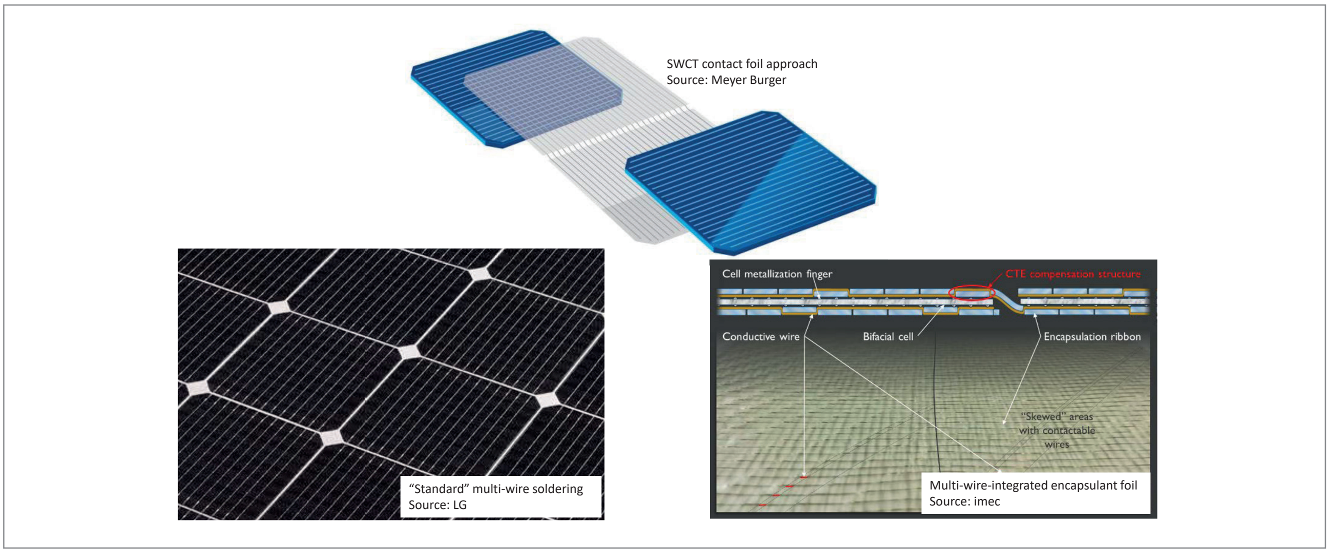

Figure 7. Illustration of the discussed multi-wire interconnection approaches.

If the cell metallization is designed with diagonal fingers on the backside, also the large ribbons to interconnect the strings can be left out. Layup of cells and interconnection fabrics can then be done immediately on the module glass, ready for feeding into a standard laminator where soldering and encapsulation is simultaneously achieved. Promising proof-of-concepts have been reported [8].

Soldering revisited

For these last evolutions, where the soldering process takes place during lamination, the standard solder materials, typically SnPbAg alloys, can no longer be used due to their melting temperatures in the range of 180°C, which is too high for most laminators. To reduce the melting temperatures, SnIn- and SnBi-based alloys are being investigated intensively [9], with a clear preference for Bi, considering the significantly higher cost of In. As a side note, also the transition to Pb-free soldering has sparked some development effort in solder materials by e.g. Alpha providing a leadfree drop-in replacement based on a SnBi-alloy [10]. First adopter of the low temperature solder alloy is the HJ cell technology, which also cannot withstand the above 200°C solder temperatures required by SnPbAg alloy. A recent review in this journal details further the technical challenges of the metallization and interconnection of this cell type [11]. The trends towards Pb-free solder might be limited now although the rising ecological concerns and novel legislations might force a rapid adaptation of these materials beyond HJ cells.

Reducing the interconnection current to reduce resistive losses: cutting cells

One rather simple solution to improve the module power and reducing the CtM losses without changing the standard interconnection technology is by using half cut cells, and this has a significant impact on the performance of PV modules. The power increase is mainly due to the reduction of resistive losses, which is achieved by halving the cell current and thereby increasing the fill factor (FF). This is simply because the electrical losses are proportional to the sum of the products of the resistances with the square of the flowing currents via the relation:

$$P_{loss} = \sum R \times I^2$$

The power loss is reduced by a factor of four when current is divided by two. In addition the extra spaces between the cells can be used to enhance reflections within the laminate, for instance by using white encapsulant layers (EVA, Polyolefins) on the rear of the cells and the backsheet resulting in short circuit gains. Both effects overcompensate the connectivity losses to a large extent, resulting in power boosts of up to 3-4% relative compared to standard technology. Additionally, junction boxes with bypass diodes can be attached in the middle of the strings, making the modules more tolerant to operation in conditions with partial shading [12], although on the other hand this involves the application of split junction boxes in the middle of the module, complicating standard manufacturing technology and bifacial considerations.

Moreover, an additional step is needed to slice the full size cells into half pieces and this needs to be done with a maximum yield and minimization of the efficiency losses caused by imperfections at the cut edge and an overall higher edge-to-area ratio. Significant improvements have been made in the development of thermal laser separation and mechanical breakage techniques [13,14] to overcome this limitation, further supported by advanced modelling approaches [15]. Additionally, modification of the stringer equipment in the module manufacturing line is required when moving to half cells to maintain the same throughputs. This has not precluded the big Tier 1 module manufacturers like REC, Jinko, Trina,

Canadian and JA Solar to increase their production capacity of half-cell modules by further fine tuning their fully automated processes, representing a smooth evolution of their existing production lines [2]. Nearly any cell technology can be used to make half cells and it is very likely that the market share of half-cell technology will significantly increase in the coming decade up to 40 % in 2028 as predicted by ITRPV [1] especially in market segments where aesthetics plays a less prominent role.

Getting rid of the wiring material: shingling

Another interesting module concept that is based on the interconnection of sliced cells is the so called shingling or tile based interconnection technology [2]. The whole concept is by no means new and dates back to 1956 as was extensively described in a recent review on singulated-cell and module architectures by Wöhrle et al [16]. The approach towards shingling was at that time largely motivated by particular design requirements and the need for high power densities on smaller available areas like car roofs. With the steady growth of the PV sector and the wish to diversify and differentiate, the potential of shingling technology has been rediscovered by a few large module manufacturers like SunPower that acquired shingle pioneer Cogenra in the recent past and commercializes the technology under its brand name P-series [17].

The beauty of this technology is that it eliminates the presence of ribbons, which clearly improves the aesthetics of the panel. A wafer sized cell is sliced into 5-6 rectangular stripe cells which are connected from the leading edge of the front cells to the opposite edge of the rear cell similar to the way roof tiles are constructed. The availability of flexible electrically conductive adhesives (ECA) as a low stress interconnecting material as well as suitable processing equipment strongly promoted the renewed interest of this technology. A schematic layout of the interconnection of shingle cells is shown in Figure 8.

The technology offers several advantages, including [18]:

- Low electrical losses due to the lower currents of the smaller shingle cells
- Improved area utilizations because of the denser packing of cells
- Processing at lower temperatures since ECA's are cured at lower temperatures than traditional tab soldering
- Smaller currents could lead to lower operating temperatures thereby improving energy yield and durability
- Application to any cell type (except back-contact) and the potential to make it bifacial
- Aesthetical appeal improves considerably because of the absence of busbars and ribbons

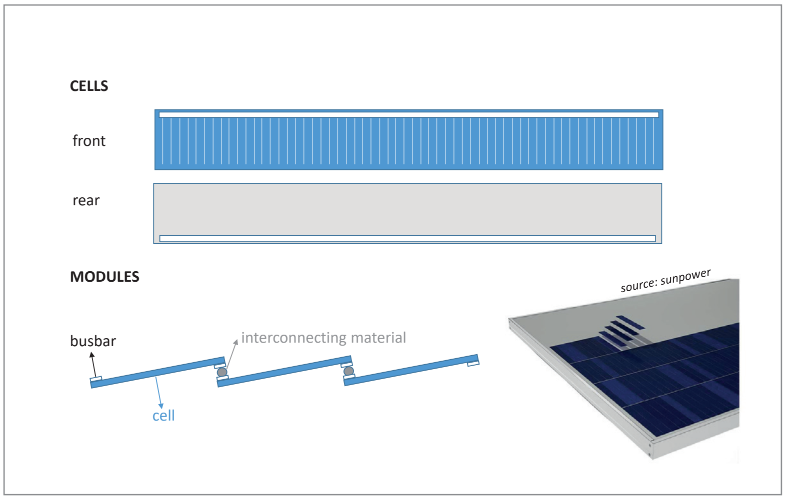

Figure 8. Schematic layout showing the principle of shingling module technology: above a top view of a monofacial sliced cell with busbars at the leading edges of front and rear cells; lower left a cross section of the interconnection of the sliced cells via an interconnecting material and lower right how cells are integrated in a full size module. Source: SunPower.

Singulation

As with half cut cells, the separation process step to cut down the full cell into stripe cells is done with laser-assisted cutting and subsequent mechanical cleavage. Specific attention should be paid to edge passivation to minimize recombination losses because of the higher edge-to-area ratio. To identify the optimum cell design with respect to cell width and corresponding front metallization finger grid design, simulations on the power output for cell stripes are carried out for standard Al-BSF cells [19] and for the so-called 'shingled passivated edge, rear emitter and rear' (SPEER) bifacial concept invented by Fraunhofer ISE [20]. This type of simulation can be applied for any future high-efficiency shingle-based cell concept based on passivated contacts leading to even higher module powers.

Interconnection

A very important requirement in a successful integration of shingled cells into modules is to create a reliable electrical interconnection between the cells that withstands the thermomechanical stresses that the module will undergo during testing and real-life operation. The interconnecting material should be flexible enough to avoid early failures due to the mismatch of thermal expansion coefficients and ECAs appear to be the most suitable class of materials that match the requirements [18]. These materials can be delivered as pastes and consist of a mixture of Ag particles within a matrix that is either based on silicones or organics. The ECAs are typically cured at temperatures between 150 and 180°C, after which the Ag particles form a percolative network and become highly conductive. The ECAs can be applied by either screen/stencil printing or dispensing/jetting. The choice of ECA as well as an optimized curing profile is required to get optimal

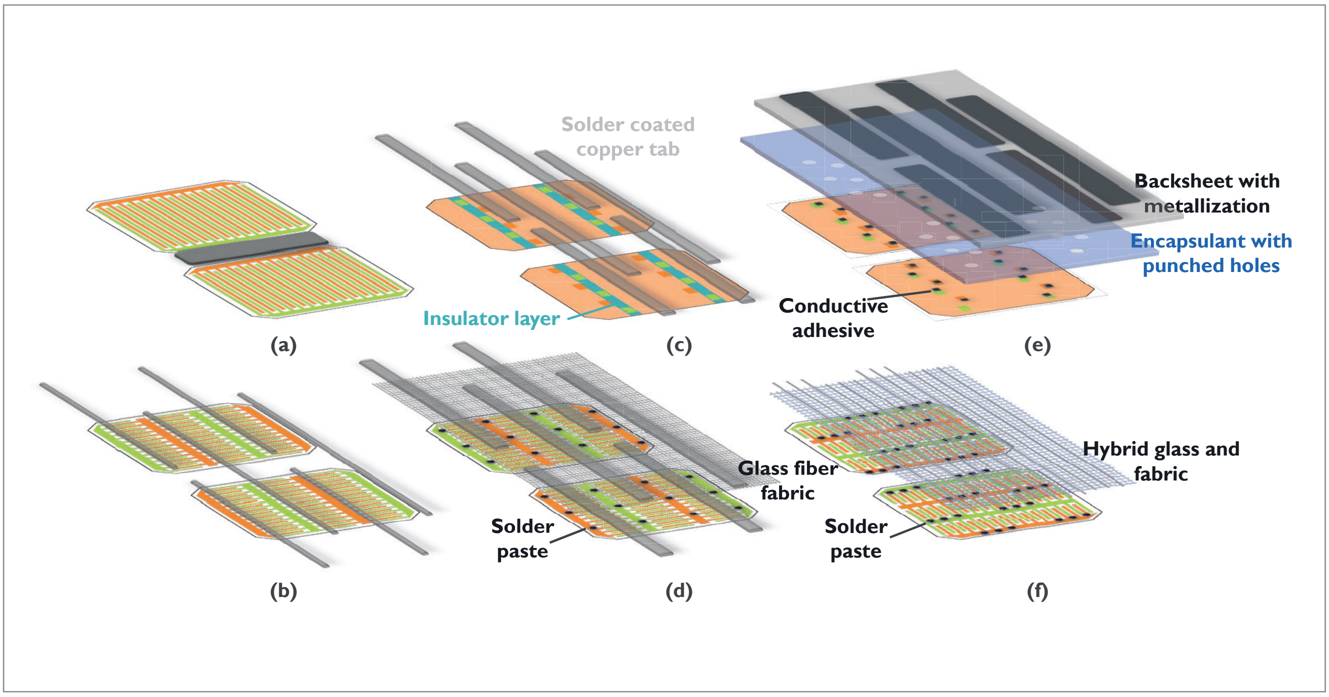

Figure 9. Schematics of various interconnection approaches for back-contact cells: (a) edge stringing, (b) busbar soldering (c) point soldering, (d) solder-through stringing, (e) foil-based interconnection and (f) woven multi-wire interconnection fabric (figure reproduced from [25] with permission).

adhesion and to pass all the critical failure tests. Some of these material challenges were addressed in a paper by Beaucarne et al. [21] where a simple analytical model was described to determine the conditions needed to avoid interconnection joint failure. It was found that interconnection materials with a low ratio of shear modulus G over shear strength is preferred for a good and robust interconnection joint. This clearly showed that ECAs with low $G/\tau_{\text{shear stress}}$ stress are superior over stiff solder joints to achieve sufficient string robustness and long term reliability.

An accurate CtM analysis done by ISE [22] revealed a clear improvement of the CtM ratio in terms of efficiency and power up to 10 % relative compared to conventional modules with ribbon or wire cell interconnection. This was further confirmed by experimental studies [22].

Concerning the long-term reliability of shingling module technology there is not a long history of test and field data so a thorough assessment cannot be made at this stage despite encouraging temperature cycling data showing <3 % power loss after 800 TC cycles [18]. SunPower further claims that its Performance Series panels are very robust since they were named as a top performer in five critical reliability tests: thermal cycling, damp heat, humidity-freeze, dynamic mechanical load and potential induced degradation as was reported in the DNV GL PV module reliability score card 2017 [17, 23].

All in all, the regained attractiveness of shingle technology has triggered the interest of more manufacturers (Seraphim, Solaria, GCL, TZS) than frontrunner SunPower, which could lead to an increased and significant market share in the coming decade.

Interconnecting back-contacted cells into modules

Despite the fact that the PV market is dominated by cell concepts which have the contacts on both sides of the cell, the world record efficiency of 26.6 % is obtained with a back-contacted cell where the current collection and contacts are all at the rear of the cell [24]. The p-n junction and metallization grid are made up of alternating parallel lines making an interdigitated pattern which gives the cell its name: interdigitated back-contact (IBC). As there is no metallization on the front of the cell, a higher current can be reached than for the two-side-contacted cells.

Another type of back-contacted cell is the metal-wrap -through cell, shortened to MWT. Here current is collected at the front and rear of the cell, but the current on the front is transported through holes or vias in the cell which are filled with a silver metallization paste to contacts at the rear of the cell. The front side contacts are isolated from the rear of the cell to prevent a short circuit. The advantages of this type of cell are the reduced metallization coverage on the front of the cell due to the absence of busbars allowing a higher current to be generated than with a standard two-side-contacted cell. Current collection is spread over the whole cell making it more efficient with lower resistance losses.

For both IBC and MWT cells, different module technologies are required to interconnect the cells due to the back-contact design. Below, we will review a number of module technologies that are currently applied in industry and various research institutes as are shown in Figure 9, largely based on and updating a previously published overview [25].

Edge stringing (Figure 9a)

SunPower is the best known manufacturer of IBC cells and produces high power PV panels for quite some years now for the high end market with module efficiencies over 22 % [26]. The cells are made of high grade n-type silicon. The metallization on the rear is completely different from conventional cells. Electroplated interdigitated copper fingers coated with tin adhere very well to the silicon and form a highly conductive pathway to busbars that are positioned at the edges of the cell. These busbars are connected using a smart tab which is designed to minimize the thermal stress on the cell during operation. The tab provides the electrical interconnection between neighbouring cells and sufficient strain relief if cells expand and shrink during temperature cycles (see Figure 10).

The edge stringing approach in fact decouples the cell interconnect from the cell contact metallization. While an elegant approach in this respect, it also implies that the cell metallization has to carry the current of the full cell. This leads to a trade-off in terms of cell metallization thickness: a low resistance requires a high thickness, however mechanical stress, as well as cost considerations ask for a thin metallization. Indeed warping due to a mismatch in coefficient of thermal expansion (CTE) between the silicon and the metallization can result in mechanical stress or cracking, which reduces the yield both in cell fabrication and module assembly. As the effect scales with size, SunPower balances this trade-off in metallization thickness by implementing this approach while keeping a limited cell size.

SunPower claims that because of this fundamentally different module design and BoM a superior reliability in real world conditions can be achieved. This was confirmed by continuous extensive qualification test programmes well beyond industry standards, supported by additional characterization and modelling, finally resulting in degradation rates <0.2 % for the optimized module designs [26,27].

Busbar stringing and point soldering (Figure 9b and 9c)

An alternative approach to overcome this trade-off is the busbar stringing approach, where the interconnect metallization on top of additional busbars within the cell area can reduce the need for a thick cell metallization [28]. In this approach, however, some electrical performance is lost as some active area is sacrificed for the busbars, causing electrical shading, unless the busbars are implemented in a second metallization level (floating busbars) [29,30,31].

To reduce electrical shading by the cell metallization, while maintaining reduced resistive losses at module level, multi-level interconnection

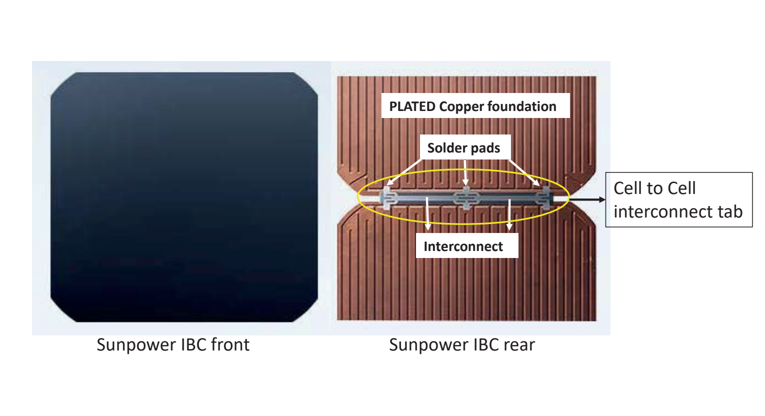

Figure 10. Layout of the edge stringing approach of IBC cells as applied by SunPower. Source: SunPower, https://us.SunPower.com

technologies are developed. These approaches require a more closely linked cell and module metallization design. Among them the point contact approach [32] is an interesting solution as the classical tabbing, where the conductive tab is directly placed over the cell, is compromised in back-contact cells due to shunts between different polarity fingers. To avoid this shunting an isolator is needed after cell fabrication (whereas in the floating busbar approach this isolator is deposited as part of the cell process). In some approaches this isolation function is also performed by the encapsulant [32]. More similar to printed circuit board assembly technology, this function could be realised by a solder mask. Another approach inspired by microelectronic circuits uses an adapter [33]. Lately, work has also been ongoing to integrate a multi-wire approach in such an isolator-based scheme [34].

Solder-through stringing (Figure 9d)

An innovative way of significantly reducing the cost is put forward by the solder-through stringing approach, where the insulation is guaranteed by a porous insulator, e.g. a woven glass fibre sheet through which a solder paste reflows and provides contact between cell contact and ribbon [35]. This approach is being commercialized by Soltech [36].

All of the above approaches use similar (solder) materials and tabbing-stringing technologies as developed for two-side contacted cells. After stringing, where cells are interconnected, these strings are traditionally then interconnected at the edge of the modules by metal (bussing) ribbons in the so-called bussing step. This implies additional resistive and area losses in the module [37, 38]. To overcome these losses module-level interconnection technologies are of interest and therefore under development. Additionally, they also enable multi-level metallization, hence reducing the thickness requirements for the cell metallization, and the elimination of a separate cell soldering step and string handling opens the door for thinner cells.

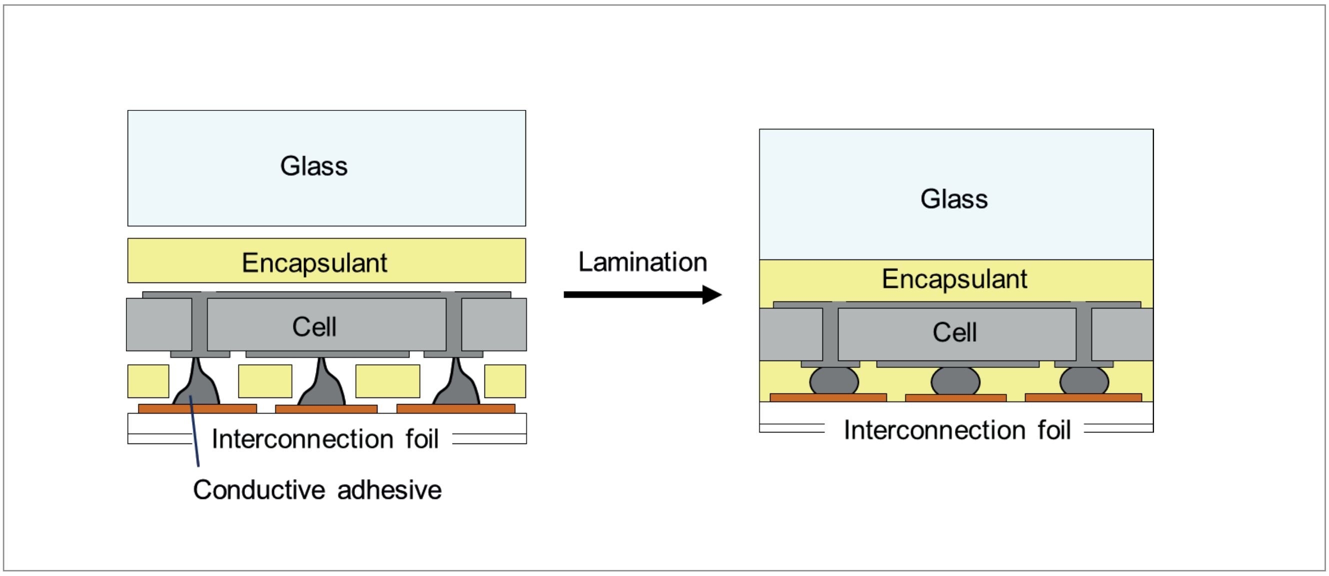

Figure 11. Schematic layout of the foil-based back contact module layer stack before and after the lamination process.

Foil-based back contact (FBC) interconnection technology (Figure 9e)

At ECN an integrated module technology for back-contact cells was developed using a back-sheet foil with an additional conductive metallic layer, usually copper or aluminium [39,40]. The conductive layer is patterned by milling, etching or other techniques to match the contact pattern on the rear of the cell so as to form a series interconnection between neighbouring cells. Contact between the cells and the copper layer is made using an interconnection paste, usually an ECA or low-temperature solder, which is applied onto the foil or the cell by stencil printing or dispensing/jetting. The cells are isolated from the foil via a layer of encapsulant with holes at the position of the conductive material. The thickness of this encapsulant layer dictates the amount of conductive material needed. The cells are then placed on top of the encapsulant and adhesive and the stack is finished with a second layer of encapsulant and a glass sheet (see Figure 11).

FBC modules have been shown to reduce cell-to-module losses when compared to other mature module technologies (soldering/tabbing and multiwire) since the total conductor cross section in FBC modules is significantly higher than for the other interconnection types [41], thereby reducing the resistive losses. FBC modules mainly based on MWT cells have proven to be reliable in selected climate chamber testing (damp heat and temperature cycling) and long-term outdoor testing, and IEC certification for MWT modules with well selected BoM has been achieved by ECN and partners [42, 43].

Dedicated industrial manufacturing equipment is available for the module manufacturing and has a very high level of automation like for instance demonstrated by equipment manufacturers as Eurotron, FormulaE and Valoe [44]. The first industrial production towards the gigawatt scale has recently started in China at Sunport Power [45], while production activities in Netherlands at a smaller scale have been started or announced [46].

In order to reach a competitive cost structure compared to the current mainstream, a large-scale industrial implementation of FBC module technology requires development of the complete value chain and availability of the materials in large volumes at low cost, in particular the conductive back-sheet and the ECA. The cost of the back-sheet is partially related to the processing used to pattern the foil and partly to the cost of the metallic conductor. The cost of the ECA is dominated by the silver content.

Recently, a number of strategies have been reported by ECN [47] to further reduce the costs of FBC technology and are summarized below:

1: Replace copper by aluminium

Originally, the patterned metal used in the conductive back sheet is a thin layer of ~35 micron copper (Cu) foil that is glued to a polymeric PV backsheet. Replacing the Cu layer in the conductive back-sheet with aluminium (Al) has the potential to reduce the overall cost of the module by more than 2% since Al is inherently cheaper than Cu. However, Al forms a native oxide on its surface which should result in an unacceptably high contact resistance to the ECA. One solution to overcome this has been explored and commercialized by the company Hanita who developed a low-cost alternative to copper foil by coating the aluminium layer with an ultrathin copper skin by Physical Vapour Deposition methods [48].

Alternatively, ECN has demonstrated the use of a cold-spray technique [40,49,50] by which Cu particles are deposited via lanes onto the Al surface at very high speeds, breaking through the oxide and making contact to the bulk Al (see Figure 12). The back contacted cells are contacted via the rear to

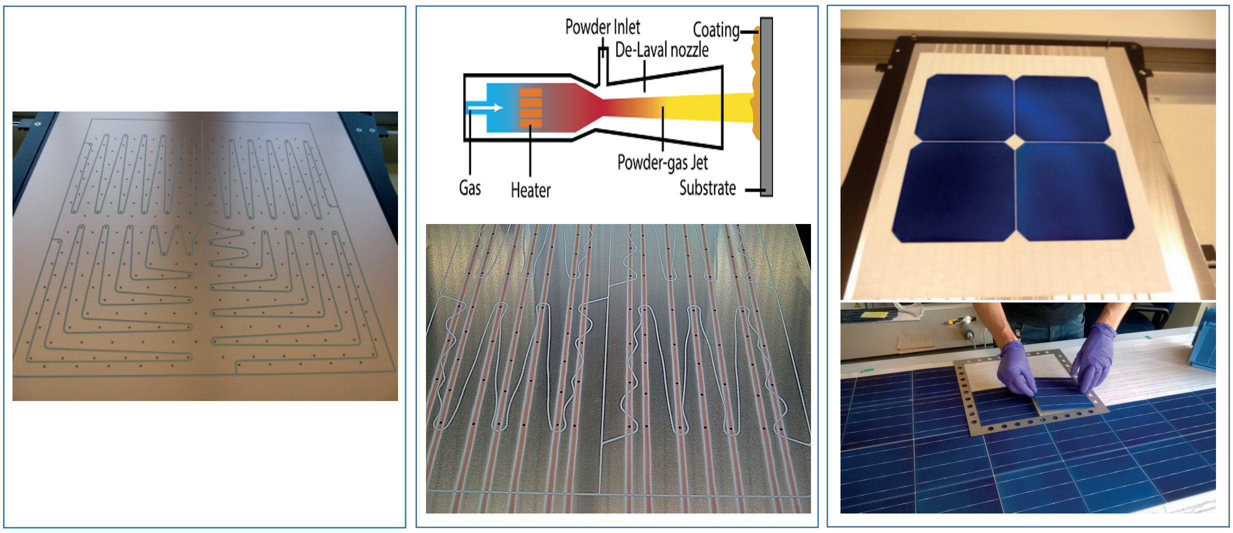

Figure 12. From left to right: a patterned copper conductive backsheet (left), a schematic representation of the spray gun used for the cold spray process and an aluminium foil with sprayed copper lines corresponding with the position of positive and negative contacts (middle); an IBC 2x2 cells mini module and the manufacturing of a MWT full size module based on copper sprayed aluminium conductive back sheets.

the Al foil via the Cu particles through an ECA with contact resistances down to 0.2 mΩ. guaranteeing a negligible CtM fill factor loss due to the interconnection. Large series of 2x2 MWT and IBC cells mini-modules have been manufactured in the ECN pilot line using this approach and are subjected to selected standard IEC reliability tests for damp heat and thermal cycling. The ageing tests clearly reveal the technical potential of the cold spray method by demonstrating >95 % power retention after three times IEC and are in line with the best test results of modules built with Cu conductive back contact foil. A prototype full size MWT module was recently manufactured at ECN with a CtM FF loss of less than 1.5 % [47].

2: Optical enhancements

FBC is also well suited for carrying the larger currents produced by larger cells, IBC, or modules with enhanced optical elements with lower resistive losses. This is because the foil makes contact at multiple points distributed across the entire cell area creating a parallel path for current conduction. Therefore, optical enhancements, such as placing a reflective material between cells (intra-module foil, IMF) can be optimized for overall improved power output for back contact modules. A highly reflective intra-module foil (IMF) is placed in all the currently inactive areas of the module, between cells and along the edges in order to reflect light back onto the high efficiency cells as can be seen in Figure 13.

As noted above, similar materials are currently available and used in standard modules. ECN has demonstrated the IMF with back contact mini-modules with 5% CtM power gain for both IBC and MWT cells [51]. For full sized 60-cell MWT modules manufactured on an existing production line for FBC modules, a CtM of more than 4% has been demonstrated [47]. To achieve this, the space between the cells was increased to 10.5mm and 6mm in the height and width respectively resulting in a 6.3% larger module area. This is then filled with IMF material. This results in more 7% gain in module power and approximately 1.5% gain in total area module efficiency.

3: High yield with thinner wafers

Another way to reduce the cost structure of PV is to save on Si usage and use thinner wafers for cell production. Since thin cells are more fragile in handling a suitable module technology is required to maintain the same production speed and yield. FBC technology, which uses pick-and-place equipment for cell placement was used to make such thin cell modules possible as was recently reported [47,52,53,54]. A larger series of ~95 µm thin n-type IBC cells were manufactured using an industrial compatible process flow [54] starting from 120 µm thick 6 inch n-type Cz diamond wire cut wafers. A selection of 60 thin-cells (process based on homojunctions and not fully optimized) with a narrow efficiency distribution was made for integration in a full sized module based on FBC module interconnection technology using dedicated industrial equipment from Eurotron and a standard module bill of materials (BoM) including ECA's. The module was produced without any breakage of cells and a cell-to-module (CtM) power loss of less than 1% while only minor issues of micro-crack formation were observed with EL. This demonstrates the feasibility of FBC technology for handling thin cells down to 80 micron thickness.

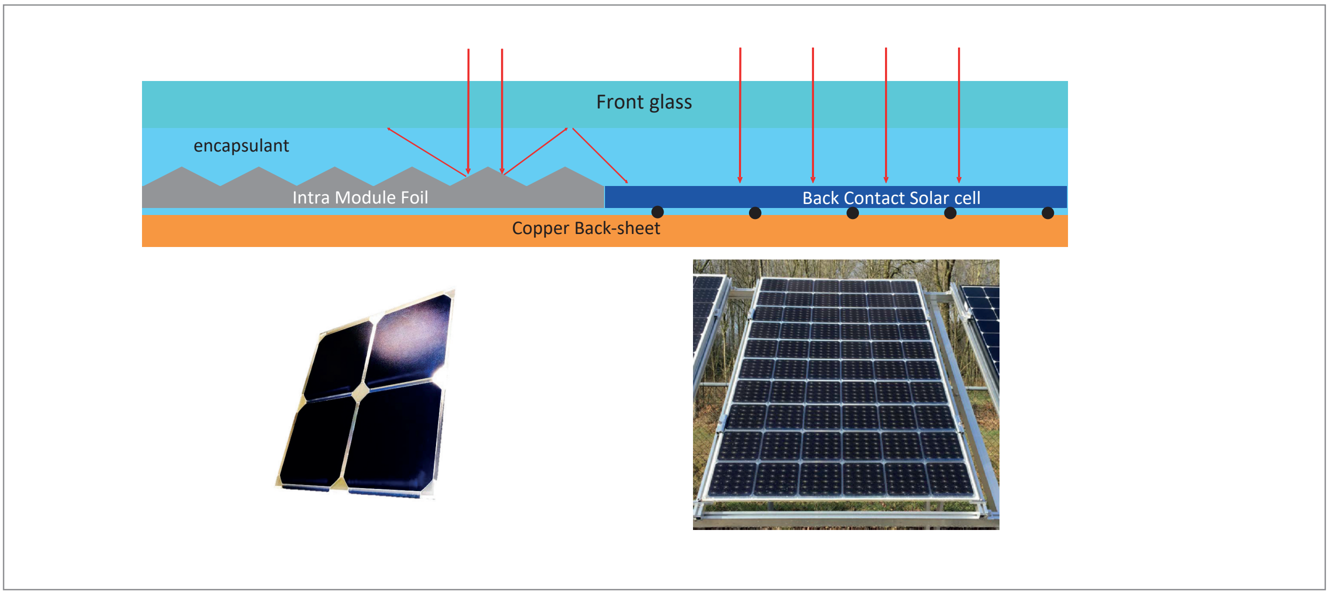

Figure 13. Upper: schematic cross-section of a Foil-based back contact module combined with reflective Intra-Module Foil (IMF). Lower left IBC mini-module with 8mm wide IMF integrated along cell edges and corners, lower right: full size 60-cell MWT module using IMF materials to increase the current by almost 6%.

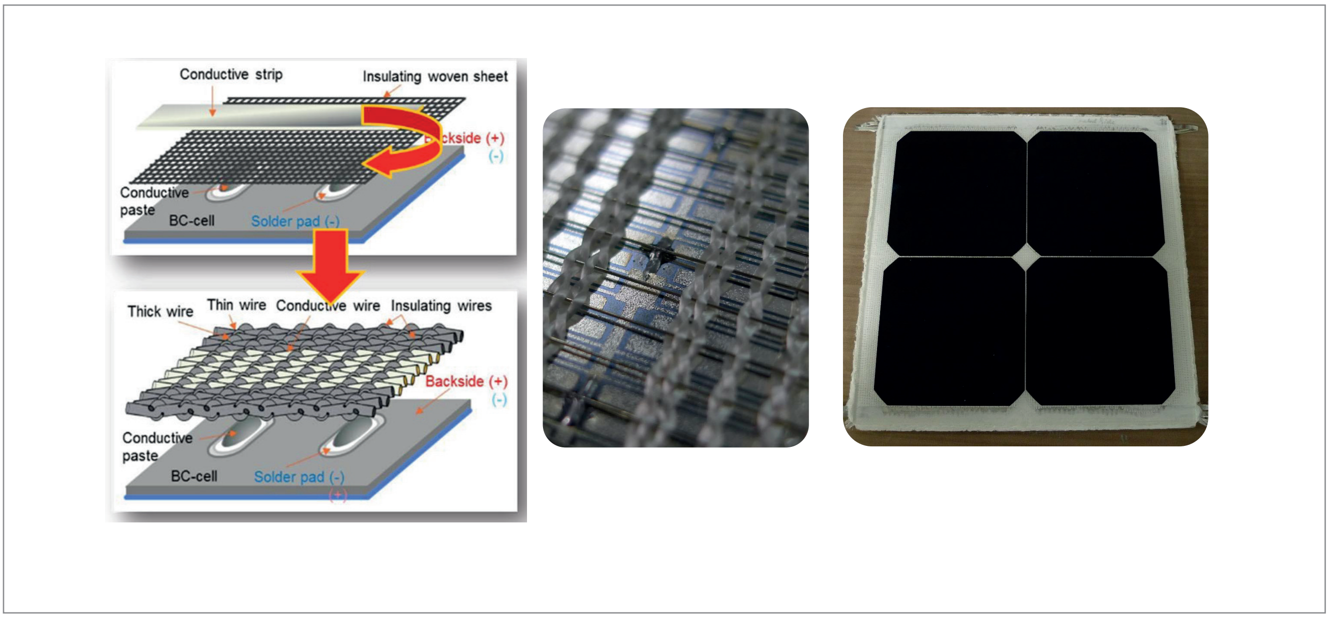

Figure 14. Schematic (left) and detail (middle) of how the interconnecting conductive ribbons in the solder-through approach can be integrated inside the woven fabric and applied in a 2x2-cell-module (right).

Woven multi-wire interconnection fabric concept (Figure 9f)

Another concept is under development at imec [35,55]. This concept is inspired by the earlier-mentioned solder-through approach and additionally brings some of the opportunities from the multi-wire interconnection technologies under development as the SWCT and MBB (multi-busbar) approach [56,57,58]. Although these are propagated mainly for two-side contacted cells currently, and not for back-contact cells, there are some features that could similarly prove beneficial here:

- Optically (not at the front obviously, but) potentially at the back for bifacial cells compared to conductive backsheets, due to the open weave structure;
- Mechanical reinforcement of the encapsulant including resilience to thermal cycling due to a reduced CTE of the glass-fibre-reinforced encapsulant;
- Reliability due to a reduced impact of cracking with the distributed wiring;
- Reduced cell metallization requirement (reduced resistance) due to the distributed contacting.

In this novel concept, insulating glass fibre and conductive wires are integrated into a hybrid woven fabric, as indicated in Figure 14. Compared to the solder-through approach, where wide metal ribbons are connecting neighbouring cells in series, the proposed novel concept uses an array of metallic wires to replace those tabbing ribbons. The metallic wires are interwoven with glass fibres to fix the metal wires' location and isolate them from the backside of the cell. Connection between the cell metallization and the metallic wires in the fabric is made through locally deposited solder paste dots. This requires an open weave pattern for solder spreading. One weave pattern that satisfies these requirements is the so-called leno weave, where pairs of fibres are twisted during the weaving process to provide an interlocked fabric. This technology can be implemented both on string and module level. The latter is achieved by integrating metallic wires at the side of the fabric in the perpendicular direction to the wires interconnecting the cells, hence enabling connection of the cell strings directly in one soldering step.

This approach of weaving together glass fibres and thin metallic wires can bring multiple improvements compared to existing interconnection technologies.

Firstly, module performance can be improved by allowing an increased metal cross-section between cells while maintaining a uniform topography of the fabric with a porous structure that can be embedded by the encapsulant. Additionally, the interconnect metallization is on a different level than the cell metallization, which allows to reduce the requirements for the cell metallization in terms of current collection (resistive losses).

Secondly, this interconnection can be designed to address strict reliability requirements through a number of features. To limit thermally-induced stresses, distributed out-of-plane stress relief in the metal wires can be easily designed and implemented into the woven fabric, e.g. by using glass fibres of different diameter within the same fabric. Though soldered contacts typically entail higher stresses than conductive adhesives [58] (but are still generally considered more reliable), multiple and distributed solder points can reduce and even eliminate the build-up of stresses across the cell. A homogenous and reduced heating over the full area during soldering creates a more homogeneous stress across the cell than local heating. With such a more evenly distributed stress, the maximum local stress may be lower, further lowering the risk of cracking compared to standard tabbing approaches. A uniform topography of the interconnecting fabric can further reduce mechanical stress on the cells and eases the lamination in glass-glass modules. Indeed, as the interconnection can be separated from the encapsulation process, the technology also allows freedom in encapsulation system, with glass-glass encapsulation eliminating humidity ingress through the backsheet which may be beneficial depending on the used encapsulation scheme and environmental conditions during operation [60]. Apart from this, realizing a more symmetrical build-up of the module is beneficial from the perspective of mechanical and thermomechanical stress on the cells inside [61]. Also, considering reliability, the used materials such as glass fibre and solder paste have already been previously validated in other PV module concepts [62] and as such lower the unknown factors that are often considered a barrier in PV module technology.

Thirdly, this selection of known materials potentially allows a low-cost technology. Weaving technology simultaneously, at limited cost in high-volume production, adapts easily to various cell metallization layouts. Avoiding the necessity of a separate stringing step and the potential of solder paste for self-alignment allows a simplified module assembly. In module assembly the ease of optical alignment due to open weave structure and relaxed alignment accuracy can also be a considerable bonus. Finally, the porous structure of the fabric allows the encapsulant to penetrate the fabric, which can thus be embedded in the encapsulant layer and potentially, depending on wire and fibre dimensions and composition, minimizes the amount and therefore cost of encapsulant material.

Concluding remarks

In the evolution towards higher cell efficiencies, new cell concepts (two-sided and back-contacted) have been introduced and for each of these concepts, new module materials and interconnection technologies have to be developed to fulfil all the demands of a good end product in terms of lowest costs, highest yield and power and above all superior quality (reliability and durability). There is no single module concept that fits all cell concepts and module application type so existing module concepts need to be adapted or innovative module technologies are required to fit the aforementioned requirements. This paper provides an overview summarizing the development of integrated cell-to-module manufacturing approaches such as multi-busbar, multi-wire, shingling module technologies for two-sided contact cells and advanced soldering, woven fabric and foil-based module technologies for back contact cells aiming for the highest power outputs, lowest costs and longest lifetimes.

With this increasing number of approaches that deviate from standardly applied technology, a versatile "toolbox" is generated to design various kind of tailored products for different applications and needs with the aim to further widen the applicability of PV. Especially by benefiting from unique features of a specific module technology or combinations thereof, specialized products can be made that are tailored for new application areas such as:

(i) BIPV (building-integrated PV), e.g. PV modules integrated in the facade of buildings, integrated in the roof of buildings, integrated in windows, …

(ii) IIPV (infrastructure-integrated PV), e.g. PV modules for sound barriers along highways and railways, PV modules integrated in roads, in-city applications such as street lightening, sub-urban and rural applications, floating PV modules...

(iii) Transportation, e.g. PV modules for cars, trains, buses, aircrafts, ...

(iv) Climate optimized PV: PV modules which are optimized for maximum energy yield in a specific climate, such as desert climate, cold and snowy climates, climates with high humidity, continental climates with large daily and yearly temperature variations...

For these emerging application fields additional criteria like improved aesthetics, flexibility of shape and size, shadow tolerance, increased resistance towards extreme weather conditions, bifaciality, three-dimensional shaping etc. are becoming more important to specify the final product. The existence of multiple module technologies, concepts and associated bill of materials might facilitate the selection whatever suits best.

References

[1] International Technology Roadmap for Photovoltaic (ITRPV), 9th Edition 2018 [http://www.itrpv.net/Reports/Downloads/]

[2] Chunduri, S.K. et al., 2017 edition Advanced Solar Module Technology http://www.apvia.org/upload/file/TaiyangNews_Report_Advanced_Solar_Module%20Technology_2017_download_version.pdf

[3] Braun, S. et al. 2012, "Solar cell improvement by using a multi busbar design as front electrode". Energy Procedia, Vol.27, pp227 – 233

[4] Braun, S et al. 2013, "Multi-Busbar Solar Cells and Modules: High Efficiencies and Low Silver Consumption". Energy Procedia, Vol: 38, pp. 334–339

[5] LG Neon2 datasheet, https://www.lg.com/global/business/solar/business-resources/download

[6] Faes, A et al.2014, "SmartWire Solar Cell Interconnection Technology". Proceedings of the 29th European Photovoltaic Solar Energy Conference and Exhibition , pp 2555 - 2561

[7] Haenni, S. et al., 2018, "The Real Power of SmartWire Connection Technology", Presentation at SNEC 2018.

[8] Govaerts, J. et al. 2019, "Progress in encapsulant-integrated multi-wire interconnection", to be published in Proceedings of the 35th European Photovoltaic Solar Energy Conference and Exhibition

[9] Geipel, T. et al. 2017, "Intermetallic compounds in solar cell interconnections: Microstructure and growth kinetics", Solar Energy Materials & Solar Cells Vol. 159 , pp. 370–388

[10] Pujari, N.S. et al.2017 "Non-Eutectic Low Melting Temperature Alloys for Standard c-Si Interconnection". Presented at the Metallization Workshop. 2017.

[11] De Rose, A. et al. 2018, "Challenges for the interconnection of crystalline silicon heterojunction solar cells", PV International, ed. 40, pp 80-89

[12] Manganiello, P. et al.2017, "A bottom-up energy simulation framework to accurately compare PV module topologies under non-uniform and dynamic operating conditions". IEEE PVSC.

[13] Schneider, J. et al., 2014 "Solar module with half size solar cells", Proceedings of the 29th European Photovoltaic Solar Energy Conference and Exhibition proceedings, pg. 185-189

[14] Röth, J. et al. 2015, "Thermal laser separation (TLS) dicing process study for cutting silicon solar cells for high efficiency half-cell modules", Proceedings of the 31st European Photovoltaic Solar Energy Conference and Exhibition, pg. 716-718

[15] Fell, A. 2017, "Modelling of edge recombination losses in half cells", Proceedings of the 33rd European Photovoltaic Solar Energy Conference and Exhibition, pp. 853-856

[16] Wöhrle, N. et al. 2017, "Solar cell demand for bifacial and singulated-cell module architectures," Photovoltaics International, Vol. 36, pp. 48–62.

[17] SunPower p-series see: https://us.SunPower.com/solar-panels-technology/p-series-solar-panels/

[18] Tonini, D. et al. 2017, "Shingling technology for cell interconnection: technology aspects and process integration", Proceedings of the 33rd European Photovoltaic Solar Energy Conference and Exhibition, pp. 38-41

[19] Rudolph, D. et al. 2017, "Cell design optimization for shingled modules", Proceedings of the 33rd European Photovoltaic Solar Energy Conference and Exhibition, pp. 880-883

[20] Wöhrle, N. et al. 2017, "The SPEER solar cell – simulation of shingled bifacial PERC-technology based stripe cells", Proceedings of the 33rd European Photovoltaic Solar Energy Conference and Exhibition, pp. 844-848

[21] Beaucarne, G. 2016, "Materials Challenge for shingled cells interconnection", Energy Procedia, Vol. 98, pp. 115–124

[22] Mittag, M. et al. 2017, "Cell-to-Module (CTM) Analysis for Photovoltaic Modules with Shingled Solar Cells", Proceedings of the 44th IEEE Photovoltaic Specialist Conference

[23] "PV module reliability scorecard 2017" To be downloaded via https://www.dnvgl.com/publications/pv-module-reliability-scorecard-2017-93448

[24] Yamamoto, K. et al. 2017, "Record-breaking efficiency back contact heterojunction crystalline Si solar cell and module", Proceedings of the 33rd European Photovoltaic Solar Energy Conference and Exhibition, pp. 201-204

[25] Borgers, T. et al. 2016, "A woven fabric for interconnecting back-contact solar cells". Prog. Photovolt: Res. Appl. (2016), Vol. 25, pp 569-582
[26] SunPower, internal report " SunPower module degradation rate", https://us.SunPower.com/sites/SunPower/files/media-library/white-papers/wp-SunPower-module-degradation-rate.pdf
[27] Bunea, G. et al., 2012, "Setting new standards in c-Si module efficiency and reliability: SunPower's roadmap to 21% efficiency production modules", Proceedings of the 27th European Photovoltaic Solar Energy Conference and Exhibition, pp. 201-204
[28] Halm, A. et al.2012, "The ZEBRA cell concept—large-area n-type interdigitated back contact solar cells and one-cell modules fabricated using standard industrial processing equipment". Proceedings of the 33rd European Photovoltaic Solar Energy Conference and Exhibition, pp. 567 - 570
[29] Galbiati, G. et al. 2012, "Large-area back-contact back-junction solar cell with efficiency exceeding 21%". IEEE Journal of Photovoltaics Vol. 3, pp 560–565
[30] Hacke, P. et al. "Interconnect technologies for back contact solar cells and modules". Patent US2008/0216887 2008.
[31] Verlinden, P. et al. 1988, "High efficiency large area back contact concentrator solar cells with a multilevel interconnection". International Journal on Solar Energy Vol. 6, pp 347–366.
[32] Eitner, U. et al. "Progress in HIP-MWT module technology". Presentation at the 5th MWT Workshop 2013.
[33] Ebert, M. et al. 2014, "Robust module integration of back contact cells by interconnection Adapters". Proceedings of the 29th European Photovoltaic Solar Energy Conference and Exhibition, pp 225–228.
[34] Faes, A. et al. 2017 "Multi-Wire Interconnection of Back-Contacted Silicon Heterojunction Solar Cells". 7th Workshop on Metallization & Interconnection for Crystalline Silicon Solar Cells –October 22-23, Konstanz.
[35] Borgers, T. et al. "The untapped potential of weaving technology for module interconnection". Presentation at the 7th Back-Contact workshop 2015.
[36] Dewallef, S. "New interconnection method for MWT cells based on tabber-stringer technology". Presentation at the 5th MWT Workshop 2013.
[37] Haedrich, I. et al. 2014, "Unified methodology for determining CTM ratios: systematic prediction of module power". Solar Energy Materials & Solar Cells , Vol. 131: pp
[38] Govaerts, J. et al. 2015, "Cell-to-module performance modeling: validation and application for advanced modules". Proceedings of the 30th European Photovoltaic Solar Energy Conference and Exhibition, pp 1997–2000.
[39] Bennett, I.J. et al. 2013, "Reducing the cost of back-contact module technology", Energy Procedia 38, 329–333 (2013).
[40] Bennett, I.J. et al. 2014, "An overview of developments in foil based back contact modules", Proceedings of the 29th EUPVSEC Conference and Exhibition, pp 5-8
[41] Van Aken, B. et al. 2016, "Positive cell-to-module change: Getting more power out of backcontact modules", Photovoltaics International, 33, pp. 97-105
[42] Rosca, V. et al. 2015, "Reliability Results for High-Efficiency Foil-Based Back-Contact PV modules", Proceedings of the 31rd European Photovoltaic Solar Energy Conference and Exhibition , pp. 2545-2548
[43] Eerenstein, W. et al., 2010, "Climate chamber test results of MWT back contact modules", Proceedings of the 25th European Photovoltaic Solar Energy Conference and Exhibition /5th World Conference on Photovoltaic Energy Conversion, pp 3854 – 385
[44] For more information on equipment manufacturers for FBC interconnection technology see: https://www.eurotron.nl/; http://www.formulaeworld.com/; https://www.valoe.com/
[45] https://www.sunportpower.eu/
[46] https://exasun.com/; https://www.energyra.com/
[47] Newman, B.N. et al. 2018, "Materials Development and Increased Module Efficiency for 15% Cost Reduction of Reduction of Back Contact Modules". Proceedings of the WCPEC-7: 45th IEEE PVSC, 28th PVSEC, 34th EUPVSEC, in press
[48] See: http://www.hanitacoatings.com/industrial/solutions-products/copper-substrates
[49] Goris, M. et al. 2014, "Aluminium Foil and Cold Spray Copper Technology as Cost Reduction Process Step in Back-contact Module Design", Energy Procedia Volume 55, pp 342-347.
[50] Goris, M. et al. 2016, "Production of low cost back contact based PV modules", Proceedings of the 32nd European Photovoltaic Solar Energy Conference and Exhibition, pp. 99-104.
[51] Guillevin, N. et al. 2017, "Cel lto module gains for high efficiency back contact cells, Proceedings of the 33rd European Photovoltaic Solar Energy Conference and Exhibition, pp 1654-1656
[52] Kroon, J.M. et al. 2017, "Highlights From The FP7 Project On Photovoltaics CHEETAH: More Power With Less Material", Proceedings of the 33rd European Photovoltaic Solar Energy Conference and Exhibition, pp 2844-2848
[53] Sommeling, P. et al. 2018, Full Size IBC Module Based on Industrially Processed 95 μm Thin Cells with a CtM Power Loss < 1%, Proceedings of the Silicon PV 2018 conference, accepted for publication
[54] Burgers, A.R. et al. 2018, "ECN's IBC solar

cells in mass production environment: rise of a competitive back-contact module concept", PV International, Vol. 39, pp. 44-54

[55] Govaerts, J, et al.2016, "Innovative approaches to interconnect back-contact cells". Proceedings of the 31st European Photovoltaic Solar Energy Conference and Exhibition 2016; pp. 1–4.

[56] Sadlik, B. et al. 2010, "DAY4™ technology for conceptually new PV module production", Proceedings of the 25th European Photovoltaic Solar Energy Conference and Exhibition; pp 4144–4147.

[57] Braun, S. et al. 2013, "Multi-busbar solar cells and modules: high efficiencies and low silver consumption". Energy Procedia; Vol. 38, pp 334–339.

[58] Söderström, T. et al. 2013, "Smart-wire connection technology". Proceedings of the 28thEuropean Photovoltaic Solar Energy Conference and Exhibition; pp. 495–499.

[59] Geipel, T. et al. 2015, "Reduction of thermomechanical stress using electrically conductive adhesives". Energy Procedia; Vol. 77, pp 346–355.

[60] Jankovec, M. et al. 2016, "In-situ monitoring of moisture ingress in PV modules using digital humidity sensors". IEEE Journal of Photovoltaics; Vol. 6(ed. 5), pp. 1152–1159.

[61] Gabor, A. et al. 2016, "Mechanical load testing of solar panels -beyond certification testing". Presented at the 43rd IEEE Photovoltaic Specialists Conference

[62] Borgers, T. et al. 2015, "Adapting conventional tabbing-stringing technology for back-contact solar cells and modules". Photovoltaics International; Vol.26(7), pp 90-94.

About the Authors

Jan Kroon studied chemistry at the University of Amsterdam and received his PhD degree in the field of physical organic chemistry in 1992. He worked as postdoctoral fellow on organic solar cells at the Wageningen University. He joined ECN Solar Energy in 1996 where he worked as project and programme manager of organic based PV technologies until June 2013. Since then, he has been active as senior project manager in the ECN PV module technology group and is currently programme coordinator back contact crystalline Si cells and modules. He is an experienced coordinator and manager of several national and international (European) projects.

Dr. Bonna Newman is a programme coordinator for PV applications and systems at ECN part of TNO. After receiving her PhD in 2008 in experimental physics at MIT, she was awarded the MIT Energy Initiative Postodoctoral Fellowship for research in materials for PV efficiency improvements. She worked in San Jose, CA, for multiple c-Si PV companies on new options for light management on c-Si cells and non-standard substrates. In 2013, she was a postodoc at the FOM Institute AMOLF, in Amsterdam, investigating the use of nanostructures in industrial scale PV. Since joining ECN part of TNO in 2014 she has moved downstream, optimizing light trapping structures for modules and working to reimagine how PV can be integrated into everyday life.

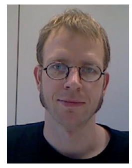

Jonathan Govaerts received his PhD in 2009 from Ghent University, Belgium, with a thesis topic of packaging and interconnection technology for (flexible) electronics. Since then Jonathan has been active in Si PV at imec on module integration of silicon solar cells. His interests relate to both cells and modules in topics across the full range from fabrication, characterization and simulation to reliability, application and dissemination. Throughout the years, sample size, lab space, number of colleagues and amount of work have steadily grown culminating in the recent move from Leuven and integration in the Energyville activities in the Thorpark in Waterschei (Genk).

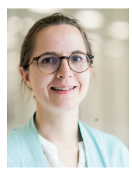

Dr. Eszter Voroshazi is group leader of the PV system activities at imec on the EnergyVille campus. This research group focuses on innovative PV module and power electronic technologies and energy yield simulations for integrated PV systems. She received her engineer title from INSA de Rennes (2008) and PhD from KU Leuven (2012). She has in-depth expertise in PV module fabrication and reliability of TFPV and SiPV modules. She is involved in the coordination or national and EU projects, and serves as expert in PV standardization committees.

Tom Borgers joined imec in 2000, working on III-V detector technologies and developing a flip-chip approach for megapixel infrared sensors. He switched to the field of photovoltaics in 2008, when he began working for Photovoltech. His interests lie in back-contact solar cell concepts, specifically the development of module technology. In 2012 Tom joined imec's reliability and modelling group, and currently works in the Si PV group, focusing on module interconnection technology.

Enquiries

ECN part of TNO: jan.kroon@tno.nl
imec: jonathan.govaerts@imec.be

State-of-the-art bifacial module technology

Hartmut Nussbaumer[1], Markus Klenk[1], Andreas Halm[2] & Andreas Schneider[3]
[1]Zurich University of Applied Sciences (ZHAW), SoE, Institute of Energy Systems and Fluid Engineering, Winterthur, Switzerland; [2]ISC Konstanz e.V., Konstanz, Germany; [3]University of Applied Sciences, Gelsenkirchen, Germany

Abstract

Bifacial PV promises a significant reduction in the levelized cost of electricity (LCOE) for PV systems, which, compared with efficiency improvements at the cell level, is still achievable with comparatively moderate effort. Almost all major PV module suppliers have bifacial modules in their product portfolios or have announced production. This paper gives an overview of the currently available bifacial modules and cell technologies and the performance of these modules. Special attention is given to the cells and the layout of the modules, including light trapping and interconnection technologies, the encapsulation materials and the adapted mounting solutions. Finally, an outlook is given on the basis of the compiled information.

Introduction

Bifacial solar cells go as far back as the 60s [1–3] and were first used in satellites [4–6] and for niche applications, such as sound barriers [7], and for shading elements [8]. The production volume remained low at the semi-industrial fabrication level [4,9], but has increased with the introduction of the Sanyo HIT Double and later the Panda [10] and EarthOn [11] modules from Yingli and PVGS. Since about 2012, interest in bifacial PV has been constantly increasing, which is reflected by the installed capacity [12], the number of available products [13] and the number of publications. As a result of technical progress, such as improved bifacial cell concepts and the availability of thin solar glass, this technology has become increasingly attractive. Furthermore, some of the new solar cell technologies, which are currently being implemented in industrial production, allow a comparatively simple adaptation to a bifacial layout. The general trend towards glass/glass modules with superior reliability, as well as the interest in 'peak shaving' and customized solutions for specific applications, further supports the development path towards bifacial technology.

In spite of the advantages, the installed capacity of bifacial systems is still small compared with monofacial mainstream systems. A major issue is the uncertainty regarding the additional 'bifacial' yield, which is due to the more complicated irradiation conditions and the power rating of bifacial modules.

It is still common to regard bifaciality as an add-on and to base the power rating/pricing on the front-side measurement under standard test conditions (STC). The effect of this is that embedding bifacial solar cells in a monofacial module structure with a reflective backsheet may allow a higher price on the market than if they were embedded in a real bifacial module version [14,15]. This is also a reasonable procedure if the cell type used is bifacial, but the modules are mounted in locations with unattractive albedos, such as shingled roofs. Panasonic offers specific modules [16] to exploit the advantages of their bifacial HIT cell technology in 'non-bifacial' modules.

While it is comparatively simple to define standardized indoor measurement conditions for a monofacial module, the measurement of a bifacial module must also include the power generated by the rear side. Standardized measurement conditions for bifacial modules are still under discussion but close to finalization [17,18].

Even if a standardized indoor measurement procedure for bifacial modules is defined, the actual yield of a bifacial PV field will always be extremely dependent on the installation conditions. For free-standing bifacial modules, the optimum orientation is a trade-off between the front- and rear-side outputs, and the efficiency is dependent on factors such as the ground reflectance, tilt angle and installation height. In extended arrays, additional factors, such as direct shading and reduced ground albedo due to adjacent rows, have to be considered. Because of the sensitivity to multiple additional factors, compared with monofacial standard installations, an accurate prediction of the yield of a bifacial PV array is, by far, more complicated. At present there are still only limited simulation tools available for bifacial arrays; however, the number of software suppliers is increasing [19–21], and there is considerable effort being devoted to improving the models and to appraising the prediction reliability [22,23].

While the improvements with regard to the simulation and measurement are important, the increasing installed capacity [12] will in itself promote the future growth of this technology. The estimates concerning the bifacial market share for the coming years vary but are most promising (Fig.

"It is still common to regard bifaciality as an add-on and to base the power rating/pricing on the front-side measurement under STC."

Figure 1. A bifacial 400kWp system from Tempress with an east–west orientation [26], which is indicative of the expected significant rise in the market share of bifacial PV: (a) view from above, and (b) view of the rear of the bifacial modules. The white gravel results in an albedo of 40%. (Source: Tempress, Amtech Group.)

1); indeed, starting from today's 3% bifacial market share the ITRPV roadmap 2017 predicts an increase to around 30% by 2027 [24], while Bloomberg even anticipates 40% by as early as 2025 [25]. Accordingly, more and more adapted components for bifacial technology will become available. In addition, the bifacial module design, which is still very similar to the standard monofacial one, may reflect specific conditions, such as increased currents or more inhomogeneous irradiation uniformity. This paper presents a comprehensive overview of the state-of-the-art technology for bifacial PV modules and of the potential trends concerning future developments.

Solar cells

Bifacial solar cells were first proposed in the 1960s [1]. Even though cells of various types were produced on a very limited scale to cover the demand (e.g. for satellite applications [6,9]), such cells were not produced in large volumes. The industrial production of bifacial cells began in 2007 with Sanyo implementing an open Ag grid for their proprietary HIT cell technology [27]. Yingli Green Energy was the first company to launch an n-PERT (passivated emitter, rear totally diffused) cell [28] in 2010; this was followed about four years later by announcements of the industrial production of bifacial p-PERC (passivated emitter and rear cell) cells and modules [29,30] by companies such as SolarWorld and NSP/ET Solar. Since then the interest in bifacial systems has been on the increase, with reports of many different technical solutions; these differ in detail but can be assigned to a limited number of technologies, which will be discussed below (HJT, PERC, PERT, IBC). More detailed comparative information concerning the technologies can be found elsewhere in the literature [2,31–33]. The technologies in question are predominantly linked to a preferred type of wafer doping: PERC is mostly related to p-type wafers, while heterojunction technology (HJT) and the PERT concept are typically linked to n-type wafer material.

Cells based on HJT were the first commercially produced bifacial solar cells. On the front and rear sides of such cells, a material other than c-Si (amorphous silicon) is deposited in order to passivate the surface and to form a second p-n junction. After Sanyo's patent on this technology expired in 2010, several module manufacturers and equipment suppliers offered comparable products based on HJT, with some differences in the processes, often using their own naming conventions, such as HCT technology from Sunpreme [34].

Today, among other companies, Panasonic, Hevel [35], 3Sun [36], Hanergy and Jinergy [37] are producing, or ramping up their production of, silicon heterojunction cells. Manufacturers, institutes (such as CSEM [38] and CEA INES [39]) and equipment providers (such as Meyer Burger [40]) are constantly working on improvements to increase efficiency and obtain more cost-effective processes. HJT cells achieve superior efficiencies of up to 23.4% on a pilot scale [39], with high bifaciality (> 0.95) as well. While the technology is attractive in many regards, cell fabrication is very different from that of homojunction c-Si cells. Existing cell manufacturers cannot therefore simply adapt the technology in an evolutionary process, like an upgrade. Nevertheless, some companies, such as Jinergy, which are already producing PERC cells have also announced the fabrication of HJT cells [37]. It is also an option for some companies to start up production, such as Sunpreme [34,41], and in particular it offers opportunities for companies which have a background in thin-film deposition, such as Hanergy [42] and 3Sun [36].

In contrast to HJT technology, the well-known

PERC concept has been (or currently is being) implemented by many mainstream p-type c-Si cell producers (p-PERC) in terms of an upgrade. Basically, the former standard Al-BSF (back surface field) type of cell is changed in such a way that the full-area rear-side aluminium layer is replaced by a passivating layer and the rear-side metallization process is correspondingly adapted. To obtain a bifacial PERC cell, which is often termed *PERC+* [43], the rear-side metallization is realized by a grid, as on the front side. SolarWorld started to produce bifacial modules in 2015 [44]. Today, the PERC+ concept is mainly implemented by Chinese and Taiwanese tier one manufacturers, such as Longi [45,46], Trina [47,48], JA Solar [49,50], NSP [51,52], EGing [53] and Jinko [54]. Because of degradation issues on multicrystalline (mc) material [55], however, all the above-mentioned PERC+ concepts are realized on p-type Cz wafers. At the PV Cell Tech conference, Canadian Solar announced it was switching all its P4 mc PERC cell production to PERC+ in 2018 [47].

A disadvantage of bifacial PERC is the comparatively low bifaciality, although Longi recently announced a significant improvement [46], with a bifaciality factor of 0.82% (at the R&D level) and reports of front efficiencies of 21.2% and higher in production. Because of the large PERC production capacity installed worldwide, the growing interest in bifacial technology, and the comparatively easy implementation of PERC+ in an existing PERC line, it is not surprising that bifacial PERC modules are increasingly becoming available.

A higher bifaciality factor is made possible by PERT technology [4], which is in principle quite similar to PERC technology. The 'T' in PERT stands for 'totally diffused' and indicates that the doping and passivation layers on both sides of the wafers are applied by diffusion. PERT is suitable for p- and n-type wafers (p-PERT; n-PERT) and also applicable to mc wafer material, as demonstrated by RCT Solutions and Shanxi Lu'An [56]. The technology has the potential for higher efficiencies than those possible with PERC, but is more complex and based on more expensive components (boron deposition, n-type wafers, silver paste consumption, etc.). In the case of p-type wafers, the rear side is exposed to boron diffusion instead of the deposition of an aluminium oxide layer in the PERC process. It should be pointed out that p-PERT has a very low market share. It has to be mentioned, though, that p-PERT was already used in the first bifacial cells for the Russian space programme; additionally, PERT is also still subject to recent research [4]. Examples of technology providers for p-PERT are RCT Solutions [57] and Schmid [58].

"A disadvantage of bifacial PERC is the comparatively low bifaciality."

The implementation of n-PERT technology is more common than p-PERT, with PERT being the standard technology on n-type wafers. Since both n-type and bifacial technology have increasingly attracted interest in the PV community, it is not surprising that numerous bifacial n-PERT processes and module types are on offer today [32], aiming at cost-effective solutions. A description of all the different processes would be beyond the scope of this paper, but suffice it to say that the aim of several processes is to introduce simplifications in order to make them more cost-effective.

All of the major suppliers of diffusion furnaces – centrotherm, Tempress, Schmid and others – offer process technology and adapted equipment. Some processes also use quite different process equipment: the diffusion process, for example, can be replaced by ion implantation [32] (Yingli [59], Jolywood [60]).

Bifacial n-PERT modules are offered, for instance, by Yingli [61–63], Jolywood [60,64], LG [65,66], Prism Solar [67], HT-SAAE [68], Linyang [69], Trina [70], Adani [71], REC [72], Jinko [73,74] and Valoe [75], with some of those mentioned being in the launch phase.

Table 1. Bifacial solar cells, main parameters and manufacturers (some products in the launch phase).

Cell concept	Bifaciality factor	Si base material	Junction and BSF doping method	Contacts	(Front) Efficiency potential	Industry
Heterojunction	>0.95	n-mono	a-Si:H p- and n-type doped	TCO / Ag TCO / Cu plated	22–25%	3Sun, Hanergy, Hevel, Jinergy, Panasonic, Sunpreme, etc.
PERT	>0.90	n-mono p-mono p-multi	B and P tube diffusion n-doped poly-Si rear side possible	Ag and Ag/ Al printed	21–23%	Adani, Jinko, Jolywood, LG, Linyang, REC, Trina, Yingli, etc.
PERC+	>70%	p-mono p- multi n-mono	B and P tube diffusion, local Al BSF	Ag and Al printed	21–23%	Eging, JA Solar, Jinko, Longi, NSP, SolarWorld, Trina, etc.
IBC	>70%	n-mono	B and P tube diffusion APCVD doped oxides	Ag and Ag/ Al printed	22–25%	Valoe

The highest lab efficiency reported so far is 22.8%, achieved by imec [38] and featuring a bifacial factor of 97% [39]. In future, the introduction of passivated contacts [60] with high-temperature firing through metallization might increase the efficiency level of industrial n-type-based solar cells to a value of 23% or higher [76].

Bifacial IBC cells are another promising option to obtain high-efficiency solar cells. 'IBC' stands for *interdigitated back contact*, which means that the contacts are solely on the rear side of the solar cell; this approach requires other fabrication procedures, while the core process equipment of n-PERT may also be used for IBC [77]. Bifacial IBC is still in its infancy, but corresponding modules have already been fabricated [78] and are even on the verge of entering industrial production [75].

Table 1 lists the most common bifacial cell architectures, including the main technological features.

Cell interconnection

The key requirement for interconnecting bifacial solar cells in terms of an optimized power output is the application of a module interconnection technique with the lowest ohmic losses. This is essential because bifacial modules experience far higher current generation because of the rear-side contribution which is added directly to the front generation. The above requirement becomes even more important in locations with increased albedo, for cells with higher bifaciality factor or for larger output currents in general (e.g. tracked modules). While most commercial PV modules based on commercially available bifacial solar cells currently utilize all the same 'standard' soldering interconnection technology, alternative technologies exist with greater benefits in terms of quality and reduced ohmic losses. Nowadays, the interconnection standard still relies mainly on an H-pattern metal grid on the front and rear sides of the cells, as applied to the very first cells decades ago. So-called *conductive fingers* collect the silicon-bulk-generated photocurrent and transfer the current to busbars (BBs), thereby creating the H pattern of the metallization. Coated (usually containing Sn and Pb) Cu ribbons are soldered to the busbars; this way a serial interconnection between the front of one solar cell and the rear of the adjacent cell is formed and so on, typically creating a string of up to 10 or 12 series-connected cells. Soldering is a mainstream interconnection technique in electronics but not necessarily the favoured process for novel high-efficiency solar cells. The applied temperature of up to 250°C jeopardizes the cells' mechanical integrity and is not suitable for all metallization schemes and materials. In addition, the resistive losses in the cell–cell interconnections usually dominate all other resistive losses in a solar panel compared with a bare solar cell.

> "The key requirement for interconnecting bifacial solar cells in terms of an optimized power output is the application of a module interconnection technique with the lowest ohmic losses."

Solar module concepts are rare and only a few have been developed over the last 12 years to specifically pass the required IEC and UL certification standards to enter the mass-production process. Several hurdles have to be overcome for any new technology in order to finally prove its superiority over soldering, which is such a simple technology that has remained virtually unchanged over the years. The easiest way to reduce ohmic losses is to instead make modifications at the cell level, specifically by increasing the number of busbars. For more than 10 years, the standard number of busbars has been three, but there are now solar cells available with four, five or six busbars. By adding more busbars, the effective transfer length for charge carriers in the emitter is significantly reduced, with the additional benefit of redundancy in case of cracks or similar flaws. The interconnection still typically relies on soldering but causes less damage to the mechanical integrity because of the much-reduced ribbon thickness. Beside this, the modifications required for mass-production equipment, such as stringers and cell flashers, are relatively minor. Ohmic losses are reduced for each busbar added, but the positive effect in terms of series resistance reduction gradually gets smaller and smaller. An optimum is typically reached somewhere between five and six busbars in terms of technological, process and financial aspects, also for bifacial cells, with 10–30% higher output current. A logical continuation of this approach would be to further reduce the diameter of the ribbon, now referred to as *connecting wire*, as the number of wires increases significantly, to far more than 10. Two mass-production techniques based on this principle are the multi-busbar technique from Schmid [79], employing typically 12 wires with a core diameter of 360μm, and the Day4Energy [80] interconnection scheme, in which 36 wires of 150μm diameter are used. The latter method was purchased and further developed by Meyer Burger and is now called *SmartWire Technology* [81]. Both technologies allow the omission of cell busbars completely, thereby significantly reducing the number of cell metallizations, emitter recombination and direct light shading. Because of the very small nature of the series resistance in both technologies, the merits for interconnecting bifacial cells are evident. In addition, because of the unique solder coating in the Day4Energy concept, the cell aluminium layer can be contacted directly, paving the way for interconnecting cells with modified metallization layouts and materials.

Cell concept	5BB	5BB HC	Conductive BS	Multi-busbar	Day4Energy / SmartWire	NICE	Shingled
PERC, PERT	+	++	In comb. with MWT	++	++	Combined with 5BB /HC ++	++
HJT	o	o	In comb. with MWT or IBC	o	++	++	++
IBC (Zebra, Mercury,...)	(√)	(√)	++ (bifacial?)	(√)	(√)	(√)	-

o = suitable, + good fit, ++ special advantages, (√) suitable, but adaptations necessary (isolating layers...)

Table 2. Ratings of interconnection technologies suited to bifacial modules.

Ohmic losses can be attributed to two sources: the series resistance, as established by the above-mentioned three technologies, and the cell current. Reduction of the latter is addressed by a module concept based on half cells [82] or by the so-called *shingling technology* [83]. Both of these concepts are very well suited to interconnecting bifacial solar cells: the standard soldering technique is used for half cells, whereas typically electrically conductive adhesive (ECA) or solder paste is applied for shingling. Half cells require only minor modifications to the cell and module process; however, shingling technology can really be regarded as a different (though not necessarily novel) approach, which is based on a different module process with significant modifications at the cell level. Although the origin of the shingling approach goes back decades, it had never been used in mass production until just recently, when its implementation was driven mainly by the need to interconnect cells with the highest output currents and the lowest ohmic losses. In fact, fill factor values at the module level exceeding 80% can be achieved, demonstrating the benefits of shingling technology [84]. Besides this, the necessity of applying an ECA also allows cell interconnection concepts which are not suitable for soldering, for example because they cannot withstand the high soldering temperatures. Currently, bifacial modules with shingled cells are also being tested at the R&D level [84,85], and the first bifacial products have even already been launched [45]. The use of conductive adhesives in combination with a structured ribbon for HJT cells was announced by Teamtechnik [86].

A technology for simplifying the interconnection and for reducing the mechanical load at the cell edges is the *flip-flop* design of bifacial solar cells [87], in which the p and n sides are respectively alternated for adjacent cells in a string. This is only possible with reasonable mismatch losses if the cells with p and n sides have a very similar power rating, which means a high bifaciality factor.

An alternative solar cell interconnection approach is the *conductive backsheet* method, invented by Eurotron and ECN [88]; this concept is based on a PCB (printed circuit board) design, typically used in electronics. All the contacts are formed inside the copper layer, which itself is integrated into the backsheet; the solar cells are interconnected on the conductive backsheet layer by either ECAs or soldering pastes. The conductive backsheet technology overcomes cell bowing issues and is therefore a perfect match for interconnecting rear-contact solar cells. The electrical polarities of the solar cell are separated by isolating trenches which form continuous circuit tracks to establish the current transport. Usually this technology results in monofacial modules; however, if a large part of the conductive backsheet layer is removed, thereby creating conductive circuit tracks with a well-defined aspect ratio, a ribbon-like interconnection can be created, allowing bifacial operation.

Finally, the NICE module concept from Apollon [89] can be mentioned as one technology that is very well suited to the interconnection of bifacial solar cells for several technological reasons. Cell interconnection is based on a pressure contact rather than soldering, allowing the use of a greater amount of ribbon to interconnect the solar cells without the detrimental effects of the soldering process. Furthermore, NICE technology is by nature a glass/glass technology, which makes it perfectly suited to bifacial application. Table 2 shows a rating for the discussed module technologies, and indicates how well the specific module technology is matched with the various bifacial solar cell types available on the market.

The light-trapping properties of the cell interconnection are discussed in a later section dedicated to optical confinement and light management.

Encapsulants

A state-of-the-art solar module contains various components, all designed and developed with specific functions for increasing longevity and for optimizing the potential to harness sunlight and convert it into electricity. The key to longevity of solar modules is the selection of the right material, which is indeed even more important for bifacial products. One of the key materials is the

"With all its advantages for bifacial solar modules, glass is currently the best choice for the front- and rear-side superstrates."

encapsulation film, which protects the solar cell and guarantees reliability and performance by protecting it against water vapour and aggressive chemical substances, as well as partly against mechanical shock and other disturbances. Its role is to provide the highest possible optical transmissivity, hinder moisture from entering the module interior, deliver a very high and durable adhesion to the adjacent materials, and guarantee a capacity to withstand high voltage.

The material of choice for many decades has been ethylene vinyl acetate (EVA), which now comes with a long track record of almost 40 years in terms of field experience and successive developments. Even today, EVA is still the most commonly used solar module encapsulation material, and dozens of experienced suppliers exist worldwide. On the negative side, three disadvantages can be listed for EVA: 1) the relatively high UV cut-off wavelength; 2) the high moisture vapour transmission rate; and 3) the materials added to improve EVA's crosslinking and adhesion properties, which generate free radicals (such as acetic acid), contributing to physical deterioration and degradation of the material properties [90]. Typical field failures here can be corrosion, yellowing or discoloration.

With all its advantages for bifacial solar modules, glass is currently the best choice for the front- and rear-side superstrates [91]. No other material delivers the same mechanical stability, transmission rate and water transmission rate of practically zero. The last of these properties also means that free radicals stemming from the encapsulation material are trapped inside the module interior, and can only be released in the limited regions of the module edges [92]. Acetic acid – in combination with photons of higher energy (meaning those in the lower visible light spectrum), heat and the time factor – acts in a deteriorative way on the module materials and can significantly reduce the module lifetime. This is particularly true for bifacial modules, given the higher operating temperature because of the significantly increased irradiation levels to which the materials are exposed. Alternatively, transparent backsheet materials can be combined with front glass, thus eliminating the above-mentioned risks but also resulting in a much-reduced mechanical strength compared with glass.

Decreasing the module temperature to a minimum is key to reducing the chemical reaction rate inside the encapsulation film [93]. For a typical glass/glass bifacial solar panel, the main chemical reaction is related to a degradation of the chemical stability of the encapsulation film, which will result in delamination or discoloration over time. Besides degradation, corrosion is aggravated by increased temperatures: the coated copper ribbon and the solar cell metallization can both suffer corrosion. The water ingress rate is significantly reduced in the case of glass/glass bifacial modules, and is therefore one of the promoting factors for degradation and corrosion that is taken out of the equation. As long as chemical by-products exist inside the encapsulation film, however, any degradation will inevitably occur over time. Therefore, there has been (and still is) an urgent need to develop new encapsulation materials.

Nowadays, various encapsulation materials – besides standard EVA – are available on the market: new EVA material developments with a lower UV cut-off (320nm), polyolefin (POE), thermoplastic polyurethane (TPU), polyvinyl butyral (PVB) and silicone-based products. Each of these materials has its advantages, and in all cases unfortunately also inevitable disadvantages, even if these (in some cases) are only related to the pricing. In terms of energy production, most of the various encapsulation materials with UV cut-off wavelengths of approximately 320nm will perform alike. Since the degradation effects of the encapsulation material are more pronounced and accelerated in bifacial modules, leading to an early material degeneration and hence a loss in transmissivity, the choice of the best materials is key to longevity. This means that module manufacturers must carefully evaluate the encapsulation material for overall long-term durability.

Junction box

The junction box electrically connects the embedded solar cells within the module with the outside world; it houses the bypass diodes and protects them, as well as the sensitive interconnections, from the environment. Overheating of bypass diodes or increased contact resistances of the clamped or soldered interconnections, caused (for example) by corrosion or faulty clamping, may lead to hazardous situations. Such defects pose a real threat and, as repeatedly reported, have caused considerable economic damage to manufacturers [94–96] and are a long-term burden [97,98]. The junction box is therefore a crucial part of the module with regard to reliability and safety.

On monofacial modules, the junction box can be placed on the module rear side without causing a detrimental shading effect. Accordingly, the size of the box is not a relevant factor, allowing sufficient volume for a thorough interconnection and enabling options which permit sufficient heat transfer, such as potting. For bifacial solar modules, however, this is obviously not the case, since any shading of the light-sensitive sections on the rear side should be avoided. Because an increase in the module dimension is also undesirable, the junction box has to be reduced in size and should preferably be placed on the rim of the module. At the same time, smaller junction boxes need to handle high currents because of the extra current generated by the module rear side; moreover, the heat generated by the bypass current has to be taken into consideration.

Because of the risks described above, it is not surprising that, in spite of the considerable rear-side shading, numerous manufacturers of bifacial modules have relied, or still rely, on conventional junction box types. Another factor favouring the use of conventional junction box types is the lower cost associated with standard components.

There are, however, also junction boxes available (or in development) which are explicitly designated for use on bifacial modules by TE Connectivity [99], Stäubli/multicontact [100,101], Leoni [102], Changzhou Almaden [103] and Amphenol [104]. These junction boxes are far smaller and are placed at the edge of the laminate [100] or at the rim of the laminate rear surface [102–104]; some are appropriate for both placements [99]. Typically, these boxes also address the market of glass/glass modules in general, which is not limited to bifacial devices, because a low visibility of the junction box is desirable for this module type.

Positioning the junction box at the edge of the module is an attractive option, because the laborious handling of the cross-connectors and the related opening of the rear-side cover are avoided and the non-productive glass area is minimized. On the other hand, this type of fixture may be more vulnerable to mechanical damage or to moisture ingress as a result of the more irregularly formed and smaller contact surface.

Another option for bifacial modules is the use of multiple junction boxes, which are generally smaller in size than the typical standard devices. While two of the already mentioned boxes for bifacial modules are of this type [99,103], there are numerous other examples which may also be suitable for bifacial modules, provided that the electrical parameters are within the specified range [105,106]. The decentralized design enables a simpler layout of the cross-connectors and attracts related material savings; it should also result in lower series resistance and improved heat transfer. Triple-pole junction boxes are used in several bifacial modules from, for example, Yingli [107], Ningbo [108], Trina [109], JA Solar [49], Jolywood [110] and Meyer Burger [111], among others. It must be mentioned, however, that the rear-side glass needs to have additional feedthroughs.

Multiple-pole junction boxes are also found on bifacial modules which are based on the half-cell approach and on the innovative interconnection scheme as presented by REC [112] in the form of a split module concept. In these cases, the splitting of the junction box into several units is adapted to the new layout; the same concept is also realized in similar modules incorporating monofacial solar cells. The half-cell approach is interesting for bifacial modules [62,113] because the impact of the increased additional current from the rear side is reduced. Such new module architectures with combined parallel and serial electrical layouts may also be a means of addressing inhomogeneous irradiation effects. With regard to the irradiation inhomogeneity, the use of integrated optimizers is also of interest for bifacial applications and has reportedly been implemented [114]. Furthermore, other developments – such as the replacement of bypass diodes by active elements [101] – may be particularly useful for bifacial modules in coping with the higher current rating of these types of module.

"For bifacial solar modules, any shading of the light-sensitive sections on the rear side should be avoided."

Optical confinement/light management

In monofacial modules, an optimized absorption of light in the cell is typically realized by using a front glass, covered with an anti-reflection coating (ARC), an encapsulant with a refractive index close to that of glass, and a highly reflective backsheet.

In the case of a bifacial module structure, the rear side needs to be transparent in order to utilize the irradiation which is usually reflected from the ground (albedo). It should be mentioned, however, that white, full-area backsheets are also used in modules with bifacial solar cells. This can be advantageous when the pricing is based on STC measurement results alone, or if the modules are intended for use in locations with low albedo. For these measurement conditions, the contribution of the bifacial module rear side due to the albedo in real installations is not taken into account. With a white, full-area backsheet, light passing through the bifacial cells or the spacing between the cells is reflected by the backsheet, and also utilized to a certain extent [14,15,115]. The specific gains and losses are dependent on the cell spacing, the spectral properties of the solar cell, and the reflectivity of the backsheet. Panasonic [16] offers modules which utilize this effect, and Dunmore [116] promotes a highly reflective backsheet particularly for this purpose. Related concepts are the structuring of the backsheet or the application of IR-reflecting coatings on the rear side [14]. Even though these measures are applied to transparent module structures to utilize the albedo, they also aim to use the reflected light from the rear side.

Light passing through the spaces between the cells of the module area contributes, after reflection from the ground, to the rear-side illumination only to a small extent. Several approaches have been proposed for reducing these power losses. One way that is effective is the use of white reflecting foil stripes in the areas between the cells [115,117]; this has now been rolled out as a commercial product (or it has been announced that it will be marketed), for example by SolarWorld [118] and Trina. These highly reflective stripes are advantageous compared with the transmission of light through the cell spacing and subsequent reflection on the ground described earlier, while leaving the electrically active rear side of the bifacial solar cells open.

Another approach aims at increasing the portion of collected light on the rear side by using a specially designed light-trapping foil (LTF) on the back of the module [119]. This specific light-trapping layer for bifacial modules was designed by the manufacturer DSM to fulfil two functions: 1) to enhance the back reflection of light coming from the front side towards the cells; and 2) to reduce the reflection of diffuse reflected light from the ground. The LTF has not yet been launched as a commercial product.

Other efforts to increase the light management are the use of structured ribbons or light-directing films which are positioned on top of the soldered ribbons, as offered, for example, by Ulbrich [120,121] and 3M [122]. The use of conductive adhesives in combination with a structured ribbon for HJT cells was announced by Teamtechnik [86]. In addition, multiwire approaches, such as the SWCT smart-wire technology from Meyer Burger, promote light-trapping properties [123].

Several years ago, the company Prism Solar developed an interesting module concept [124,125]. In this layout, a wide spacing between the cells results in a module area coverage by solar cells of around 50%. An optical film called *holographic planar concentrator (HPC)* is embedded between the solar cells; this layer guides the incoming light via total internal reflection at the glass–air interface to the strings of solar cells, resulting in a concentration of energy per unit area of PV material. This low-concentration design is especially suited to a bifacial module structure. Other low-concentration concepts have been proposed but have not yet been integrated into the module structure [126–130].

Modules

As with monofacial modules, a common attribute of bifacial modules is the cell technology used; often the module names do not directly refer to the underlying technology, such as n-PERT, HJT or p-PERC+, but are instead chosen by the manufacturer for their specific process. As shown in the solar cell section of this paper, there is a wide range of different technologies that allow a differentiation of cell types. Apart from the cell technology, the layout of bifacial modules is still quite homogeneous.

Aside from some products which use bifacial cells in a monofacial module with a white reflective backsheet (as offered, for example, by Panasonic [16]), the rear side of a bifacial module has to be transparent in at least in one direction. In addition, modules which partly utilize internal reflection, by covering the cell spacing with a white reflective material [115], have a transparent rear side, as implemented in some commercial modules (e.g. SolarWorld [118], Trina or Linyang). For details of both of these approaches, see also the internal reflection section of this paper.

To obtain a transparent rear side, there are two options available on the market: laminates with a transparent backsheet or a glass/glass layout. By far, most of the suppliers choose a double glass design, which promises better reliability and is also being increasingly used for monofacial modules; on the other hand, some very large bifacial manufacturers, such as LG and Jolywood (which is also a leading producer of backsheets), offer transparent backsheet modules. (Jolywood offers bifacial modules with glass/glass and glass/transparent backsheet structures [110].) Interestingly, in the authors' market screening, modules with the highest STC efficiency (Jolywood: 20% [110]) and the highest overall front power (LG: 395W [66]) were found to be those assembled using a transparent backsheet. DuPont recently announced its release of a transparent Tedlar backsheet [131], whereas manufacturers such as Krempel [132], Dunmore [116], Coveme [133] and Isovoltaic among others offer a transparent backsheet or are currently working on its development. SolarWorld changed the module layout and replaced the version with a transparent backsheet [134] by a glass/glass version [135].

The advantages and disadvantages of both layouts are widely discussed in the PV community. Glass/glass has obvious advantages concerning the mechanical stability and shielding capability of the inner components. In a symmetrical structure, the cell matrix is also located along the neutral fibre, which means that any bending of the laminate does not result in tensile or compressive stresses to the cells. On the other hand, a backsheet allows undesirable chemicals, such as acetic acid (which is a result of EVA degradation), to diffuse out of the laminate [92], as described earlier in more detail in the encapsulant section. A backsheet also promises a lower cell operating temperature, may result in a lighter module and allows a faster lamination process.

While glass/backsheet modules almost always have a circumferential frame, with glass/glass modules (dependent on glass thickness, size and the intended mechanical load resistance) frameless configurations are also standard. In the case of monofacial modules, most are currently 156mm × 156mm in size and incorporate 60 cells, but the share of 72-cell modules is increasing. The number of cells also defines the module size and is therefore often dependent on the application.

Other trends, such as half cells and shingle cells, are relevant to bifacial modules as well as to monofacial ones. With regard to half cells, the lower current is particularly interesting; because of the additional rear-side contribution, bifacial modules

> "Interestingly, in the authors' market screening, modules with the highest STC efficiency and the highest overall front power were found to be those assembled using a transparent backsheet."

have higher currents and consequently greater ohmic losses than monofacial modules. Accordingly, the highest promoted module efficiency has also been demonstrated with a half-cell module [110]. Innovative layouts for half-cell modules [72,136,137] with non-standard interconnection schemes may be advantageous for bifacial modules in other respects too, because the performance in shaded conditions could be improved.

Measures, particularly the multi-busbar approach, to reduce the series resistance affect bifacial modules even more than monofacial ones because of the higher currents. Currently, bifacial modules with shingled cells are also undergoing testing at the R&D level [84,85], and the first bifacial products have even already been launched [45].

Another trend, which is also implemented in monofacial devices, is the use of optimizers [138]; because of the more inhomogeneous irradiation conditions, the technique might even be more relevant to bifacial installations or at the bifacial module level, as implemented by Sunpreme [114].

Today, bifacial state-of-the-art modules are framed glass/glass modules with 2.5mm sheet thickness, POE encapsulation, 60 or 72 full-size n-SHJ, n-PERT or p-PERC+ five-busbar ribbon-connected cells, three separate junction boxes and an Al frame. The most common module variations are a transparent backsheet, cells with three or four busbars, half-cut cells, interconnections based on round wires (multi-busbar, SWCT or similar), single junction boxes or single module power optimizers, and a frameless structure. Efficiencies range between 17 and 20% at STC for front illumination. Not all companies state the bifacial factor of their products, nor is it yet common practice to give a quantitative statement on the bifacial energy gain under specific irradiation conditions. For double-glass modules, the thickness of the glass could be reduced to 2mm or below, from a technical point of view. There is no real cost-reduction potential, however, since a thickness reduction of hardened solar glass to under 2mm is complicated and at present only feasible using expensive techniques, such as chemical treatment. In addition, the module layout would need a redesign, with supporting structures located on the rear [139], since the mechanical stiffness of such thin laminates would not be adequate.

Table 3 is an attempt to summarize bifacial modules of different types, without claiming to be complete. It also has to be mentioned that manufacturers usually promote several types with different properties; in the list, however, typically only one product has been arbitrarily chosen as an example, except where there are striking differences, such as half-cell and full-cell versions, which are interesting for comparison. Generally, the version with the highest power output has been selected. Note also that the products are subject to change,

Table 3. A selection of bifacial modules implementing different technologies.

	STC front [W]	Eta front [%]	Cell	No. of busbars	No. of cells	Cover	Frame	Junction box	Remarks
JA	370	18.6	p-PERC	5	72 full	GG	yes	3 edge	short frame optional
Jinko	310	18.7	n-PERT	5	60 full	GG 2x2.5mm	no	edge	
Jolywood	325	19.8	n-PERT	4	60 full	GG 2x2.5mm	no	3 edge	
Jolywood	330	20	n-PERT	4	120 half	G/BS 3.2mm	yes	edge	high voltage
LG	395	18.7	n-PERT	12 round wires	72 full	G/BS 3.2mm	yes	edge	large cell size
Longi	310	18.7	p-PERC	5	60 full	GG	yes	3 edge	
Megacell	280	16.9	n-PERT	3	60	GG 2x2mm	yes	rear	~2015
Ningbo	340	17.1	n-PERT	4	72 full	GG 2x2.5mm	yes	3 edge	
NSP	310	18.5	p-PERC	5	60 full	GG 2x2.5mm	yes	3 edge	POE
Prism	295	17.7	n-PERT	3	60 full	GG 2x3.2mm	no	edge	
Panasonic	225	15.7	HJT	3	72 full	GG	yes	edge	~2014 small cell size
SolarWorld	290	17.3	p-PERC	5	60 full	GG	yes	edge	white cell spacing
Sunpreme	410	19.5	HCT (HJT)	5	150 half	GG 2x2.8mm	yes	2 edge	
Sunpreme	380	19.5	HCT (HJT)	3	72 full	GG 2x2.9mm	no	edge	Tigo optimizer
Trina	310	18.6	p-PERC	5 (12)	60 full	GG 2x2.5mm	no & yes	3 edge	POE
Yingli	295	17.8	n-PERT	5	60 full	GG 2x2.5mm	no	3 edge	
Yingli	360	17.8	n-PERT	5	144 half	GG 2x2.5mm	no	3 edge	

and the data shown may differ from information found on the manufacturers' websites.

A bifacial module which matches the typical description above is the DUOMAX Twin from Trina, as shown in Fig. 2. This is a frameless glass/glass module with 60 monocrystalline cells (5BB) and p-type PERC technology, with a bifaciality factor of greater than 70%. It is constructed with split junction boxes on the edge with three bypass diodes. The standard glass thickness is 2.5mm on both sides. The module efficiency ranges from 17.6 to 18.9% under STC conditions.

Modules with various modifications may be acquired from other manufacturers. According to Trina, their bifacial modules are also available with white reflective covering in the spaces between the cells, with an alternative glass thickness of 2mm, and also in a framed version. Trina also offers modules with 12 busbars. On the Trina website, a 72-cell DUOMAX Twin version is promoted [140].

Another non-standard feature is the use of POE instead of EVA as the encapsulant for bifacial modules.

Figure 2. The DUOMAX Twin bifacial module from Trina, featuring a frameless glass/glass configuration with 60 monocrystalline cells (5BB) and p-type PERC cell technology; the reported bifaciality factor is greater than 70%. The module incorporates split junction boxes at the edge with three bypass diodes. The standard glass thickness is 2.5mm on both sides. The module efficiency ranges from 17.6 to 18.9% under STC conditions. (Source: Trina Solar.)

Module mounts and single-axis trackers

In contrast to standard monofacial PV modules, the output performance of bifacial module installations is much more dependent on the mounting and on the condition of the ground. Four installation configurations exist, namely fixed-tilt and vertical, along with one-axis and two-axis tracking. In all cases, the rear-side irradiation reaching the bifacial cells needs to be maximized, the rear-side light has to be uniformity optimized, and the portion of rear-side shading must be prevented. All the parameters mentioned earlier have an impact on the energy yield of bifacial module plants; they therefore have to be taken into account and if relevant will need to be optimized. This also applies to the cable guiding and the junction box, which must be installed outside the active area of the cells.

Since bifacial solar modules are categorized either as *framed* (typically glass on the front and transparent backsheet foil on the rear) or as *frameless* (typically glass on the front and rear) products, depending on the mounting structure, it is essential that the right module type be carefully chosen. For framed bifacial modules, the solar cells adjacent to the frame parts (i.e. the cells located directly beside the frame) are specifically subject to excessive shading under certain light conditions (usually in the early morning and late afternoon) [141]. Consequently, frameless bifacial modules are favoured over framed ones. Nevertheless, this is only a valid assumption if the mounting structure itself is arranged in such a way as to prevent any additional shading on the rear side. In other words, the uniformity of the indirect irradiation (the diffuse and reflected portion) over the entire module rear side is a key parameter to be optimized. The rear-side light uniformity is significantly improved with increasing module height above ground, affecting the rear-side irradiance level as well [142]. SolarWorld, for example, recommends an installation height of at least 1m for their current fixed-tilt-installed bifacial products [143]. This parameter, in combination with the ground reflectivity (typically called the *ground albedo value*), defines the amount of light reaching the rear side of the bifacial solar module. These two parameters play no significant role in monofacial PV plants but require a careful pre-evaluation to be performed by the installers/planners in order to squeeze the maximum energy yield out of a bifacial installation.

Solar trackers are a highly efficient way to mount PV modules: the sun's position in the sky is tracked, which maximizes the energy yield throughout the day, and indeed throughout the year. Since the sun's position constantly changes, it is impossible to achieve optimal energy production with fixed-tilt or vertical PV installations. The use of tracking systems entails higher installation and maintenance costs than for fixed systems but ensures a higher energy output during the whole year. Single-axis trackers have only one axis of

"The output performance of bifacial module installations is much more dependent on the mounting and on the condition of the ground."

movement, allowing the installed panels to move from east to west, thereby tracking the sun as it rises, moves across the sky and finally sets. On the other hand, dual-axis trackers possess two axes of movement, allowing the tracking to also take into account the change in seasons. The major advantages of dual-axis tracking are evident during the winter months.

The yield gain for tracked PV installations finally depends on the geographic location, the type of module tracker used and the module temperature coefficients, since the module operating temperature increases with the light level and exposure time.

According to new data from GTM Research, global solar tracker shipments hit a record of 14.5GW in 2017 [144]. With the significant benefits associated with tracked solar modules, the tracker market is now also adapting to bifacial module technology. The necessary adaptations, however, mean a redesign of existing trackers. The mounting structure must not cause shading of the rear side of the module; this argument is also valid for any driving and actuator units, and the cabling needs to be arranged accordingly. With such specifically designed tracking devices, suppliers such as Arctech Solar promise energy yield gains ranging from 15 to 50%; if the tracker system using bifacial modules is installed over a water surface, the achieved increase in yield can approach 60%, compared with a fixed-tilt system utilizing monofacial modules, as reported by Big Sun Energy.

Fig. 3 shows a specifically designed single-axis tracking system for PV systems which avoids shading of the rear side of the modules.

Figure 3. Independent horizontal single-axis tracker from Arctech Solar, designed for bifacial modules [145]. The modules are fixed using aluminium elements at the module edges, overlapping with the long purlins to avoid covering the back of the bifacial modules. Junction boxes at the module edges in such a system, as shown, can be integrated without shading caused by cables. (Source: Arctech Solar.)

Outlook

At the moment, it is impossible to predict which cell technology will be superior for bifacial applications. HJT and IBC, both with more complex processes and more expensive n-type wafers, promise the highest efficiencies in bifacial systems, although HJT is superior with regard to the bifaciality factor. Bifacial IBC is the most complex but least investigated technology. The most common bifacial cell types today are n-PERT and PERC+, with n-PERT yielding a higher bifaciality and higher efficiency potential, but at a higher cost. There are a large number of n-type manufacturers, but there are also a steadily growing number of p-type PERC+ competitors.

PERC+ has the advantage that the current switch from Al-BSF as a mainstream cell technology to PERC, combined with the growing interest in bifacial and the comparatively simple implementation of the bifacial PERC+ layout, will lead to increased efforts in this direction. Considering the historical development and the focus on mainstream technology in the PV industry that has repeatedly been demonstrated, this is an impressive argument. On the basis of these observations, it may be reasonable to assume that PERC+ will increasingly dominate in the short to mid term, while the improvements in n-type processing will make this technology superior in the mid to long term.

Besides cell selection, the module layout is of great interest. While there is a lot of activity in backsheet manufacturing, there is a general trend towards glass/glass modules (also true for monofacial modules) in order to improve durability and reliability. Since glass/glass is adaptable to bifacial demands, it is also very likely that this approach will dominate in the future. Glass thicknesses below 2mm will not be standard in the mid term. If modules are available as a framed or unframed product, the choice will mostly depend on the size and the application. Some developments which are innovative today show a lot of promise concerning their application to bifacial systems. In particular, the more inhomogeneous irradiation conditions over the module area make corresponding techniques that have been developed for monofacial modules (such as innovative interconnection schemes or optimizers at the module level) even more attractive for bifacial modules. The use of innovative interconnection schemes, especially the split module type, is often linked to half cells, which, because of the lower current, are an obvious alternative for bifacial devices anyway. Ultimately, the price–performance ratio and the observed reliability will, as always, be the decisive factor for the success of all innovative approaches.

“HJT and IBC promise the highest efficiencies in bifacial systems, although HJT is superior with regard to the bifaciality factor.”

References

[1] Mori, H. 1960, "Radiation energy transducing device", U.S. Patent 3.278.811.
[2] Cuevas, A. 2005, "The early history of bifacial solar cells", *Proc. 20th EU PVSEC*, Barcelona, Spain.
[3] Romijn, I. 2016, "Bifacial modules – Review", bifi PV Workshop, Miyazaki, Japan [http://bifipv-workshop.com/index.php?id=myazaki-program].
[4] Kreinin, L. & Eisenberg, N. 2017, "P-PERT bifacial solar cell technology past and future", bifi PV Workshop, Konstanz, Germany [http://bifipv-workshop.com/index.php?id=konstanz-2017-program].
[5] Letin, V.A. et al. 2000, "Bifacial solar arrays of Russian space crafts", *Proc. 28th IEEE PVSC*, Anchorage, USA, pp. 1067–1070.
[6] Strobl, G. et al. 1985, "Bifacial space silicon solar cell", *Proc. 18th IEEE PVSC*, Las Vegas, USA, p. 454.
[7] Nordmann, T., Vontobel, T. & Clavadetscher, L. 2012, "15 years of practical experience in development and improvement of bifacial photovoltaic noise barriers along highways and railway lines in Switzerland", *Proc. 27th EUPVSEC*, Frankfurt, Germany, pp. 3843–3847.
[8] R. Hezel 2003, "Novel applications of bifacial solar cells", *Prog. Photovolt: Res. Appl.*, Vol. 11, pp. 549–556.
[9] Made in Zelenograd 2018, "Solar wind" [http://www.made-in-zelenograd.com/companies/solar-wind/#page4].
[10] Burgers, T. 2011, "19.5% efficient n-type solar cells made in production", *Proc. 26th EUPVSEC*, Hamburg, Germany.
[11] Goda, S. 2015, Talk, 11th CSPV, Hangzhou, China.
[12] Joanny, M. et al. 2017, "Bifacial systems overview", bifi PV workshop, Konstanz, Germany [http://bifipv-workshop.com/index.php?id=konstanz-2017-program].
[13] Osborne, M. 2017, "SNEC 2017: The next big solar module trend on display", *PV Tech* [https://www.pv-tech.org/editors-blog/snec-2017-the-next-big-solar-module-trend-on-display].
[14] Saw, M.H. et al. 2017, "Enhancing optical performance of bifacial PV modules", *Energy Procedia*, Vol. 124, pp. 484–494.
[15] Singh, J.P. et al. 2015, "Comparison of glass/glass and glass/backsheet PV modules using bifacial silicon solar cells", *IEEE J. Photovolt.*, Vol. 5, pp. 783–791.
[16] Panasonic 2018, "Silicon heterojunction solar cell" [https://panasonic.net/ecosolutions/solar/technology/index.html].
[17] Fakhfouri, V. 2016, "IEC 60904-1-2: Measurement of current-voltage characteristics of bifacial photovoltaic devices", bifi PV Workshop, Miyazaki, Japan [http://bifipv-workshop.com/index.php?id=myazaki-program].
[18] Zhang, X. et al. 2018, "Power rating and qualification of bifacial PV modules", *PV Tech*, Vol. 40, pp. 90–96.
[19] Wittmer, B. 2017, "PVsyst bifacial shed simulations with PVsyst", bifi PV Workshop, Konstanz, Germany [http://bifipv-workshop.com/index.php?id=konstanz-2017-program].
[20] Kutzer, M. 2016, "Ertragssteigerung durch bifaciale Modultechnologie", 31. OTTI Symposium Photovoltaische Solarenergie, Kloster Banz, Germany.
[21] Zhao, X.S. & Khan, M.R. 2018, "Purdue University bifacial module calculator (PUB)" [https://nanohub.org/resources/pub].
[22] "PV performance modeling collaborative – Bifacial PV performance models" [https://pvpmc.sandia.gov/pv-research/bifacial-pv-project/bifacial-pv-performance-models/].
[23] Van Aken, B. 2016, "Bifacial modelling – Review", bifi PV workshop, Miyazaki, Japan [http://bifipv-workshop.com/index.php?id=myazaki-program].
[24] ITRPV 2018, "International technology roadmap for photovoltaic (ITRPV): 2017 results", 9th edn (Mar.) [http://www.itrpv.net/Reports/Downloads/].
[25] Martin, C. 2018, "Double-sided solar panels are taking off in China – Bloomberg" [https://www.bloomberg.com/news/articles/2018-05-17/watch-out-for-double-sided-solar-panels-taking-off-in-china].
[26] Vermeulen, W. 2017, "400kW bifacial system in NL and comparison with two other systems", bifi PV Workshop, Konstanz, Germany [http://bifipv-workshop.com/index.php?id=konstanz-2017-program].
[27] Sanyo 2010, "HIT Double 190", Data Sheet [http://www.panasonic.com/business/pesna/includes/pdf/eco-construction-solution/HIT_Double_190_Datasheet.pdf].
[28] Yingli Green Energy 2010, "Yingli green energy unveils high-efficiency monocrystalline Panda module at Intersolar trade shows", Press Release [http://ir.yinglisolar.com/phoenix.zhtml?c=213018&p=irol-newsArticle&ID=1435603].
[29] Asbeck 2014, "Asbeck versucht Neustart: Ex-Sonnenkönig kündigt neue Modultechnik an", *Handelsblatt* [http://www.genios.de/presse-archiv/artikel/HB/20141215/ asbeck-versucht-neustart/6E27CF9D-B436-48EF-9CEA-EFC3080CD8F5.html].
[30] prnnewswire 2014, "ET Solar to launch double glass bifacial module at pv expo 2014", News Release [https://www.prnewswire.com/news-releases/et-solar-to-launch-double-glass-bifacial-module-at-pv-expo-2014-247053621.html].
[31] Chunduri, S.K. & Schmela, M. 2017, "Taiyang news – About solar power", *Taiyang News – Sol. Power,* Vol. Bifacial Solar Module Technology 2017 Edition.
[32] Veschetti, Y. 2017, "Review on bifacial cells", bifi PV workshop, Miyazaki, Japan [http://bifipv-workshop.com/index.php?id=myazaki-program].
[33] Romijn, I. 2017, "Bifacial solar cells – A brief overview", bifi PV workshop, Konstanz, Germany [http://bifipv-workshop.com/index.php?id=konstanz-2017-program].
[34] Sinha, A. 2016, "Technology behind the world's largest bifacial PV power plant", bifi PV workshop, Miyazaki, Japan [http://bifipv-workshop.com/index.php?id=myazaki-program].

[35] Zaripova, A. 2016, "Russia: Hevel develops high-efficiency HJT modules", *pv magazine* [https://www.pv-magazine.com/2016/08/10/russia-hevel-develops-high-efficiency-hjt-modules_100025725/].
[36] Osborne, M. 2018, "3sun outlines transition to heterojunction bifacial module production", *PV Tech* [https://www.pv-tech.org/news/3sun-outlines-transition-to-heterojunction-bifacial-module-production].
[37] Presseportal 2018, "Jinergy gibt Fortschritte bei der Serienproduktion von PERC- und HJT-Solarmodulen bekannt – Medienmitteilung jinneng clean energy technology ltd." [https://www.presseportal.ch/de/pm/100064834/100816110].
[38] Bundesamt für Energie BFE 2014, "Eine Testfabrik für HJT-Solarzellen".
[39] Meyer Burger & CEA-INES 2018, "Record 410 watt module with heterojunction solar cell technology", Press Release (May) [http://e1.marco.ch/publish/meyerburger/10_7752/Press_Release.pdf].
[40] Clover, I. 2017, "Simple, powerful, demonstrable: Meyer Burger on why HJT is poised for the mainstream", *Pv Mag.* [https://www.pv-magazine.com/2017/12/13/simple-powerful-demonstrable-why-hjt-is-poised-for-the-mainstream/].
[41] Sunpreme 2015, "Sunpreme launches the world's first bi-facial smart module incorporating integrated Tigo optimizers in partnership with JDS Power thereby achieving 10% higher system energy output and up to 30% longer strings – Sunpreme" [http://sunpreme.com/2015/09/10/httpwww-prnewswire-comnews-releasessunpreme-launches-the-worlds-first-bi-facial-smart-module-incorporating-integrated-tigo-optimizers-300141113-htmltceml_cleartime/].
[42] Hanergy Thin Film Power Group Limited, "Technology roadmap", [http://en.hanergythin-filmpower.com/index.php?m=content&c=index-&a=lists&catid=27&id=7#slide=1].
[43] Dullweber, T. et al. 2016, "PERC+: Industrial PERC solar cells with rear Al grid enabling bifaciality and reduced Al paste consumption", *Prog. Photovolt: Res. Appl.,* Vol. 24, pp. 1487–1498.
[44] Colthorpe, A. 2015, "SolarWorld launches 72-cell bifacial PV module" [https://www.pv-tech.org/news/solarworld_launches_72_cell_bifacial_pv_module].
[45] Osborne, M. 2018, "Longi Solar's p-type mono bifacial shingled cell module sets 20.66% efficiency record" [https://www.pv-tech.org/news/longi-solars-p-type-mono-bifacial-shingled-cell-module-sets-20.66-efficienc].
[46] Osborne, M. 2017, "Longi touts record bifaciality value of 82.15% for mono PERC bifacial module" [https://www.pv-tech.org/news/longi-touts-record-bifaciality-value-of-82.15-for-mono-perc-bifacial-module].
[47] Trina Solar 2017, "Trina solar launches bifacial PERC module 'DUOMAX Twin'" [http://www.trinasolar.com/en-uk/resources/newsroom/mon-05012017-1500].
[48] Osborne, M. 2017, "Trina solar launches 60-cell mono-PERC 'DUOMAX Twin' bifacial 300w module" [https://www.pv-tech.org/products/trina-solar-launches-60-cell-mono-perc-duomax-twin-bifacial-300w-module].
[49] JA Solar 2018, "72-cell bifacial mono PERC double glass module – Bifacial mono perc double glass module" [http://www.jasolar.com/index.php?m=content&c=index&a=show&catid=82&id=2].
[50] Shan, W. 2018, "Innovative double-glass bifacial PERC modules by JA Solar yield cost-effectively for pv systems" [https://www.pv-tech.org/guest-blog/innovative-double-glass-bifacial-perc-modules-by-ja-solar-yield-cost-effect].
[51] Osborne, M. 2018, "Neo solar power's mono PERC bifacial modules selected for 100mw pv plant in Taiwan" [https://www.pv-tech.org/news/neo-solar-powers-mono-perc-bifacial-modules-selected-for-100mw-pv-plant-in].
[52] NSP 2017, "NSP solar module" [https://www.nsp.com/nspsolarmodules?lang=en].
[53] Sraisth 2017, "Only perc", *Pv Mag. Int.* [https://www.pv-magazine.com/magazine-archive/only-perc/].
[54] Zheng, P. et al. 2018, "Bifacial solar products light new pathway to future pv", *Photovolt. Int.,* 39th Edn.
[55] Fuhs, M. 2015, "Schmid: Pert statt Perc", *pv magazine* [https://www.pv-magazine.de/2015/03/16/schmid-pert-statt-perc/].
[56] Teppe, A. et al. 2015, "Progress in the industrial evaluation of the mc-Si PERCT technology based on boron diffusion", *Energy Procedia,* Vol. 77, pp. 208–214.
[57] "Technology – RCT – the technology company" [http://www.rct-solutions.com//technology-10.html].
[58] "PERT – Schmid Group" [https://schmid-group.com/business-units/photovoltaics/zelle/zelltechnologien/pert/].
[59] Osborne, M. 2014, "Spi 2014: Yingli Green includes mwt and ion implant to 'panda' technology roadmap" [https://www.pv-tech.org/news/spi_2014_yingli_green_includes_mwt_and_ion_implant_to_panda_technology_road].
[60] Yong, L. 2017, "Jolywood npert technology and its application", Presented at the Bifacial PV workshop, Konstanz, Germany [http://bifipv-workshop.com/fileadmin/layout/images/Konstanz-2017/3__Liuyong_JOLYWOOD_nPERT_technology_and_its_application.pdf].
[61] "Panda bifacial 60cf – Yingli Solar" [http://www.yinglisolar.com/en/products/monocrystalline/panda-bifacial-60cf/].
[62] "Panda bifacial 144hcl – Yingli Solar" [http://www.yinglisolar.com/en/products/monocrystalline/panda-bifacial-144hcl/].
[63] Nee, J. 2017, "Process and outlook of industrial n-type bifacial PV module", Presented at the SNEC.
[64] Osborne, M. 2018, "Jolywood taps imec to support development of n-type bifacial solar cells", *PV Tech* [https://www.pv-tech.org/news/jolywood-taps-imec-to-support-development-of-n-type-

bifacial-solar-cells].
[65] "LG: steigert Spitzenleistung des Neon 2 bifacial auf 390 Watt (ee-news.ch)" [https://www.ee-news.ch/de/article/38304/lg-steigert-spitzenleistung-des-neon-2-bifacial-auf-390-watt].
[66] "Neon 2 bifacial – LG Deutschland business" [https://www.lg.com/de/business/solar-panel/neon/lg-neon-2-bifacial].
[67] "Our products — Prism Solar" [https://www.prismsolar.com/s/bi60specs.pdf].
[68] Osborne, M. 2017, "Ht-SAAE launches second-generation n-type pert bifacial module", *PV Tech* [https://www.pv-tech.org/products/ht-saae-launches-second-generation-n-type-pert-bifacial-module].
[69] 2017, "Interview – Linyang", *Taiyang News – Sol. Power,* Vol. 2017 Edition Bifacial Solar Module Technology, pp. 29–30.
[70] "Trina solar: the first TrinaPro project with 250mW is on the way – Trina Solar" [https://www.trinasolar.com/en-uk/resources/newsroom/uktrina-solar-first-trinapro-project-250mw-way].
[71] "Adani: Dual glass bifacial 60 cells" [http://www.adanisolar.com/products/60-cell-modules-dual-glass-bifacial].
[72] Hsu, A. 2016, "315W 60-cell bifacial module using n-type mono cells with 21.5% efficiency manufactured on production scale equipment", Presented at the bifi PV workshop, Miyazaki, Japan,
[73] "Jinko Solar – Your best supplier of modules, cells & wafers" [https://www.jinkosolar.com/press_detail_1669.html].
[74] "Eagle bifacial solar modules – building your trust in solar" [https://www.jinkosolar.eu/en/solar-modules/bifacial.html].
[75] Osborne, M. 2018, "ISC Konstanz signs n-type bifacial and IBC cell technology transfer to Valoe for commercialisation", *PV Tech* [https://www.pv-tech.org/news/isc-konstanz-signs-n-type-bifacial-and-ibc-cell-technology-transfer-to-valo].
[76] 2017, "Fully screen-printed monopoly silicon solar cell technology", *PHYS.ORG* [https://phys.org/news/2017-12-fully-screen-printed-monopoly-silicon-solar.html].
[77] Mihailetchi, V.D. et al. 2015, "A comparison study of n-type PERT and IBC cell concepts with screen printed contacts", *Energy Procedia, Vol. 77*, pp. 534–539.
[78] Osborne, M. 2017, "SNEC 2017: World's first full-size IBC bifacial module to be displayed", *PV Tech* [https://www.pv-tech.org/news/snec-2017-worlds-first-full-size-ibc-bifacial-module-to-be-displayed].
[79] Braun, S., Hahn, G. & Nissler, R. 2013, "Multi-busbar solar cells and modules: high efficiencies and low silver consumption", *Energy Procedia,* Vol. 38, pp. 334 – 339.
[80] Schneider, A., Rubin, L. & Rubin, G. 2006, "Solar cell efficiency improvement by new metallization techniques – the day4 electrode concept", *Conf. Rec. 2006 IEEE 4th World Conf. Photovolt. Energy Convers.,* pp. 1095–1098.
[81] Söderström, T. 2017, "Bifacial HJT SWCT gg modules", Presented at the bifi PV workshop, Konstanz, Germany [http://bifipv-workshop.com/index.php?id=konstanz-2017-program].
[82] Joanny, M. "Module architecture optimization for bifacial applications, presented at the bifi pv workshop, Miyazaki, Japan, 2016" [http://bifipv-workshop.com/index.php?id=myazaki-program].
[83] Zhao, J. 1997, "20000 PERL silicon cells for the '1996 World Solar Challenge' solar car race", *Prog Photovolt Res Appl,* Vol. 5, pp. 269–276.
[84] Mittag, M. et al. 2017, "Cell-to-module (CTM) analysis for photovoltaic modules with shingled solar cells", *Proc. 44th IEEE PVSC*, Washington, D.C., USA
[85] Singh, J.P. 2017, "Shingled bifacial photovoltaic modules", Presented at the bifi PV workshop, Konstanz, Germany [http://bifipv-workshop.com/index.php?id=konstanz-2017-program].
[86] Hutchins, M. 2018, "Teamtechnik receives stringer order for HJT module line", *PV Mag.* [https://www.pv-magazine.com/2018/02/12/teamtechnik-receives-stringer-order-for-hjt-module-line/].
[87] Schulte-Huxel, H. et al. 2016, "Flip-flop cell interconnection enabled by an extremely high bifacial factor of screen-printed ion implanted n-PERT Si solar cells", *Proc. 32nd EU PVSEC*, pp. 407–412.
[88] Späth, M. 2008, "A novel module assembly line using back contact solar cells", *Proc. 33rd IEEE PVSC* 2008, San Diego, USA
[89] Einhaus, R. 2004, "Nice – new industrial solar cell encapsulation (NICE) technology for pv module fabrication at drastically reduced costs", *Proc. 19th EUPVSEC*, Paris, France
[90] Schneider, A. 2015, "Material developments allowing for new applications, increased long term stability and minimized cell to module power losses", *Proc. 31st EUPVSEC*, Hamburg, Germany
[91] Tang, J. 2017, "The performance of double glass photovoltaic modules under composite test conditions", *Energy Procedia,* Vol. 130, pp. 87–93.
[92] Oreski, G. 2017, "Acetic acid permeation through photovoltaic backsheets: influence of the composition on the permeation rate", *Polym. Test.*, Vol. 60, pp. 374–380.
[93] Koehl, M., Hoffman, S. & Wiesmeier, S. 2017, "Evaluation of damp-heat testing of photovoltaic modules", *Prog. Photovolt.*, Vol. 25, pp. 175–183.
[94] Osborne, M. 2013, "Fire risk fiasco as Dutch government warns over 650,000 Scheuten solar modules", *PV Tech* [https://www.pv-tech.org/news/fire_risk_fiasco_as_dutch_government_warns_about_650000_scheuten_solar_modu].
[95] Osborne, M. 2015, "Solar-Fabrik to issue junction box failure warning on risk of fires", *PV Tech* [https://www.pv-tech.org/news/solar_fabrik_to_issue_junction_box_failure_warning_on_risk_of_fires].
[96] 2017, "Anschlussdosen von Yamaichi fehlerhaft", *photovoltaik* [https://www.photovoltaik.eu/Archiv/

Heftarchiv/article-766823-110453/anschlussdosen-von-yamaichi-fehlerhaft-.html].
[97] 2010, "Zahl defekter Solarmodule weiter offen", *photovoltaik* [https://www.photovoltaik.eu/article-439909-30021/zahl-defekter-solarmodule-weiter-offen-.html].
[98] Allagas, M. 2016, "BP solar settlement" [http://www.bpsolarsettlement.com/].
[99] "Solarlok pv edge junction box for bifacial and half-cut solar panel applications – TE Connectivity" [http://www.te.com/usa-en/about-te/news-center/solarlok-pv-edge.html].
[100] Stäubli Electrical Connectors AG/Switzerland, photovoltaic main catalogue, index e, 01.2018, p. 63.
[101] Madon, F. et al. 2015, "Bifacial NICE modules from high efficiency n-type Bison solar cells", *Energy Procedia,* Vol. 77, pp. 382–385.
[102] "Betasolar® psbo-x junction box lsb-00190 / lsb-00192" [https://www.leoni-solar-windpower.com/en/products-services/junction-boxes/potted-jb/product-information/].
[103] "Changzhou Almaden co., ltd." [http://www.czamd.com/en/product/18_20.
[104] "Amphenol about us", *Triple Pole J-Box* [http://www.amphenol-solar.com/EN/Product/2/67.html].
[105] "QC junction box-171721", *QC Categ.* [http://www.qc-solar.com/product/junction-box-171721.html].
[106] "Zhejiang Zhonghuan Sunter pv technology co., ltd." [http://www.pvzh.com/e_productshow.asp?id=3224].
[107] "Panda bifacial 60cf – Yingli Solar" [http://www.yinglisolar.com/en/products/monocrystalline/panda-bifacial-60cf/].
[108] "Ningbo Nbqxsolar bifacial solar module" [http://www.nbqxsolar.com/en/productsd.php?tid=114&tids=114&pid=561].
[109] "Durable frameless dual-glass panels for ground mount installations – Trina Solar" [http://www.trinasolar.com/us/product/duomax72].
[110] "Jolywood" [http://www.solarsystems.pro/en/jolywood.html].
[111] "Product detail" [https://www.meyerburger.com/ch/de/meyer-burger/produkte-und-systeme/detail/skyslate-bifacial/].
[112] Hsu, A. 2016, "315W 60-cell bifacial module using n-type mono cells with 21.5% efficiency manufactured on production scale equipment",, Presented at the bifi PV workshop, Miyazaki, Japan.
[113] 2017, "Jolywood n-type bifacial half-cell double glass module – Jolywood Solar – product search – world smart energy week – reed exhibitions japan" [http://d.wsew.jp/en/Exhibitors/4019394/JOLYWOOD-SOLAR/Products/1284841/Jolywood-N-type-Bifacial-Half-cell-Double-Glass-Module].
[114] "Sunpreme launches the world's first bi-facial smart module incorporating integrated Tigo optimizers in partnership with JDS Power thereby achieving 10% higher system energy output and up to 30% longer strings – Sunpreme" [http://sunpreme.com/2015/09/10/httpwww-prnewswire-comnews-releasessunpreme-launches-the-worlds-first-bi-facial-smart-module-incorporating-integrated-tigo-optimizers-300141113-htmltceml_cleartime/].
[115] Mittag, M. et al. 2017, "Analysis of backsheet and rear cover reflection gains for bifacial solar cells", *Proc. 33rd EUPVSEC*, Amsterdam, Netherlands, pp. 18–22.
[116] "High voltage pv backsheet, clear pv backsheets – Dunmore" [https://www.dunmore.com/products/specialty-pv-backsheet.html].
[117] van Roosmalen, J. a. M. et al. 2016, "White bifacial modules – Improved STC performance combined with bifacial energy yield", *32nd Eur. Photovolt. Sol. Energy Conf. Exhib.,* Munich, Germany, pp. 42–47 [http://www.eupvsec-proceedings.com/proceedings?paper=38754].
[118] "SolarWorld's bisun solar module with bifacial extra yield – pv Europe – solar technology and applications" [http://www.pveurope.eu/Products/Solar-Generator/Solar-modules/Solarworld-s-Bisun-solar-module-with-bifacial-extra-yield].
[119] Mrcarica, M. 2016, "DSM materials application in bifacial modules light management", Presented at the bifi PV workshop, Miyazaki, Japan,
[120] "LCR – light capturing ribbon – grooved pv interconnect wire" [https://www.pvribbon.com/pv-ribbon-products/light-capturing-ribbon/].
[121] Muehleisen, W. et al. 2016, "Comparison of output power for solar cells with standard and structured ribbons", *EPJ Photovolt*, Vol. 7, pp. 70701.
[122] "3m solar light redirecting film (LRF) T80" [http://multimedia.3m.com/mws/media/1360537O/3m-solar-light-redirecting-film-lrf-t80-white-paper.pdf].
[123] "SmartWire connection technology – Meyer Burger" [https://www.meyerburger.com/user_upload/dashboard_news_bundle/376409e022f7d2ae6f6e29318f8055410774c7fd.pdf].
[124] Russo, J. et al. 2012, "Characterization of diffuse anisotropic illumination effects to the output of bifacial and holographic planar concentrating photovoltaic panel configurations", *Proc. 38th IEEE PVSC,* Austin, USA, pp. 1312–1317 [http://ieeexplore.ieee.org/document/6317842/].
[125] 2008, "Optics for solar energy: holographic planar concentrator increases solar-panel efficiency", *Laser Focus World* [https://www.laserfocusworld.com/articles/2008/12/optics-for-solar-energy-holographic-planar-concentrator-increases-solar-panel-efficiency.html].
[126] João, G. 2013, "Testing bifacial PV cells in symmetric and asymmetric concentrating cpc collectors", *Engineering*, Vol. 5, pp. 185–190.
[127] Moehlecke, A., Febras, F.S. & Zanesco, I. 2013, "Electrical performance analysis of pv modules with bifacial silicon solar cells and white diffuse reflector", *Sol. Energy*, Vol. 96, pp. 253–262.
[128] Ooshaksaraei, P. et al. 2013, "Characterization of a bifacial photovoltaic panel integrated with

external diffuse and semimirror type reflectors", *Int. J. Photoenergy*, Vol. 2013, pp. 1–7.
[129] Lim, Y.S. et al. 2014, "Design and evaluation of passive concentrator and reflector systems for bifacial solar panel on a highly cloudy region – a case study in Malaysia", *Renew. Energy*, Vol. 63, pp. 415–425.
[130] Poulek, V., Khudysh, A. & Libra, M. 2015, "Innovative low concentration pv systems with bifacial solar panels", *Sol. Energy*, Vol. 120, pp. 113–116.
[131] Osborne, M. 2018, "SNEC 2018: DuPont surprises with transparent backsheet for bifacial modules", *PV Tech* [https://www.pv-tech.org/news/snec-2018-dupont-surprises-with-transparent-backsheet-for-bifacial-modules].
[132] "Backsheet with fluoropolymer – Krempel GmbH" [https://www.krempel-group.com/en/solutions/solar-materials/backsheet-with-fluoropolymer-for-crystalline-modules/].
[133] "Clrpye® – pv backsheet for building integrated photovoltaics – Coveme" [http://www.coveme.com/dymat-clr-pye-backsheet-mono].
[134] "Datasheet sunmodule bisun sw 325 xl duo", *SolarWorld* [https://d3g1qce46u5dao.cloudfront.net/data_sheet/sunmodule_bisun_xl_solar_panel_325_datasheet.pdf].
[135] "Datasheets Sunmodule Bisun Protect", *SolarWorld* [https://www.solarworld.de/en/products/sunmodule-bisun-protect/].
[136] "Poly crystalline half-cut cell module – amur leopard", *RECOM* [https://www.recom-solar.com/half-cut-cell/].
[137] "Quadpower – qp60 tpg", *LinYang Renew.* [http://www.linyang.com/pv/products/module/2549/20715.html].
[138] Photovoltaik4all "Solaredge p505-5 (mc4) leistungsoptimierer", *Photovoltaik4all – Online Shop* [https://www.photovoltaik4all.de/leistungsoptimierer/solaredge-p505-5-mc4].
[139] Kreutzmann, A. 2016, "Gitter statt Rahmen", *Photon*, pp. 32.
[140] "Trina Solar datasheet 72 cell DUOMAX Twin", *Trina Sol.* [https://static.trinasolar.com/sites/default/files/Datasheet%20DUOMAX%20Twin_DEG14C.07%28II%29_July_2017_B_web.pdf].
[141] Rabanal-Arabach, J., Schneider, A. & Cabrera, E. 2015, "Minimization of electrical losses of pv modules located in places with high solar irradiance", *Energy Procedia,* Vol. 77, pp. 402–406.
[142] Kreinin, L. et al. 2017, "Pv systems based on bifacial modules: performance simulation vs. design factors", *Photovolt. Spec. Conf. PVSC 2017 IEEE 44th, IEEE,* pp. 1–4.
[143] "Calculating-additional-energy-yield-through-bifacial-solar-technology-sw9002us.pdf" [www.solarworld-usa.com/~/media/www/files/white-papers/calculating-additional-energy-yield-through-bifacial-solar-technology-sw9002us.pdf].
[144] Munsell, M. 2017, "Global solar tracker shipments grow 32% in 2017, NEXTracker leads the market – Greentech Media", *GTM Res. Spotlight* [https://www.greentechmedia.com/articles/read/global-solar-tracker-shipments-grow-32-in-2017-nextracker-leads-the-market].
[145] "Arctech Solar, product 'SkySmart', tracking type: independent horizontal single axis tracker" [www.arctechsolar.com].

About the Authors

Dr. Hartmut Nussbaumer dedicated his academic career to PV and completed his Ph.D. in 1996. After postdoctoral work he held several management positions in the PV industry, and was CTO of RENA GmbH from 2010 to 2014. He then became a lecturer at the Zurich University of Applied Sciences (ZHAW) in Winterthur, Switzerland, and is currently head of the PV modules group.

Dr. Markus Klenk received his Ph.D. in 2001, after which he worked for Sunways AG, first in R&D and later as head of cell and module quality assurance. This was followed by senior technologist positions at centrotherm and RCT Solutions. Since 2015 he has been at the ZHAW, where he continues his PV activities.

Andreas Halm joined ISC in 2008, working on solar cells made of SoG (solar-grade) silicon. In 2010 he switched to developing n-type IBC solar cells, and in 2013 began to focus on module integration. In 2016 he became group leader of the module development group, and has been head of the module department since 2017.

Prof. Dr. Andreas Schneider obtained his Ph.D. at the University of Konstanz in 2004. From 2005 to 2011 he worked for Day4Energy as head of R&D, subsequently joining Jabil and then ISC Konstanz in 2011, where he was responsible for module development. Since 2016 he has been a professor at the University of Applied Sciences Gelsenkirchen.

Enquiries

Dr. Hartmut Nussbaumer
Dr. Markus Klenk
Technikumstrasse 9
8401 Winterthur, Switzerland

Tel: +41 58 934 4799 or +41 58 934 4804
Email: hartmut.nussbaumer@zhaw.ch
Email: markus.klenk@zhaw.ch

Advertisers and web index

To advertise within Photovoltaics International, please contact the sales department: Tel +44 (0) 20 7871 0122

SNEC PV POWER EXPO
Dialogue & Conference & Exhibition

www.snec.org.cn

SNEC 13th (2019) International Photovoltaic Power Generation and Smart Energy Exhibition & Conference

◎Asian Photovoltaic Industry Association / Shanghai New Energy Industry Association

◎Show Management: Follow Me Int'l Exhibition (Shanghai), Inc.

Add: RM905-907 No 425 Yishan Rd, Xuhui District, Shanghai 200235, PRC

Tel: +86-21-33685117 / 33683167

◎For exhibition: info@snec.org.cn   For conference: office@snec.org.cn

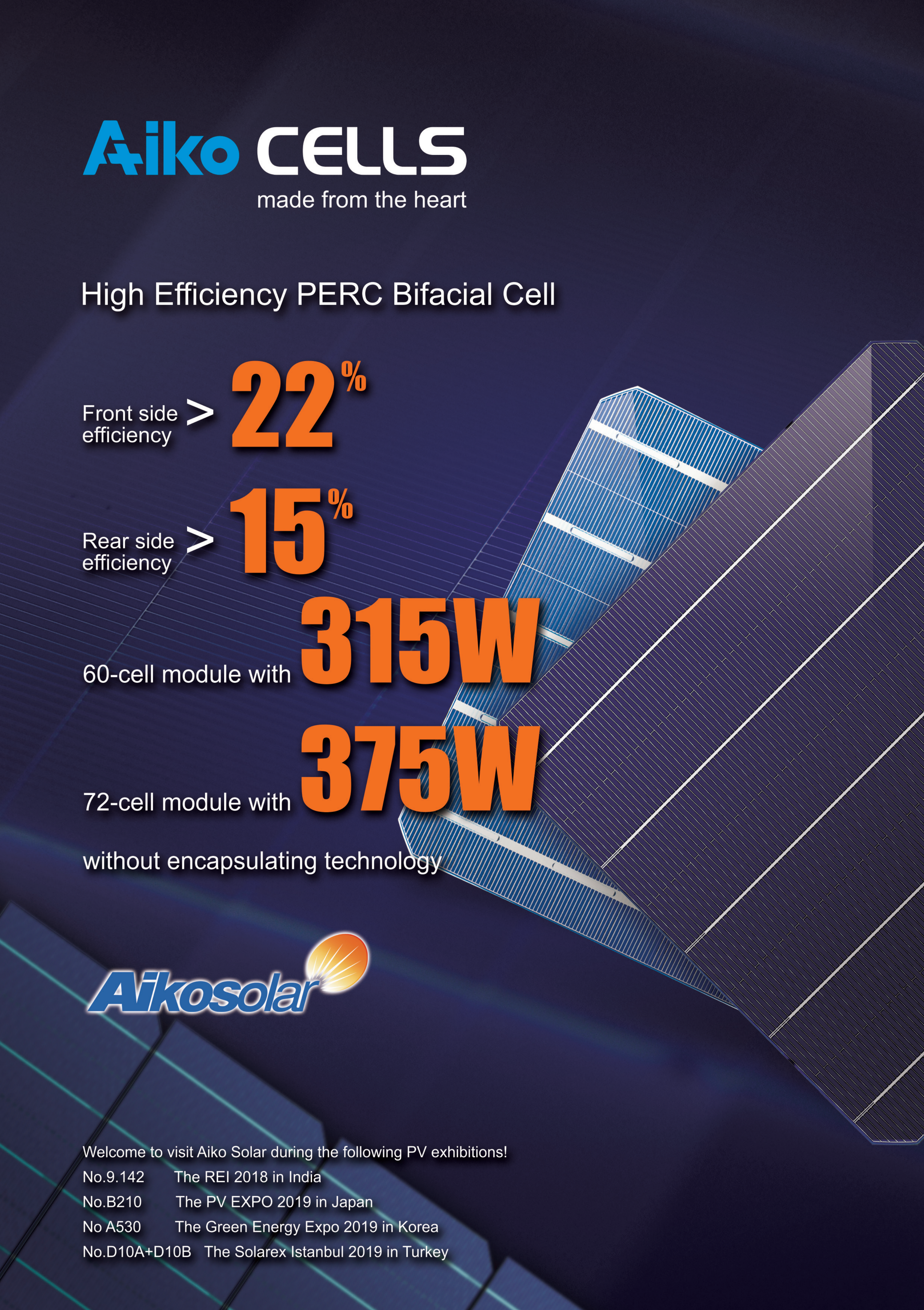
Aiko CELLS
made from the heart
High Efficiency PERC Bifacial Cell
Front side efficiency > 22%
Rear side efficiency > 15%
60-cell module with 315W
72-cell module with 375W
without encapsulating technology
Aikosolar
Welcome to visit Aiko Solar during the following PV exhibitions!
No.9.142 The REI 2018 in India
No.B210 The PV EXPO 2019 in Japan
No A530 The Green Energy Expo 2019 in Korea
No.D10A+D10B The Solarex Istanbul 2019 in Turkey